UNIONE EUROPEA
Fondo sociale europeo

Repubblica Italiana

REGIONE AUTÒNOMA DE SARDIGNA
REGIONE AUTONOMA DELLA SARDEGNA

FSE 2007-2013
POR SARDEGNA
obiettivo competitività regionale e occupazione

Fondazione di Sardegna

uniss
UNIVERSITÀ DEGLI STUDI DI SASSARI

A.D. MDLXII

UNIVERSITÀ DEGLI STUDI DI SASSARI

CORSO DI DOTTORATO DI RICERCA

Scienze Agrarie

RVRALIS ET SILVESTRIS SAPIENTIA

Curriculum Agrometeorologia ed Ecofisiologia dei Sistemi Agrari e Forestali

Ciclo XXIX

A modeling tool to assess local and regional impact of climate change on crop water requirement in Euro-Mediterranean Countries, and assessment of Mediterranean irrigated agriculture vulnerability

dr. Sara Masia

Coordinatore del Corso	Prof. Antonello Cannas
Referente di Curriculum	Prof. Donatella Spano
Docente Guida	Dr. Serena Marras
Tutor	Dr. Costantino Sirca
Co-tutor	Dr. Antonio Trabucco

Anno Accademico 2015 - 2016

UNIONE EUROPEA
Fondo sociale europeo

Repubblica Italiana

REGIONE AUTÒNOMA DE SARDIGNA
REGIONE AUTONOMA DELLA SARDEGNA

FSE 2007-2013
POR SARDEGNA
obiettivo competitività regionale e occupazione

Fondazione di Sardegna

uniss
UNIVERSITÀ DEGLI STUDI DI SASSARI

UNIVERSITÀ DEGLI STUDI DI SASSARI

CORSO DI DOTTORATO DI RICERCA

Scienze Agrarie

Curriculum Agrometeorologia ed Ecofisiologia dei Sistemi Agrari e Forestali

Ciclo XXIX

La presente tesi è stata prodotta durante la frequenza del corso di dottorato in Scienze Agrarie dell'Università degli Studi di Sassari, a.a. 2015/2016 - XXIX ciclo, con il sostegno di una borsa di studio cofinanziata con le risorse del P.O.R. SARDEGNA F.S.E. 2007-2013 - Obiettivo competitività regionale e occupazione, Asse IV Capitale umano, Linea di Attività l.3.1 "Finanziamento di corsi di dottorato finalizzati alla formazione di capitale umano altamente specializzato, in particolare per i settori dell'ICT, delle nanotecnologie e delle biotecnologie, dell'energia e dello sviluppo sostenibile, dell'agroalimentare e dei materiali tradizionali".

La tesi è stata prodotta, altresì, grazie al contributo della Fondazione di Sardegna.

Sara Masia presents her sincere thanks to the Sardinian Regional Government for the financial support of her PhD scholarship (P.O.R. Sardegna F.S.E. Operational Programme of the Autonomous Region of Sardinia, European Social Fund 2007-2013 - Axis IV Human Resources, Objective l.3, Line of Activity l.3.1.).
Sincere thanks also to the Fondazione di Sardegna for the financial contribution.

Table of Contents

ABSTRACT

Climate change is recognized to have a strong impact on water availability, especially in the Mediterranean areas, by enhancing drought conditions and water scarcity issues. The availability of water is crucial in the agriculture sector and affects crop growth and yield. Irrigation practices are then quite diffuse for sustaining crop production, so the assessment of crop water requirement becomes extremely important. In addition, to cope with the changing crop water needs due to global warming, strategies to find the best balance between water application and crop yield need to be developed.

This work aims to develop a tool able to estimate crop water consumption and irrigation requirement for economically relevant crops, at local and regional scale, for both actual and future climate conditions. Specifically, the developed tool will allow to quantify, per each crop and per each crop growth stage, the amount of water effectively consumed by plants and the irrigation volumes and scheduling. Based on that, this work aims to evaluate the impact of climate change on future water needs for three crops (maize, wheat, and grape) at Euro-Mediterranean basin scale. In addition, the vulnerability of Mediterranean irrigated agriculture is investigated.

The Simulation of Evapotranspiration of Applied Water model was selected and converted in a R programming language, and implemented in R platform (SIMETAW_R) to estimate crop irrigation requirements at different scales, and with large dataset generated by climate models. The new tool, originally developed to work at farm level, was included into a GIS platform under R, named SIMETAW_GIS, fully developed in this work, which could process geospatial environmental data and reiterate simulations over regional scale.

This work is organized in different sections: an introductive part and three chapters.

The introductive part would aim to briefly introduce climate changes issues, their implication for agriculture, and to describe the main concepts related to the estimation of crop water consumption.

The first chapter aims at identifying and evaluating the flexible tool needed to estimate crop water needs. It then describes the improvement made on the Simulation of Evapotranspiration of Applied Water (SIMETAW_R) model, and evaluates its

performance in estimating crop evapotranspiration and irrigation requirement at local scale and under several pedo-climatic conditions. SIMETAW_R model was applied in 10 European sites selected through the international FLUXNET network. Model estimates of actual evapotranspiration (ETa) where validated through the comparison with ETa values directly measured by Eddy Covariance stations at each site. In addition, the performance of the Hargreaves-Samani and standardized Penman-Monteith equations were assessed in order to identify the one more accurate in estimating reference evapotranspiration with the available input, that was then selected to be used for the estimation of crop and actual evapotranspiration.

The second chapter illustrates the development and the application of SIMETAW_GIS as a tool to simulate crop water use and water application at regional scale. The analysis was conducted for past climate conditions (1976-2005) and under future climate (2036-2065) by using two Representative Concentration Pathway scenarios, RCP 4.5 and 8.5. The analysis allowed to estimate the impact of climate change on crop water needs per each Euro-Mediterranean Country of the domain under investigation.

SIMETAW_R and its platform SIMETAW_GIS allow to compute the daily soil water balance, reference, crop, and actual evapotranspiration, as well as the evapotranspiration of applied water, i.e. the total amount of water applied per each event. The model schedules also the number of irrigation events.

Finally, the third chapter indicates the assessment of the irrigation supply vulnerabilities for specific watersheds in the Euro-Mediterranean basin including the changes of irrigation requirements and of water availability into dams as a result of climate change, and the study of potential future conflicts among sectors in the use of water resources.

Results showed higher values of reference, crop, and actual evapotranspiration, as well as irrigation requirement, under future climate conditions, and differences were often greater under RCP 4.5 than 8.5 scenario. The impact of global warming on maize, grape, and wheat water consumption and irrigation was more severe in Mediterranean Countries, already affected by water scarcity. In term of yield losses, the best response to future increasing CO_2 concentration in the atmosphere was given by wheat and grape (C3 crops).

The new SIMETAW_R model outcomes at local scale, as well as the SIMETAW_GIS platform gridded outcomes at regional scale may be useful to increase awareness on

climate change impact in Euro-Mediterranean regions, thus to address farmers, decision makers, and politicians in developing sustainable strategies in agriculture target to better manage water resource.

INTRODUCTION

Impact of climate change in European regions

According to the Intergovernmental Panel on Climate Change (IPCC), "*Climate change refers to a change in the state of the climate that can be identified (e.g., by using statistical tests) by changes in the mean and/or the variability of its properties, and that persists for an extended period, typically decades or longer. Climate change may be due to natural internal processes or external forcings such as modulations of the solar cycles, volcanic eruptions, and persistent anthropogenic changes in the composition of the atmosphere or in land use. Note that the Framework Convention on Climate Change (UNFCCC), in its Article 1, defines climate change as: 'a change of climate which is attributed directly or indirectly to human activity that alters the composition of the global atmosphere and which is in addition to natural climate variability observed over comparable time periods'. The UNFCCC thus makes a distinction between climate change attributable to human activities altering the atmospheric composition, and climate variability attributable to natural causes."* (IPCC, 2014).

Climate is a very complex system characterized by the interactions among factors such as vegetation, oceans, atmosphere, and so on. This system is prone to natural or anthropogenic changes, and depend on space and time scale. One of the main cause of global warming is the constant increasing concentration of the anthropogenic greenhouse gas emissions (GHGs) in the atmosphere since the pre-industrial revolution (IPCC, 2014).

Climate change is one of the most important challenge for our society in the 21st century. According to the Fifth Assessment Report of the IPCC this challenge is expected to worsen in the next few decades due to the quick demographic growth, the socio-economic development, the increasing demand of raw materials and energy, the extension of residential centres, as well as the improvement of quality of life.

The quick increasing temperature from 2005 onward is related to the increasing concentration of GHGs in the atmosphere (Collins et al., 2013). The contribution of each GHG emission to the long-term future radiative forcing, and projections of global

surface temperature change, for each Representative Concentration Pathway scenario (RCP), obtained through a models ensemble, is shown in Figure 1a and 1b.

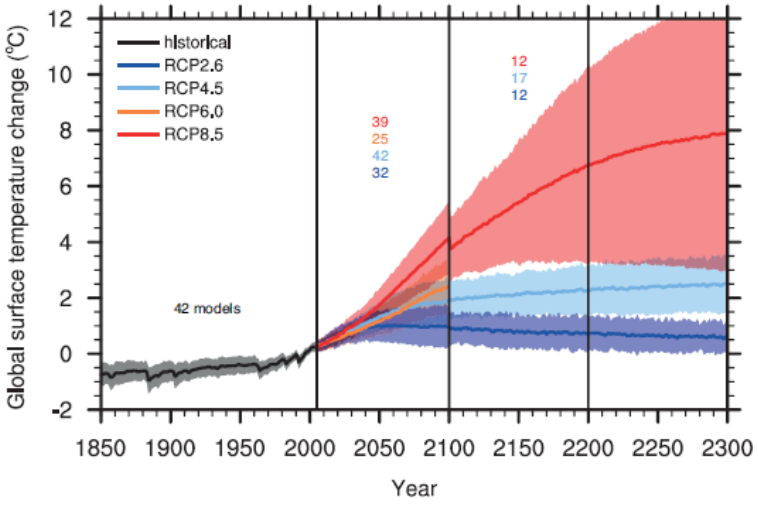

1a

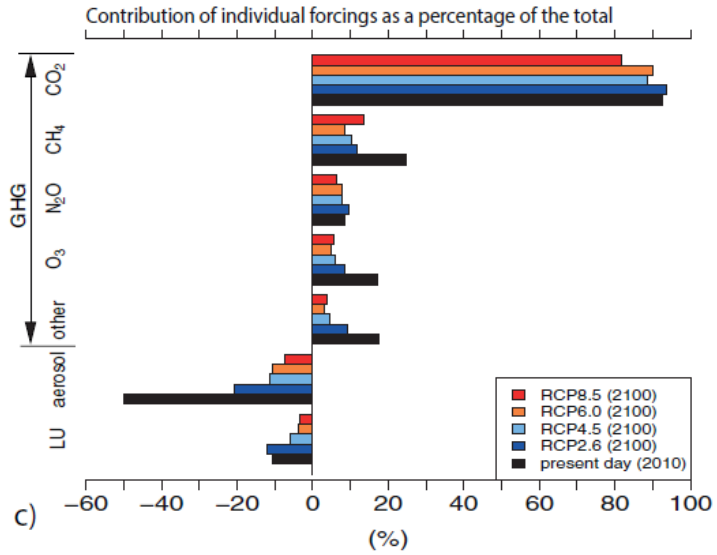

1b

Fig. 1a. Changes of global annual mean surface temperature (°C) from 1980 to 2300. Fig. 1b. Percentage of the contribution of each GHGs expressed considering each RCP used in CMIP5. CO_2 is the Carbon dioxide, CH_4 the methane, N_2O the nitrous oxide, O_3 the ozone, and LU the land use from 2010 to 2100 (Collins et al., 2013).

In parallel with increasing temperature, saturation vapor pressure is also expected to increase. In addition, strong changes in water cycle are expected, but these are more difficult to characterize, because of the random patterns that precipitation events can assume. According to the phrase, "the wet get wetter and the dry get drier", rainfall is projected to increase in fact in the already wet areas near the equator, and to decrease in

areas already characterized by low precipitation as the subtropical one, particularly under RCP 8.5 (IPCC, 2013). This fact happens because the water vapor is constantly transported from subtropics (around 20° to 40° latitude in both Hemispheres) to the higher latitude (50 and 70° latitude in the Northen and Southern Hemisphers), thus as a consequence of the increasing temperature, the amount of water vapor which moves from subtropic to subpolar region will be higher (Held and Vecchi, 2008) (Figure 2).

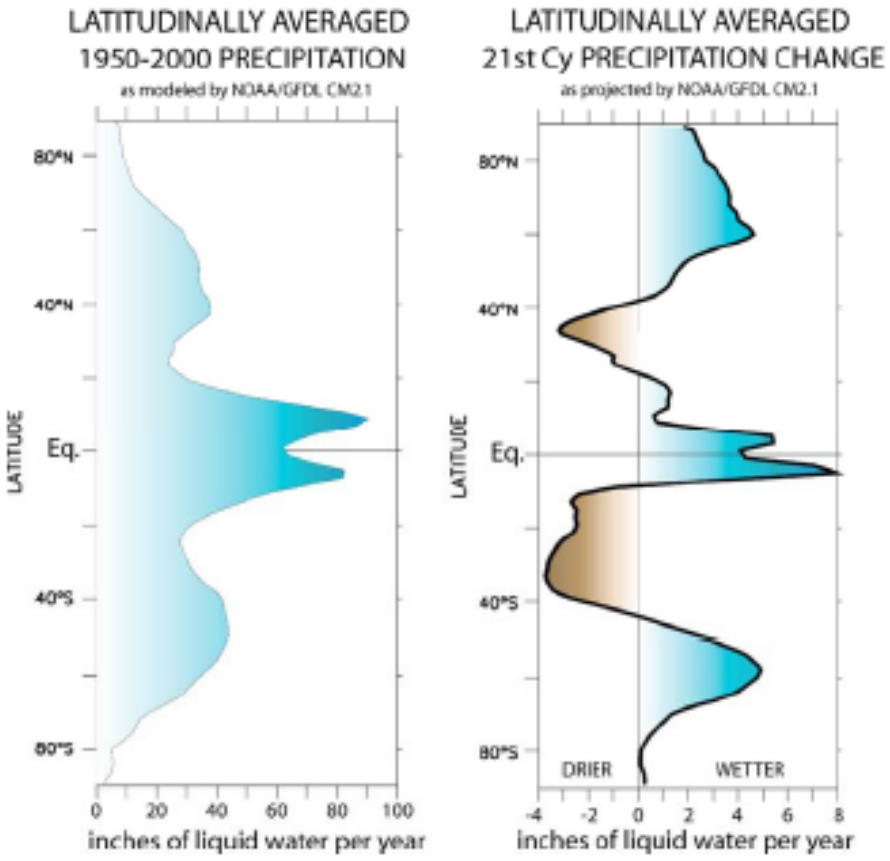

Fig. 2. Latitudinally averaged precipitation simulated by the GFLD CM2.1 model over the period 1951-2000 and 2081-2100 (Held and Vecchi, 2008).

The impact of climate change (CC) in Europe is different from region to region, and it is strictly dependent on social, economic, climatic, and geographic factors (Figure 3).

Since future projections indicate large impact over different sectors across Europe, the European Countries decided to adopt a medium-term strategies which aims at a more sustainable economy to cope with climate changes. The European 2020 strategy aims to reduce the GHGs concentration in the atmosphere by 20%, in comparison to 1990 level,

to reach 20% energy dependencies by renewable sources, and to increase the energy efficiency up to 20% (EEA, 2015).

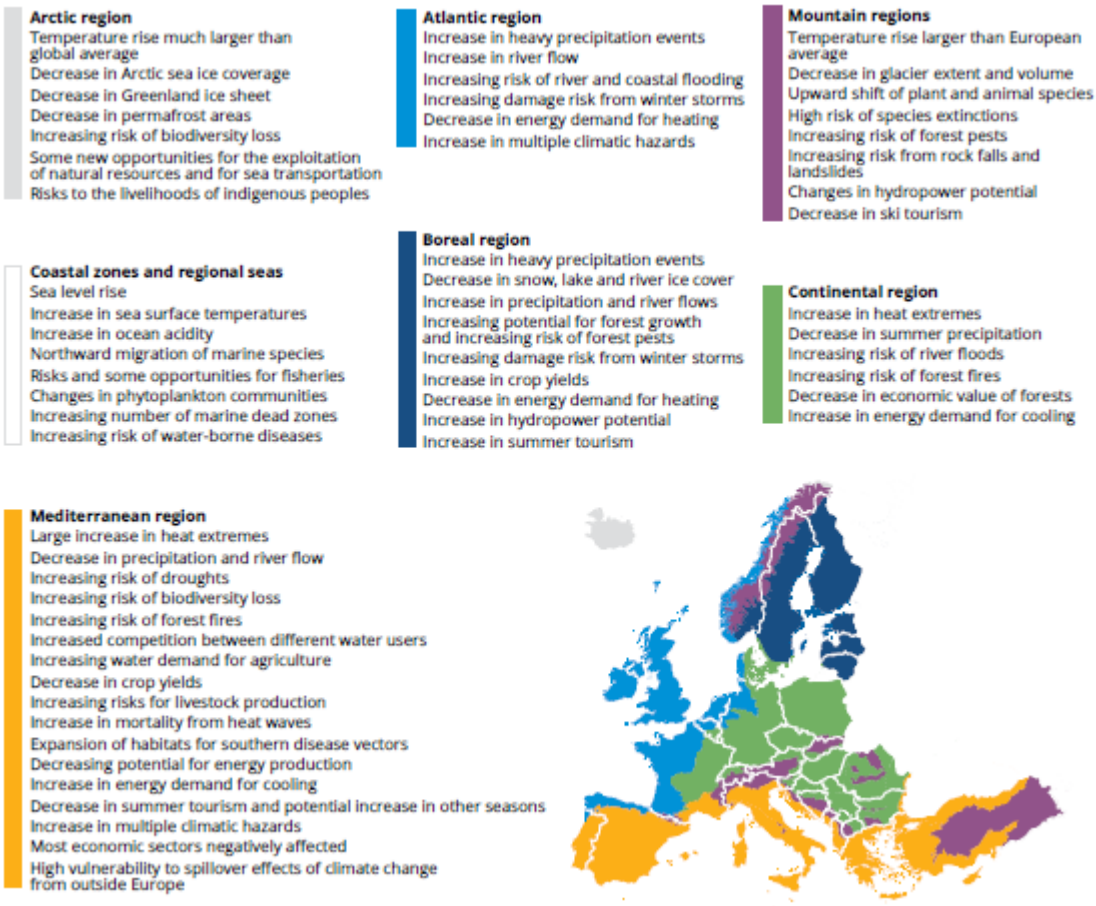

Fig. 3. Impact of climate change in Europen regions (EEA, 2017).

Modeling the climate system

Physics and mathematics are the bases of climate models, which are able to represent future climate conditions with a range of confidence that is higher for certain variables such as temperature and lower for others as precipitation. The confidence of climate model outcomes is measured also by their ability in reproducing past climate change and observed climate (Randall et al., 2007). Although models are simplification of the reality, they are essential to predict future impacts, and to assess adaptation and mitigation strategies.

Global Climate Models (GCMs) are used to reproduce the climate system at global scale, thus all the interactions among changes in GHGs concentration, land surface, sea level, and so on. They are built to reconstruct and simulate the main Earth's system components using a three dimensional grid (Figure 4).

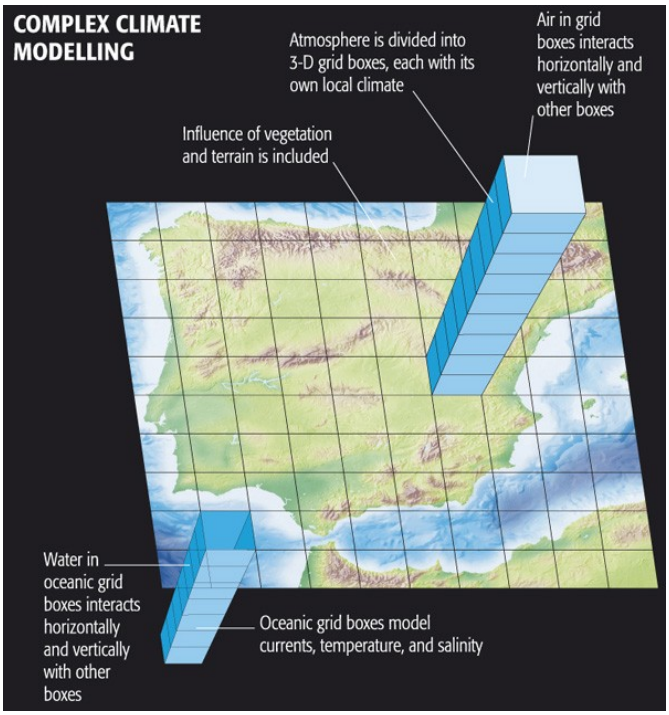

Fig. 4. General scheme of the complex, gridded Global Climate Model.

Atmosphere, land and oceans are divided in small grids evaluating the interactions with the surrounding grid boxes. Any variable, such as humidity, temperature, and cloud coverage, is considered uniform for the entire cell.

Although the spatial GCMs resolution has increased from 1990 (around 500 km, 1st Assessment Report) until 2010 (around 80 km, 5th Assessment Report) (IPCC, 2013), a downscaling technique is needed to reproduce the climate system at regional scale and at higher resolution. The downscaling process (Figure 5a and 5b) provides an increase of GCM spatial resolution (around 25 km), thus more detailed features (e.g. topography) in the studied domain.

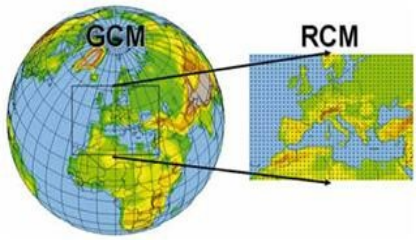

Fig. 5a. Scheme of downscaling from Global Climate Model (GCM) to Regional Climate Model (RCM) (Giorgi., 2008).

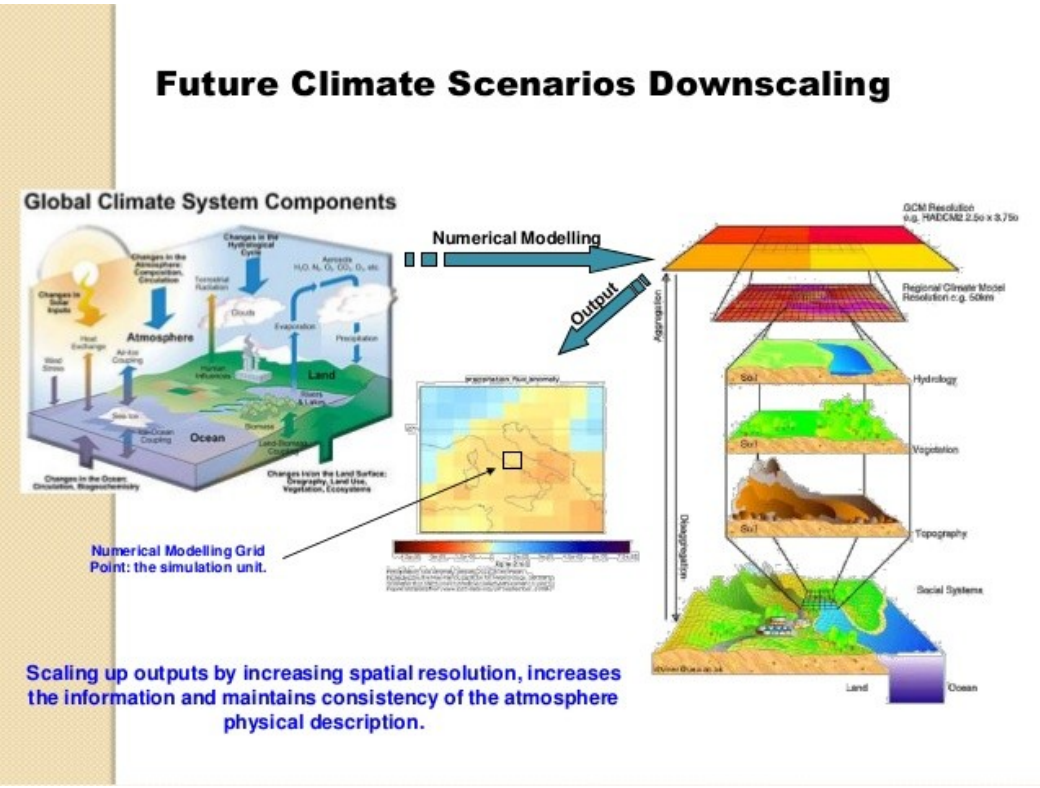

Fig. 5b. Downscaling process of future climate scenarios (http://www.slideshare.net/GRFDavos/bonn-lr).

Representative Concentration Pathways (RCPs) climate scenarios

One of the main cause of climate change is the increase of natural or anthropogenic emissions of greenhouse gases in the atmosphere. According to the last report of the European Environmental Agency (2009), the CO_2 concentration in the atmosphere increased up to 400 parts per million (ppm) in 2016, specifically compared to the the pre-industrial revolution, the level was about 40% higher.

It is stated that there is a direct relationship between air temperature and the variation of GHGs concentrations (IPCC, 2007; Lüthi et al., 2008) (Figure 6).

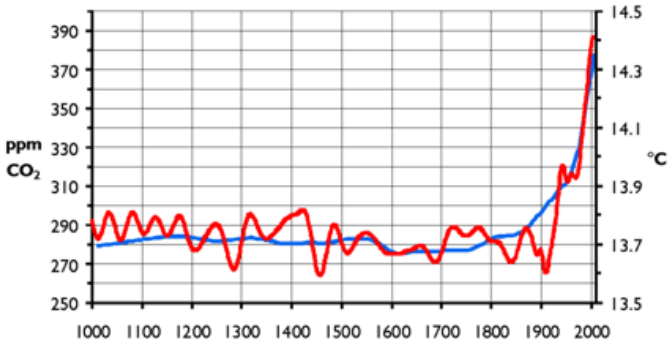

Fig. 6. Direct relationship between air temperature (red line) and carbon dioxide (blue line) (from www.riscaldamentoglobale.it).

According to the IPCC, the GHGs emissions are constantly increasing, leading to a continuous raise in surface temperature. At global level, according to Hartmann et al. (2013), the mean surface temperature is increase with a range of 0.49 °C to 0.89 °C, with an average of 0.72 °C, in the period from 1951 to 2012. Despite the huge number of policies developed in order to mitigate climate change, 2014 and 2015 were the warmest years in the last decades (ISPRA, 2016). According to the IPCC scenarios, without mitigation policies the mean surface temperature will rise up to 3.7 – 4.8 °C by 2100 compared to the pre-industrial time (IPCC, 2014).

Since climate is influenced by the concentration of GHG, the research and definition of climate change needs to consider plausible scenarios of GHG emissions. At the moment, four Representative Concentration Pathways (RCPs) are mostly taken as reference (Figure 7), considering their total radiative forcing (W m^{-2}) pathway (trajectories over time), i.e. the total amount of GHGs emissions due to human activities until 2100. RCPs scenarios are useful frameworks for the scientific community to describe the influence of anthropogenic emissions on future climate (http://sedac.ipcc-data.org/ddc/ar5_scenario_process/RCPs.html). The radiative forcing ranges from 2.6 to 8.5 W m^{-2}, and are considered rather "representative" because each of them refers to a substantial large number of scenarios available in literature. The definition "concentration pathways" is used to underline that they are sets of future projections of the radiative forcing components (van Vuuren et al., 2011).

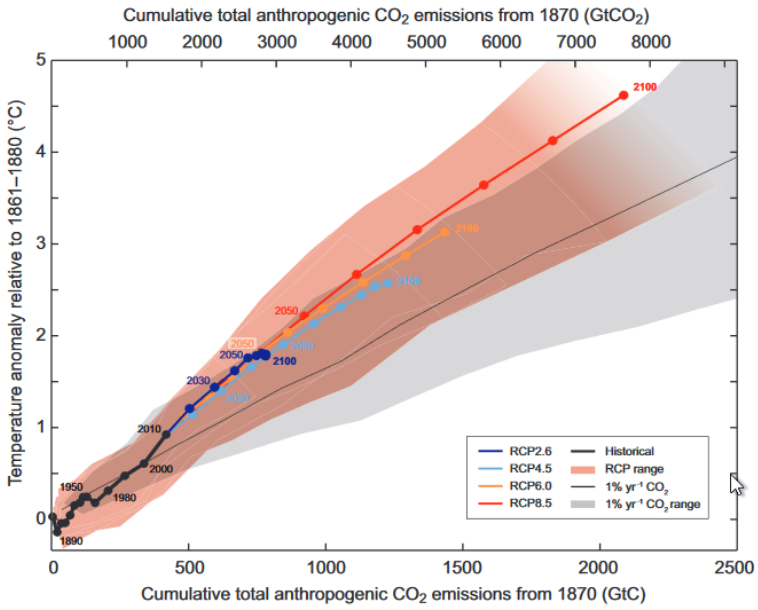

Fig. 7. Cumulative total anthropogenic CO_2 emissions and temperature anomalies (IPCC, 2013).

A brief description of the sets of RCPs and their main features is reported in Table 1.

Tab. 1. Description of the four Representative Concentration Pathways Scenarios and their main characteristics. IA model=Integration Assessment Model (modified from http://sedac.ipcc-data.org/ddc/ar5_scenario_process/RCPs.html and van Vuuren et al. (2011)).

				Scenario components		
	Description	**IA Model**	**Publication – IA Model**	**Greenhouse gas emissions**	**Agricultural area**	**Air pollution**
RCP8.5	Rising radiative forcing pathway leading to 8.5 W/m^2 (~ 1370 ppm CO_2 eq) by 2100.	MESSAGE	Riahi et al. (2007) Rao & Riahi (2006)	High baseline	Medium for both cropland and pasture	Medium-high
RCP6	Stabilization without overshoot pathway to 6 W/m^2 (~ 850 ppm CO_2 eq) at stabilization after 2100	AIM	Fujino et al. (2006) Hijioka et al. (2008)	Medium baseline; high mitigation	Medium for cropland but very low for pasture (total low)	Medium
RCP4.5	Stabilization without overshoot pathway to 4.5 W/m^2 (~ 650 ppm CO_2 eq) at stabilization after 2100	GCAM	Smith and Wigley (2006) Clarke et al. (2007) Wise et al. (2009)	Medium-low mitigation Very low baseline	Very low for both cropland and pasture	Medium
RCP2.6	Peak in radiative forcing at ~ 3 W/m^2 (~ 490 ppm CO_2 eq) before 2100 and then decline	IMAGE	van Vuuren et al. (2006 and 2007)	Very low	Medium for cropland and pasture	Medium-low

RCPs are expected to be used as input for climate models and mitigation analysis, as well as for the assessment of climate change impact.

Agriculture and water resources in the Euro-Mediterranean regions

Agriculture is a sector with large relevance for water needs, and definitively the most responsible for water use in semi arid areas like southern Europe and Mediterranean areas. Around 2010, the mean total water withdrawal for agriculture, which includes irrigation, livestock, and aquaculture, is accounted for about 25% at European level (Figure 8a), where the percentage accounted for in Western and Central Europe (27%) is higher than the one estimated in Eastern Europe (21%). The 57% (Figure 8b) of the total water use is estimated in Mediterranean Countries. In Northern Africa the percentage of water withdrawal for agricultural use is about the 84% (Figure 8c) (http://www.fao.org/nr/water/aquastat/tables/WorldData-Withdrawal_eng.pdf).

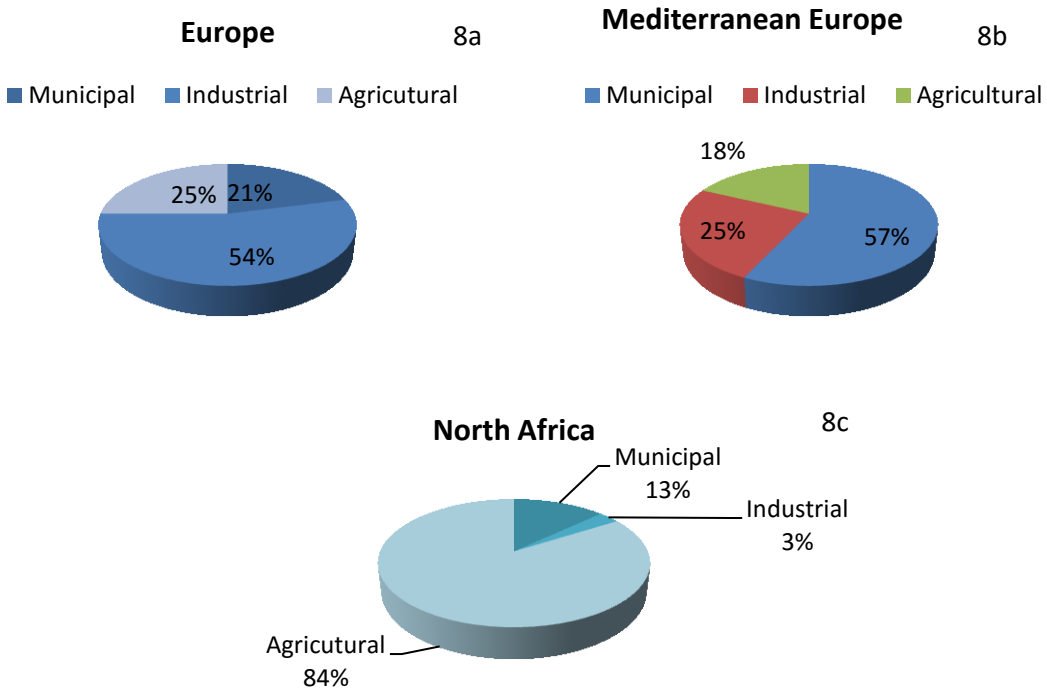

Fig. 8a, 8b, and 8c. Mean total percentage of water withdrawal by sector in Europe, Mediterranean Countries, and North Africa, respectively, around 2010. (http://www.fao.org/nr/water/aquastat/tables/WorldData-Withdrawal_eng.pdf).

The recently increasing temperature associated with decreasing precipitation result in a limited water availability in the Southern regions, where irrigation is an essential practice for agricultural production. In the Northern areas, most of the water resources is used for livestock, while in the Southern arid and semi-arid areas, with particular attention to the Mediterranean regions, it is used for irrigation (EEA, 2009).

The highest percentage (around 60%) of the total freshwater abstraction used for irrigation is in fact accounted for in Southern and Southern East Europe (http://ec.europa.eu/eurostat/statistics-explained/index.php/Agri-environmental_indicator_-_water_abstraction). A brief overview of the agricultural areas and water resources in Euro-Mediterranean Countries is presented in this section.

The cultivated area, the total area equipped for irrigation (Figure 9a), and specifically the area actually irrigated, the irrigation water withdrawal (Figure 9b), the total harvested irrigated area, as well as the total area equipped for surface irrigation, sprinkler and localized irrigation are reported in Table 2 for European Countries and in Table 3 for the Mediterranean Countries.

Tab. 2. Cultivated area, total area equipped for irrigation, area actually irrigated, irrigation water withdrawal, total harvested irrigated area, and total area equipped for surface irrigation, sprinkler and localized irrigation in European Countries. Areas are expressed in ha (x 1000), and water abstraction in $10^{\wedge 9}$ m^3 yr^{-1} (http://www.fao.org/nr/water/aquastat/data/query/index.html?lang=en).

	Cultivated area (1000 ha)	**Area equipped for full control irrigation (1000 ha)**	**Area equipped for irrigation: actually irrigated (1000 ha)**	**Irrigation water withdrawal ($10^{\wedge 9}$ m^3 yr^{-1})**	**Total harvested irrigated crop area (1000 ha)**	**Area equipped for surface irrigation (1000 ha)**	**Area equipped for sprinkler irrigation (1000 ha)**	**Area equipped for localized irrigation (1000 ha)**
Austria	1417 *(2014)*	119.80 *(2013)*	51.68 *(2013)*	0.01 *(2010)*	43.40 *(2008)*		131 *(1993)*	
Belgium	839.30 *(2014)*	19.18 *(2013)*	5.74 *(2013)*		5.70 *(2008)*			
Bulgaria	3613 *(2014)*	115.50 *(2013)*	40.51 *(2011)*	0.31 *(2011)*	72.64 *(2008)*	80.60 *(2007)*	21 *(2007)*	3 *(2007)*
Czechia	3219 *(2014)*	34.07 *(2013)*	17.84 *(2013)*	0.01 *(2013)*	19.91 *(2007)*	22.53 *(2007)*	11 *(2007)*	5 *(2007)*
Denmark	2436 *(2014)*	439 *(2013)*	242 *(2013)*	0.09 *(2012)*	254.10 *(2008)*			
Estonia	654.30 *(2014)*	0.45 *(2010)*	0.32 *(2010)*	0 *(2010)*	0.32 *(2010)*		3.68 *(1995)*	
Finland	2234 *(2014)*	102.10 *(2013)*	15.02 *(2010)*	0.04 *(2005)*	15.02 *(2010)*		58.78 *(2010)*	9.80 *(2010)*
Germany	12074 *(2014)*	639 *(2010)*	372.80 *(2010)*	0.17 *(2010)*	234.60 *(2006)*	10.70 *(2006)*	500 *(2006)*	5 *(2006)*
Ireland	1059 *(2014)*	1.10 *(1998)*	1.10 *(1998)*	0.003 *(1998)*	1.10 *(1998)*		60 *(2000)*	
Latvia	1215 *(2014)*	0.63 *(2013)*	0.41 *(2013)*		0.62 *(2007)*			
Lithuania	2384	4.44	1.60	0	1.53		9.24	

	(2014)	*(2012)*	*(2013)*	*(2011)*	*(2010)*		*(1995)*	
Luxembourg	64.16 *(2014)*	0 *(2007)*		0 *(2013)*				
Hungary	4585 *(2014)*	184.8 *(2014)*	99.32 *(2014)*	0.23 *(2013)*	87.62 *(2008)*	18.9 *(2007)*	118 *(2007)*	4 (2007)
Netherlands	1081 *(2014)*	499.40 *(2013)*	101.80 *(2013)*	0.02 *(2012)*	202.30 *(2008)*			
Norway	811.10 *(2014)*	88.91 *(2013)*	19.45 *(2013)*	0.11 *(2006)*	55 *(2007)*			
Poland	11304 *(2014)*	75.81 *(2013)*	45.55 *(2013)*	0.08 *(2012)*	72.06 *(2007)*	102.70 *(2007)*	5 *(2007)*	8 *(2007)*
Portugal	1885 *(2014)*	583.70 *(2007)*	421.50 *2007)*	3.76 *(2009)*	421.50 *(2008)*		40 *(1999)*	25 *(1999)*
Romania	9203 *(2014)*	230.40 *(2013)*	152.80 *(2013)*	0.34 *(2013)*	173.40 *(2008)*		448 *(2003)*	4 *(2003)*
Serbia	2794 *(2014)*	91.96 *(2011)*	34.17 *(2011)*	0.08 *(2013)*	34.17 *(2011)*			
Slovakia	1413 *(2014)*	99.64 *(2013)*	24.60 *(2013)*	0.01 *(2014)*	39.09 *(2008)*			
Sweden	2597 *(2014)*	155.50 *(2013)*	51.87 *(2013)*	0.06 *(2010)*	54.17 *(2007)*			
Switzerland	425.70 *(2014)*	61 *(2010)*	36.18 *(2010)*	0.13 *(2012)*	36.18 *(2010)*			
Macedonia	452 *(2014)*	127.80 *(2004)*	79.64 *(2007)*	0.15 *(2013)*	79.64 *(2007)*			
United Kingdom	6279 *(2014)*	228 *(2005)*	49.13 *(2013)*	0.04 *(2012)*	138.20 *(2007)*	117 *(2005)*	105 *(2005)*	6 *(2005)*

Tab. 3. Cultivated area, total area equipped for irrigation, and specifically the area actually irrigated, irrigation water withdrawal, total harvested irrigated area, and total area equipped for surface irrigation, sprinkler and localized irrigation for Mediterranean Countries. Areas are expressed in ha (x 1000) and water abstraction in $10^{\wedge 9}$ m^3 yr^{-1} (http://www.fao.org/nr/water/aquastat/data/query/index.html?lang=en).

	Cultivated area (1000 ha)	**Area equipped for irrigation (1000 ha)**	**Area equipped for irrigation: actually irrigated (1000 ha)**	**Irrigation water withdrawal ($10^{\wedge 9}$ m^3 yr^{-1})**	**Total harvested irrigated crop area (1000 ha)**	**Area equipped for surface irrigation (1000 ha)**	**Area equipped for sprinkler irrigation (1000 ha)**	**Area equipped for localized irrigation (1000 ha)**
Albania	696 *(2014)*	337.60 *(2013)*	205.30 *(2013)*	0.51 *(2006)*	102.70 *(2006)*			
Algeria	8439 *(2014)*	1177 *(2012)*	1012 *(2012)*	3.50 *(2001)*	858.20 *(2008)*	686.90 *(2012)*	270 *(2012)*	220 *(2012)*
Bosnia and Herzegovina	1117 *(2014)*	3 *(2000)*						
Croatia	890.80 *(2014)*	25.87 *(2013)*	13.43 *(2013)*	0.01 *(2010)*		4.86 *(2002)*	0.25 *(2002)*	0.01 *(2002)*
Cyprus	106.30 *(2014)*	39.54 *(1994)*		0.16 *(2013)*	31.26 *(2008)*			35.59 *(1994)*
Egypt	3745 *(2014)*	3610 *(2010)*			6333 *(2010)*	2730 *(2010)*	410 *(2010)*	470 *(2010)*
France	19328 *(2014)*	2811 *(2013)*	1424 *(2013)*	3.14 *(2009)*	1512 *(2008)*	115 *(2007)*	2420 *(2007)*	107.50 *(2007)*
Greece	3725 *(2014)*	1517 *(2013)*	1165 *(2013)*	7.86 *(2011)*	1280 *(2008)*			
Israel	397.70 *(2014)*	225 *(2004)*	181.50 *(2006)*		183.60 *(2006)*			168.80 *(2004)*
Italy	9121 *(2014)*	4004 *(2013)*	2866 *(2013)*	12.89 *(2007)*	2666 *(2008)*	2399 *(2007)*	981.20 *(2007)*	570.60 *(2007)*
Lebanon	258 *(2014)*	104 *(1998)*	90 *(1998)*		105.30 *(2003)*	66.13 *(1998)*	29.04 *(1998)*	8.83 *(1998)*
Libya	2050 *(2014)*	400 *(2008)*	335 *(2008)*		406 *(2000)*			
Malta	10.23	4.20	3.66	0.02	2.81			

	(2014)	*(2013)*	*(2013)*	*(2013)*	*(2008)*			
Montenegro	13.74 *(2014)*	2.41 *(2010)*	2.41 *(2010)*		2.41 *(2010)*	0 *(2010)*	0.90 *(2010)*	1.50 *(2010)*
Morocco	9592 *(2014)*	1458 *(2011)*	1341 *(2012)*		1711 *(2011)*	1044 *(2011)*	125.80 *(2011)*	288.2 *(2011)*
Slovenia	237.30 *(2014)*	7.60 *(2010)*	3.50 *(2010)*	0.003 *(2013)*	3.50 *(2010)*		5.26 *(2010)*	2.33 *(2010)*
Spain	17188 *(2014)*	3923 *(2012)*	3504 *(2012)*	23.37 *(2012)*	3093 *(2009)*			
Syria	5733 *(2014)*	1341 *(2010)*	1210 *(2000)*		1334 *(2000)*	1043 *(2010)*	187.10 *(2010)*	110.90 *(2010)*
Tunisia	5232 *(2014)*	459.60 *(2012)*	380 *(2011)*		419 *(2011)*	189.40 *(2012)*	115.20 *(2012)*	155 *(2012)*
Turkey	23944 *(2014)*	5340 *(2012)*	4206 *(2004)*		4206 *(2004)*	4690 *(2012)*	500 *(2012)*	150 *(2012)*

The cultivated area, given by the sum of arable lands and permanent crops, is estimated higher than 8 million hectares in Algeria, France, Germany, Morocco, Polonia, Italy, Romania, Spain, and Turkey. It is worth noting that the areas equipped for full control irrigation are higher than the ones actually irrigated in all Euro-Mediterranean Countries. Most of the areas equipped for irrigation and actually irrigated are in the Mediterranean basin, in particular areas larger than 1 million hectares are located in Algeria, France, Greece, Italy, Morocco, Spain, Syria, and Turkey. The highest values ($> 3 \times 10^{\wedge 9}$ m^3 yr^{-1}) of annual water withdrawal for irrigation are in general always in correspondence with the largest cultivated and irrigated areas. Southern regions are also accounted for the highest total harvested irrigated crop lands. Egypt, Italy, Syria, Turkey, and Morocco are the Countries where surface irrigation is mainly used. More than 500,000 ha are irrigated using sprinkler system in France, Germany, Italy, and Turkey. In addition, land irrigated using localized irrigation are also located in Mediterranean basin where the total hectares were higher than 100,000 in most of the Countries.

Total harvested irrigated crop area refers to specific crops irrigated for their entire growing season. Since the same area may be under double irrigated cropping, it could be counted twice, hence the total harvested irrigated crop area may be larger than the area equipped for full control irrigation (Egypt, Lebanon, Libya, and Morocco). It is evident that, in the wet Northern-East Countries such as Austria, Bulgaria, Czechia, Denmark, Finland, Germany, Lithuania, Netherlands, Norway, Romania, Slovakia, Sweden, Switzerland, and United Kingdom, despite the large areas equipped for irrigation, the harvested irrigated crop lands are lower.

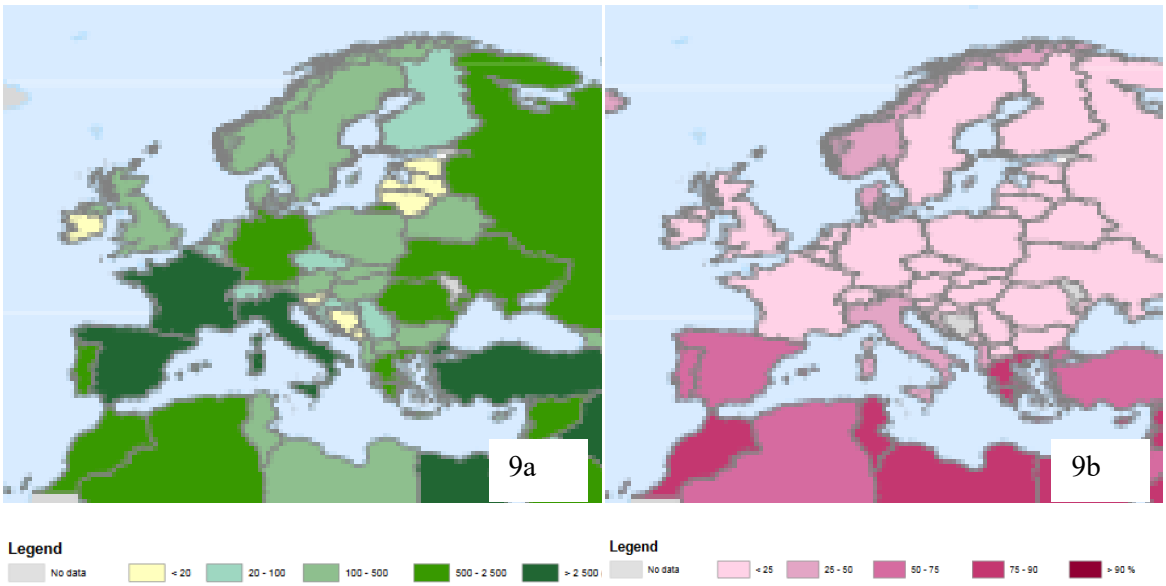

Fig. 9a. Total area equipped for irrigation expressed in ha (1000 ha) (http://www.fao.org/nr/water/aquastat/maps/EqIrr_eng.pdf). Fig. 9b. Percentage of total water withdrawal abstracted for agriculture in Euro-Mediterranean Countries (http://www.fao.org/nr/water/aquastat/maps/WithA.WithT_eng.pdf).

Due to the water losses in the supply system, the abstraction rates is generally higher than the water demand (OECD, 2006). In order to solve this issue, strategies to improve water efficiency are necessary to develop a more sustainable agriculture in particular in areas already affected by water scarcity.

The impact of climate change on hydrological cycle

The hydrological cycle is a natural process characterized by a constant movement of water on, above, and below the Earth surface (Figure 10). The sun drives the changes of water state between ice, liquid, and vapor through physical processes. Water moves from liquid to vapor through the processes of 1) evaporation from water bodies and soil, and 2) transpiration from plants. Water vapor moves to the atmosphere where it is stored in clouds. Water changes its state from vapor to liquid or solid through the process of condensation, and falls to the surface where it returns naturally as rainfall or snowfall to the surface (Trenberth et al., 2006).

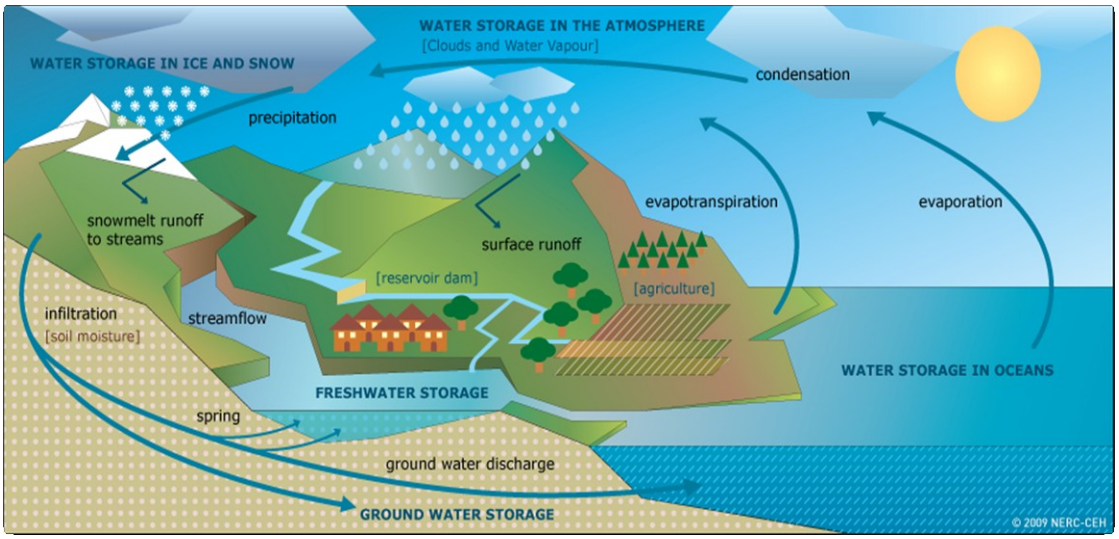

Fig. 10. The hydrological cycle. Movement of water molecules through physical processes in the Earth system.

It is widely known that the physical processes involved in the water cycle are influenced by climate and its changes. One of the most serious consequences of the increasing concentrations of GHGs in the atmosphere may be a variation of the water amount and distribution in the Earth system. The impact of climate change on water resources is expected to be exacerbated by the end of the current century creating several areas characterized by perennial droughts and others by frequent floods (Graham et al., 2010). Christensen et al. (2007) stated that there will be no uniform changes in global water cycle. Climate models foresee an increase of annual precipitation in Northern Europe and a decrease in Southern Europe. In central Europe and in Mediterranean areas a reduction of the number of rainy days, with a high risk of consequently drought summer, is expected in the next few years (IPCC, 2013). Water availability is predicted to be increasingly scarcer worldwide, and this trend will be exacerbated not only by climate change conditions but also by the quick and significant population growth, the socio-economic development, the increasing demand for raw materials, as well as changes in lifestyle. The reduction of available water may trigger a competition among sectors for water use, making difficult to find a balance between demand and supply.

The impact of climate change on plant physiology

The increasing GHG concentration in the atmosphere is the main responsible for the increasing temperature, but also variation of the relative humidity in the atmosphere are

expected. This affects transpiration process, thus, warming will have a direct and strong impact on evapotranspiration. Additionally, plants react to higher values of CO_2 concentration with the partially closure of stomata that results in the reduction of conductance (Bernacchi et al., 2007; Snyder et al., 2011).

Plants need to absorb carbon dioxide (CO_2) from the atmosphere to carry on the photosynthetic process and to loose water to regulate internal temperature. The water lost from the leaves during the plant's lifetime is equivalent to hundred times the fresh weight of the specific plant (Taiz and Zeiger, 2008). The transpiration is basic for plant physiology. Nowadays, it is known as one of the most important processes thanks to which the plant can regulate internal temperature in order to not impact metabolism (Cocucci, 2006). The conversion of water from liquid to vapor requires energy, which is provided by the plant through the dissipation of heat; evaporative process leads to cool plant structures (Taiz and Zeiger, 2008). Water passes from cell to cell through membranes following a water potential gradient from soil to leaves which is important also to measure the "water status" of a plant (Taiz and Zeiger, 2008). The movement of water in the atmosphere occurs through small pores named stomata located in the leaves surface. Stomata are generally closed as a response to water stress due to increasing temperature; this reduces the exchange of water vapor and CO_2 between plant and atmosphere (Taiz and Zeiger, 2008).

The impact of global warming on plant physiology is still controversial. It is crucial to understand and to quantify the effect of rising CO_2 concentration and consequently increasing temperature on photosynthetic process (Bernacchi et al., 2003) because this can influence crop yield (Streck, 2005). The response of C3 and C4 plants to the climate change is different due to their attitude in fixing and reducing CO_2. Several studies stated that competitiveness of C3 plants increases with the increasing concentration of CO_2 in the atmosphere. It stimulates C3 photosynthesis, that results in a more vigorous growth and higher yields (Patterson et al., 1984; Cure and Acok, 1986). C3 plants respond reducing photorespiration and increasing photosynthesis until the point where both CO_2 uptake and release are balanced (Taiz and Zeiger, 2008). The efficiency of C3 and C4 plants related to carbon dioxide concentration and temperature is shown in Figure 11.

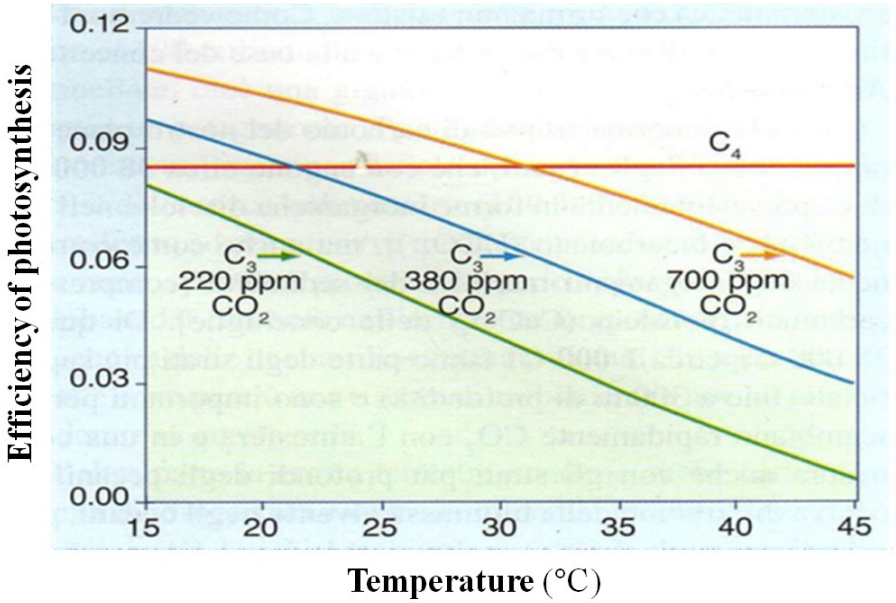

Fig. 11. C3 and C4 plants photosynthetic efficiency in relation to temperature and atmospheric CO_2 concentration (modified from Rascio et al., 2012).

Cure and Acok (1986) stated that in case of doubling CO_2 concentration in the atmosphere, the leaf area tends to increase, while transpiration tends to decrease by about 23% as a direct consequence of water stress. In that case, water efficiency is improved, and that results in a lower crop water needs that tends to be an advantage during dry periods (Samarkoon and Gifford, 1995).

Evapotranspiration concept

Evapotranspiration (ET) is the combination of two processes, evaporation and transpiration. Water is converted from liquid to gas simultaneously from several surfaces and open water bodies such as soil, wet vegetation, rivers, oceans, seas, and lakes by evaporation (E), and from plant tissues by transpiration (T) (Allen et al., 1998). Air temperature, wind speed, solar radiation, as well as relative humidity are the key factors in the transfer of water vapor to the atmosphere.

The energy necessary to change the state of water molecules from liquid to vapor from the abovementioned surfaces in the evaporation process is provided by the sun. The process is a direct function of the temperature and an inverse function of the air humidity. The sun is the driving force also in the transpiration process. Stomata control the loss of water from leaves. The process is influenced not only by the climatological

parameters involved in direct evaporation but also by the crop, the environment, and plant management.

The two processes are simultaneous but the percentage of water lost by each is different, and varies during the growing season. Taking into account the leaf area index (LAI) development in the growing season, at sowing the 100% of water lost is determined by evaporation, while for a well developed crop, where canopy covers a high percentage of soil, nearly the 90% of water losses are due to transpiration (Figure 12) (Allen et al., 1998).

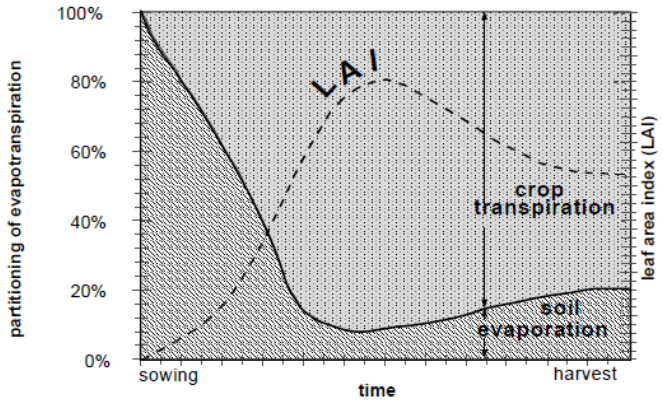

Fig. 12. Evaporation and transpiration ratio during the crop growing season (Allen et al., 1998).

The evapotranspiration values are usually referred to the depth of water lost in a time period through both evaporation and transpiration processes. ET is expressed in millimetres (mm) per unit of time. The ET data can be reported annually (mm yr^{-1}), montly (mm $month^{-1}$), daily (mm day^{-1}), hourly (mm h^{-1}), or seasonally (mm $season^{-1}$). Evapotranspiration is expressed also in terms of millimeters of water lost per unit of area or considering the amount of energy per unit of area (Table 4) (Allen et al., 1998).

Tab. 4. Conversion factors and units used to express evapotranspiration. Values are referred to a temperature of 20 °C and to a water density of 1000 kg m^{-3} (Allen et al., 1998).

	Depth	**Volume per unit area**		**Energy per unit area**
	mm day^{-1}	**m^3 ha^{-1} day^{-1}**	**L s^{-1} ha^{-1}**	**MJ m^{-2} day^{-1}**
1 mm day^{-1}	1	10	0.116	2.45
1 m^3 ha^{-1} day^{-1}	0.1	1	0.012	0.245
1 l s^{-1} ha^{-1}	8.640	86.40	1	21.17
1 MJ m^{-2} day^{-1}	0.408	4.082	0.047	1

When the process of evapotranspiration is referred to a hypothetical well watered crop, which covers entirely the soil, with a uniform height of 12 cm, an albedo of 0.23, and a surface resistance fixed to 70 s m^{-1}, it is named *reference evapotranspiration (ETo)* (Allen et al., 1998).

Thus ETo refers to the evaporative request of the atmosphere for an hypothetical crop independent by crop features, stage of growth, and management. The water lost is referred to a reference surface, that can be used to make comparison of ET measured from other surfaces, at different places or at different time scales. Reference evapotranspiration is only affected by meteorological variables; for this reason it is calculated using weather data without regard to crop and soil features (Figure 13) (Allen et al., 1998).

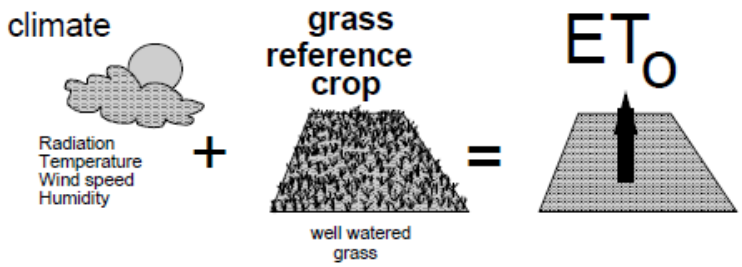

Fig. 13. Reference evapotranspiration (ETo) conceptual scheme (Allen et al., 1998).

Solar radiation, wind speed, relative humidity and air temperature are the weather variables which mainly have an impact on evapotranspiration.

Hot temperature, low humidity, strong wind, and sunny days result in higher values of crop water requirements than values achieved in sites characterized by cool temperature, high humidity, little wind, and cloudy sky (http://www.fao.org/docrep/x0490e/x0490e04.htm).

ETo is related to *crop evapotranspiration (ETc)* (eq.1) through a crop coefficient (*Kc*) obtained by the ratio between ETo and ETc.

$$ETc = ETo * Kc \qquad \text{(mm)} \quad \text{eq. 1}$$

ETc refers to the total water amount used by a specific crop to grow up in standard conditions, that is to say a crop well-watered and fertilized, free from disease, grown in a large field (Allen et al., 1998).

The crop coefficient depends on the considered crop, the stage in the growing season, the crop physiology, the soil humidity, the absorbed light, as well as the plant age, morphology and ecophysiology. Since Kc is the ratio between ETc and ETo, it can be used to "adjust" the differences between the evapotranspiration of a specific and the reference crop. Kc values during the crop growing season are determined through the crop coefficient curve that is characterized by a different shape that is typical for each crop. In well-watered condition, the ET process mostly depend on the energy needed to vaporize water both from the soil and the canopy, thus the solar radiation plays a key role in the daily process. Considering the components of ET separately, i.e. E and T, in field or row crops, higher values of evaporation are measured before the sowing/budbreak, and after harvest/leaf fall. In this condition, the soil is bare and mostly exposed to the sunlight. Only the 10% of the canopy covers the ground since this period represents the first step of the growing season (stage AB, Figure 14).

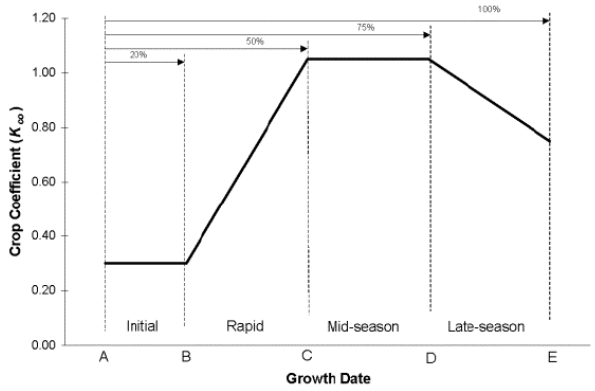

Fig. 14. Example of pattern of crop coefficient during the growing season of annual crops (Snyder et al., 2007).

The transpiration values increase depending on the crop growth; the process is dominant during the midseason (stage CD, Figure 14) when the solar radiation is mostly intercepted by the canopy, with only a small reaching the soil. The ratio of evaporation to ET increases again when the crop is near to the senescence.

The different growth stages during the growing season are different in deciduous plants and vine crops, where the initial growth stage is omitted (Figure 15) (Snyder et al.,

2007), and the midseason starts with canopy covering 70% of soil. The growing season begins rapidly at the budbreak, and it ends when transpiration is equal to zero, i.e. when leaf drop (Snyder et al., 2005).

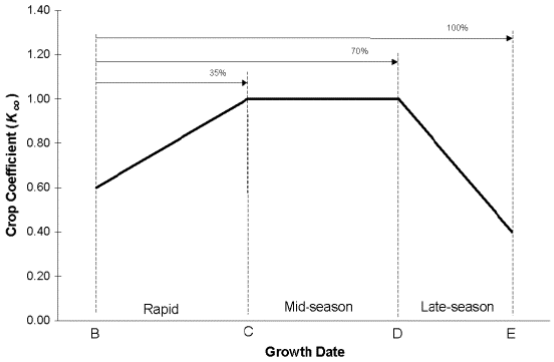

Fig. 15. Crop growing season of deciduous plants and grape (Snyder et al., 2007).

Since during initial growing period and off-season the evaporation process is dominant, rather than transpiration, the crop coefficient for bare soil should be computed to estimate water lost through ET. Crop coefficient for bare soil during these periods is a function of the reference evapotranspiration and soil wetness (Snyder et al., 2005).

Crops do not always grows under standard or optimal conditions. Most of the time in fact they are affected by disease, limited water resources, and low soil fertility. Under these conditions, crop yield and quality decrease. The evapotranspiration of a crop under no-standard conditions is called *Actual Evapotranspiration (ETa)* (Figure 16). It refers to an adjusted crop evapotranspiration (ETc adj) computed taking into account a stress coefficient (Ks).

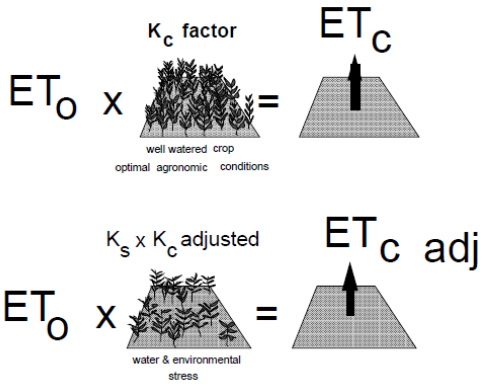

Fig. 16. Crop and actual evapotranspiration under standard and no-standard growing conditions conceptual scheme (Allen et al., 1998).

ETa is calculated multiplying the ETc by a Ks (Allen et al., 1998) (eq.2).

$$ETa = ETc * Ks \qquad \text{(mm)} \quad \text{eq. 2}$$

The amount of water lost through the evapotranspiration process should be replenished to guarantee a well-watered condition for an optimal crop growth. The water necessary to refill the losses due to evapotranspiration is named "Crop Water Requirement" (CWR) (Allen et al., 1998).

Evapotranspiration, and thus crop water requirements are influenced by several environmental, crop, weather, and management factors. Crop diseases, chemical and physicals soil properties can reduce crop growth and consequently the evapotranspiration. The amount of water lost by the crop depends also on the variety, the cultivar, the ground cover, the rooting depth, the canopy height and roughness.

The depth of water applied to refill the soil up to the field capacity is named *Net water Application* (NA). In addition, differences in frequency and intensity of irrigation as well as the irrigation system, should be taken into account to assess the process, and to define strategies to reduce water losses (Allen et al., 1998).

Methods to compute reference and actual evapotranspiration

Reference evapotranspiration calculation

In the past years, three different approaches were followed to estimate ETo: radiation model, temperature model, and or the combination of different models (Jacobs, 2001) (Table 5).

Many equations were developed to compute ETo, and many changes were done in the past to develop the best procedure. Most of the equations proposed were strictly related to the specific climatic condition where they were developed (Allen et al., 1998).

In 1990, the Expert Consulation stated that "the FAO Penman-Monteith is recommended as the sole standard method for the definition and computation of the reference evapotranspiration" (http://www.fao.org/docrep/x0490e/x0490e06.htm).

The FAO Penman-Monteith method is considered the most precise equation, because it is based on a detailed theoretical base (Buttafuoco et al, 2010). It requires detailed climate data such as air temperature, relative humidity, net radiation, and wind speed as

well as other crop parameters. A simpler method is the Hargreaves Samani equation (Buttafuoco et al., 2010), which requests only data on extra-terrestrial solar radiation, maximum and minimum temperature (Samani, 2000). A brief description of these two equations is reported below.

Tab. 5. Different approaches to compute Reference evapotranspiration (ETo) (Jacobs., 2001).

Abbreviation	Approach	Source and Description
McCloud	Temperature	IFAS golf course and turf publications
Thornthwaite	Temperature	Thornthwaite and Mather (1957)
MBC	Temperature	Modified Blaney-Criddle
SFWMD	Temperature	Modified Blaney-Criddle with SFWMD crop coefficients
MMBC	Radiation	SFWMD Modified-Modified Blaney-Criddle (Shih, 1981)
Harg	Radiation	1985, Hargreaves (Hargreaves et al., 1985)
Turc	Radiation	1961, (Turc, 1961)
Pen48	Combination	1948 Original Version of Penman (Penman, 1948)
Pen63	Combination	1963 Version of Penman (Penman, 1963)
Pen77	Combination	FAO24 Modified Penman (Doorenbos and Pruitt, 1977)
IFAS Pen	Combination	IFAS Florida Modified Penman (Jones et al, 1984)
ASCE PM-90	Combination	ASCE-Penman Monteith, Jensen et al. (1990) w/Rn56, G56, r_a & r_s = F(ht) , λ=F(T)
Pen, FAO	Combination	ASCE-PM w/ht = 0.12 m , r_s = 70 s/m and albedo = 0.23 , R_n 56, G = 0 , λ = 2.45 MJ kg^{-1} (Allen et al., 1998)
ASCE00	Combination	ASCE-PM, r_a = f(ht) , albedo=0.23 , daily Et_0 r_s = 70 s/m , hourly Et_0 r_s = 50 & 200 s m^{-1} , daily Et_r r_s = 45 s m^{-1} hourly Et_r r_s = 30 s/m & 200 s m^{-1} (Walter et al., 2000)

Standardized reference evapotranspiration for short canopies

Based on the FAO-56 Penman-Monteith equation, the daily standardized reference evapotranspiration rates for short canopies (ETos) is calculated using daily data of solar net radiation (MJ m^2), minimum and maximum relative humidity (%), wind speed (m s^{-1}), and minimum and maximum air temperature (°C) (Allen et al., 1998; Allen et al., 2005) (eq. 3). The equation is calculated considering either relative humidity or dew point temperature (°C).

$$ET_0 = \frac{0.408\Delta(R_n - G) + \gamma\left(\frac{900}{T+273}\right)u_2(e_s - e_a)}{\Delta + \gamma\left(1 + \frac{rc}{ra}\right)} \qquad \text{(mm)} \quad \text{eq. 3}$$

where Δ is the slope of the saturation vapour pressure-temperature at the mean air temperature curve (kPa °C^{-1}), *Rn* is the net radiation measured or calculated at the crop surface (MJ m^2 d^{-1}), *T* is the mean daily air temperature (°C) calculated by the minimum and maximum daily temperature, u_2 is the mean wind speed measured at 2 m height (m s^{-1}), *G* is the ground heat flux density measured at the soil surface (MJ m^2 d^{-1}), *es* is computed as the mean of saturation vapor pressure at the maximum and minimum air temperature, and it is the saturation vapor pressure at 1.5 to 2.5 m height (kPa), *ea* is the mean actual vapor pressure at 1.5 to 2.5 m height (kPa), γ is the psychometric costant, *rc* and *ra* are the surface and aerodynamic resistance (m s^{-1}), respectively.

The elevation of the site is basic to calculate the mean atmospheric pressure (P) following the Universal Gas Law, as:

$$P = 101.3\left(\frac{293 - 0.0065z}{293}\right)^{5.26} \qquad \text{(kPa)} \quad \text{eq. 4}$$

where *P* is the mean atmospheric pressure at the station elevation "*z*" above mean sea level (m).

The *Psycometric Costant* (γ) is calculated as:

$$\gamma = \frac{c_p P}{\varepsilon\lambda} = 0.665x10^{-3}P \qquad \text{(kPa °C}^{-1}\text{)} \quad \text{eq. 5}$$

where *P* is the mean atmospheric pressure at the station elevation "z", λ is the latent heat of vaporization, c_p the specific heat measured considering a constant pressure, and ε is the ratio between molecular weight of vapor and dry air (Allen et al., 1998).

According to Allen et al. (1998, 2005) the slope of Saturation Vapor Pressure curve (Δ) is computed as:

$$\Delta = \frac{4098[0.6108\ exp\left(\frac{17.27T}{T+237.3}\right)]}{(T+237.3)^2} \qquad \text{(kPa °C}^{-1}\text{)} \quad \text{eq. 6}$$

where Δ is the slope of saturation vapor pressure curve and T is the daily mean air temperature (°C).

The saturation Vapor Pressure Deficit equation is:

$$VPD = es - ea \qquad \text{(kPa)} \qquad \text{eq. 7}$$

where *es* is the saturation vapor pressure and *ea* the actual vapor pressure

The capacity of the air to hold water is named as Saturation Vapor Pressure (es), and it is calculated as:

$$e_s = \frac{e^0(T_{max}) + e^0(T_{min})}{2} \qquad \text{(kPa)} \quad \text{eq. 8}$$

where e^0 is the saturation vapor pressure function:

$$e^0(T) = 0.6108exp\left(\frac{17.27T}{T+237.3}\right) \qquad \text{(kPa)} \quad \text{eq. 9}$$

The actual vapor pressure at the dew point temperature (*ea*), can be computed following several equations. The choice of the method to calculated ea depends on the available data. When dew point temperature (*Tdew*) values are available, the equation to compute *ea* is:

$$e_a = e^0(T_{dew}) = 0.6108exp\left[\frac{17.27T_{dew}}{T_{dew}+237.3}\right] \qquad \text{(kPa)} \quad \text{eq. 10}$$

The Tdew is a measure of the atmospheric moisture. It represents the temperature to which the air is saturated with water vapor. Higher dew point temperature means more moisture in the atmosphere. When minimum and maximum air temperature, and relative humidity are known, ea is calculated following the equation:

$$e_a = \frac{e^0(T_{min})\frac{RH_{max}}{100} + e^0(T_{max})\frac{RH_{min}}{100}}{2} \qquad \text{(kPa) eq. 11}$$

where e^0 (Tmin) is the saturation vapor pressure (kPa) at daily minimum temperature, e^0 (Tmax) is the saturation vapor pressure at daily maximum temperature (kPa), RH_{max} is the daily maximum relative humidity (%), and RH_{min} is the daily minimum relative humidity (%). Most of the time both daily maximum and minimum relative humidity values are not available. In this case, ea is calculated with mean relative humidity as:

$$e_a = \frac{RH_{mean}}{100} e^0(T_{mean}) \qquad \text{(kPa) eq. 12}$$

where RH_{mean} is the mean daily relative humidity and T_{mean} is the mean daily air temperature.

The net radiation (Rn) is the difference between both the longwave and shortwave radiation at the crop surface. It is the total amount of energy available for the Earth system. It is calculated as:

$$R_n = R_{ns} - R_{nl} \qquad \text{(MJ m}^{-2}\text{ d}^{-1}\text{) eq. 13}$$

where Rns is the net shortwave radiation, and Rnl is the longwave radiation. Rns is considered to be positive downwards and negative upwards, while Rnl is defined with reversed signs. Net radiation values are mostly positive or equal to zero, and negative at higher latitudes during winter time.

The net short wave radiation (Rns) is calculated as:

$$R_{ns} = R_s - \alpha R_s = (1 - \alpha) R_s \qquad \text{(MJ m}^{-2}\text{ d}^{-1}\text{) eq. 14}$$

where α is the albedo and Rs is the incoming solar radiation. Albedo, which represents the canopy reflection coefficient, is fixed at 0.23 referring to standardized short and tall canopies.

The net long wave radiation (Rnl) is computed as:

$$R_{nl} = \sigma f_{cd}\left(0.34 - 0.14\sqrt{e_a}\right)\left[\frac{T_{K\,max}^4 + T_{K\,min}^4}{2}\right] \qquad (\text{MJ m}^{-2}\,\text{d}^{-1}) \quad \text{eq. 15}$$

Where σ is the Stefan-Boltzmann constant equal to 4.901 x 10-9, f_{cd} is the function of the cloudiness whose values are limited to 0.05<=f_{cd}>=1.0, *ea* is the actual vapor pressure (kPa), $T_{k\,min}$ and $T_{k\,max}$ are the minimum and maximum absolute temperature respectively during the 24h period (K).

The soil heat flux density (G_{day}) is equal to zero when a daily time step is considered (Allen at al., 1998).

$$G_{day} = 0 \qquad (\text{MJ m}^{-2}\,\text{d}^{-1}) \quad \text{eq. 16}$$

The aerodynamic resistance (*ra*) is basic to define the movement of vapor and heat from the surface to the atmosphere. Its computation for the reference crop (0.12 cm tall) is:

$$r_a = \frac{\ln\left[\frac{Z_m - d}{Z_{om}}\right]\ln\left[\frac{Z_h - d}{Z_{oh}}\right]}{\text{K}^2\ \text{u}_z} = \frac{In\left[\frac{2-2/3(0.12)}{0.123(0.12)}\right] In\left[\frac{2-2/3(0.12)}{(0.1)0.123(0.12)}\right]}{(0.41)^2 u_2} = \frac{208}{u_2} \qquad (\text{m s}^{-1}) \quad \text{eq. 17}$$

where Z_m and Z_h are the height of the wind and humidity measurements (m, usually 2 m), respectively, *d* is the zero plane displacement height (m), Z_{om} and Z_{oh} are the roughness length governing momentum or heat and vapor transfer, respectively. *K* is the constant of von Karman, and u_z is the wind speed at the *z* height m (Allen et al., 1998).

The canopy resistance is the ratio between the bulk stomata resistance (*rc*) expressed as s m^{-1} and the active Leaf Area Index (*LAI*) expressed as meter of leaf area per meter of soil area:

$$active\ LAI = 0.5 * LAI \qquad \text{eq. 18}$$

Thus the canopy resistance is computed following the equation:

$$rc = \frac{rs}{0.5 * LAI} \qquad (\text{s m}^{-1}) \quad \text{eq. 19}$$

Hargreaves - Samani equation

The Hargreaves-Samani equation (HS) is an alternative method for the calculation of reference evapotranspiration (Hargreaves and Samani 1985). Since the most difficult variables to collect are wind speed, relative humidity, and net radiation (de Sousa Lima et al., 2013), HS equation can be used to estimate reference evapotranspiration using only the daily minimum (Tmin) and maximum air temperature (Tmax), and the extraterrestrial radiation (Ra) (eq. 20).

The strength of this equation is that it does not require a local calibration. The applicability of this equation was tested making comparison with several other equation methods in Australia, Bangladesh, Haiti, and the United States in order to state its accuracy to calculate evapotranspiration (Hargreaves and Samani 1985).

$$ET_{0,harg} = \alpha R_a (T_{max} - T_{min})^{0.5} \left(\frac{T_{max}+T_{min}}{2} + 17.78\right) \qquad \text{(mm) eq. 20}$$

where *Ra* is expressed in MJ m^{-2} d^{-1}, T_{max} and T_{min} are in °C, while α is a constant equal to 0.0023.

Actual evapotranspiration calculation

The amount of water lost by the process of evapotranspiration by a surface can be measured through direct methods such as soil water balance, lysimeter, energy balance, and micrometeorological method. The use of direct methods is often limited due to the equipment cost and the difficulty of measuring data directly in the field. Despite their expensive application and management, they are widely use in the field of scientific research. They are often used to validate models.

The pan evaporimeter, the standardized reference evapotranspiration equation, the Hargreaves-Samani equation and some other approaches are considered indirect methods. They are based on the computation of crop and actual evapotranspiration (ETc) from reference evapotranspiration (ETo) values.

Indirect methods

Crop evapotranspiration (ETc) is expressed as the product of reference evapotranspiration (ETo) and crop coefficient (Kc) (see eq. 1). The effect of water

deficit on crop evapotranspiration is defined by a stress coefficient (Ks) which allows to calculate the actual evapotranspiration (ETa) (see eq. 2).

- *Pan evaporation method*

In addition to the standardized PM and HS equations, the pan evaporimeter is widely used to estimate ETo. The integrated effect of weather parameter on water evaporation from a specific open water surface is measured by a pan. The water depth measured in the pan in a day without rain is equal to the evaporated water. The amount of water evaporated by the pan is strictly dependent on the pedo-climatic conditions and the surrounding crop (Figure 17).

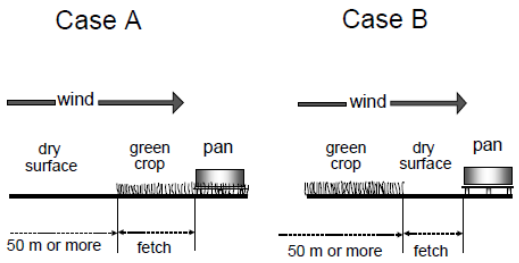

Fig. 17. Different pan positions: on the grass (Case A) and on the bare soil (Case B) (Doorenbos and Pruitt., 1977).

The equation applied to compute ETo through the pan evaporimeter (eq. 21) takes into account a pan coefficient which depends on the site, the climatic factors, the size and the pan type (Maidment, 1992).

$$ETo = Kp * Epan \qquad \text{(mm)} \quad \text{eq. 21}$$

where *ETo* is the reference evapotranspiration expressed in mm d^{-1}, *Kp* is the pan coefficient, and *Epan* is the amount of water evaporated by the pan expressed in mm d^{-1} (Doorenbos and Pruitt, 1977).

Direct methods

- *Soil water balance*

Water is added externally to the soil system through rainfall and irrigation, and part of it is lost by percolation and runoff. The root zone as well as the water table can be recharged not only by percolation but also by the water which rises through *capillary* action (Figure 18).

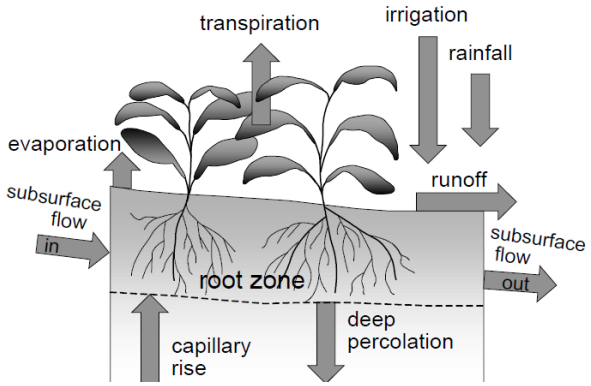

Fig. 18. Soil water balance components (Allen et al., 1998).

Crop evapotranspiration is one of the main soil water balance components and it can be calculated through equation 22:

$$ETc = I + P - R_o - DP + CR \pm \Delta SF \pm \Delta SW \qquad (mm) \quad eq.\ 22$$

where I is the irrigation, P the precipitation, R_o the surface runoff, DP the deep percolation, CR the capillarity rise, ΔSF the subsurface flow in or out of the root zone, and ΔSW the soil water content.

The method is based on the estimation of water inflow and outflow into root zone in a period of time. Since ΔSF, CR, and DP are difficult to compute, they are not considered for short period of time (Allen et al., 1998).

- *Lysimeter*

Lysimeters are tanks used to isolate soil and vegetation in order to measure the amount of evapotranspiration under natural conditions (Figure 19).

The equipment is characterized by a drainage system which allows to measure the water volume drained at the bottom. Lysimeters should contain an undisturbed soil, the same or at least the most similar crops cultivated outside it, and a reduced oasis effect (Jensen et al., 1990).

Fig. 19. Lysimeter just installed in a field (Source: http://hydropedologie.agrobiologie.cz/en-lyzimetr.html).

Evapotranspiration is defined by measuring the change of mass through weighing lysimeters and drainage water through non-weighing lysimeters (Allen et al., 1998).
ETc is measured through the continuity equation:

$$ETc = P-Q-\Delta V \quad (mm) \quad \text{eq. 23}$$

where P is the water applied or the rain (incoming water), Q is the drained water (outcoming water), and ΔV is the change of soil water content.
Since they are quite expensive, their use is limited.

- *Energy balance method*

The energy budget is the estimative balance of the energy emanated by the sun and absorbed or reflected from the Earth, so the net radiation (Rn) is the main source of energy for the ecosystem.
Energy fluxes direction within the system are defined by sign. Positive values of Rn means that the surface is acquiring energy while positive values of all the other components mean that they are removing energy from the surface (Castellvì et al., 2008) (Figure 20).

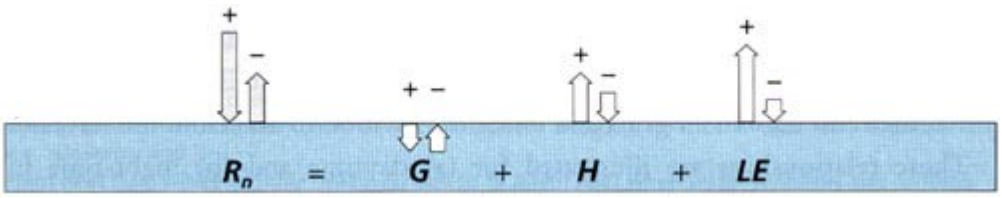

Fig. 20 Energy balance equation and signs of its components (http://www.fao.org/docrep/008/y7223e/y7223e09.htm).

The direct measurement of crop evapotranspiration can be obtained according to the first law of thermodynamics through the equation:

$$Rn - H - LE - G - M = 0 \qquad \text{eq. 24}$$

where *Rn* is the net radiation, *H* is the sensible heat flux, *LE* is the latent heat flux, *M* is the metabolic term, and *G* is the ground heat soil flux. All fluxes are noted in W m^{-2}, and they are converted at daily scale through the factor of 0.0864 in MJ m^{-2} d^{-1}. Referring to a cropped surface and atmosphere, G values is considered equal to zero at daily scale, and M can be ignored because its negligible consumption of energy (Castellvì et al., 2008).

Though the energy balance equation, the latent heat flux (LE) which represents the evapotranspiration fraction of the total energy, can be derived,. LE is the combination between two components: the amount of energy necessary to vaporize a unit mass of water (L), and the mass which goes through a square meter surface in a unit of time (E). When LE is characterized by a downward flux (i.e. it is removed from the air) the sign is negative, and reverse (Snyder and Paulo de Melo-Abreu, 2005).

- *Micrometeorological methods*

Micrometeorological techniques are based on the energy balance equation. One of the most used to directly quantify crop evapotranspiration is the Eddy Covariance (EC) technique.

The Eddy Covariance technique is widely known and common used because it provides direct and accurate measurements of fluxes exchanged within the complex atmosphere-surface system.

The movement upward and downward of the air is the most responsible of the transport of water vapor, momentum and heat from and to the cropped surface. The transport of mass and energy is carried out by very small air parcel named "eddies" (Allen et al., 1998). The EC technique measure and compute the vertical movements through samples of turbulent fluxes used to determine the difference of the mass transferred in the canopy-atmosphere system (Baldocchi, 2003).

The measurements made at one point represent an averaged ensemble of the exchanges, with a length scale of 100 m to 2 km.

The scalar flux is equal to the covariance between the vertical wind velocity and scalar concentration fluctuations:

$$F = \overline{W'C'} \qquad \text{eq. 25}$$

where *c* is the gas concentration, the temperature or the humidity, and *w* is the vertical wind speed. The prime indicates the fluctuation of an instantaneous value (*w)* from the average ($\overline{w}$) and the overbar the time average as shown in the equation below.

$$W' = W - \overline{W} \qquad \text{eq. 26}$$

The flux is directed upward when F>0 and downward when F<0 (Baldocchi et al., 1988).

According to Rosenberg et al. (1983) and Verma (1990), the EC method allows to estimate the latent heat flux following the equation 27:

$$LE = L\overline{w'q'} \qquad (\text{W m}^{-2}) \quad \text{eq. 27}$$

where *w* is the vertical wind speed, *q* the absolute humidity, and *L* is the latent heat of vaporization.

Negative flux density represents energy and mass which moves from the atmosphere to the surface, and positive the reverse. The instrumentation used in this technique (Figure 21) is composed by a three-dimensional sonic anemometer to measure wind speed and direction, and a gas analyzer to measure scalar concentrations (https://fluxnet.ornl.gov/methodology).

Fig. 21. Eddy Covariance station established in a vineyard to measure turbulent fluxes.

REFERENCES

Allen, R.G., Pereira, L. S., Raes, D., & Smith, M., 1998. Crop evapotranspiration: Guidelines for computing crop requirements. Irrigation and Drainage Paper No. 56, FAO 56, 300, https://doi.org/10.1016/j.eja.2010.12.001.

Allen, R.G., Walter, I.A., Elliott, R.L., Howell, T.A., Itenfisu, D., Jensen, M.E., Snyder, R.L., 2005. The ASCE Standardized Reference Evapotranspiration Equation. American Society of Civil Engeneers, Reston, VA.

Baldocchi, D.D., Hincks, B.B., Meyers, T.P., 1988. Measuring biosphere-atmosphere exchanges of biologically related gases with micrometeorological methods. Ecology 69, No. 5.

Baldocchi, D.D., 2003. Assessing the eddy covariance technique for evaluating carbon dioxide exchange rates of ecosystems: past, present and future. Global Change Biology 9 (4), 479–492, https://doi.org/10.1046/j.1365-2486.2003.00629.x.

Bernacchi, C.J., Calfapietra, C., Davey, P. A., Wittig, V. E., Scarascia-Mugnozza, G. E., Raines, C. A., Long, S.P., 2003. Photosynthesis and stomatal conductance responses of poplars to free-air CO_2 enrichment (PopFACE) during the first growth cycle and immediately following coppice. New Phytologist 159, 609–621.

Bernacchi, C.J., Kimball, B.A., Quarles, D.R., Long, S.P., Ort, D.R., 2007. Decreases in Stomatal Conductance of Soybean under Open-Air Elevation of [CO_2] Are Closely Coupled with Decreases in Ecosystem Evapotranspiration. Plant Physiology vol. 143, No. 1, 134-144. American Society of Plant Biologists.

Buttafuoco, G., Caloiero, T., Coscarelli, R., 2010. Spatial uncertainty assessment in modelling reference evapotranspiration at regional scale. Hydrology and Earth System Sciences 14 (11), 2319–2327, https://doi.org/10.5194/hess-14-2319-2010.

Castellví, F., Snyder, R.L., Baldocchi, D.D., 2008. Surface energy-balance closure over rangeland grass using the eddy covariance method and surface renewal analysis.

Agricultural and Forest Meteorology 148 (6–7), 1147–1160, https://doi.org/10.1016/j.agrformet.2008.02.012.

Christensen, J.H., B. Hewitson, A. Busuioc, A. Chen, X. Gao, I. Held, R. Jones, R.K. Kolli, W.-T. Kwon, R. Laprise, V. Magaña Rueda, L. Mearns, C.G. Menéndez, J. Räisänen, A. Rinke, A. Sarr and P. Whetton, 2007. Regional Climate Projections. In: Climate Change 2007: The Physical Science Basis. Contribution of Working Group I to the Fourth Assessment Report of the Intergovernmental Panel on Climate Change [Solomon, S., D. Qin, M. Manning, Z. Chen, M. Marquis, K.B. Averyt, M. Tignor and H.L. Miller (eds.)]. Cambridge University Press, Cambridge, United Kingdom and New York, NY, USA.

Clarke, L., Edmonds, J., Jacoby, H., Pitcher, H., Reilly, J., Richels, R., 2007. Scenarios of Greenhouse Gas Emissions and Atmospheric Concentrations. Sub-report 2.1A of Synthesis and Assessment Product 2.1 by the U.S. Climate Change Science Program and the Subcommittee on Global Change Research. Department of Energy, Office of Biological & Environmental Research, Washington, DC., USA, 154.

Cocucci, M., 2006. Ruolo dell'acqua nella fisiologia della pianta: aspetti termodinamici e cinetici. Italian Journal of agronomy 3, 609-615.

Collins, M., Knutti, R., Arblaster, J., Dufresne, J.-L., Fichefet, T., Friedlingstein, P., Gao, X., Gutowski, W.J., Johns, T., Krinner, G., Shongwe, M., Tebaldi, C., Weaver A.J., Wehner,M., 2013. Long-term Climate Change: Projections, Commitments and Irreversibility. In: Climate Change 2013: The Physical Science Basis. Contribution of Working Group I to the Fifth Assessment Report of the Intergovernmental Panel on Climate Change [Stocker, T.F., D. Qin, G.-K. Plattner, M. Tignor, S.K. Allen, J. Boschung, A. Nauels, Y. Xia, V. Bex and P.M. Midgley (eds.)]. Cambridge University Press, Cambridge, United Kingdom and New York, NY, USA.

Cure, J. D., Acock, B., 1986. Crop responses to carbon dioxide doubling: a literature survey. Agricultural and Forest Meteorology 38, 127-145.

de Sousa Lima, J., Antonino, A., Souza, E., Hammecker, C., Montenegro, S., Lira, C., 2013. Calibration of Hargreaves-Samani equation for estimating reference evapotranspiration in the sub-humid region of Brazil. Journal of Water Resource and Protection 5, 12A.

Doorenbos, J., Pruitt, W.O., 1977. Guidelines for predicting crop water requirements. FAO Irrigation and Drainage Paper 24, 144.

EEA, 2009. Water resources across Europe — confronting water scarcity and drought. EEA Report No 2/2009. European Environment Agency, Copenhagen, Denmark.

EEA, 2015. The European environment: state and outlook 2015. European Environment Agency, Copenhagen, Denmark.

EEA, 2017. Climate change, impacts and vulnerability in Europe 2016. EEA Report No 1/2017. European Environment Agency, Copenhagen, Denmark.

Fujino, J., Nair, R., Kainuma, M., Masui, T., Matsuoka, Y., 2006. Multi-gas mitigation analysis on stabilization scenarios using AIM global model. The Energy Journal 3 (Special Issue #3), 343-354.

Giorgi, F., 2008. Regionalization of climate change information for impact assessment and adaptation. WMO Bulletin 57 (2) – April 2008, 86 – 92. Retrieved April 15th, 2014, https://www.wmo.int/pages/publications/bulletin_en/archive/57_2_en/documents/giorgi_sub _en.pdf.

Graham, S., Parkinson, C., Chahine, M., 2010. The Water Cycle. Nasa earth observatory. http://earthobservatory.nasa.gov/Features/Water/.

Hargreaves, G.L., Hargreaves, G.H., Riley, J.P., 1985. Agricultural benefits for Senegal River Basin. Journal of Irrigation and Drainage Engineering, ASCE 111 (2), 113-124.

Hargreaves, G.H., & Samani, Z.A., 1985. Reference crop evapotranspiration from temperature. Applied Engineering in Agriculture 1 (2), 96–99, https://doi.org/10.13031/2013.26773.

Hartmann, D.L., A.M.G. Klein Tank, M. Rusticucci, L.V. Alexander, S. Brönnimann, Y. Charabi, F.J. Dentener, E.J. Dlugokencky, D.R. Easterling, A. Kaplan, B.J. Soden, P.W. Thorne, M. Wild and P.M. Zhai, 2013: Observations: Atmosphere and Surface. In: Climate Change 2013: The Physical Science Basis. Contribution of Working Group I to the Fifth Assessment Report of the Intergovernmental Panel on Climate Change [Stocker, T.F., D. Qin, G.-K. Plattner, M. Tignor, S.K. Allen, J. Boschung, A. Nauels, Y. Xia, V. Bex and P.M. Midgley (eds.)]. Cambridge University Press, Cambridge, United Kingdom and New York, NY, USA.

Held, I., Vecchi, G., 2008. Will the wet get wetter and the dry drier?. The National Oceanic and Atmospheric Administration (NOAA) Geophysical Fluid Dynamics Laboratory (GFDL) - Princeton, NJ. 1, No. 5.

Hijioka, Y., Matsuoka, Y., Nishimoto, H., Masui, M., Kainuma, M., 2008. Global GHG emissions scenarios under GHG concentration stabilization targets. Journal of Global Environmental Engineering 13, 97-108.

IPCC, 2007. Fourth IPCC Assessment Report (AR4): Climate Change 2007. Cambridge University Press.

IPCC, 2013. Summary for Policymakers. In: Climate Change 2013: The Physical Science Basis. Contribution of Working Group I to the Fifth Assessment Report of the Intergovernmental Panel on Climate Change Stocker, T.F., D. Qin, G.-K. Plattner, M. Tignor, S. K. Allen, J. Boschung, A. Nauels, Y. Xia, V. Bex and P.M. Midgley. Cambridge University Press, Cambridge, United Kingdom and New York, NY, USA.

IPCC, 2014. Summary for Policymakers. In: Climate Change 2014: Mitigation of Climate Change. Contribution of Working Group III to the Fifth Assessment Report of the Intergovernmental Panel on Climate Change Edenhofer, O., R. Pichs-

Madruga, Y. Sokona, E. Farahani, S. Kadner, K. Seyboth, A. Adler, I. Baum, S. Brunner, P. Eickemeier, B. Kriemann, J. Savolainen, S. Schlömer, C. von Stechow, T. Zwickel and J.C. Minx. Cambridge University Press, Cambridge, United Kingdom and New York, NY, USA.

ISPRA, 2016. Gli indicatori del clima in italia nel 2015. Stato dell'Ambiente 65/2016. Desiato, F., Fioravanti, G., Fraschetti, P., Perconti, W., Piervitali, E., Pavan, V. ISPRA Settore Editoria, ISBN978-88-448-0779-5.

Jacobs, J.M., 2001. Evaluation of Reference Evapotranspiration Methodologies. Water Resources Management, 24 April, 2311–2337, https://doi.org/10.1007/s11269-009-9553-8.

Jensen, M.E., Burman, R.D., Allen, R.G., 1990. Evapotranspiration and Irrigation Water Requirements. American Society of Civil Engineers. Manuals and reports on engineering practice No. 70, 360, ISBN 0-87262-763-2.

Jones, J.W., Allen, L.H., Shih, S.F., Rogers, J.S., Hammond, L.C., Smajstrla, A.G., Martsolf, J.D., 1984. Estimated and measured evapotranspiration for Florida climate, crops and soils. Bulletin 840 (Tech.), IFAS, University of Florida, Gainesville, FL.

Lüthi, D., Le Floch, M., Bereiter, B., Blunier, T., Barnola, J-M., Siegenthaler, U., Raynaud, D., Jouzel, J., Fischer, H., Kawamura, K., Stocker, T.F., 2008. High-resolution carbon dioxide concentration record 650,000–800,000 years before present. Nature 453, 379-382, doi:10.1038/nature06949.

Maidment, D.R., 1992. Handbook of hydrology. McGraw-Hill Inc., New York, USA, ISBN: 0070397325.

OECD, 2006. Report on the OECD Workshop on agriculture and water: Sustainability, markets and policies. Adelaide, Australia, 14.-18. November 2005, COM/AGR/CA/ENV/EPOC/RD(2005)71.

Patterson, D.T., Flint, E.P., Beyers, J.L., 1984. Effects of CO_2 Enrichment on Competition between a C4 Weed and a C3 Crop. Weed Science 32, No. 1, 101-105.

Penman, H.L., 1948. Natural Evaporation from open water, bare soil and grass. Proceedings of the Royal Society, Series A. 193, 120-145.

Penman, H.L., 1963. Vegetation and Hydrology. Tech. Comm. No. 53, Commonwealth Bureau of Soils, Harpenden, England, 125 pp.

Rao, S., Riahi, K., 2006. The role of non-CO_2 greenhouse gases in climate change mitigation: long-term scenarios for the 21st century. The Energy Journal 27 (3),177-200.

Randall, D.A., Wood, R.A., Bony, S., Colman, R., Fichefet, T., Fyfe, J., Kattsov, V., Pitman, A., Shukla, J., Srinivasan, J., Stouffer, R.J., Sumi, A., Taylor, K.E., 2007. Cilmate Models and Their Evaluation. In: Climate Change 2007: The Physical Science Basis. Contribution of Working Group I to the Fourth Assessment Report of the Intergovernmental Panel on Climate Change [Solomon, S., D. Qin, M. Manning, Z. Chen, M. Marquis, K.B. Averyt, M.Tignor and H.L. Miller (eds.)]. Cambridge University Press, Cambridge, United Kingdom and New York, NY, USA.

Rascio, N., Carfagna, S., Esposito, S., La Rocca, N., Lo Gullo, M.A., Trost, P., Vona,V. 2012. Elementi di Fisiologia Vegetale, EdiSES, Napoli.

Riahi, K., Grübler, A., Nakicenovic, N., 2007. Scenarios of long-term socioeconomic and environmental development under climate stabilization. Technological Forecasting and Social Change 74 (7), 887-935.

Rosenberg, N.J., Blad, B.L., Verma, B.S., 1983. Microclimate. The biological environment. John Wiley & Sons, New York-Chichester-Brisbane-Toronto-Singapore.

Samani, Z., 2000. Estimating Solar Radiation and Evapotranspiration Using Minimum Climatological Data (Hargreaves-Samani equation). Journal of Irrigation and Drainage Engineering 126 (4), doi: 10.1061/(ASCE)0733-9437(2000)126:4(265).

Samarkoon, A.B., Gifford, R.M., 1995. Soil water content under plants at high CO_2 concentration and interactions with the direct CO_2 effects, a species comparison. Journal of Biogeography 22, 193-202.

Shih, S.F., Allen, L.H., Jr., Hammond, L.C., Jones, J.W., Rogers, J.S., Smajstrala, A.G., 1981. Comparison of Methods of Evapotranspiration Estimates, American Society of Agricultural Engineers Summer meeting, Orlando June 21-24 1981, Paper No. 81-2015.

Smith, S.J., Wigley, T.M.L., 2006. Multi-gas forcing stabilization with MiniCAM. The Energy Journal 3 (Special Issue #3), 373-392.

Snyder, R.L., De Melo-Abreu, J.P., 2005. Frost Protection: fundamentals, practice and economics. Food and Agriculture Organization of the United Nations. Rome. pp. 223, ISBN 92-5-105328-6.

Snyder, R.L., Orang, M., Geng, S., Matyac, S., Sarreshteh, S., 2005. SIMETAW (Simulation of Evapotranspiration of Applied Water) Simulation of Evapotranspiration of Applied Water, 211–226.

Snyder, R.L., Orang, M., Matyac, S., Eching, S., 2007. Crop Coefficients. Copyright - Regents Of The University Of California.

Snyder, R.L., Moratiel, R., Song, Z., Swelam, A., Jomaa, I., Shapland, T., 2011. Evapotranspiration response to climate change. Acta Horticulturae, doi:10.17660/ActaHortic.2011.922.11.

Streck, N. A., 2005. Climate change and agroecosystems: the effect of elevated atmospheric CO_2 and temperature on crop growth, development and yield. Ciencia Rural 35 (3), 730-740.

Taiz, L., Zeiger, E., 2008. Fisiologia Vegetale, Piccin, Padova.

Thornthwaite, C.W., Mather, J.R., 1957. Instruction and Tables for Computing Potential Evapotranspiration and the Water Balance. Drexel Institute of Technology, Laboratory of Climatology, Publications in Climatology 10 (3), 311.

Trenberth, K.E., Smith, L., Qian, T., Dai, A., Fasullo, J., 2006. Estimates of the Global Water Budget and Its Annual Cycle Using Observational and Model Data. Journal of hydrometeorology, special section 8, doi:10.1175/JHM600.1.

Turc, L., 1961. Evaluation des besoins en eau d'irrigation, Èvapotranspiration potentielle, formulation simplifiè et mise à jour. Annales agronomiques 12, 13-49.

van Vuuren, D.P., Eickhout, B., Lucas, P.L., den Elzen, M.G.J., 2006. Long-term multi-gas scenarios to stabilise radiative forcing − Exploring costs and benefits within an integrated assessment framework. The Energy Journal 27, 201-233.

van Vuuren, D.P., den Elzen, M.G.J., Lucas, P.L., Eickhout, B., Strengers, B.J., van Ruijven, B., Wonink, S., van Houdt, R., 2007. Stabilizing greenhouse gas concentrations at low levels: an assessment of reduction strategies and costs. Climatic Change 81 (2), 119-159.

van Vuuren, D.P., Edmonds, J., Kainuma, M., Riahi, K., Thomson, A., Hibbard, K., Hurtt, G.C., Kram, T., Krey, V., Lamarque, J.F., Masui, T., Meinshausen, M., Nakicenovic, N., Smith, S.J., Rose, S.K., 2011. The representative concentration pathways: an overview. Climatic Change 109, 5–31. Springer, doi:10.1007/s10584-011-0148-z.

Verma, S.B., 1990. Micrometeorological methods for measuring surface fluxes. Remote Sensing Reviews 5, 99–115.

Walter, I.A. R.G. Allen, R. Elliott, B. Mecham, M.E. Jensen, D. Itenfisu, T.A. Howell, R. Snyder, P. Brown, S. Echings, T. Spofford, M. Hattendorf, R.H. Cuenca, J.L. Right, D. Martin. 2000. ASCE Standardized Reference Evapotranspiration Equation.pages 209-215 in Evans, R.G., B.L. Benham, and T.P. Trooien (ed.) Proceedings of the National Irrigation Symposium, ASAE, Nov. 14-16, 2000, Phoenix, AZ.

Wise, M., Calvin, K., Thomson, A., Clarke, L., Bond-Lamberty, B., Sands, R., Smith, S. J., Janetos, A., Edmonds, J., 2009. Implications of limiting CO_2 concentrations for land use and energy. Science 324, 1183-1186.

Websites

http://www.slideshare.net/GRFDavos/bonn-lr

www.riscaldamentoglobale.it

http://sedac.ipcc-data.org/ddc/ar5_scenario_process/RCPs.html

http://www.fao.org/nr/water/aquastat/tables/WorldData-Withdrawal_eng.pdf

http://ec.europa.eu/eurostat/statistics-explained/index.php/Agri-environmental_indicator_-_water_abstraction

http://www.fao.org/nr/water/aquastat/data/query/index.html?lang=en

http://www.fao.org/nr/water/aquastat/maps/WithA.WithT_eng.pdf

http://www.fao.org/nr/water/aquastat/maps/EqIrr_eng.pdf

http://www.fao.org/docrep/x0490e/x0490e04.htm

http://www.fao.org/docrep/x0490e/x0490e06.htm

http://hydropedologie.agrobiologie.cz/en-lyzimetr.html

http://www.fao.org/docrep/008/y7223e/y7223e09.htm

https://fluxnet.ornl.gov/methodology

OBJECTIVE

Climate change will have an impact on the hydrological cycle, thus on the availability of water resource for sectors, particularly for agriculture (Bates et al., 2008). The change in climatic parameters will affect crop evapotranspiration with a great influence on water applications, and this will be more evident in Mediterranean regions where water scarcity is expected to be more severe (IPCC, 2013).

It is widely known that more efforts are needed to improve and identify strategies target to a sustainable agriculture in Mediterranean Countries. The knowledge of crop water consumption is surely one of the most important step to reduce water losses and to better schedule irrigation events. In this contest, in recent years, several models have been developed to investigate crop water consumption at local and regional scale (Brisson et al., 2003; Jones et al., 2003; Stockle et al., 2003; Raes et al., 2012), but only a few of them allow to also estimate irrigation requirements. In addition, only a few models have been applied at Mediterranean basin scale (Braud et al., 2013; Saadi et al., 2014; Fader et al., 2015) to compute water application. Most of them have been applied in other Continents or at global scale (Gosain et al., 2005; Santhi et al., 2005; Siebert et al., 2010; Zheng et al., 2010).

This work was carried out to improve the knowledge related to climate change impact on crop evapotranspiration and net irrigation water demand in Euro-Mediterranean Countries. In this context, the Simulation of Evapotranspiration of Applied Water (SIMETAW_R) model was selected, improved and converted in a R programming language, to study the impact of climate change on three economically relevant crops, such as grape, maize, and wheat, both at local and regional scale.

Three specific objectives were identified in this work:

1. the improvement and the evaluation of SIMETAW_R model performance in estimating crop evapotranspiration and irrigation demand at local scale
2. the development of SIMETAW_GIS platform as a tool to assess the impact of climate change on crop consumption and water application at regional scale
3. the assessment of the vulnerability of Euro-Mediterranean irrigated agriculture under climate change conditions

The improvement and the evaluation of SIMETAW_R model was done by pursuing the following achievements: (i) the evaluation of the Hargreaves Samani (HS) and Penman Monteith (PM) equations to estimate reference evapotranspiration (ETo) in order to identify the one to be used for the calculation of crop water requirements; (ii) the estimation of crop and actual evapotranspiration, and irrigation demand for maize, grape, and wheat at local scale; and (iii) the evaluation of the model performance over different pedo-climatic conditions through the validation of modeled results with *in situ* measurements.

The development of the SIMETAW_GIS platform required a further comparison of the modeled variables used to estimate ETo using both the HS and PM equations with site measurements. This allowed to evaluate the performance of the two equations in estimating ETo also at regional scale. The final objective of this part was then the estimation of crop water consumption and water application for maize, grape, and wheat at regional scale, for both past and future climate.

Finally, the assessment of the Euro-Mediterranean vulnerability of irrigated agriculture under climate change conditions was pursued by following two more objectives: (i) the identification of most vulnerable reservoirs under drought conditions due to global warming in the Euro-Mediterranean area; and (ii) the assessment of climate change impact on both irrigation requirements and changes in water inflow to reservoirs granting irrigation supplies for the main crops (maize, wheat, and grape, also vegetables) over the domain.

PART 1. The SIMETAW_R model: evaluation of model performance in estimating crop evapotranspiration and irrigation requirements at local scale

1.1 INTRODUCTION

Nowadays the sustainable management of available water is the base of the territorial resource planning programs, and becomes crucial in the agricultural sector.

Although agriculture is considered one of the sectors which mainly contributes to water consumption, its products are fundamental to ensure the supply of food, to reduce poverty, and to stimulate the rural socio-economic development.

The important role of agriculture in food production increases the need to find strategies target to save water affecting as less as possible crop yield. In order to answering to this need, knowledge on crop water requirement is basic. Since crop growth is strictly related to the local pedo-climatic conditions, the estimation of reference, crop and actual evapotranspiration is the first step in crop water management.

Crop water consumption is related to reference evapotranspiration by a specific crop coefficient (ETc). Since crop growth is influenced by the actual field conditions, such as the water availability, the soil depth, as well as the crop management, a stress coefficient is considered in order to assess the actual crop water consumption (ETa). Several works applied the reference evapotranspiration using the FAO Penman-Monteith methodology (Kotsopoulos et al., 2003; Rana et al., 2012; Longobardi and Villani 2013; Mancosu et al., 2015) and the Hargreaves Samani equation in European experimental site (Najafi and Asgari 2008; Mancosu et al., 2013; Sheikh and Mohammadi 2013; Campi et al., 2014; Mancosu et al., 2014; Khandelwal and Dhiman, 2015) to assess crop water requirements.

Taking into account the large areas irrigated in Euro-Mediterranean regions, the ongoing climate change and its projected influence, the introduction of models in agricultural sector becomes fundamental to simulate crop yield and water needs in

different water conditions. This may help farmers, politicians, as well as decision makers in developing crop management strategies target to find the right balance between economy and environment.

Crop yield can be simulated by crop models. The first crop model was developed in the Netherlands in 1965 by de Wit. Later, some other models have been studied, and a few of them are reported in Table 6.

Hydrological models such as CROPWAT (Smith, 1991), SWAP (Kroes and van Dam, 2003), HYDRUS-1D (Simunek et al., 2009), SIMETAW# (Mancosu et al., 2015), CRITERIA (Marletto and Zinoni, 1998; Marletto et al., 2005), and BUDGET (Raes., 2002) are used by the scientific community to estimate reference and crop evapotranspiration, and to simulate irrigation scheduling to plan a sustainable management of the water resource. The soil water balance in the crop root zone is considered a necessary information to develop water planning also by Feddes et al. (1974), Rowse et al. (1983), Camp et al. (1988), Foroud et al. (1992), and George et al. (2000).

Tab. 6. List of crop models used to developed management sustainable strategies.

Name	Acronym	Literature
Decision Support System for Agrotechology Tranfer	DSSAT	Jones et al., 2003
Cropping System Simulation model	CropSyst	Stockle et al., 2003
Crop Estimation through Resource and Environment Synthesis	CERES	Ritchie and Otter, 1985 Jones and Kiniry, 1986
Interdisciplinary simulator for standard crop	STICS	Brisson et al., 2003
Erosion Productivity Impact Calculator	EPIC	Williams et al., 1984
FAO cropwater productivity model to simulate yield response to water	AquaCrop	Raes et al., 2012

This chapter aims to select and improve a tool able to estimate crop water consumption and irrigation requirement for economically relevant crops, per each crop growth stage, and under different pedo-climatic characteristics. SIMETAW model was used to develop this research because it not only computes the crop water requirement but it is able also to estimate the total amount of water necessary to satisfy crop needs. Based on a daily soil water balance it allows to plan the timing and the number of irrigation events under different pedoclimatic and management conditions. The original SIMETAW# model (Snyder et al. 2004; Snyder et al., 2012; Mancosu et al., 2015) was improved in R programming language and applied in 10 European sites.

In addition, since many studies stated that the application of the standardized reference evapotranspiration equation for short canopies (ETo_PM) (Allen et al., 2005a) is not always easy, due to the specific input data required (Allen et al., 1998; Allen et al. 2005a; Popova et al., 2006; Todorovic et al., 2013; Pereira et al., 2015), the simulation of daily reference evapotranspiration using Hargreaves Samani equation (ETo_HS) (Hargreaves and Samani, 1985) was also performed in each site, in order to identify the one more accurate with the available input, that was then selected to be used for the estimation of ETc, and ETa.

1.2 MATERIALS AND METHODS

1.2.1 SWOT analysis

A SWOT analysis was performed in order to better define the SIMETAW_R model strengths, weaknesses, opportunities, and treats (Figure 22). This analysis allowed to select it as the flexbile tool needed for the further work carried out.

SIMETAW_R could be used as an instrument to better manage water resource in agriculture, thus to develop water use sustainable strategies. These opportunities are emphasized by the model strengths. It is in fact able to compute reference evapotranspiration by applying both Hargreaves Samani and standardized Penman Monteith equation. In addition, it allows the estimation of crop and actual evapotranspiration. The crop coefficients are related to the percentage of the growing season. Kc can be modified during the midseason as a function of local climate. A

modified Kc in case of vineyard or deciduos trees is also allowed. The model estimates a daily soil water balance in case of deficit, rainfed, and full irrigation. Moreover, it allows to schedule irrigation, and specifically the number of events and the net water amount to apply per each. In order to make SIMETAW_R easier to stakeholders, more efforts are needed to develop a comprehensible interface.

Strengths	***Weaknesses***
• It allows to work at local scale • It calculates the potential evapotranspiration (ETo) using the equation of Penman-Monteith (PM) and Hargreaves-Samani (HS) • It includes the CO_2 concentration in the calculation of ETo • It allows to modify the crop coefficient (Kc) of the midseason as a function of the local climate • It allows to modify the Kc in case of deciduous trees or vineyards • It relates the Kc to the percentage of the growing season • It computes a daily soil water balance • It computes the number of irrigation events • It computes the water net application per event • It computes the evapotranspiration of applied water (ETaw) • It allows to choose the irrigation method • It calculates the water balance in case of non-uniform irrigation • It estimates the water balance in rain-fed, deficit and full irrigation • It takes into account a stress coefficient, which is used to compute ETa • It considers Kc from by the FAO 24 (Doorenbos and Pruitt, 1977), FAO 56 (Allen et al., 1998), and several more recent papers	• It does not consider soil salinity • It requires many inputs • It does not have an easy and quickly comprehensible interface
Opportunities	***Threats***
• It allows to better manage water resources • It is useful as an instrument of service to society (institutions, farmers, hobbyists, etc.) • It is useful as a tool for raising awareness on climate change	• Difficulties in the involvement of stakeholders for using it • Difficulties in dealing with conservative mentality

Fig. 22. SWOT analysis.

1.2.2 SIMETAW_R model

The Simulation of Evapotranspiration of Applied Water (SIMETAW_R) model is the improved version of SIMETAW# model developed by the University of California, Davis, and the California Department of Water Resources (Snyder et al., 2004, Snyder et al., 2012) and recently modified by Mancosu et al. (2015). In this work, the original model was re-written using "R" statistics language, the most widely used statistical software, and called SIMETAW_R.

R is a programming language and environment for graphics and statistical computing. The model was converted in R language to provide users with an open source program, available for different operating systems (Microsoft Windows, Macintosh, and Linux on both 32 and 64 bit processors) and easily modificable. R does not have any license restriction, thus it is possible to use it everywhere. It is composed by around 4800 packages divided in main topics, a large collections of graphical facilities, tool for analysis, functions, and operators that can be easily used. It can be considered as an interactive software thanks to an active group which replies to questions and gives support (http://analyticstrainings.com/?p=101). Although at the beginning R was mostly based on other program languages such as C and Fortran, nowadays the most common programming languages (Java, C++, and Python) are strictly connected with it.

SIMETAW_R is a user friendly daily soil water balance program developed to compute the reference evapotranspiration (ETo), the crop evapotranspiration (ETc), and the actual evapotranspiration (ETa), as well as the evapotranspiration of applied water (ETaw). The model estimates the amount of water required by irrigated crops (CWR), schedules the number of irrigation events, and the amount of water applied per each event (NA) (Mancosu et al., 2015).

The availability of climate, crop, soil, and management data is basic to run simulations with SIMETAW_R model. Daily weather data such as maximum and minimum temperature (°C), wind speed (m s^{-1}), solar radiation (MJ m^{-2} d^{-1}), dew point temperature (°C) or relative humidity (%), and precipitation (mm) are used to compute ETo. The crop water requirement (CWR) of a specific crop in a specific area, is estimated including in the model the crop planting and harvesting date, the presence of cover crops, the soil water holding capacity, the maximum rooting depth, the maximum soil

depth, the percentage of full area planted, and the water allocation. Information on rain-fed or irrigated conditions, irrigation system and distribution uniformity should be also included into the model (Snyder et al., 2004; Snyder et al., 2012; Mancosu et al., 2015).

1.2.2.1 Main equations used to estimate crop water consumption and irrigation demand

Reference evapotranspiration is estimated by the SIMETAW_R model following the standardized reference evapotranspiration equation for short canopies (ETo_PM) (Allen et al., 1998; Allen et al., 2005a; Allen et al., 2006) and the Hargreaves-Samani (ETo_HS) (Hargreaves and Samani, 1985) as reported in equations 3 and 20, respectively. ETo_PM is used as an input to estimate ETc and ETa following the equations 1 and 2, respectively.

SIMETAW_R model takes into account the effect of increasing CO_2 concentration in the atmosphere in ETo_PM, precisely in the stomatal conductance equation (eq. 28). The equation 28 revised by Snyder et al. (2011) was applied in this study allowing the calculation of crop water requirement for future periods under climate change scenarios. The revised stomatal conductance equation (gs) is:

$$g_s = 14.18 - 0.0112\ CO_2 \qquad (\text{m s}^{-1}) \quad \text{eq. 28}$$

Stomatal conductance is the rate of passage of CO_2 entering or water vapor coming out through the stomata (Taiz and Zeiger, 2008). Consequently, the stomata resistance (*rs*), i.e. the mean resistance of a single leaf, is computed as:

$$rs = \frac{1}{gs} \qquad (\text{m s}^{-1}) \quad \text{eq. 29}$$

It depends on the specific crop and the step of the growing season. It is usually a direct function of the age of the plant. The revised canopy resistance equation (*rc*) is:

$$\mathrm{r_c} = \frac{1000}{1.44(14.18 - 0.0112\ \mathrm{CO_2})} \qquad (\text{m s}^{-1}) \quad \text{eq. 30}$$

Since the Kc is known to depend on the local climate (Doorenbos and Pruitt, 1977, Allen et al., 2005b), SIMETAW_R model modifies the equation as:

$$K_{Cmid} = K_{ctab} + 0.261(ET_0 - 7.3)(K_{Ctab} - 1) \qquad \text{eq. 31}$$

where K_{Ctab} is the tabular Kc value that is possible to calculate in a climate where reference evapotranspiration value is similar to 7.3 mm day^{-1} (Guerra et al., 2014), and Kc_{mid} is the adjusted crop coefficient.

The effect of immature deciduous plants and vine crops on crop coefficient is accounted for in the model through the percentage of soil covered by the canopy:

$$If \sin\left(\frac{C_g}{70}\frac{\pi}{2}\right) \geq 1.0 \; then \; K_c = K_{cm} \; else \; K_c = K_{cm}\left[\sin\left(\frac{C_g}{70}\frac{\pi}{2}\right)\right] \qquad \text{eq. 32}$$

where *Cg* is the percentage of soil shaded by the crop. If cover crops are present, a value of 0.35 is added to the crop coefficient. The Kc can not be lower than 0.90 and higher than 1.15. In SIMETAW_R model it is possible to include the presence of cover crops during the crop growth; specifically a maximum of two different cover crop growing season can be included.

The crop tabular coefficient of immature subtropical orchards is also modified (eq. 33) (Snyder et al., 2005).

$$If \sin\left(\frac{C_g}{70}\frac{\pi}{2}\right) \geq 1.0 \; then \; K_c = K_{cm} \; else \; K_c = K_{cm}\sqrt{\sin\left(\frac{C_g}{70}\frac{\pi}{2}\right)} \qquad \text{eq. 33}$$

Since during the initial crop growth and the off season, evaporation process (E) is dominant on transpiration (T), the crop coefficient for bare soil should be computed in order to estimate water lost through E, during the off-season, and ETc in the first step of the growing season. Stroosnijder (1987) and Snyder et al. (2000) proposed a two stage method to compute the evaporation from the soil surface, which is used to estimate the crop coefficient for bare soil. The computation of the crop coefficient for bare soil is obtained considering the daily reference evapotranspiration and the number of days

between precipitation that are considered significant (precipitation is considered significant when its value is higher than the double value of ETo) (Snyder et al., 2005). In Figure 23 are reported Kc values for nearly bare soil simulated using the original SIMETAW model (solid line) and the defined ones by Doorenbos and Pruitt (1977) (dashed line).

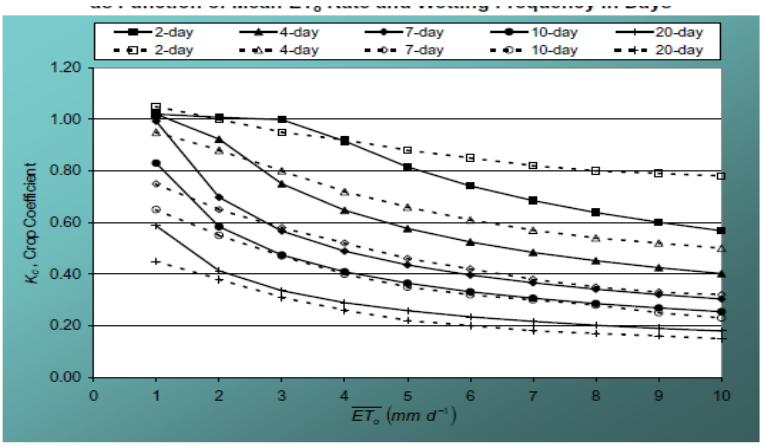

Fig. 23. Daily mean ETo rate and days between wetting used to estimate crop evapotranspiration for bare soil (Snyder et al., 2005).

Since crops are not always cultivated in well-watered conditions, a stress coefficient needs to be accounted. The Ks computation is obtained by considering the soil water depletion (*SWD*), the plant water availability (*PAW*), and the allowable depletion (*AD*):

$$K_s = 1 - \frac{100\left(\frac{SWD}{PAW}\right) - AD}{100 - AD} \qquad \text{eq. 34}$$

Ks assumes values from 0 to 1. Values lower than 1 result in a water stress condition. The AD represents to the amount of available water which corresponds to the yield threshold depletion. AD is usually considered as 50% of the plant available water, and generally plants characterized by small root system have a low allowable depletion value (Snyder et al., 2012).

The Yield Threshold Depletion YTD is the difference between field capacity (FC) and yield threshold (YT), that is to say the amount of water that can be depleted before

incurring in a yield reduction. FC represents the water that remains in the soil after a drainage of 24 hours in a saturated condition, and it is considered as the total amount of water stored in the soil and available for the plant (AW). YT is the amount of water stored in the soil at the threshold, and that influences the yield. The SWD represents the difference in water content below the field capacity. It is calculated adding the SWD of the previous day, the crop evapotranspiration of the current day, the capillary rise, percolation below the root layer, the depth of irrigation and the runoff (eq. 35). When precipitation value is higher than SWD, the latter is equal to the effective rainfall (Re), otherwise, it assumes the same value of the Re, considering that, in this case, Re is equal to precipitation (Mancosu et al., 2015):

$$SWD_i = SWD_{i-1} + ET_{ci} + P_{cpi} + C_i - D_i - R_{offi} + I_i \qquad \text{(mm)} \quad \text{eq. 35}$$

where ET_{ci} is the crop evapotranspiration, P_{cpi} the precipitation, *Ci* and *Di* the capillary and the deep percolation, respectively, R_{offi} the runoff, and I_i the depth of irrigation.

The calculation of a daily soil water depletion (eq. 35) is necessary to define the irrigation events, that occur before than the SWD is higher than the management of allowable depletion (MAD, mm), thus the computation of MAD is basic to define irrigation scheduling.

MAD is the amount of water that can be depleted between water irrigation applications without incurring in water deficit. It can be considered also as the water amount necessary to refill the soil to the field capacity (NA, mm). The model also computes the evapotranspiration of the applied water (ET_{aw}, mm), i.e. the sum of the net irrigation application (NA). The computation of the net application is obtained by multiplying the total amount of water that should be applied in order to supply crop needs, i.e. the gross application (GA, mm), by the percentage of application efficiency (AE, %), i.e. the water entered in the soil during an irrigation event, stored in the root zone, and available for plant. The GA is the total amount of water that is necessary to apply in order to replace water in the root zone to satisfy crop water need. Application Efficiency (AE) depends on the irrigation system, and it takes into account the amount of water lost during the water application. It is considered as the ratio between NA and GA during irrigation (http://www.fao.org/docrep/t7202e/t7202e06.htm).

Since during the initial crop growth season only the 10% of soil is covered by the crop, the crop evaporation is considered equal to the evaporation process, thus NA is computed as:

$$NA_c = \overline{ET}_0 \cdot K_e \cdot d_e \qquad \text{(mm)} \quad \text{eq. 36}$$

where *Ke* is the crop coefficient of the bare and nearly bare soil, the *ETo* represents the mean daily reference evapotranspiration during the stage AB of the growing season, and d_e the number of water application during this time step (Mancosu et al., 2015).
The Ke is computed as:

$$K_e \frac{2.54}{\sqrt{CET_0}} \qquad \text{eq. 37}$$

where the values 2.54 represents the hydraulic factor and *CETo* is the cumulative ETo.
At the beginning of the mid-season NA is computed as:

$$NA_c = \left(1 - R_{off}\right) \cdot RT \cdot AR \cdot D_u \qquad \text{(mm)} \quad \text{eq. 38}$$

where *RT* is the runtime that depends on the irrigation method, *AR* is the application rate (mm h^{-1}), and D_u is the distribution uniformity (%) (Mancosu et al., 2015).
SIMETAW_R allows to plan number and frequency of the irrigation events during the midseason in case of full (WAP = 100%, water allocation percentage) or deficit irrigation (WAP < 100%).
For fully irrigated crops, the number of water applications (N_{ic}) is computed as a ratio between the evapotranspiration of the applied water of a well-watered crop (ET_{awe}) and the management allowable depletion in well watered conditions (MAD_c):

$$N_{ic} = \frac{ET_{awe}}{MAD_c} \qquad \text{(mm)} \quad \text{eq. 39}$$

The number of water application in case of deficit conditions (N_{ia}) is computed considering that the plant irrigation requirement (PIR) is lower than 100%:

$$N_{ia} = \frac{\sum NA_a}{MAD_c} \quad \text{(mm)} \quad \text{eq. 40}$$

where the sum of the irrigation depth to the low quarter of a crop cultivated in stressed conditions ($\sum NAa$) is:

$$\sum NA_a = (WA - \sum R_o) \times D_u \quad \text{(mm)} \quad \text{eq. 41}$$

where *WA* is the water allocation, i.e. the mean amount of water available for irrigation, R_o is the runoff coefficient and D_U the distribution uniformity.
Consequently, the MAD in case of water deficit (MADa) is:

$$MAD_a = \frac{\sum NA_a}{N_{ia}} \quad \text{(mm)} \quad \text{eq. 42}$$

The evapotranspiration of the applied water of a well-water crop (ET_{awe}) is then computed as:

$$ET_{awe} = CET_c - \left(YTD_c - \frac{YTD_{os}}{2}\right) \quad \text{(mm)} \quad \text{eq. 43}$$

where *CETc* is the cumulate value of ETc during the entire growing season, *YTDc* is the yield threshold depletion during the mid-season, and YTD_{os} represents the yield threshold depletion during the off-season (Mancosu et al., 2015).
SIMETAW_R model allows the estimation of ET_{aw} also in non-uniform fields by dividing the field into four quarters. The low quarter application is the mean irrigation applied to the quarter which receives the least amount of water (1° quarter), while the high quarter is the mean depth of water applied to the quarter which receives the largest quantity of water. The second and the third application are the mean depths of water applied to the intermediate quarters (Mancosu et al., 2015).
If WA and Nic are known, the ET_{aw}, i.e. the amount of water necessary to refill the water lost by crop evapotranspiration from the effective soil root area, and not replaced by any other resources, is computed as:

$$ET_{aw} = \sum_{i=1}^{n} NA_{c,i} \quad \text{(mm)} \quad \text{eq. 44}$$

where *n* is the number of net application and ET_{aw} is equal to the mean depth of applied water infiltrated into the low quarter during the growing season.

During stress condition, the WA is lower than the percentage of full irrigation (PIR, %), and the sum of the net application to the low quarter ($\sum NA_a$) (Mancosu eta al., 2015) is computed as:

$$\sum NA_a = \sum GA_c \left(\frac{PIR}{100}\right) = WA \cdot D_u \quad \text{(mm)} \quad \text{eq. 45}$$

In addition, following Allen et al. (1998) it is possible to investigate on the relationship between soil moisture stress and yield by applying the following equation:

$$1 - \frac{Ya}{Ym} = Ky\,(1 - \frac{ETa}{ETc}) \quad \text{eq. 46}$$

where *Ya* is the actual crop yield, *Ym* the maximum crop yield expected, and *Ky* the yield response factor.

1.2.3 Experimental sites

Experimental sites were selected in the framework of the Euro-Mediterranean basin, to evaluate the performance of the SIMETAW_R model in estimating crop water consumption (ETa). Ten experimental sites located at different latitude were selected from the Fluxnet international monitoring network: three in Italy, two in Germany and France, one in Switzeland, Belgium, and in the Netherlands (Figure 24) (Table 7).

The considered crops are maize, wheat, and grape. Evapotranspiration was estimated during the crop growing season. The selection of these crops was related to their relevance from the economical point of view, assessed by the Statistical Office of the European Communities (EUROSTAT), which stated that in 2014 the production of

durum wheat was equal to 7.6 million tons, maize grain produced 84.8 million tons, while grape a total of 26.1 million tons (EUROSTAT, 2014).

Fig. 24. Map of the experimental sites.

Tab. 7. Experimental sites and crop characteristics used for model simulations.

Code	SITE	Country	Latitude	Longitude	Elevation	Year	Crop	Sowing-Harvest date
IT-Neg	Negrisia	Italy	45.75	12.45	11	2007	grape	01.04.2007/15.10.2007
IT-Neg	Negrisia	Italy	45.75	12.45	11	2008	grape	01.04.2008/27.10.2008
IT-VdA	Valle dell'Adige	Italy	46.20	11.11	207	2009	grape	15.04.2009/05.09.2009
IT-BCi	Borgo Cioffi	Italy	40.52	14.96	13	2005	maize	17.05.2005/24.08.2005
IT-BCi	Borgo Cioffi	Italy	40.52	14.96	13	2006	maize	27.04.2006/22.08.2006
IT-BCi	Borgo Cioffi	Italy	40.52	14.96	13	2007	maize	09.05.2007/24.08.2007
IT-BCi	Borgo Cioffi	Italy	40.52	14.96	13	2009	maize	12.06.2009/08.10.2009
DE-Kli	Klingenberg	Germany	50.89	13.52	468	2005-2006	wheat	25.09.2005/06.09.2006
DE-Kli	Klingenberg	Germany	50.89	13.52	469	2007	maize	23.04.2007/2.10.2007
DE-Geb	Gebesee	Germany	51.10	10.91	157	2006-2007	wheat	09.11.2006/07.08.2007
FR-Lam	Lamasquere	France	43.50	1.24	182	2006-07	wheat	18.10.2006/15.07.2007
FR-Lam	Lamasquere	France	43.50	1.24	182	2007	maize	01.05.2006/31.08.2006
FR-Gri	Grignon	France	48.84	1.95	117	2005-2006	wheat	28.10.2005/15.07.2006
FR-Gri	Grignon	France	48.84	1.95	117	2005-2006	maize	05.5.2005/28.09.2005
CH-Oe2	Oensingen	Switzerland	47.29	7.73	450	2006-2007	wheat	19.10.2006/16.07.2007
BE-Lon	Lonzee	Belgium	50.55	4.75	165	2004-2005	wheat	14.10.2004/03.8.2005
BE-Lon	Lonzee	Belgium	50.55	4.75	165	2006-2007	wheat	10.10.2006/05.08.2007
NL-Dij	Dijagraaf	The Netherlands	51.99	5.65	9	2007	maize	05.05.2007/29.09.2007

Eddy Covariance fluxes and climate data of each site were provided by meteorological, radiometric, and micrometeorological stations set up in each selected site.

In addition, a questionnaire was circulated in each site to collect information about crop management, soil and crop characteristic, and irrigation management. The soil details

focused on soil texture and maximum depth. Information on crop type, sowing and harvesting date, maximum rooting depth were also collected, as well as management data concerning applied water, irrigation system, and distribution uniformity. Information were obtained also through a literature review.

Negrisia (IT-Neg)

Negrisia is part of the municipality of Ponte di Piave, Veneto. The soil is silty-clay loam and it is classified by FAO (2008) as a Vertic Eutrudent soil. The fluxes exchanged between vegetation and atmosphere have been measured since 2005. The station is set up in the centre of a 25 hectares vineyard, where the main cultivar is the *Carmenère N.* grafted on SO_4 rootstock, planted in 1992. The number of the wine grapes per hectare is 3.076. The crop is trained in a cordon system, and the canopy reaches its maximum height at 2.70 m. The ground cover on the rows is chemically treated (Papale et al., 2015).

The years considered to test SIMETAW_R model performance are 2007 and 2008. The period under investigation was defined from budbreak to harverst. Since phenological data were not available, the default SIMETAW_R grape growing season from April 1st to October 27th was used in both years. Allen et al. (1998) was followed to determine the maximum and soil rooting depth that were 2 m and 1.5 m, respectively. Plants were wet only occasionally using a gravity system. No information on water amount provided by irrigation were obtained.

Valle dell'Adige (IT-VdA)

Valle dell'Adige is a site located in Trentino-Alto Adige. The soil (Gleyic-Haplic Fluvisol) is composed by silt 47%, clay 11%, and sand 42%. The area (2.5×1 km^2) is mainly a vineyard where the cultivar *Teroldego rotaliano* is cultivated. The canopy is about 2 m high and covers the ground for 50%.

The model test was carried on during the wine grape growing season in 2009, from April 15th (budbreak) to September 5th (harvest).

The maximum rooting depth is 1 m, while the maximum soil depth is 1.5 m. Plants were wet using a gravity method during the summer months. The total amount of water

provided was around 150-200 mm per month, specifically about 400-700 mm per season (from the beginning of June to the middle of August).

Borgo Cioffi (IT-BCi)

The experimental site is located in Salerno, in Campania region, in the Southern Italy. The 16 hectares area is covered by an arable field mainly planted with maize and alfalfa. The texture of the Calcic Kastanozem Skeletic soil is clay to sandy clay (Papale et al., 2015).

Simulations were run for the maize growing season using data collected in the years 2005, 2006, 2007, and 2009. The growing season in 2005 started on May 17th and it finished in August 24th, in 2006 the sowing and the harverst date were anticipated at April 27th and August 22nd, respectively. Data were elaborated from May 9th to August 24th in 2007, and from June 12th to October 8th in 2009. Values of 1.5 and 2 m were considered for the maximum rooting depth and the maximum soil depth, respectively (Allen et al., 1998). The sprinkler method was used for a total amount of water per year of 330 mm in 2005, 300 mm in 2006 (Moors et al., 2010), 396 mm in 2007, and 291 in 2009 (Ranucci et al., 2011).

Klingenberg (DE-Kli)

The Eddy Covariance station was set up in Saxonia, Germany. Slightly sandy-clay and clay-sandy-loam are the textures found in the B horizon of the soil classified by FAO 2008 as a Gleysoil (Kutsch et al., 2010). Data on wheat growing season were provided from September, 25th 2005 to September 6th 2006 (Wattenbach et al., 2010), while maize data were available from April 23rd 2007 to October 2nd 2007. The maximum soil depth is 0.69 m and the maximum rooting depth is defined equal to 1 m. Both crops grew up in rainfed conditions (Moors et al., 2010). The water requirement was equal to 150 kg water per kg of biomass (Wattenbach et al., 2010).

Gebesee (DE-Geb)

Gebesee is an experimental site located in Thuringia, Germany. The soil is a Chernozem one (FAO, 2008) with silty-clay-loam texture (Kutsch et al., 2010). Maximum rooting and soil depth are 1.5 m and 2 m, respectively (FAO, 2008). SIMETAW_R model was

tested for wheat from November 9th 2006 to August 7th 2007. The crop was not irrigated (Moors et al., 2010). The kilograms of water per kilograms of biomass required by the wheat were 150 (Wattenbach et al., 2010).

Lamasquère (FR-Lam)

The agricultural field of Lamasquère is located in Southwestern France. The soil classified by FAO as a Luvisol on Alluvium has a clay-loam texture (Van den Hoof et al., 2010). Maximum rooting and soil depth are 1.5 m and 2 m, respectively (FAO, 2008). Data were processed from October 18th 2006 to July 15th 2007 to test the model performance on wheat (Revill et al., 2013), and from May 5th 2006 to August 31st 2006 on maize.

A static sprinkler was used to irrigate maize for a total amount of 147.8 mm (Béziat et al., 2009; Li et al., 2011). Wheat was cultivated in rainfed condition (Ceschia et al., 2010; Moors et al., 2010).

Grignon (FR-Gri)

The experimental site is located in south-eastern France. FAO 2008 classified the soil as Luvisol with a silt-loam texture (Van den Hoof et al., 2010).

Maize and wheat were investigated in this site. Maize was sowed on May 9th and harvested on September 28th (in 2005), while the wheat growing season began on October 28th 2005 and finished on July 15th 2006. Both crops were not irrigated (Moors et al., 2010).

Oensingen (CH-Oe2)

The study site is located in the canton of Solothurn, in Switzeland. The soil is Eutri-stagnic Cambisol (Hastings et al., 2010) with a silty-clay texture (Kutsch et al., 2010). The model simulated wheat growing season from October 19th 2006 to July 16th 2007. The suggested FAO (2008) values of 1.5 m and 2 m of maximum rooting and soil depth were used, respectively. Wheat was not irrigated (Moors et al., 2010, Hastings et al., 2010).

Lonzee (BE-Lon)

The site is located in Belgium. The soil texture is silty-clay-loam (Van den Hoof et al., 2010), and the soil is classified as a Luvisol (Kutsch et al., 2010). The maximum rooting (1.5 m) and soil depth (2 m) were included in the model as suggested by FAO. Wheat was cultivated from 2004 to 2007. The growing season started on October 14th, 2004 to August 3th, 2005, and on October 13th, 2006 to August 5th, 2007. Wheat was not irrigated during the growing season (Moors et al., 2010).

Dijkgraaf (NL-Dij)

The site is located in the Netherlands. The Haplic Gleysol soil is typical of the site. FAO (2008) values of maximum rooting and soil depth were used. The model performance was tested during maize growing season from May 4th to September 27th, in 2007 (Li et al., 2011). The crop grew up in rainfed conditions (Moors et al., 2010, Li et al., 2011).

1.2.4 Eddy Covariance measurements

The selection of the field with Eddy Covariance stations was done following the Fluxnet international monitoring network. Fluxnet is considered a "network of regional network" involved in five continents with a range of latitude from 70 degree north to 30 degree south, where 650 EC tower operates on. In each station, data are available at a time step of 30-minutes. Different biomes such as temperate, boreal, and tropical forests, as well as wetlands, grasslands, crops, and tundra are represented in the network.

Fluxnet database includes measured fluxes and ancillary data, i.e. information about the site. Data are available to be freely downloaded under three different processing levels, which correspond to different level of quality checks and aggregation performed (https://fluxnet.ornl.gov/). The levels considered in this research were both level three (L3) and level four (L4). In L3 data are provided with a time step of 30 minutes, while in L4 hourly, daily, weekly, and monthly aggregated data are reported. Data in both levels were downloaded and gap-filled following Falge et al. (2001) method.

The variables downloaded from Fluxnet website were:

- carbon dioxide (CO_2) concentration measured at top of the tower (ppm)
- air temperature (Ta, °C)
- net radiation (Rn, W m^{-2})
- wind horizontal speed (WS, m s^{-1})
- precipitation (precip, mm)
- saturation vapor pressure (VPD, kPa)
- latent heat flux (LE, W m^{-2})

Carbon dioxide, air temperature, net radiation, wind speed as well as the latent heat flux were downloaded at the third level, gap filled and processed to daily values. Saturation vapor pressure and precipitation data where directly downloaded at the fourth level, with a daily time step.

The net radiation and the latent heat flux were converted from W m^{-2} to MJ m^{-2} d^{-1} using the conversion factor of 0.0864. Latent heat flux was then converted from MJ m^{-2} d^{-1} to mm d^{-1} using the conversion factor of 0.408 to represent the measured crop water. Days with more than 30% half hour gaps were removed from the LE original database.

1.2.5 Statistical model validation

SIMETAW_R model performance was assessed by comparing actual evapotranspiration simulated by the model and the latent heat flux measured by the Eddy Covariance station at each selected site.

The correlation between observed and modeled data is determined through the Person's coefficient (r, %) and the coefficient of determination (R^2, %). Pearson's coefficient is a well known measure of the magnitude and the direction of the linear or non linear association between variables, and its values range from -1 to +1. The perfect agreement results in a coefficient equal to 1, where all data are on the 1:1 line and increasing values along *x* axis results in increasing values in *y* axis. Negative *r* values denote a negative linear association among variables, thus as *x* value increases while *y* values decreases. Any linear correlation between *x* and *y* exists if the *r* value is 0. The Person's coefficient is calculated as:

$$r = \frac{\sum(x-\bar{x})(y-\bar{y})}{\sqrt{\sum(x-\bar{x})^2 \sum(y-\bar{y})^2}} \qquad \text{eq. 47}$$

where x and y are the two variables under investigation.

The coefficient of determination is computed as the square of Pearson's coefficient. It defines the proportion of the variance of one variable that is explained through the other one. It ranges from 0 to 1.

Root Mean Square Error (RMSE, mm), Mean Absolute Error (MAE, mm), Mean Bias Error (MBE, mm), and the Index of Agreement (IA, %) were also used to assess the SIMETAW_R performance.

The RMSE is widely used to compute the differences between observed and modeled values, thus to assess model accuracy:

$$RMSE = \sqrt{\frac{\sum_{i=1}^{n}(X_{\mathrm{mod}} - X_{obs})^2}{n}} \qquad \text{eq. 48}$$

where X_{obs} is the observed data and X_{mod} the simulated one, and n is the number of the considered values. RMSE depends on the dependent variable. It is used to measure the accuracy of the model with small values resulting in a better model forecast ability.

The MAE depends also on the dependent variable but it is less sensitive to large deviation:

$$MAE = \frac{\sum_{i=1}^{n} | X_{\mathrm{mod}} - X_{obs} |^2}{n} \qquad \text{eq. 49}$$

The MBE is the measure of systematic errors, and is computed as:

$$MBE = \frac{\sum_{i=1}^{n} X_{\mathrm{mod}} - X_{obs}}{n} \quad \text{eq. 50}$$

It gives a measure of the overestimation (positive values) or underestimation (negative values) of the modeled value respect to the observed one.

The IA gives the percentage of the model accuracy:

$$IA = 1 - \frac{\sum_{i=1}^{n}(Xmod - Xobs)^2}{\sum_{i=1}^{n}(|Xmod - \overline{Xobs}| + |Xobs - \overline{Xobs}|)^2} \qquad \text{eq. 51}$$

Higher IA values result in better model performance.
The relationship between simulated actual evapotranspiration (dependent variable) and the observed actual evapotranspiration (independent variable) is explained through the linear regression and it is computed following the equation:

$$y = a + bx \qquad \text{eq. 52}$$

where *a* is the intercept and *b* is the angular coefficient.

1.3 RESULTS

The application of SIMETAW_R model enabled to compute the evapotranspiration of applied water (ETaw) for irrigated crops, that is equal to the sum of the net irrigation applied during the growing season (NA). ETaw is the portion of crop water requirement (CWR) relative to the total amount of water supplied by irrigation without considering other water supply, such as the effective precipitation (Mancosu et al., 2015). The generalized crop coefficient was considered equal to its default value suggested by the FAO 24 (Doorenbos and Pruitt, 1977), FAO 56 (Allen et al., 1998), and many others recent work, from the initial growth to the mid-season, and for all the late season. Crop coefficient values modified during the midseason as a function of the local climate were computed. The trend of the generalized crop coefficient (IKc), crop coefficient (Kc), crop coefficient for the nearly bare soil (Ke, when the percentage of the ground cover is lower than 10%), as well as the stress coefficient (Ks) are shown for each crop. The model performance are reported as the comparison between measured and simulated daily actual evapotranspiration. The simulated ETo values used to show the daily trends

were obtained using the standardized Penman Monteith equation (ETo_PM), which was in turn used as an input to compute ETc and ETa. Statistical indeces were used to evaluate the SIMETAW_R performance and results are reported per each site. In addition, model performance are explained by taking into account the percentage of gap filled observed data and the energy balance closure. The energy budget closure was used to assess measured data reliability, and it is obtained by the assessment of Rn-G and H+LE. The slope of the 1:1 line was computed. Slope values equal to 1 defined the best measurements accurancy. According to Baldocchi et al. (1988) the closure can be considered acceptable if the differences between the perfect and the real conditions are lower than 20-30%.

1.3.1 Klingenberg (DE-Kli)

Meteorological characterization

Climate and fluxes data were elaborated for both wheat and maize growing season, from September 25th, 2005 to September 6th, 2006, and from April 23rd to October 2nd, 2007, respectively.

According to Köppen climate classification, the site is characterized by a warm temperate fully humid with warm summer. Based on measured meteorological values, results that the mean maximum air temperature was 11.13 °C and 18.29 °C, respectively, while the mean minimum temperature was 4.30 °C and 9.42 °C, in both seasons. A peak of temperature of about 32 °C was measured in both years in July. The mean seasonal temperature was higher in 2007 (14.38 °C) than in 2005-2006 (6.38 °C) but the period of investigation was characterized by a different length.

During the two growing seasons, the higher values of precipitation were measured from May to September. Comparing the meteorological summer months (June, July, and August) of both years, the highest cumulative precipitation value was measured in 2007 (310 mm). In 2005-2006, the precipitation for the same period was about 60 mm less, and the drier month was July. The highest Vapour Pressure Deficit (VPD) cumulative value was measured in the 2007 season. The mean VPD value was 0.56 kPa, i.e. 0.10 kPa less than in the 2005-2006 season (Figure 25). Peaks of saturation vapor pressure were measured equal to 1.99 kPa on July 16th 2007 and 2.24 kPa on July 20th 2006.

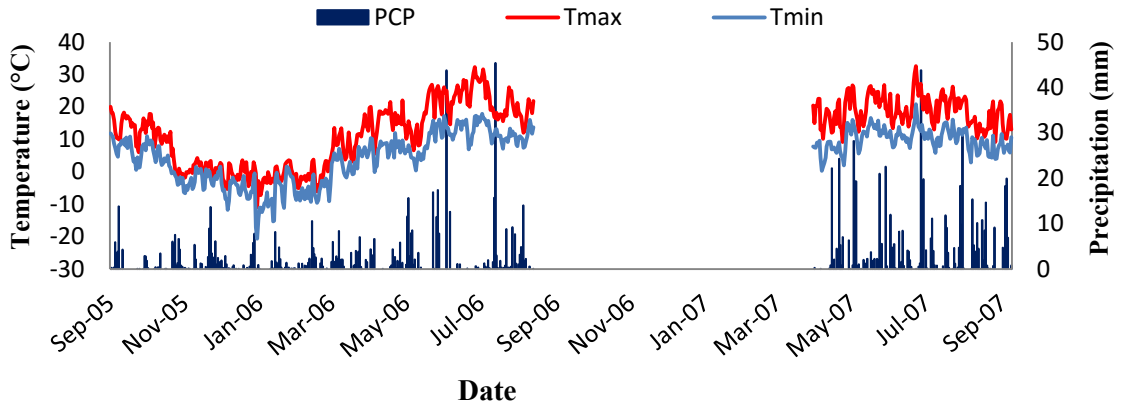

Fig. 25. Trend of daily maximum temperature (Tmax), minimum temperature (Tmin), mean temperature (Tmean), and precipitation (PCP), in Klingenberg, in 2005-2006 and 2007.

The cumulative value of net radiation from June to August was 945.07 MJ m^{-2} in 2005-2006, and 841.71 MJ m^{-2} considering the same period in 2007, while the maximum peak was equal to 14.33 MJ m^{-2} d^{-1} in 2007.

The mean wind speed was about 2 m s^{-1} considering the common months for both seasons. From sowing to harvest, both seasons were characterized by the peaks of minimum and maximum wind speed values around 0.8 and 8 m s^{-1}, respectively.

Reference evapotranspiration

The evaporative demand of the atmosphere (ETo) was computed in this work using both Hargreaves-Samani (ETo_HS) and standardized reference evapotranspiration rates for short canopies (ETo_PM). The cumulative ETo_PM and ETo_HS value were 568 and 461 mm in 2005-2006 season, respectively. ETo_PM and ETo_HS values were lower, 441 mm and 342 mm, respectively, in 2007, and this was due to the different length of the two seasons, (the first from 25-09-2005 to 06-09-2006, and the second one from 23-04-2007 to 2-10-2007). The highest daily ETo value was around 6 mm, and it was computed using ETo_PM. Both equations followed the same trend from around September to the end of May, in 2005-2006 season (Figure 26); higher values of ETo_PM than ETo_HS were measured from June onward, and this difference could be due to the influence of high values of air temperature, net radiation and saturation vapor pressure, as well as a low wind speed measured in that period. The ETo_PM values decreased from the beginning of August in correspondence to lower temperature and saturation vapor pressure. In season 2007, ETo_PM values changed directly

proportional to the VPD, Tmean, and Rn measurements. Values were higher since the first week of August and then they tended to decrease. Maximum peaks of ETo_PM were estimated in July 20th 2006 (6.09 mm) and July 16th 2007 (6.31 mm), in correspondence with the maximum peak of VPD.

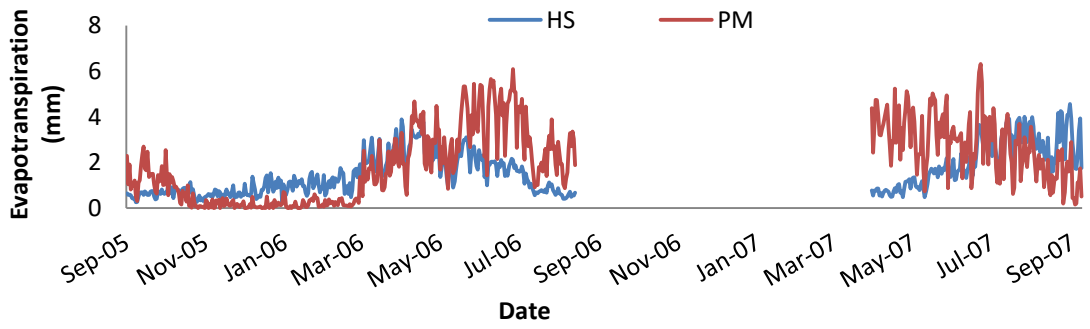

Fig. 26. Trend of daily reference evapotranspiration computed using Hargreaves Samani (ETo_HS) and the standardized reference evapotranspiration equation (ETo_PM), in Klingenberg, in 2005-2006 and 2007.

Model results evaluation

Klingenberg, wheat, 2005-2006

The wheat cultivated at the site during 2005-2006 season was not irrigated, hence water supply came only from precipitation. During the mid-season, Kc values were adjusted depending on the local climate conditions. The mid-season generalized crop coefficient (IKc) computed was 0.05 lower than SIMETAW_R default value (1.05).

The Ke and the Kc values were the same during the first step of the growing season. Ke values were lower than Kc values during the mid-season, when the soil was well covered by plants, and the amount of water evaporated from it was lower. Ks values were lower than 1 in a few days from May to August (Figure 27) when the absence or lower values of precipitation were measured. Since the maximum soil depth is around 700 mm, water deficit conditions are shown by the low Ks coefficient during midseason and late season, specifically from the middle of May to the beginning of August.

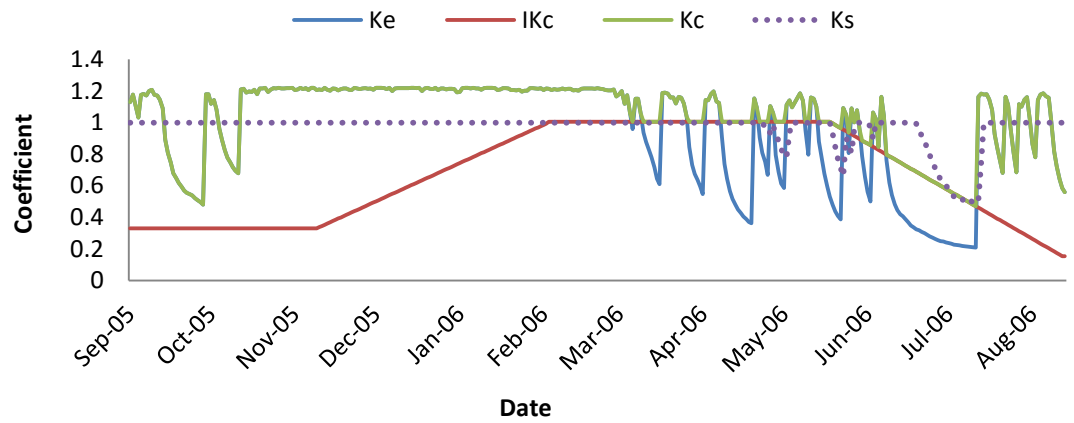

Fig. 27. Daily trend of the crop coefficient for the bare soil (Ke), the generalized crop coefficient (IKc), the crop coefficient (Kc), and the stress coefficient (Ks) during wheat growing season, in Klingenberg 2005-2006.

Since the site was characterized by a cumulative precipitation value of 607 mm, and events were frequent, ETc values were in line with ETa values for almost the entire season (Figure 28).

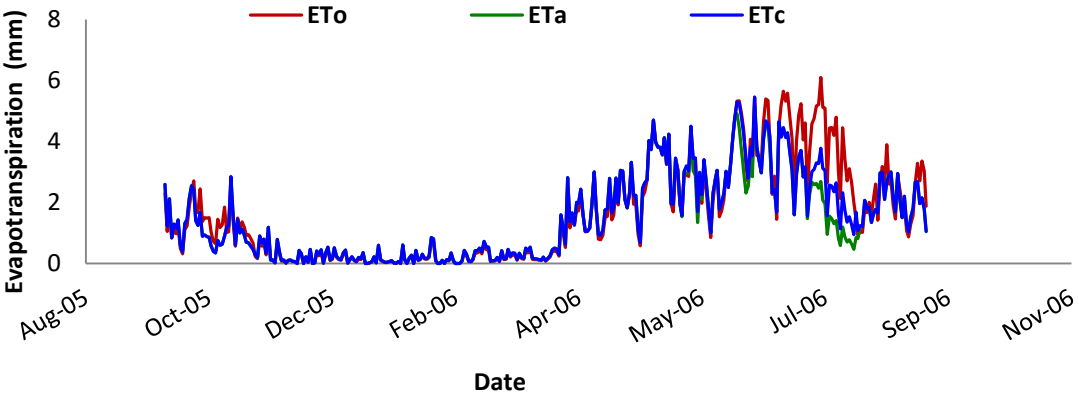

Fig. 28. Daily trend of reference, crop, and actual evapotranspiration (ETo, ETc, and ETa, respectively), in Klingenberg, in 2005-2006.

Differences are shown in the middle of October 2005 and the last two weeks of July 2006, when water deficit conditions (lower values of Ks, Figure 27), due to a reduction in precipitation, led to reduce ETa values.

A general agreement was observed between simulated and observed ETa, in particular from the beginning of the season until March and in July. Although the peak of ETa were both in June, the simulated value (5.2 mm) was 0.40 mm higher than the observed one (Figure 29).

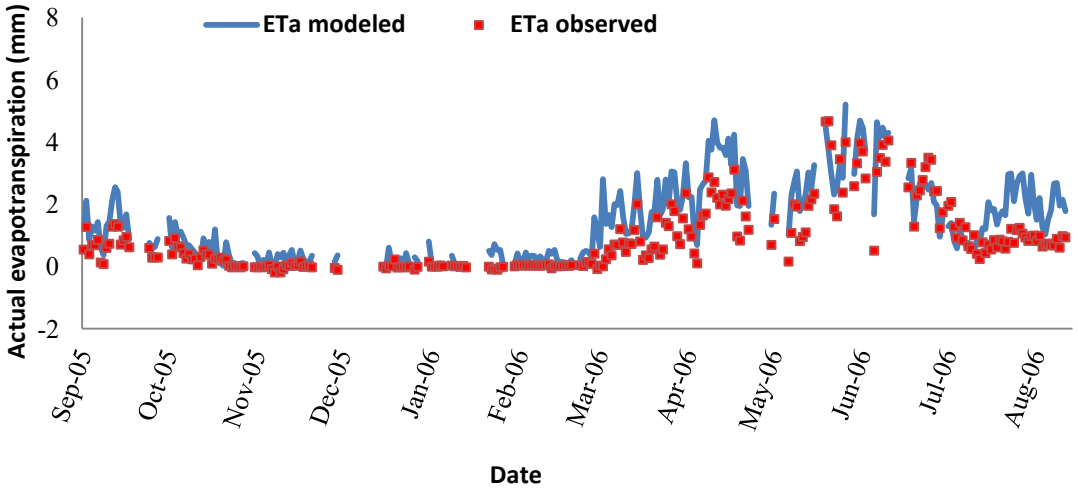

Fig. 29. Daily trend of modeled and observed actual evapotranspiration, in Klingenberg, in 2005-2006.

The good model performance were confirmed by the RMSE, the R^2 and IA values (0.82 mm, 78%, and 88%, respectively) (Table 8). Modeled and measured ETa values were highly correlated. The Pearson's coefficient value was significant for $P \leq 0.001$. In this season in fact the regression line fitted well the data (R^2=78%). In addition, the index of agreement between simulated and observed data was high. The accuracy of the model was explained also by the high value of the slope of the regression line (1.04), and the low value of the intercept (0.52).

Tab. 8. Statistical indices used to assess SIMETAW_R performance, in Klingenberg, in 2005-2006.

SITE	YEAR	CROP	r	RMSE	MBA	MBE	IA	RE	R^2	a	b
				mm	mm	mm	%	%	%		
Klingenberg	05-06	WHEAT	0.88***	0.82	0.65	0.57	88	16.85	78	0.52	1.04

*P ≤ 0.05; **P ≤ 0.01; ***P ≤ 0.001

From March to the end of the season differences could be linked to the percentage of gap filled (Table 9) latent heat flux data (19%), and by the accuracy of LE measurements which could be influenced by the precipitation frequency and intensity observed in that period. The slope of 0.38 and the R^2 of 45% defined the energy budget closure linear regression.

Tab. 9. Percentage of gap filled data in the original dataset, in Klingenberg, in 2005-2006.

SITE	YEAR	CROP	CO_2	Rn	Ta	WS	H	LE	VPD	PCP
			%	%	%	%	%	%	%	%
Klingenberg	05-06	WHEAT	19.47	0.02	0.01	8.41	11.80	19.65	0.00	0.00

Klingenberg, maize, 2007

Maize was sown in Klingenberg in 2007. The crop was not irrigated but thanks to the high frequency of precipitation events, with a total amount of 592 mm, any water deficit was recorded (Ks=1 during the growing period, Figure 30). Considering the local climate, the IKc value computed during the mid-season was 1.01 instead than 1.05, i.e. 0.04 lower than the model default value.

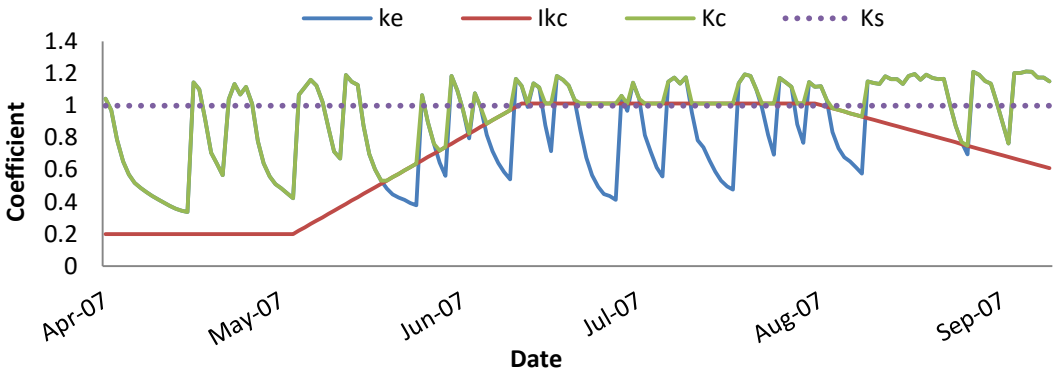

Fig. 30. Daily trend of the crop coefficient for the bare soil (Ke), the generalized crop coefficient (IKc), the crop coefficient (Kc), and the stress coefficient (Ks) during maize growing season, in Klingenberg, in 2007.

The first part of the season was characterized by ETo values higher than ETc, it means that the evaporative demand of the atmosphere was higher than the amount of water consumed by the crop during the initial growth stage.

Since no water deficit was measured ETa resulted equal to ETc (Figure 31).

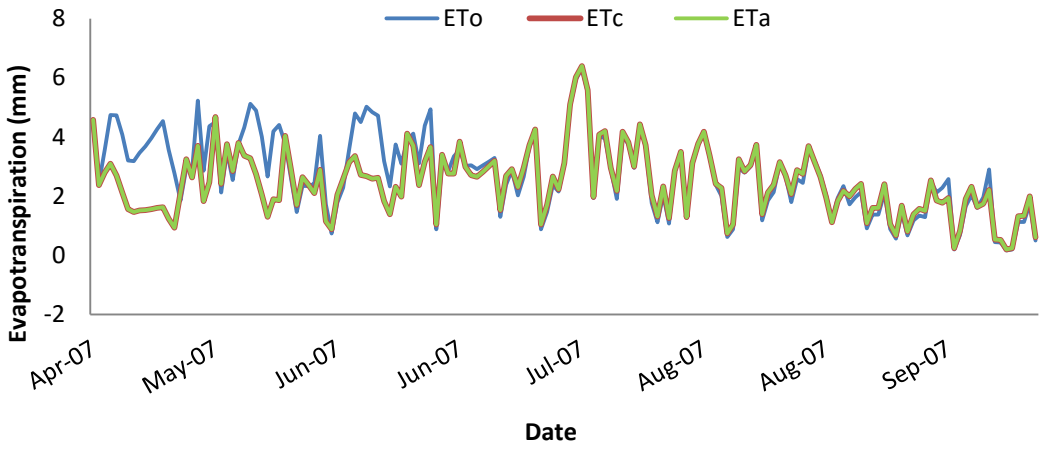

Fig. 31. Daily trend of reference, crop, and actual evapotranspiration (ETo, ETc, and ETa, respectively), in Klingenberg, in 2007.

The model captured the observed trend in ETa values even if a slightly overestimation (1.23 mm) was found during the entire maize growing season. A maximum ETa peak (6.03 mm) was computed in July, in correspondence with the highest precipitation value, and the difference between simulated (6.39 mm) and observed (3.48 mm) was equal to 2.91 mm (Figure 32).

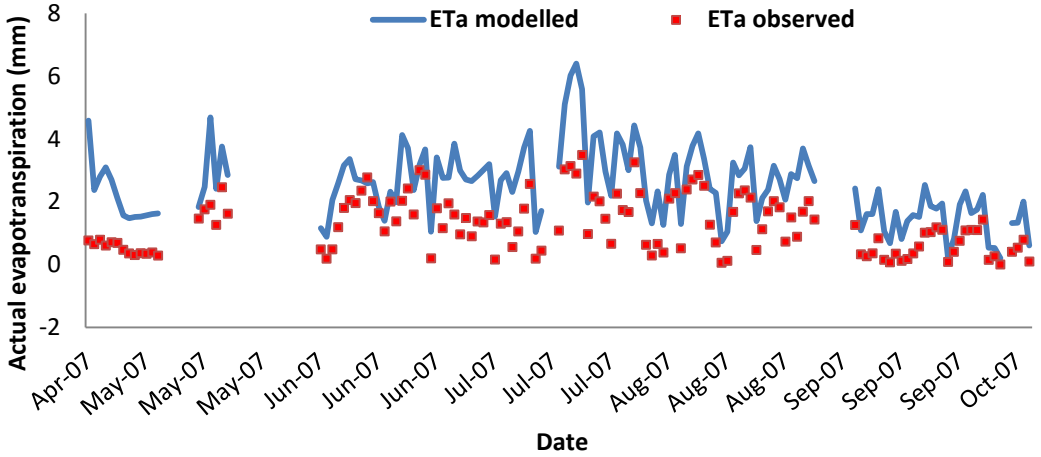

Fig. 32. Daily trend of modeled and observed actual evapotranspiration, in Klingenberg, in 2007.

The Person's coefficient value (0.84) was significant for $P \leq 0.001$. The R^2 equal to 71% confirmed the low data dispersion, thus the good SIMETAW_R performance in this season, and this was also affirmed by the angular coefficient (1.13) value of the

regression line. The statistical indices used to assess SIMETAW_R performance are shown in Table 10.

Tab. 10. Statistical indices used to assess SIMETAW_R performance, in Klingenberg, in 2007.

SITE	YEAR	CROP	r	RMSE	MBA	MBE	IA	RE	R^2	a	b
				mm	mm	mm	%	%	%		
Klingenberg	07	MAIZE	0.84***	1.39	1.24	1.23	67	39.72	71	1.07	1.13

*P ≤ 0.05; **P ≤ 0.01; ***P ≤ 0.001

The high RE value was related to a high RMSE value, and it may be affect by the energy balance closure of the measured fluxes lower (0.42) than the standard value (0.70). LE values accuracy may be compromised by the frequency and the intensity of precipitation which is known to alter sensor sensivity. Table 11 showed the percentage of values gap filled.

Tab. 11. Percentage of gap filled data in the original dataset, in Klingenberg, in 2007.

SITE	YEAR	CROP	CO_2	Rn	Ta	WS	H	LE	VPD	PCP
			%	%	%	%	%	%	%	%
Klingenberg	07	MAIZE	17.15	2.36	0.10	1.29	1.37	1.37	0.00	0.00

1.3.2 Grignon (FR-Gri)

Meteorological characterization

Climate and fluxes data were elaborated for both wheat and maize growing seasons, from October 28th 2005 to July 15th 2006, and from May 5th to September 28th, 2005, respectively. Grignon climate is characterized by a "warm temperate fully humid with warm summer" by Koppen climate classification.

The maximum air temperature measured in the site for maize and wheat growing seasons was 32 °C in both seasons, while the minimum temperature were 2.78 °C and -6.58 °C during maize and wheat, respectively. The mean seasonal temperature was higher during maize season (16.97 °C) than in wheat season (8.08 °C). The cumulative values of precipitation were 329 mm and 172 mm during wheat and maize growing season, respectively. Differences in temperature and precipitation values were due to the different period under study (summer months for maize and from autumn to summer for wheat) The cumulative precipitation value from the middle of May to the middle of July

in 2006 was 66 mm, with a peak of 21 mm in June. In the same period, 2005 was wetter with a total rainfall of 80 mm and a peak of 16.4 mm in July (Figure 33). Although in different years, these months were characterized by the same maximum (1.65 kPa), and mean value (0.68 kPa) of saturation vapor pressure.

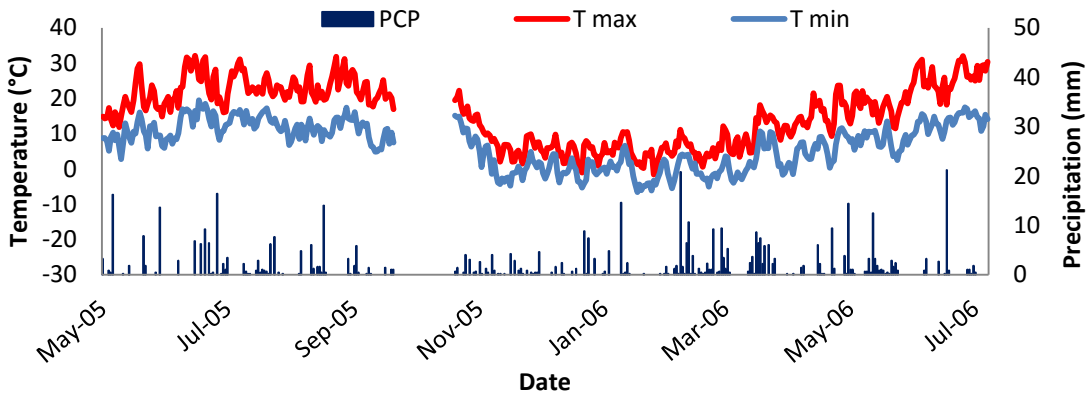

Fig. 33. Trend of daily maximum temperature (Tmax), minimum temperature (Tmin), mean temperature (Tmean), and precipitation (PCP), in Grignon, in 2005 and 2005-2006.

Peaks of net radiation were equal to 16.96 and 17.42 MJ m^{-2} d^{-1} in June for maize and wheat, respectively. The lowest value of net radiation was -2.60 MJ m^{-2} d^{-1} in December 2005. The cumulated net radiation during wheat growing season was equal to 1041 MJ m^{-2}, while it was 1292 MJ m^{-2} during maize growing season. The cumulated net radiation considering the period in common between the two seasons, was higher in 2006 (695 MJ m^{-2}) than in 2005 (687 MJ m^{-2}). The mean wind speed was 2.72 m s^{-1} in 2005-2006 season and 2.36 m s^{-1} in 2005. The windiest day was in December 2005 with a measured value of 6.74 m s^{-1}. The period in common was characterized by a mean value of wind speed equal to 2.84 m s^{-1} in 2005 with a maximum value of 4.34 m s^{-1}, and 2.12 m s^{-1} in 2006 with a maximum peak of 5.81 m s^{-1}.

Reference evapotranspiration

The cumulated value of ETo_PM was lower (419 mm) than ETo_HS value (557 mm) in 2005-2006, during wheat season. The application of the standardized reference evapotranspiration rates for short canopies led to calculate a higher value of ETo (451 mm) than Hargreaves-Samani (356 mm), in 2005, during maize season. The maximum

daily values of ETo_PM and ETo_HS were about 6.4 mm and 5.3 mm respectively, in both seasons (Figure 34).

ETo_HS equation tended to be higher than ETo_PM in correspondence with rainy periods, for instance from the beginning of 2006 to May, while it was lower than ETo_PM during the driest periods in both seasons. The trend of ETo_HS followed the same trend of temperature, and this was noticeable in both seasons. ETo_PM low values observed from around January to March 2006 may be related to the lowest VPD values (0.12 kPa as mean value), and temperature observed in this period.

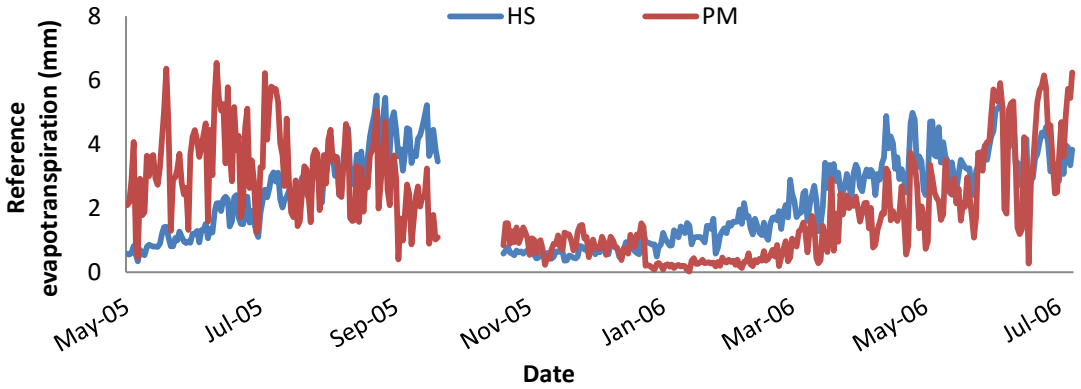

Fig. 34. Trend of daily reference evapotranspiration calculated using both Hargreaves-Samani and the standardized reference evapotranspiration rates for short canopies, in Grignon, in 2005 and 2005-2006.

Model results evaluation

Grignon, wheat, 2005-2006

The crop was not irrigated, but any water deficit condition was observed because of the frequency and the intensity of the precipitation. The stress coefficient slightly lower than 1 was found during the late season in correspondence with dry days. The local climate was considered to adjust wheat midseason generalized crop coefficient value that,at this stage, was equal to 1 instead than 1.05 (i.e. 0.05 lower than SIMETAW_R default value) (Figure 35).

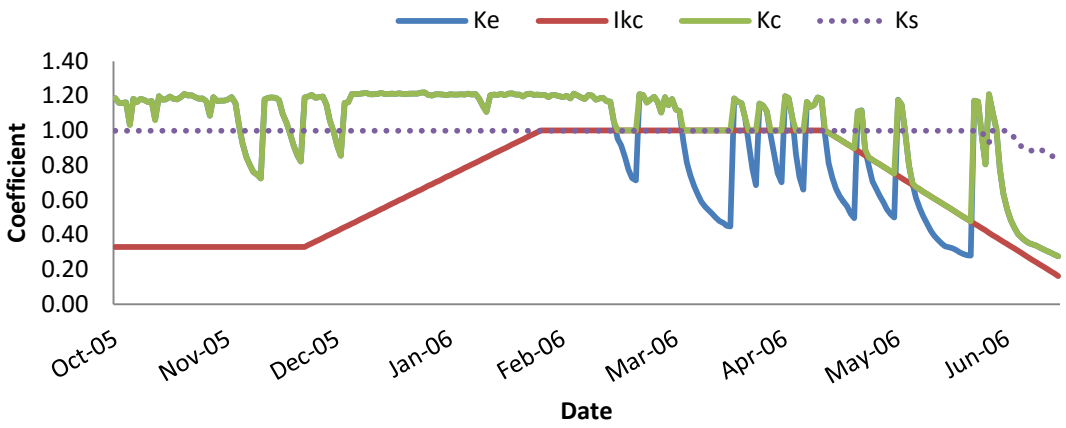

Fig. 35. Daily trend of the crop coefficient for the bare soil (Ke), the generalized crop coefficient (IKc), the crop coefficient (Kc), and the stress coefficient (Ks) during wheat growing season, in Grignon, in 2005-2006.

ETc and ETa values were identical for almost the whole growing season (Figure 36), with only a small difference in the late season due to a Ks value slightly smaller than 1. The maximum daily value of ETa was measured in June (4.12 mm), while the lower one was equal to 0.01 mm, in January. ETo values were slightly higher than ETc during the late season in correspondence with plant senescence, high temperature and low precipitation values.

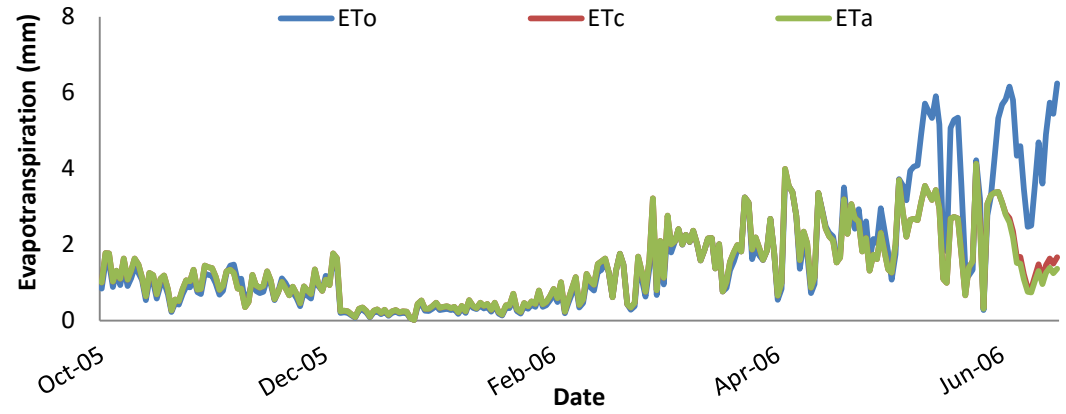

Fig. 36. Daily trend of reference, crop, and actual evapotranspiration (ETo, ETc, and ETa, respectively), in Grignon, in 2005-2006.

Figure 37 shows that the trend of observed and modeled data was almost the same. The difference between the cumulated modeled ETa value (306 mm) and the observed (278 mm) one was lower than 30 mm. SIMETAW_R model well matched the observed values for the entire season, in particular during the midseason.

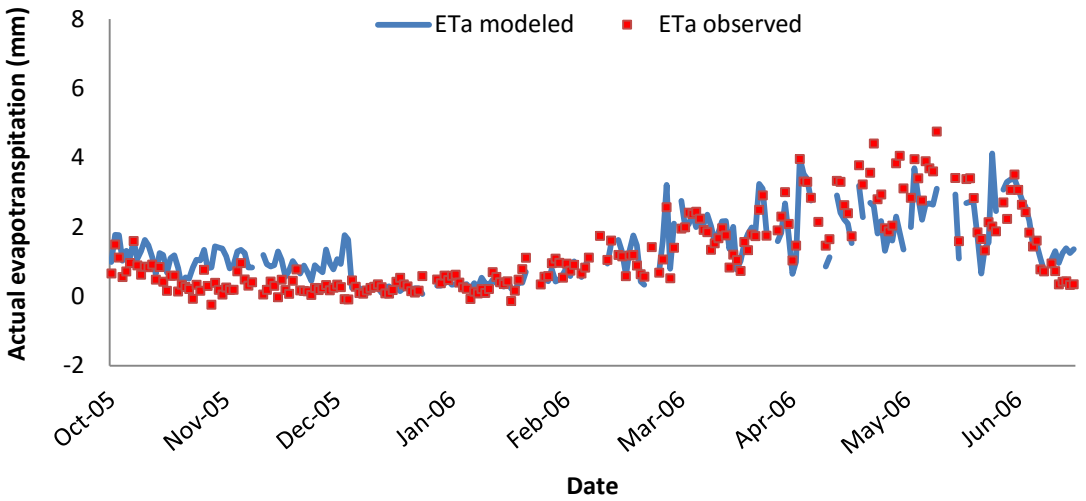

Fig. 37. Daily trend of modeled and observed actual evapotranspiration,in Grignon, in 2005-2006.

Simulated and observed ETa data were strongly and significantly correlated ($r=0.85$, $P \leq 0.001$). The good SIMETAW_R model performance was also stated by the low RMSE and consequently low RE, and the high index of agreement. The model overestimation was low in this season (MBE=0.12 mm) (Table 12). The high model accuracy was also confirmed by a slope of the regression line equal to 0.69.

Tab. 12. Statistical indices used to assess SIMETAW_R performance, in Grignon, in 2005-2006.

SITE	YEAR	CROP	r	RMSE	MBA	MBE	IA	RE	R^2	a	b
				mm	mm	mm	%	%	%		
Grignon	05-06	WHEAT	0.85***	0.61	0.45	0.12	91	12.12	72	0.50	0.69

*P ≤ 0.05; **P ≤ 0.01; ***P ≤ 0.001

Considering the period from October to December the percentage of gap filled data was 28.05 (Table 13), and that could explain the model overestimation observed in these months.

Tab. 13 Percentage of gap filled data in the original dataset, in Grignon, in 2005-2006.

SITE	YEAR	CROP	CO_2	Rn	Ta	WS	H	LE	VPD	PCP
			%	%	%	%	%	%	%	%
Grignon	05-06	WHEAT	29.59	20.40	19.80	19.90	22.39	28.05	2.68	0.77

Grignon, maize, 2005

In 2005, from May to July the experimental field in Grignon was cultivated with maize. The crop was not irrigated, and water deficit conditions happened from maize midseason until the harvest (Figure 38).

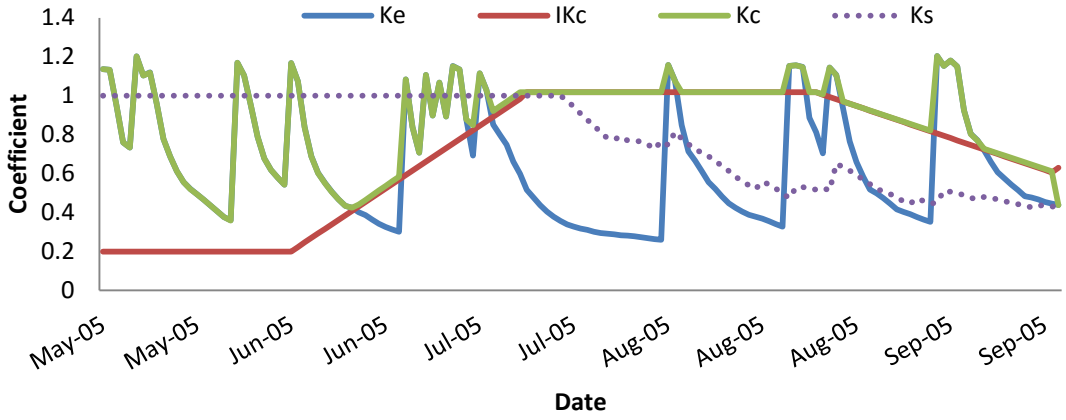

Fig. 38. Daily trend of the crop coefficient for the bare soil (Ke), the generalized crop coefficient (IKc), the crop coefficient (Kc), and the stress coefficient (Ks) during maize growing season, in Grignon, in 2005.

The amount of water consumed by the plant in water deficit conditions is shown in Figure 39 by the green line. Lower values of ETa were in correspondence with the lower values of Ks, hence ETc was higher than ETa from June onward.

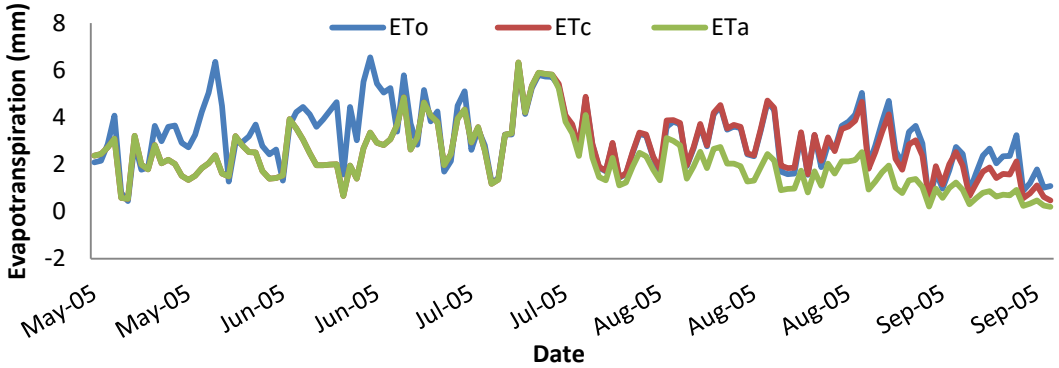

Fig. 39. Daily trend of reference, crop, and actual evapotranspiration (ETo, ETc, and ETa, respectively), in Grignon, in 2005.

The simulated ETa values were in line with the observation for the entire growing season. Figure 40 showed an overestimation of the model in the first part of the maize growing season (from about the initial growth to the end of the rapid growth) and an underestimation during the second part (from mid-season to the harvest).

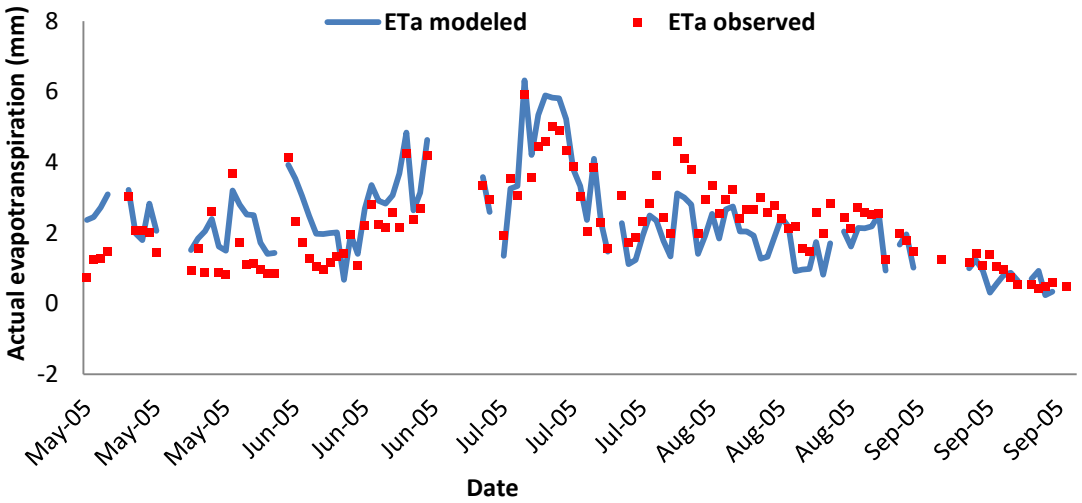

Fig. 40. Daily trend of modeled and observed actual evapotranspiration, in Grignon, in 2005.

Simulated and measured ETa values were significantly correlated (r=0.81, $P \leq 0.001$) Data dispersion is identified by the coefficient of determination which was equal to 65%. The agreement between observed and model actual evapotranspiration values reached the 89% (Table 14). In this season the model overestimation was negligible (0.04 mm). The slope (0.88), as well as the intercept (0.32) of the 1:1 line confirmed a good model accuracy.

Tab. 14. Statistical indices used to assess SIMETAW_R performance, in Grignon, in 2005.

SITE	YEAR	CROP	r	RMSE	MBA	MBE	IA	RE	R^2	a	b
				mm	mm	mm	%	%	%		
Grignon	05	MAIZE	0.81***	0.75	0.63	0.04	89	13.73	65	0.32	0.88

*P ≤ 0.05; **P ≤ 0.01; ***P ≤ 0.001

Table 15 shows the percentage of LE and CO_2 gap filled in the original dataset. Any gap was found in VPD original dataset. The Eddy Covariance measurements were accurate, and this was confirmed by the slope of the energy balance closure linear regression equal to 0.65 and the coefficient of determination of 78%.

Tab. 15. Percentage of gap filled data in the original dataset, in Grignon, in 2005.

SITE	YEAR	CROP	CO2	Rn	Ta	WS	H	LE	VPD	PCP
			%	%	%	%	%	%	%	%
Grignon	05	MAIZE	15.76	2.53	1.89	1.89	7.09	15.69	0.00	0.70

1.3.3 Dijgraaf (NL-Dij)

Meteorological conditions

Climate and fluxes data were elaborated for maize growing season, from May 5th to September 29th, 2007. Climate in Dijgraaf is warm temperate, fully humid, with warm summer (https://fluxnet.ornl.gov/). The maximum air temperature reached during maize growing season was 31.10 °C in June, and the minimum 5.07°C in September. The mean air temperature was equal to 15.98°C. The maximum precipitation value was 18.40 mm in May. The cumulative precipitation from May to September was 299 mm. Maximum and minimum saturation vapor pressure were 1.12 kPa in August and 0.11 kPa in September, respectively, with an average of 0.40 kPa (Figure 41).

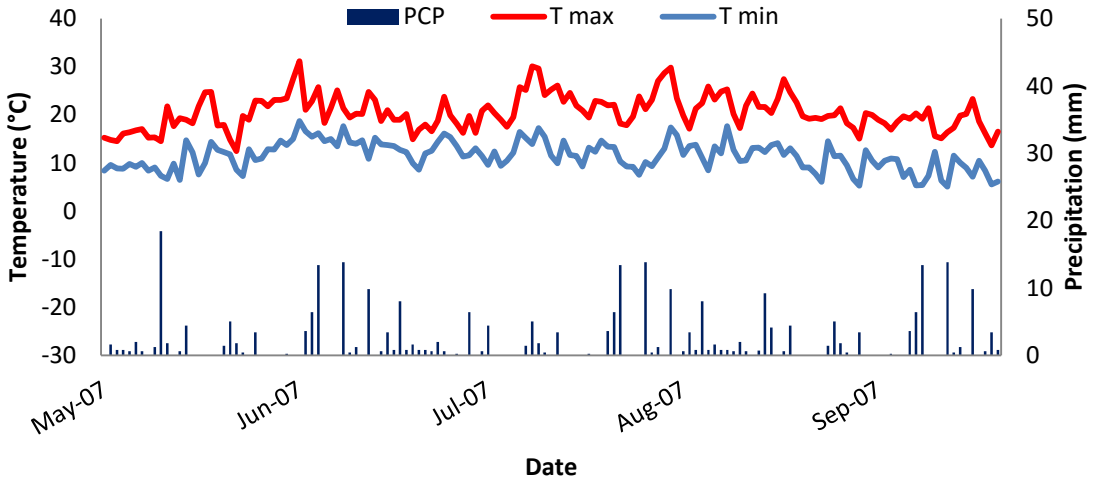

Fig. 41. Trend of daily maximum temperature (Tmax), minimum temperature (Tmin), mean temperature (Tmean), and precipitation (PCP), in Dijgraaf, in 2007.

The maximum value of net radiation was 17.02 MJ m^{-2} in June and the minimum 1.11 MJ m^{-2} in August. The cumulative value for the entire season was 1250 MJ m^{-2}. The windiest day during maize growing season was in May, and the maximum wind speed value was 3.65 m s^{-1}. The mean value was 1.64 m s^{-1} and the lowest value was 0.48 m s^{-1}.

Reference evapotranspiration

The trend of ETo_PM and ETo_HS tended to be reversed from the end of the midseason to the late season, when ETo_HS values were higher than ETo_PM (Figure

42). The cumulative ETo_HS value was 295 mm and the cumulated ETo_PM was 356 mm. Minimum and maximum daily values were similar considering both equations, 0.40 mm and 4.80 mm, respectively. Higher ETo_HS values were found in the last part of the season, specifically from the end of August onward, when the mean precipitation value was higher (2.36 mm) than in the previous months (1.98 mm). In addition, the mean wind speed value was lower (1.32 m s^{-1}) in the last two months than before (1.77 m s^{-1}). ETo_HS underestimation was in fact found in the first part of the period under investigation.

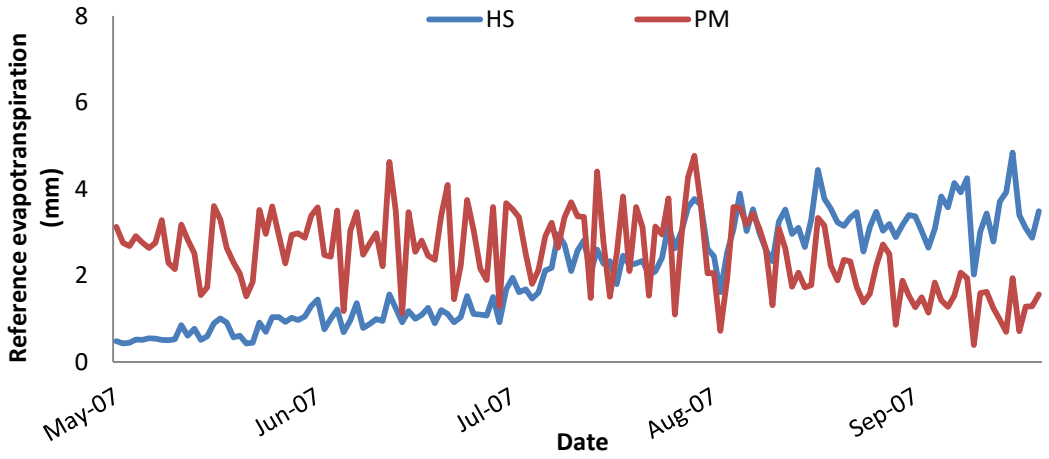

Fig. 42. Trend of daily reference evapotranspiration calculated using both Hargreaves-Samani and the standardized reference evapotranspiration rates for short canopies, in Dijgraaf, in 2007.

Model results evaluation

The cumulative precipitation in summer was enough to satisfy crop water requirement, in fact no water deficit was defined during maize growing season. The IKc during the crop growing season was 1.01, i.e. 0.04 lower than the model default value (Figure 43). Figure 44 shows the trend of ETo, ETc, and ETa where ETc and ETa were characterized by the same values during the entire growing season. The maximum and minimum daily values of ETc measured were 4.9 mm and 0.40 mm, respectively.

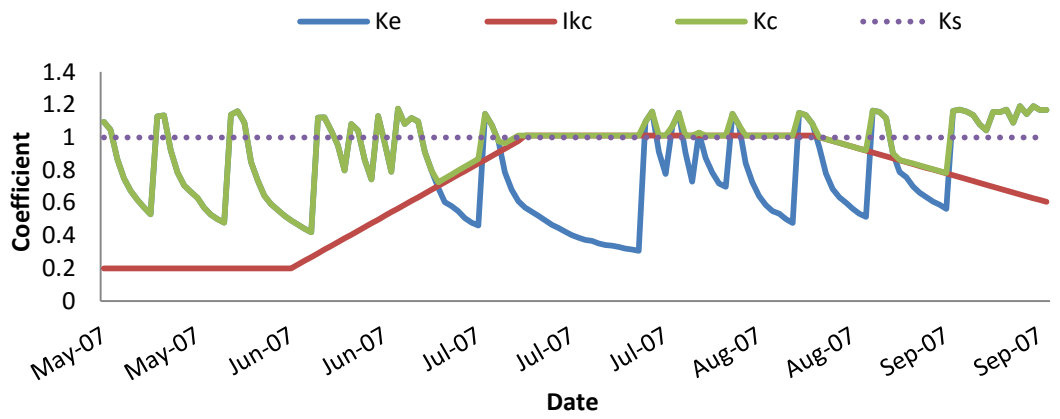

Fig. 43. Daily trend of the crop coefficient for the bare soil (Ke), the generalized crop coefficient (IKc), the crop coefficient (Kc), and the stress coefficient (Ks) during maize growing season, in Dijgraaf, in 2007.

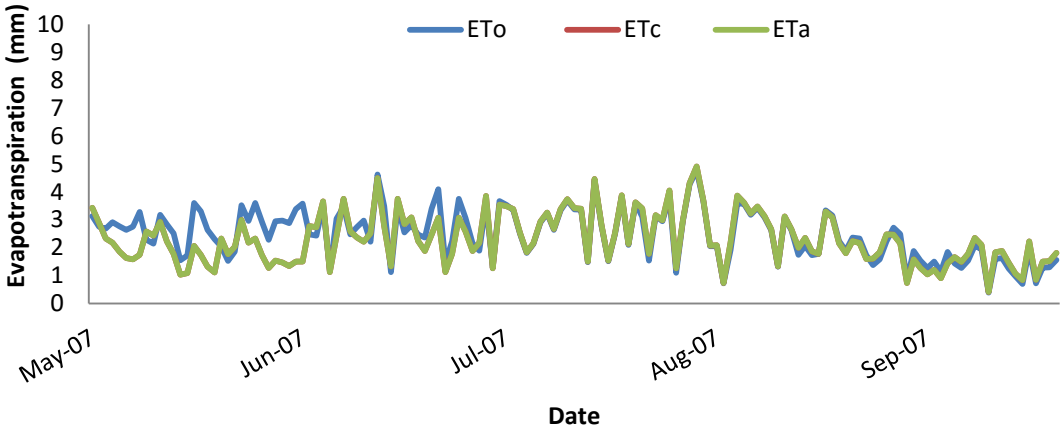

Fig. 44. Daily trend of reference, crop, and actual evapotranspiration (ETo, ETc, and ETa, respectively), in Dijgraaf, in 2007.

Figure 45 shows that measured and observed data followed the same trend during maize growing season. The cumulated simulated and observed ETa values were 296 mm and 314 mm, respectively. The maximum ETa peak (4.9 mm) was computed in correspondence with the maximum peak of VPD (1.12 kPa).

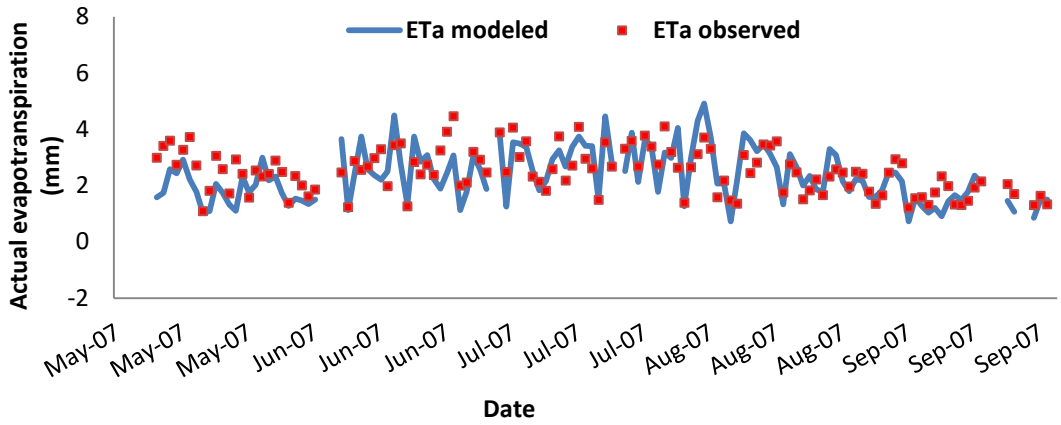

Fig. 45. Daily trend of modeled and observed actual evapotranspiration, in Dijgraaf, in 2007.

The *r* coefficient value was signicant for $P \leq 0.001$. The RMSE (0.68) and the index of agreement (82%), indicated a good model performance. This was also confirmed by the high slope value (0.83) and low intercept (0.27) of the 1:1 regression line. (Table 16).

Tab. 16. Statistical indices used to assess SIMETAW_R performance, in Dijgraaf, in 2007.

SITE	YEAR	CROP	r	RMSE	MBA	MBE	IA	RE	R^2	a	b
				mm	mm	mm	%	%	%		
Dijagraaf	07	MAIZE	0.71***	0.68	0.54	-0.14	82	20.12	50	0.27	0.83

*$P \leq 0.05$; **$P \leq 0.01$; ***$P \leq 0.001$

The determination coefficient of the energy balance closure was equal to 84% with a slope of 0.80, and it stressed the high accuracy of Eddy Covariance measurements. The energy balance closure results indicated a good accuracy in ETa measurements, that, in part, contributed to the good agreement between simulations and observations in this site compared to the others. In Table 17, the percentage of gap filled variable from the original dataset was reported.

Tab. 17. Percentage of gap filled data in the original dataset, in Dijgraaf, in 2007.

SITE	YEAR	CROP	CO_2	Rn	Ta	WS	H	LE	VPD	PCP
			%	%	%	%	%	%	%	%
Dijagraaf	07	MAIZE	13.04	4.66	4.65	6.35	10.82	17.78	0.00	0.00

1.3.4 Oensingen (CH-Oe2)

Meteorological conditions

Climate and fluxes data were elaborated for wheat growing season, from October 19th 2006 to July 16th 2007. Climate in Oensingen is warm temperate, fully humid, with warm summer. The maximum and minimum temperature recorded in Oensingen were 37.65 °C and -10.19 °C, respectively, with a mean air temperature of 10.32 °C.

Precipitation were mostly concentrated from May to the end of the season. The rainiest day was in June, when a peak of precipitation of 47.84 mm was measured (Figure 46). The cumulative rainfall was 1101 mm. Winter was characterized by a mean VPD value of 0.07 kPa, then values increased reaching a peak of 2.5 kPa in April. The mean VPD was equal to 0.34 kPa during the whole growing season. High mean temperature, scarce precipitation event, and high value of saturation vapor pressure characterized the period from March to May 2007.

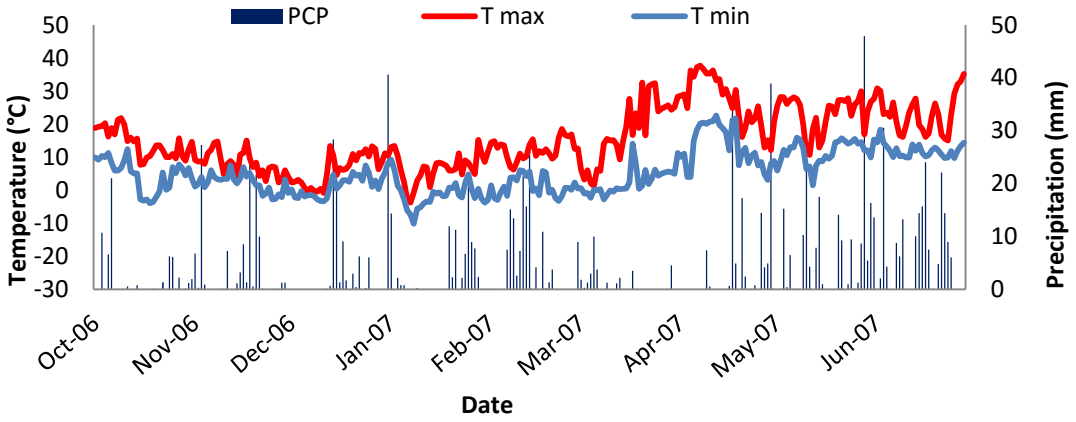

Fig. 46. Trend of daily maximum temperature (Tmax), minimum temperature (Tmin), mean temperature (Tmean), and precipitation (PCP), in Oensingen, in 2006-2007.

The cumulative net radiation in Oensingen was equal to 1438 MJ m^{-2}, with a peak in June equal to 18.60 MJ m^{-2} d^{-1}. Wheat growing season was characterized by windy days, particularly in winter when the maximum value of 7.6 m s^{-1} was measured in January. The mean wind value was equal to 1.87 m s^{-1}.

Reference evapotranspiration

Daily ETo_HS values were higher than ETo_PM for almost the entire period under investigation. The cumulated ETo_HS value (720 mm) was higher than ETo_PM (441mm). ETo_HS followed the temperature trend. The highest temperature observed in April influenced probably ETo_HS which tended to increase considerably. ETo_PM was maybe influenced by the high values of temperature and VPD in particular from spring onward (Figure 47) where its values tended to be higher. The mean VPD value was in fact lower (about 0.08 kPa) until the beginning of April than in the last part (0.74 kPa).

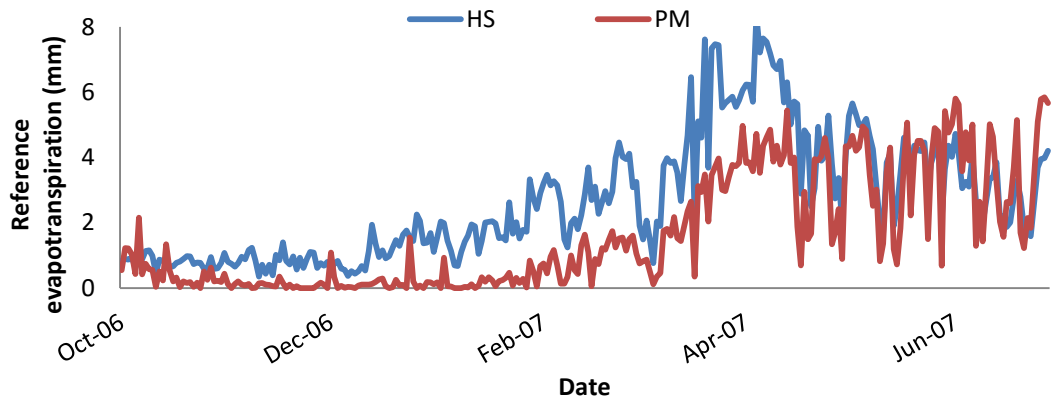

Fig. 47. Trend of daily reference evapotranspiration calculated using both Hargreaves-Samani and the standardized reference evapotranspiration rates for short canopies, in Oensingen, in 2006-2007.

Model results evaluation

The period was characterized by no water deficit. The IKc during the crop growing season was 1.00, thus 0.05 lower than the model default coefficient value. Low values of Ke were measured during the mid season in correspondence with a dry period (Figure 48).

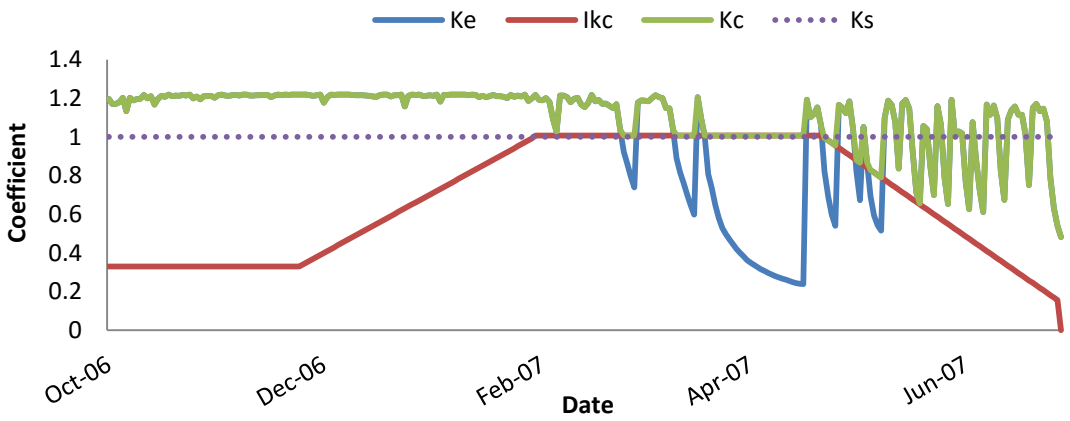

Fig. 48. Daily trend of the crop coefficient for the bare soil (Ke), the generalized crop coefficient (IKc), the crop coefficient (Kc), and the stress coefficient (Ks) during wheat growing season, in Oensingen, in 2006-2007.

ETc and ETa values were equal because no water deficit was computed (Figure 49). The maximum ETc was 5.48 mm, and the cumulative ETc was 429 mm.

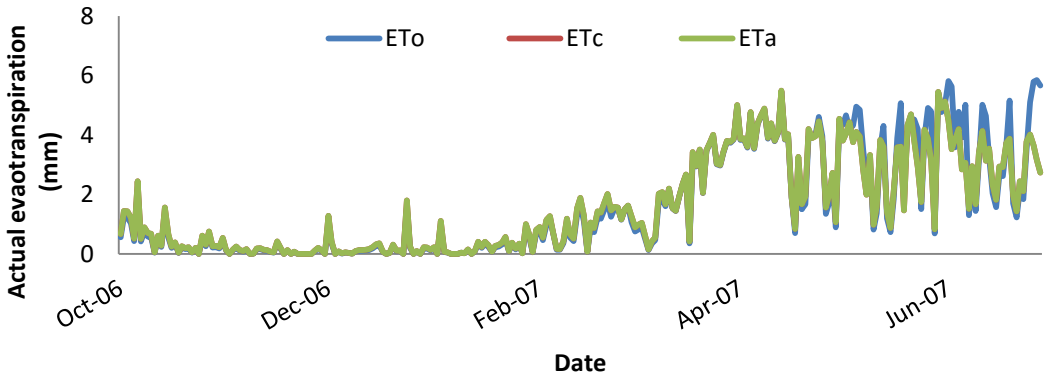

Fig. 49. Daily trend of reference, crop, and actual evapotranspiration, in Oensingen, in 2006-2007.

The ETa values estimated by the model (211 mm) were closed to the measured ones (274 mm), The trend followed by the measured and observed data was almost the same during the maize growing season (Figure 50). SIMETAW_R model well fitted the observed ETa values for the entire season, in particular from the beginning of October to the end of April.

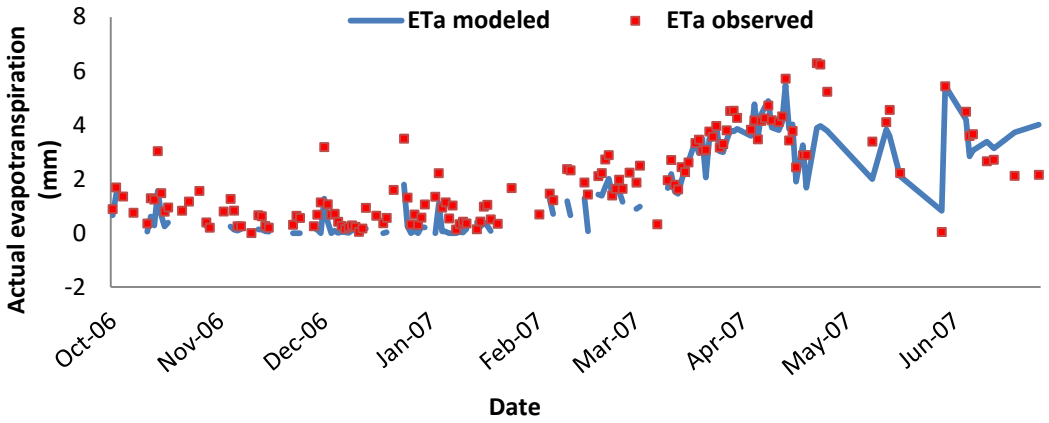

Fig. 50. Daily trend of modeled and observed actual evapotranspiration, in Oensingen, 2006-2007.

The Pearson's coefficient value (0.92) was significant for $P \leq 0.001$ The good model performance were determined by the high index of agreement (94%), the low percentage of relative error (12%), and the high value of the slope of the linear regression equation (0.94) (Table 18).

Tab. 18. Statistical indices used to assess SIMETAW_R model performance, in Oensingen, in 2006-2007.

SITE	YEAR	CROP	r	RMSE	MBA	MBE	IA	RE	R^2	a	b
				mm	mm	mm	%	%	%		
Oensingen	06-07	WHEAT	0.92***	0.75	0.58	-0.44	0.94	12	85	-0.33	0.94

*P ≤ 0.05; **P ≤ 0.01; ***P ≤ 0.001

The percentage of gap filled data was very low for all variables except for CO_2 values (Table 19). The great performance of the model may be also related to the absence of gaps in LE dataset. In addition, any gap was found in H, VPD, and PCP dataset.

Tab. 19. Percentage of gap filled data in the original dataset, in Oensingen, in 2006-2007.

SITE	YEAR	CROP	CO_2	Rn	Ta	WS	H	LE	VPD	PCP
			%	%	%	%	%	%	%	%
Oensingen	06-07	WHEAT	28.75	1.10	1.11	1.08	0	0	0	0

1.3.5 Lamasquère (FR-Lam)

Meteorological characterization

Climate and fluxes data were elaborated for both wheat and maize growing season, from October 18th 2006 to July 15th 2007, and from May 1st to August 31st 2006, respectively. Köppen climate classification indicates the Lamasquère climate as "warm temperate, fully humid with warm summer".

The mean temperature measured in the site during wheat and maize growing season were 14.85 °C and 19.94 °C, respectively. The maximum and minimum values during wheat season were 30.82 °C and -6.80 °C, and 35.33 °C and 2.04°C during maize cultivation. Comparing the months in common between the two crops, from May to the first two weeks of July, the mean temperature was about 19 °C in both years, with a maximum values of 23.39 °C measured in 2007 (Figure 51). The cumulative value of precipitation for the whole wheat and maize growing seasons were 531 mm and 286 mm, respectively, and the mean saturation vapor pressure values were 0.17 kPa and 0.75 kPa. From May to July the cumulative precipitation was higher (245 mm) in 2007 than in 2006 (158 mm). In the same period, the mean value of VPD was 0.72 kPa in 2006 and 0.38 kPa in 2007.

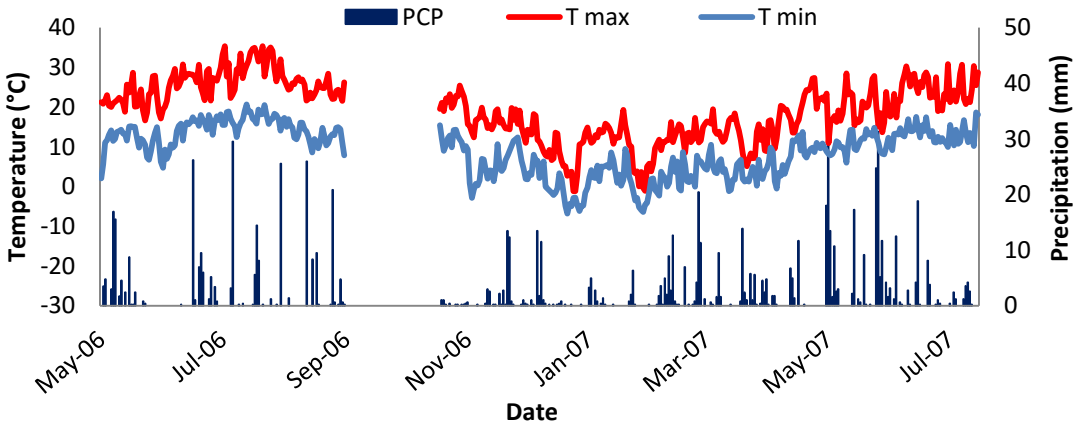

Fig. 51. Trend of daily maximum temperature (Tmax), minimum temperature (Tmin), mean temperature (Tmean), and precipitation (PCP), in Lamasquère, in 2006-2007.

The highest cumulative Rn value equal to 1483 MJ m^{-2} was measured during maize growing season, and it was about 180 MJ m^{-2} lower than in 2006-2007 season.

Comparing the common months, the cumulative net radiation was higher (924 MJ m^{-2}) in 2006 than in 2006-2007 (807 MJ m^{-2}).

The mean wind speed during the entire wheat season was 1.68 m s^{-1} and 1.80 m s^{-1} during maize season. The maximum value measured was 5.78 m s^{-1} in 2007.

Reference evapotranspiration

The cumulative value of ETo_PM and ETo_HS were 384 mm and 705 mm in the 2006-2007 seasons. During the 2006 season, the ETo_HS values was 351 mm and ETo_PM 483 mm.

Comparing the period from May to July, the highest mean evaporative demand was obtained using ETo_PM (301 mm), in 2006. Lower values were measured using both ETo_HS (264 mm) and ETo_PM (227 mm) in 2007 (Figure 52). During maize growing season, ETo_PM was influenced by T, VPD and WS: high values of T and VPD, and low values of WS resulted in higher values of ETo_PM. The influence of net radiation was also considered to explain the variability of ETo_PM, in fact the highest net radiation values were observed in summer months, specifically during the maize growing season.

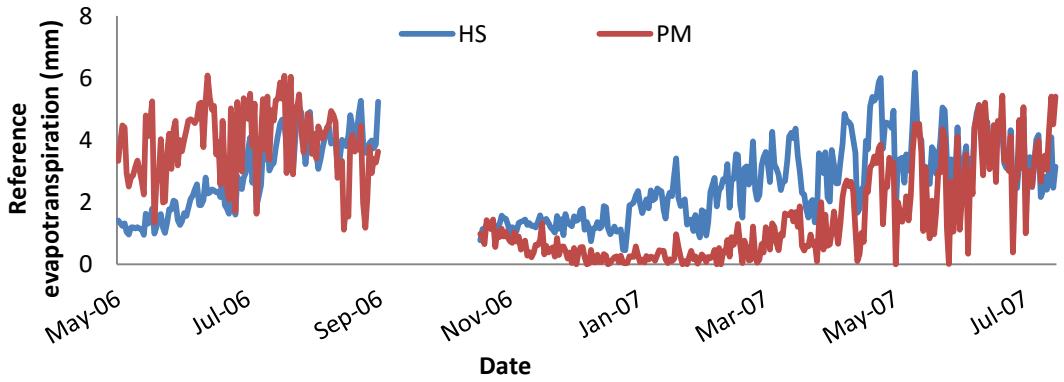

Fig. 52. Trend of daily reference evapotranspiration, in Lamasquère, in 2006 and 2006-2007.

Model results evalutation

Lamasquère, wheat, 2006-2007

The crop under study was not irrigated, hence water supply came only from precipitation. Since the rainfall supplied the water necessary to grow up the crop, no water deficit was measured, hence the stress coefficient was equal to 1 (Figure 53).

During the mid-season, crop coefficient values were adjusted depending on the local climate and conditions. The mid-season IKc was 0.05 higher than the model default value (1.05).

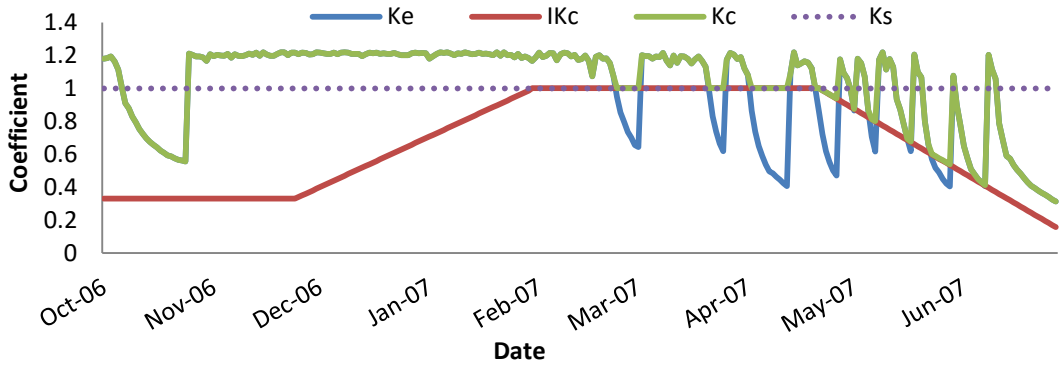

Fig. 53. Daily trend of the crop coefficient for the bare soil (Ke), the generalized crop coefficient (IKc), the crop coefficient (Kc), and the stress coefficient (Ks) during wheat growing season, in Lamasquère, in 2006-2007.

In Figure 54, the daily values of ETo, ETc, and ETa referred to wheat growing season are shown. The water consumed by the crop was a bit lower (328 mm) than the evaporative demand of the atmosphere (384 mm). Since the precipitation was 531 mm, no water deficit was measured, thus ETc and ETa values were identical.

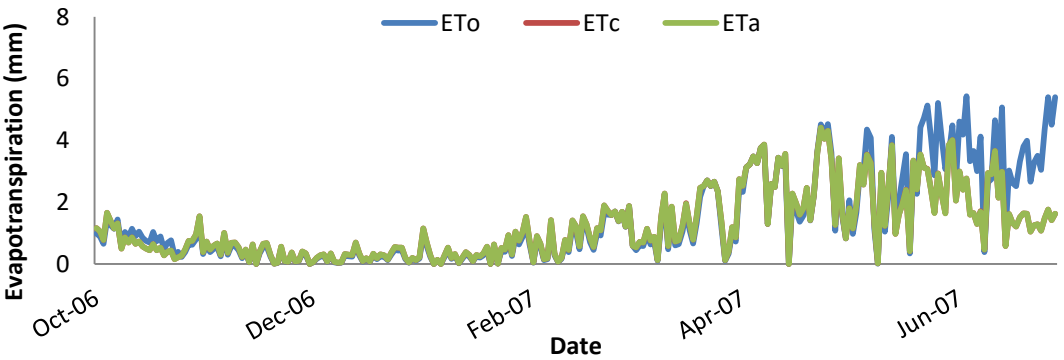

Fig. 54. Daily trend of reference, crop, and actual evapotranspiration (ETo, ETc, and ETa, respectively), in Lamasquère, in 2006-2007.

ETa modeled values were very similar to the observed values (Figure 55), until the midseason. The cumulated ETa observed values was 195 mm, and the modeled one was 170 mm.

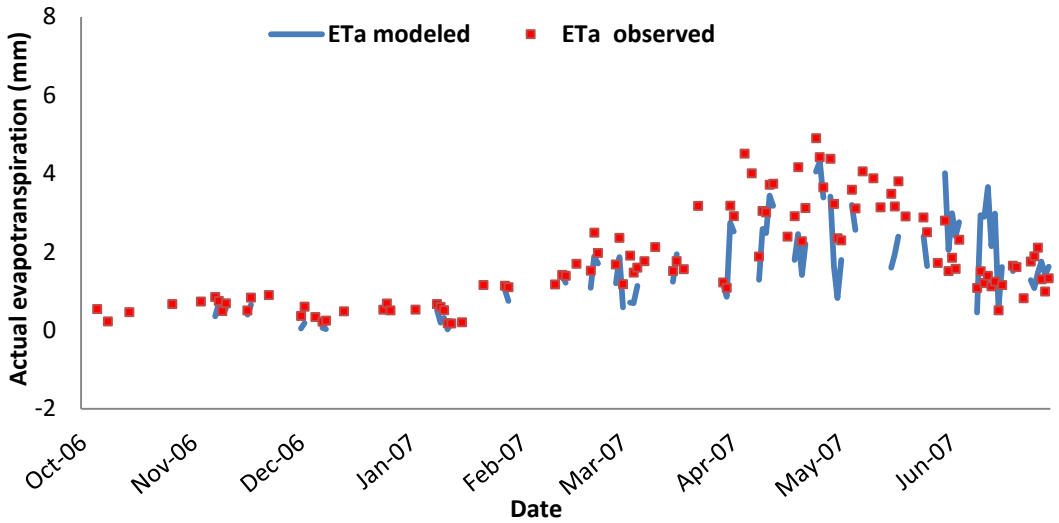

Fig. 55. Daily trend of modeled and observed wheat actual evapotranspiration, in Lamasquère, in 2006-2007.

The difference between cumulated observed and simulated ETa value was lower than 30 mm in season 2006-2007. The SIMETAW_R well captured observed data during the season. Measured and simulated ETa values were highly and significantly correlated ($r=0.82$, $P \leq 0.001$). The data dispersion identified by the determination coefficient was low (Table 20). The RMSE equal to 0.72 mm, the index of agreement of 90%, as well as the high slope and the low intercept value of the regression line confirmed the good accuracy of SIMETAW_R model.

Tab. 20. Statistical indices used to assess SIMETAW_R model performance, in Lamasquère, in 2006-2007.

SITE	YEAR	CROP	r	RMSE	MBA	MBE	IA	RE	R^2	a	b
				mm	mm	mm	%	%	%		
Lamasquere	06-07	WHEAT	0.82***	0.72	0.55	-0.23	0.90	15.16	69	0.22	0.75

*P ≤ 0.05; **P ≤ 0.01; ***P ≤ 0.001

Any gap was found in VPD and PCP dataset in season 2006-2007, while the highest percentage of gap filled data was computed for LE values (Table 21).

Tab. 21. Percentage of gap filled data in the original dataset, in Lamasquère, in 2006-2007.

SITE	YEAR	CROP	CO_2	Rn	Ta	WS	H	LE	VPD	PCP
			%	%	%	%	%	%	%	%
Lamasquere	06-07	WHEAT	19.09	2.72	0.01	4.51	25.58	37.01	0.00	0.00

Lamasquère, maize, 2006

Maize was not irrigated in the experimental site. Since the cumulated precipitation in the last months of the growing season (73 mm) was not able to satisfy the water lost by the actual evapotranspiration (90 mm), the Ks was lower than 1 (Figure 56).

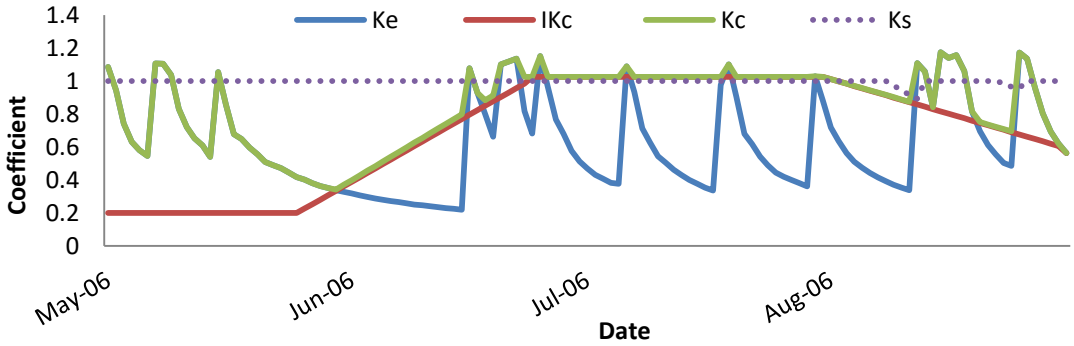

Fig. 56. Daily trend of the crop coefficient for the bare soil (Ke), the generalized crop coefficient (IKc), the crop coefficient (Kc), and the stress coefficient (Ks) during maize growing season, in Lamasquère, in 2006.

The water deficit is shown in Figure 57, and it stresses a lower value of ETa due to a stress coefficient values lower than 1. During the driest period (from May to June), ETo values were higher than ETc.

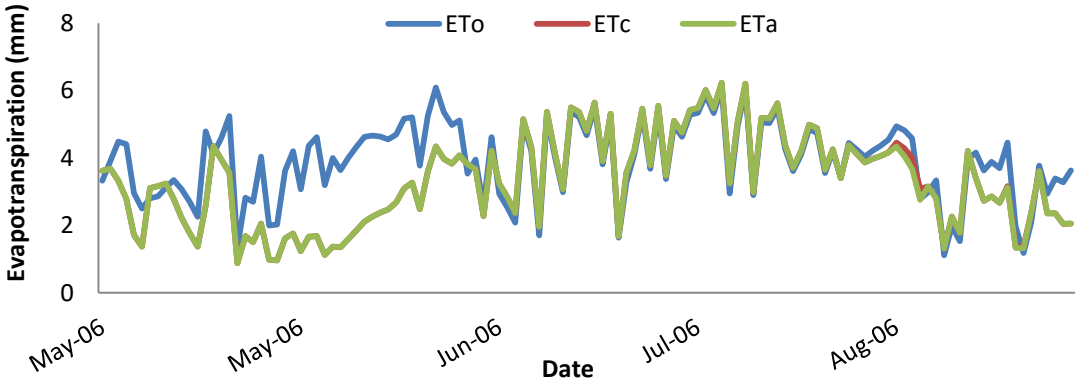

Fig. 57. Daily trend of reference, crop, and actual evapotranspiration (ETo, ETc, and ETa, respectively), in Lamasquère, in 2006.

Model performance are shown in Figure 58. Similar values of cumulated modeled (206 mm) and observed (179 mm) ETa were computed in this site during the maize growing season.

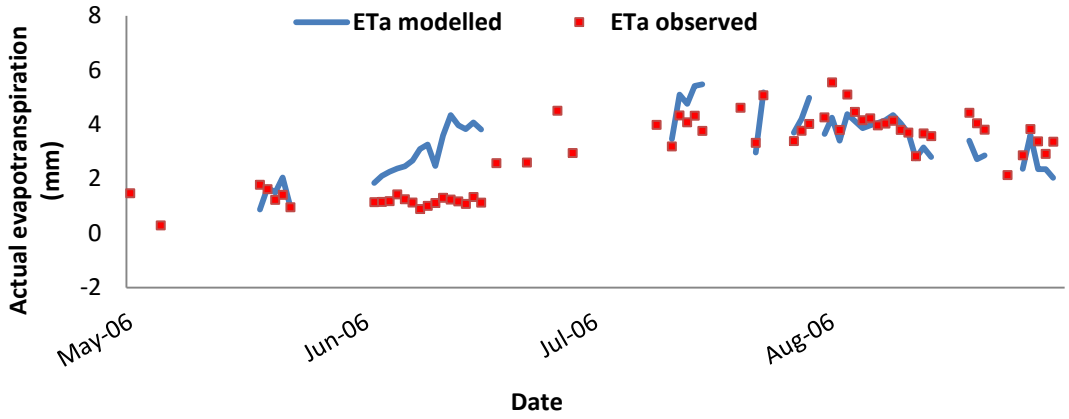

Fig. 58. Daily trend of modeled and observed actual evapotranspiration, in Lamasquère, in 2006.

The *r* coefficient value was significant for $P \leq 0.001$. SIMETAW_R model performance were defined by a index of agreement of 76% and a root mean square error of 1.22 mm. The mean bias error confirmed a model overestimation of 0.43 mm. Table 22 shows the statistical indices used to assess SIMETAW_R model performance.

Tab. 22. Statistical indices used to assess SIMETAW_R model performance, in Lamasquère, in 2006.

SITE	YEAR	CROP	r	RMSE	MBA	MBE	IA	RE	R^2	a	b
				mm	mm	mm	%	%	%		
Lamasquere	06	MAIZE	0.61***	1.22	0.92	0.43	76	23.13	37	1.88	0.50

*P ≤ 0.05; **P ≤ 0.01; ***P ≤ 0.001

The low coefficient of determination (37%) indicated a high data dispersion around the 1:1 regresion line. The model better matched observed data in August, when any LE gap was found in the original dataset. The low R^2 and slope, both equal to 0.57, which characterized the energy balance closure, as well as the high percentage of gap filled LE data (38.74%) (Table 23), could explain the differences between measured and simulated ETa values, as well as the high RE (23.13) and RMSE (1.22) value.

Tab. 23. Percentage of gap filled data in the original dataset, in Lamasquère, in 2006.

SITE	YEAR	CROP	CO_2	Rn	Ta	WS	H	LE	VPD	PCP
			%	%	%	%	%	%	%	%
Lamasquere	06	MAIZE	27.13	8.28	8.28	5.76	33.30	38.74	0.00	0.00

1.3.6 Lonzee (BE-Lon)

Meteorological characterization

Climate and fluxes data were elaborated for wheat growing season, from October 14th 2004 to August 3rd 2005, and from October 10th to August 5th 2007, respectively. Köppen climate classification indicates the Lonzee climate as "warm temperate, fully humid with warm summer" (https://fluxnet.ornl.gov/).

The mean temperature in Lonzee was 9.67 °C in 2006-2007, and 8.7 °C in 2004-2005. The maximum and minimum mean temperature were higher in 2006 season, 13.35 °C and 6.00 °C, respectively. The cumulative precipitation values was 529 mm and 550 mm in 2004-2005 and 2006-2007, respectively (Figure 59). The mean saturation vapor pressure was 0.25 kPa in the first season, about 0.10 kPa less than in the second one.

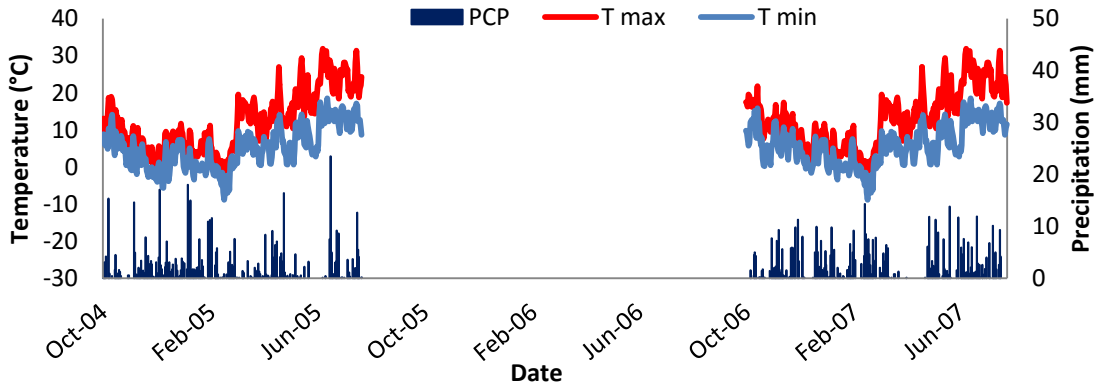

Fig. 59. Trend of daily maximum temperature (Tmax), minimum temperature (Tmin), mean temperature (Tmean), and precipitation (PCP), in Lonzee, in 2004-2005 and 2006-2007.

The cumulated net radiation in 2004-2005 was 1504 MJ m^{-2} and 1449 MJ m^{-2} in 2007. The mean wind speed value of 3.24 m s^{-1} was recorded in 2006-2007, and 2.98 m s^{-1} in 2004-2005. The maximum value of around 8.40 m s^{-1} was measured in both seasons.

Reference evapotranspiration

The cumulative values of ETo_PM and ETo_HS were 458 mm and 553 mm in 2004-2005 season, and 468 mm and 559 mm in 2006-2007. The maximum ETo value was computed using ETo_PM, and it was equal to 6.13 mm, in 2004-2005, while ETo_HS maximum value was 5.47 mm. Lower values of ETo_HS (5.44 mm) and ETo_PM (4.97 mm) were computed in season 2006-2007 (Figure 60). Values of ETo_PM were higher

in 2004-2005 than in 2006-2007, and this was consistent with the highest values of VPD measured in the first season, in particular from about April 2005 onward, in correspondence also with the highest temperature.

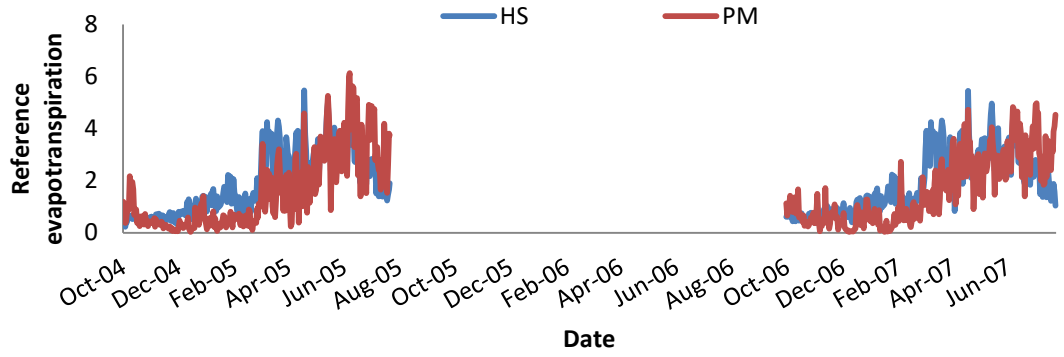

Fig. 60. Trend of daily reference evapotranspiration, in Lonzee, in 2004-2005 and 2006-2007.

Modeling results evaluation

Lonzee, wheat, 2004-2005

The crop under study was not irrigated, hence water supply came only from precipitation. Water deficit was measured during the late season and this was confirmed by the low values of Ks during the late season (Figure 61). During the mid-season IKc values were adjusted depending on the local climate and conditions.

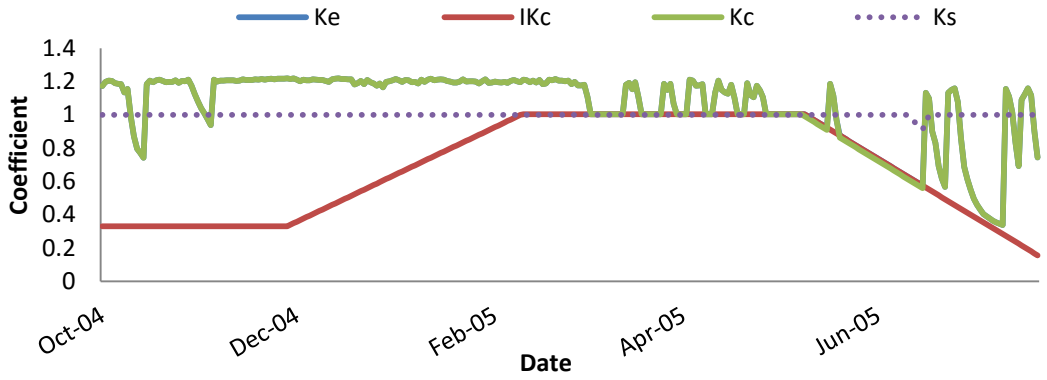

Fig. 61. Daily trend of the crop coefficient for the bare soil (Ke), the generalized crop coefficient (IKc), the crop coefficient (Kc), and the stress coefficient (Ks) during wheat growing season, in Lonzee, in 2004-2005.

In Figure 62, the daily values of ETo, ETc, and ETa referred to wheat growing season are shown.

ETa was a bit lower than ETc in a few days of wheat growing season because of the available water was not enough to satisfy crop water requirement.

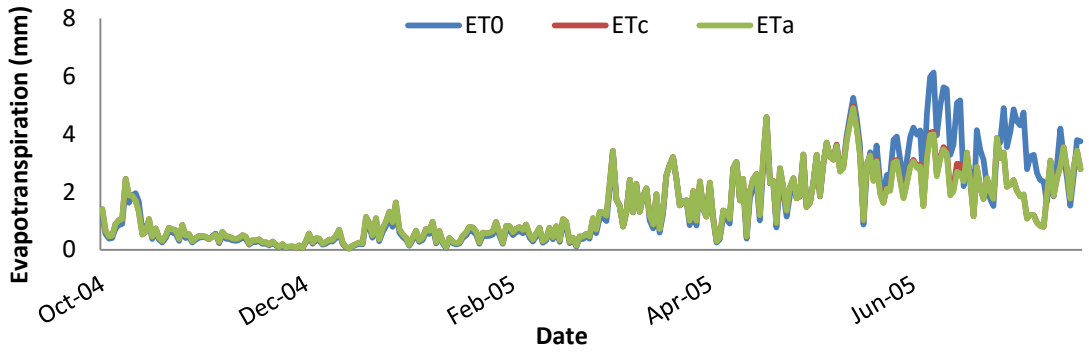

Fig. 62. Daily trend of reference, crop, and actual evapotranspiration (ETo, ETc, and ETa, respectively), in Lonzee, in 2004-2005.

ETa modeled values were very similar to observations. The cumulated ETa observed values was in fact computed equal to 337 mm and the modeled one was372 mm. SIMETAW_R well matched the Eddy Covariance measurements for the entire growing season (Figure 63).

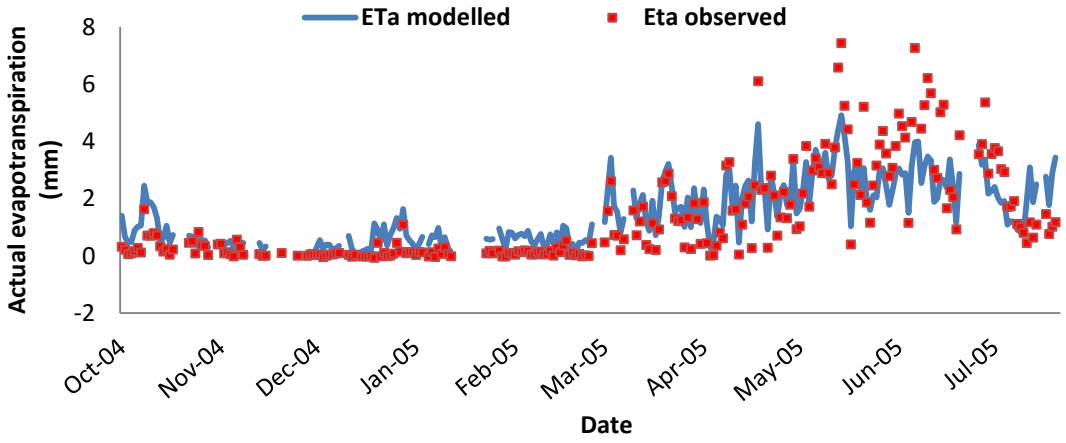

Fig. 63. Daily trend of modeled and observed actual evapotranspiration, in Lonzee, in 2004-2005.

Modeled data and Eddy Covariance data were strongly and significantly correlated (r=0.89, P ≤ 0.001). The index of agreement was equal to 90% (Table 24). The overestimation of SIMETAW_R model was very low (MBE=0.14 mm) in this season.

Tab. 24. Statistical indices used to assess SIMETAW_R model performance, in Lonzee, in 2004-2005.

SITE	YEAR	CROP	r	RMSE	MBA	MBE	IA	RE	R^2	a	b
				mm	mm	mm	%	%	%		
Lonzee	04-05	WHEAT	0.89***	0.89	0.65	0.14	90	10.64	79	0.71	0.58

*P ≤ 0.05; **P ≤ 0.01; ***P ≤ 0.001

Table 25 explains the percentage of data gap filled in the original dataset.. The energy closure balance equation was characterized by a slope and R^2 equal to 0.79 and 77%, respectively, and this underlined the good accuracy of the measured data, since they are in line with the standard value.

Tab. 25. Percentage of gap filled data in the original dataset, in Lonzee, in 2004-2005.

SITE	YEAR	CROP	CO_2	Rn	Ta	WS	H	LE	VPD	PCP
			%	%	%	%	%	%	%	%
Lonzee	2004-2005	WHEAT	4.64	6.10	8.31	2.70	26.00	20.39	0.00	7.82

Lonzee, wheat, 2006-2007

Wheat was not irrigated in the experimental site. Since the cumulated precipitation was enough to supply crop water requirement the Ks was equal to 1, and there was not any stress condition (Figure 64).

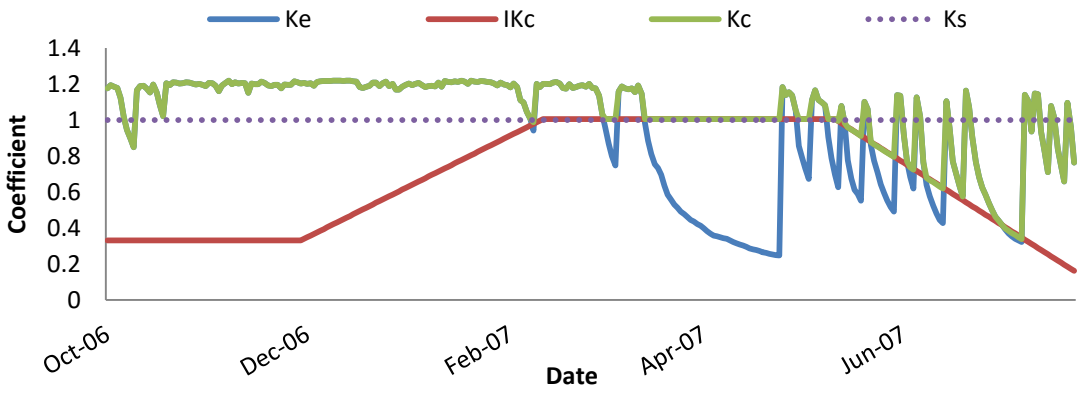

Fig. 64. Daily trend of the crop coefficient for the bare soil (Ke), the generalized crop coefficient (IKc), the crop coefficient (Kc), and the stress coefficient (Ks) during wheat growing season, in Lonzee, in 2006-2007.

ETa values were equal to ETc values because any water deficit was measured (Figure 65). ETo values were higher than ETc at the end of the growing season and this is maybe due to the high temperature measured in this period.

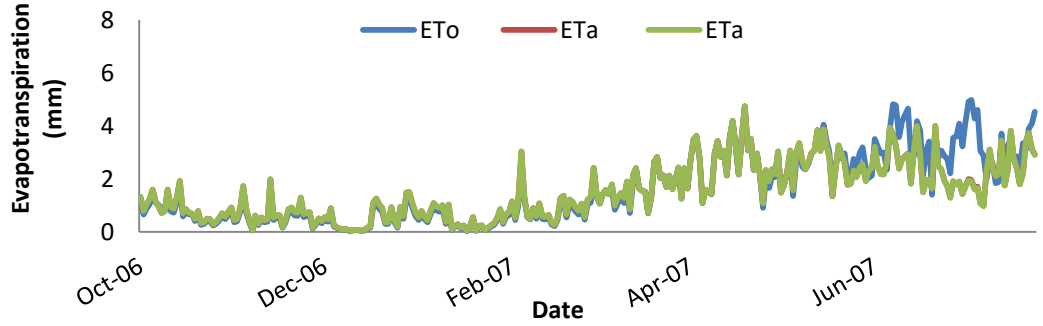

Fig. 65. Daily trend of reference, crop, and actual evapotranspiration (ETo, ETc, and ETa, respectively), in Lonzee, in 2006-2007.

The performance of SIMETAW_R model were assessed comparing observed and modeled ETa.The cumulated modeled and observed ETa values were 411 mm and 260 mm, respectively. Simulated values tended to be slightly higher than the observed ones from sowing to about April (Figure 66).

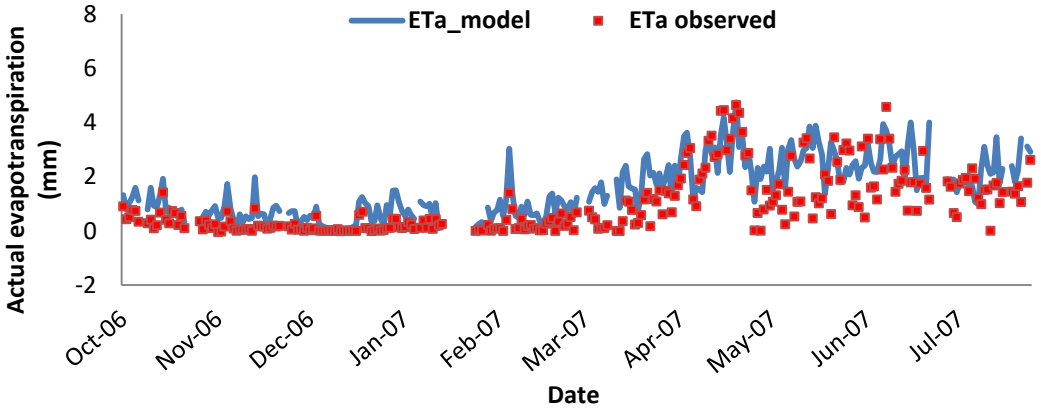

Fig. 66. Daily trend of modeled and observed actual evapotranspiration, in Lonzee, in 2006-2007.

Model performance are shown in Table 26. The Pearson's coefficient value (0.78) was significant for $P \leq 0.001$. The coefficient of determination was equal to 61% and the index of agreement was the 82% as well as the high angular coefficient (b=0.82) confirmed the model accuracy.

Tab. 26. Statistical indices used to assess SIMETAW_R model performance, in Lonzee, in 2006-2007.

SITE	YEAR	CROP	r	RMSE	MBA	MBE	IA	RE	R^2	a	b
				mm	mm	mm	%	%	%		
Lonzee	06-07	WHEAT	0.78***	0.91	0.72	0.57	82	19.47	61	0.76	0.82

*P ≤ 0.05; **P ≤ 0.01; ***P ≤ 0.001

Table 27 indicates the data gap filled in the original dataset. The percentage of LE gap filled values in this site was equal to about the 3%. The energy balance closure is defined by a slope of 79 and a R^2 of 77%, and this highlighted the good accuracy of the measured variables, which may explain the good model performance .

Tab. 27. Percentage of gap filled data in the original dataset, in Lonzee, in 2006-2007.

SITE	YEAR	CROP	CO_2	Rn	Ta	WS	H	LE	VPD	PCP
			%	%	%	%	%	%	%	%
Lonzee	06-07	WHEAT	4.38	4.13	4.69	3.33	0.00	3.03	16.09	9.18

1.3.7 Borgo Cioffi (IT-BCi)

Meteorological characterization

Climate and fluxes data were elaborated for maize growing season in four years, from May 17th to August 24th 2005, from April 27th to August 22nd 2006, from May 9th to August 24th 2007, from June 12th to October 8th 2009.

According to Köppen climate classification Borgo Cioffi climate is classified as "warm temperate with dry, hot summer" (https://fluxnet.ornl.gov/).

The mean temperature in Borgo Cioffi was 22.26 °C in 2005, 21.32 °C in 2006, 22.47 °C in 2007, and 24.50 °C in 2009. The maximum and minimum mean temperature were 27.35 °C and 16.87 °C in 2005, 25.35 °C and 15 °C in 2006, 27.32 °C and 17.40 °C in 2007, and 28.71 °C and 19.97 °C in 2009 (Figure 67).

The cumulative precipitation values were 105 mm, 144 mm, 112 mm , and 25 mm in 2005, 2006, 2007, and 2009, respectively. A peak of precipitation was measured in summer 2007 (56.89 mm). The lowest value of saturation vapor pressure was 0.80 kPa in 2006. In all the other years, the VPD value was about 0.86 kPa. The maximum VPD peak (3.26 kPa) was measured in August 2007.

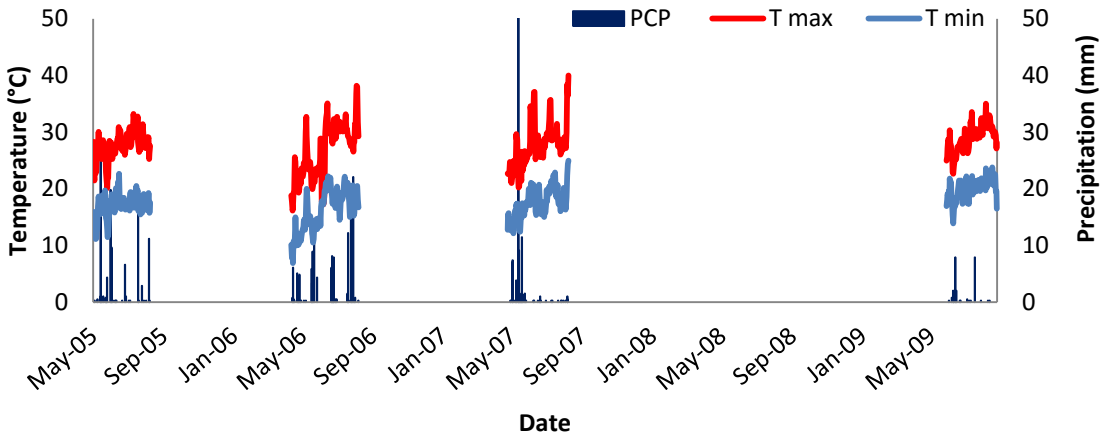

Fig. 67. Trend of daily maximum temperature (Tmax), minimum temperature (Tmin), mean temperature (Tmean), and precipitation (PCP) in Borgo Cioffi, in 2005, 2006, 2007, 2009.

The cumulated net radiation was 1410 MJ m^{-2}, 1665 MJ m^{-2}, 1537 MJ m^{-2}, and 1273 MJ m^{-2} in 2005, 2006, 2007, and 2009, respectively. The mean wind speed was measured equal to 1.79 m s^{-1}, 1.67 m s^{-1}, 1.64 m s^{-1}, 1.84 m s^{-1} in 2005, 2006, 2007, and 2009, respectively.

Reference evapotranspiration

The cumulative value of ETo_PM and ETo_HS were 472 mm and 270 mm in 2005, 525 mm and 314 mm in 2006, 499 mm and 300 mm in 2007, and 424 mm and 220 mm in 2009 (Figure 68). The low ETo_HS values were maybe related to the high temperature and low relative umidity which characterized the site. ETo_PM values were mainly influenced by the trend of temperature and saturation vapor pressure and wind speed, specifically peaks of ETo_PM were observed in correspondence with the highest temperature and VPD values observed in each season.

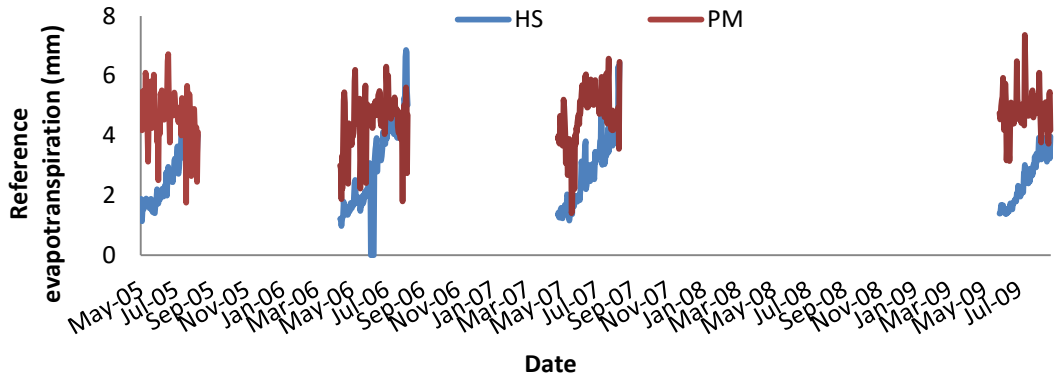

Fig. 68. Trend of daily reference evapotranspiration, in Borgo Cioffi, in 2005, 2006, 2007, and 2009.

Model results evaluation

The crop under study was irrigated, hence water supply did not come only from precipitation. No water deficit was defined according to the model because the net irrigation application totally supplied crop water requirement (Figures 69 and 70). The observed net irrigation was compared in this work with the modeled one. The site received 330 mm, 300 mm, 396 mm, and 291 mm of water in the growing seasons 2005, 2006, 2007, and 2009, respectively. The model simulated a total amount of water per season equal to 259 mm, 288 mm, 317 mm, and 230 mm. The difference between the observed value and the modeled one was less than 80 mm. The model simulated also the number of hypothetical irrigation that was equal to 9, 10, 11, and 8, during the four seasons.

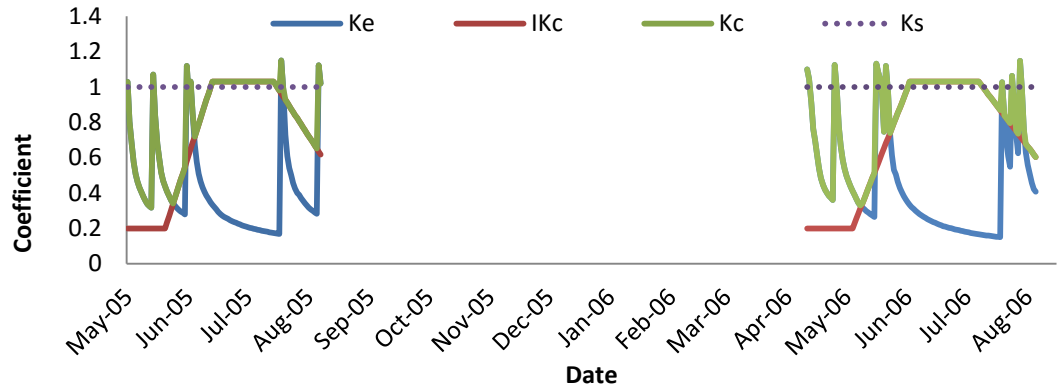

Fig. 69. Daily trend of the crop coefficient for the bare soil (Ke), the generalized crop coefficient (IKc), the crop coefficient (Kc), and the stress coefficient (Ks) during maize growing season, in Borgo Cioffi, in 2005 and 2006.

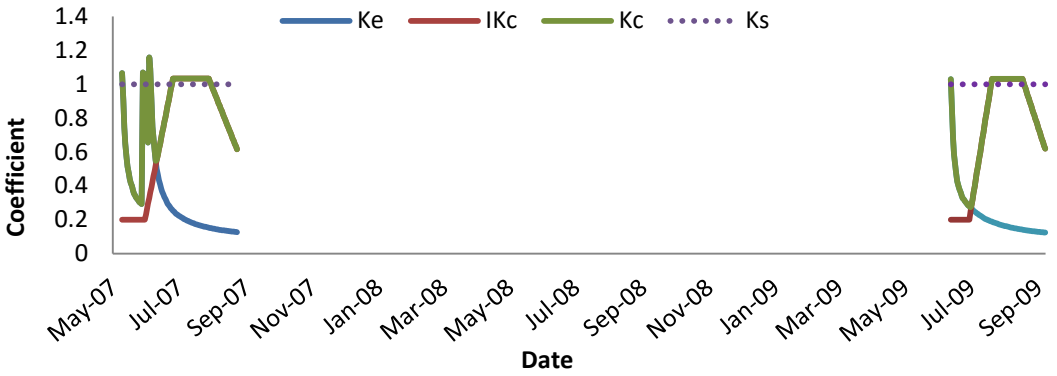

Fig. 70. Daily trend of the crop coefficient for the bare soil (Ke), the generalized crop coefficient (IKc), the crop coefficient (Kc), and the stress coefficient (Ks) during maize growing season, in Borgo Cioffi, in 2007 and 2009.

Since any water deficit occurred, ETa was equal to ETc (Figure 71 and 72).

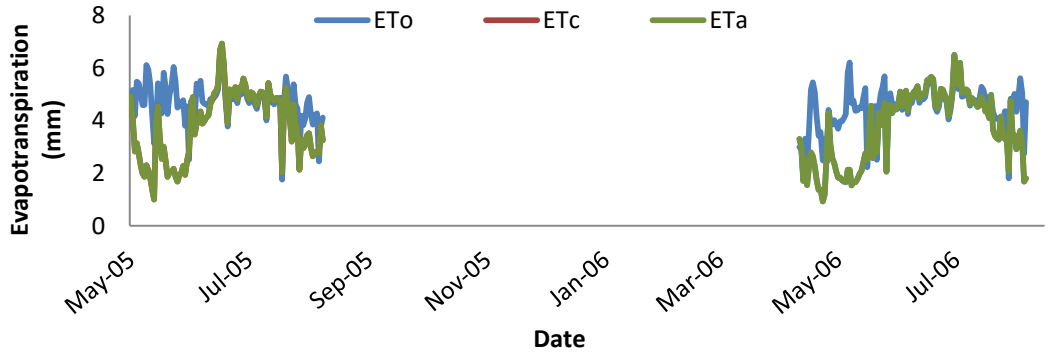

Fig. 71. Daily trend of reference, crop, and actual evapotranspiration (ETo, ETc, and ETa, respectively), in Borgo Cioffi, in 2005 and 2006.

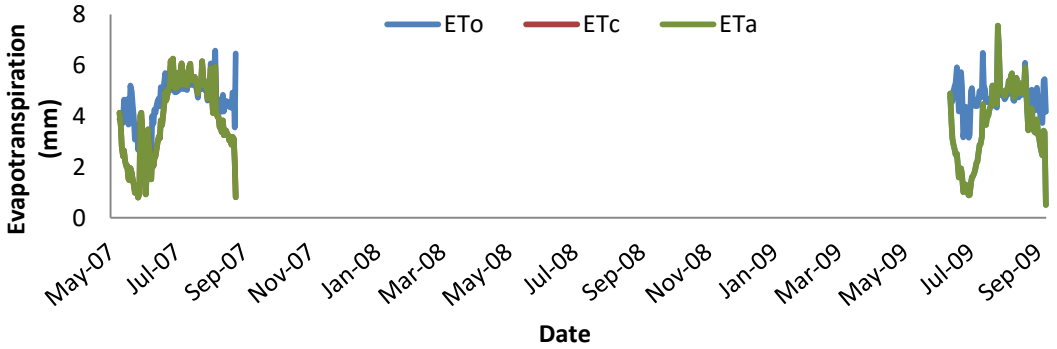

Fig. 72. Daily trend of reference, crop, and actual evapotranspiration (ETo, ETc, and ETa, respectively), in Borgo Cioffi, in 2007 and 2009.

Model performance were assessed comparing modeled and observed ETa values (Figures 73, 74, 75, and 76). The cumulated observed ETa values was 257 mm and the modeled 304 mm in 2005, while lower values were found in season 2006 where the observed ETa cumulated value was 223 and the modeled 282 mm. The highest

measured (335 mm) and simulated (414 mm) ETa values were found in season 2007, while the lowest were shown in 2009 where measured and simulated ETa values were 221 and 258 mm, respectively. Diffferences between ETa values simulated using SIMETAW_R and measured by the EC stations were never higher than 80 mm.

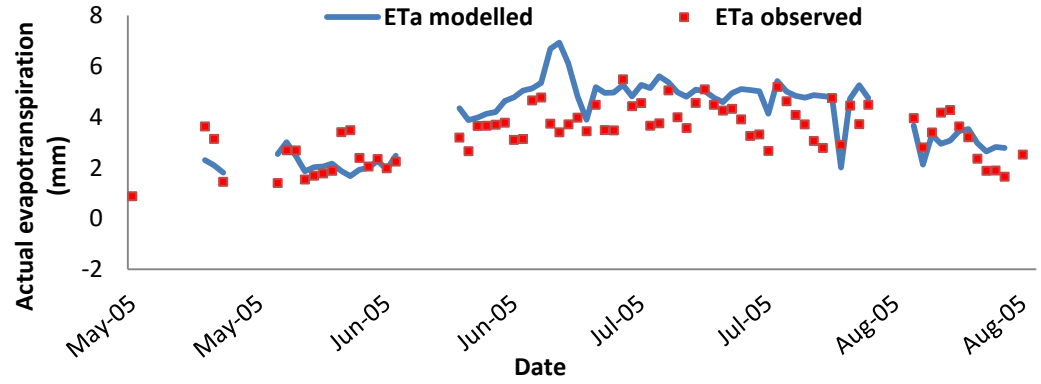

Fig.73. Daily trend of modeled and observed actual evapotranspiration, in Borgo Cioffi, in 2005.

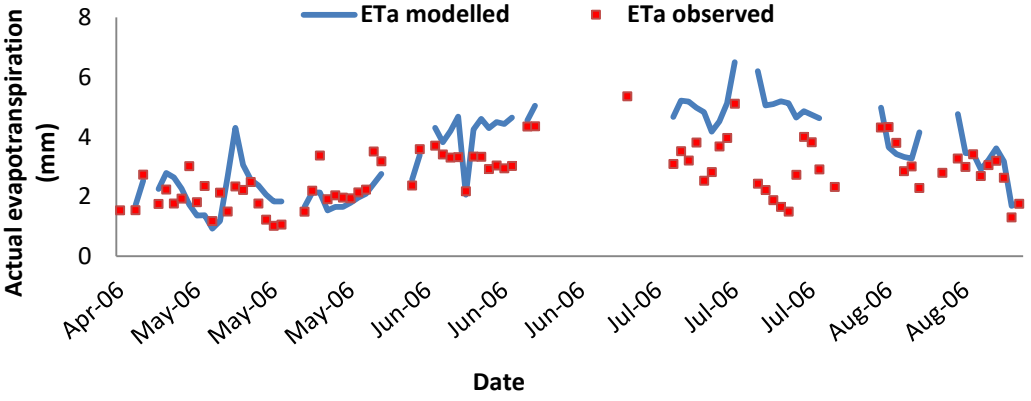

Fig. 74. Daily trend of modeled and observed actual evapotranspiration, in Borgo Cioffi, in 2006.

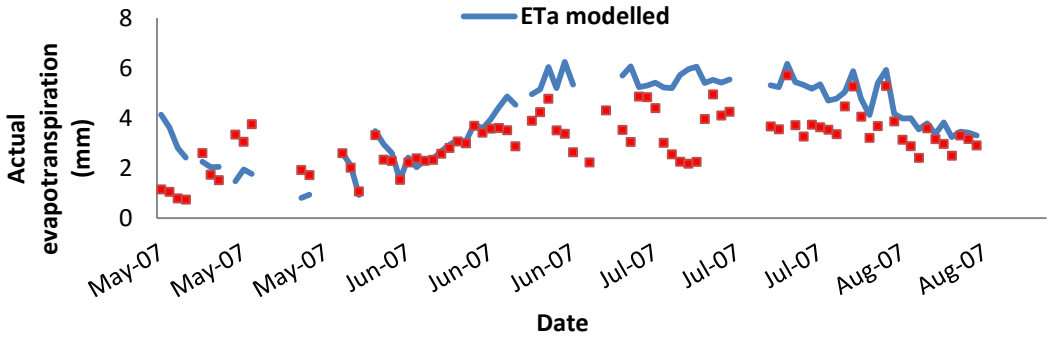

Fig. 75. Daily trend of modeled and observed actual evapotranspiration, in Borgo Cioffi, in 2007.

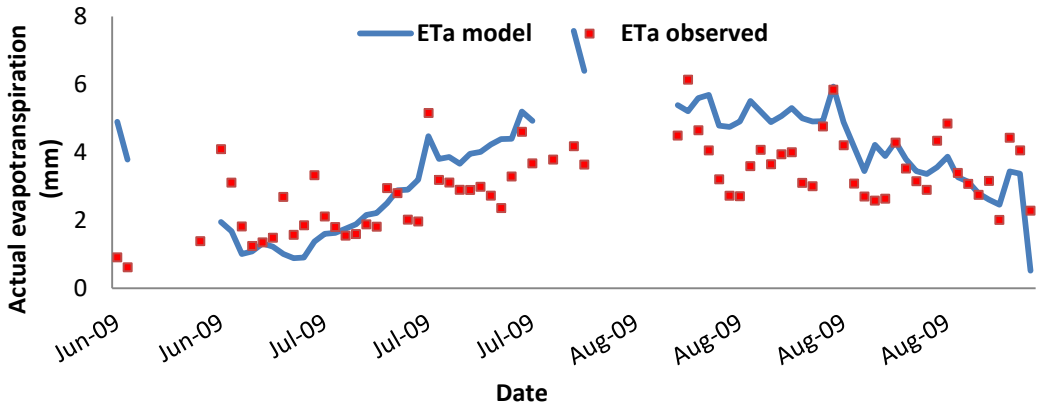

Fig. 76. Daily trend of modeled and observed actual evapotranspiration, in Borgo Cioffi, in 2009.

The Pearson's coefficient value was never higher than 0.65 in all seasons. The performance of the model were defined by the high RMSE and RE. The root mean square error was in fact always higher than 1 mm and the relative error close to 30%. Data dispersion was high, and this is affirmed by a R^2 never higher than 40 (Table 28).

Tab. 28. Statistical indices used to assess SIMETAW_R performance, in Borgo Cioffi, in 2005, 2006, 2007, and 2009.

SITE	YEAR	CROP	r	RMSE	MBA	MBE	IA	RE	R^2	a	b
				mm	mm	mm	%	%	%		
Borgo Cioffi	05	MAIZE	0.64***	1.21	0.92	0.62	0.73	26.24	41	1.19	0.82
Borgo Cioffi	06	MAIZE	0.62***	1.29	0.97	0.73	0.69	29.73	39	0.99	0.90
Borgo Cioffi	07	MAIZE	0.63***	1.48	1.12	0.93	0.68	29.70	40	1.29	0.88
Borgo Cioffi	09	MAIZE	0.63***	1.32	1.03	0.51	0.75	23.86	40	0.95	0.86

*P ≤ 0.05; **P ≤ 0.01; ***P ≤ 0.001

The performance of SIMETAW_R model in each season under investigation, in Borgo Cioffi, coud be explained through both the high percentage of gap filled data (Table 29), which was always around the 23%, and the energy balance closure. The regression line of the energy balance closure showed a slope of the 1:1 line between 0.58 and 0.65 which was lower than 0.70, i.e. the standard acceptable value. In addition the R^2 was never higher than 70%.

Tab. 29. Percentage of gap filled data in the original dataset, in Borgo Cioffi, in 2005, 2006, 2007, and 2009.

SITE	YEAR	CROP	CO_2	Rn	Ta	WS	H	LE	VPD	PCP
			%	%	%	%	%	%	%	%
Borgo Cioffi	05	MAIZE	17.73	4.63	0.00	16.71	16.75	21.60	0.00	0.00
Borgo Cioffi	06	MAIZE	13.05	24.15	1.48	9.52	16.97	26.73	0.00	3.39
Borgo Cioffi	07	MAIZE	11.01	1.66	0.04	7.79	14.87	23.75	0.00	0.00
Borgo Cioffi	09	MAIZE	4.66	5.08	0.00	0.84	4.75	18.63	0.00	0.00

1.3.8 Negrisia (IT-Neg)

Meteorological characterization

Climate and fluxes data were elaborated from April 1st to October 15th, in 2007 and 2008 and grape was cultivated in the field.

According to Köppen climate classification Negrisia climate is classified as "warm temperate with dry, hot summer" (https://fluxnet.ornl.gov/).

The mean temperature in Negrisia was 18.86 °C in both seasons. The maximum and minimum temperature were 36.49 °C and -2.09 °C in 2007, 35.81 °C and 8.08 °C in 2008. The cumulative precipitation values were 440 and 599 mm, in 2007 and 2008, respectively, with a maximum value of precipitation equal to 104 mm measured in May (Figure 77). The saturation vapor pressure value was 0.79 kPa in 2007, and 10 kPa less in 2008.

The cumulated net radiation value was 2291 MJ m^{-2} and 2227 MJ m^{-2} in 2007 and 2008, respectively. The maximum daily value (18.80 MJ m^{-2} d^{-1}) was measured in June 2007. The mean wind speed was 1.4 m s^{-1} in 2007 and 1.44 m s^{-1} in 2008.

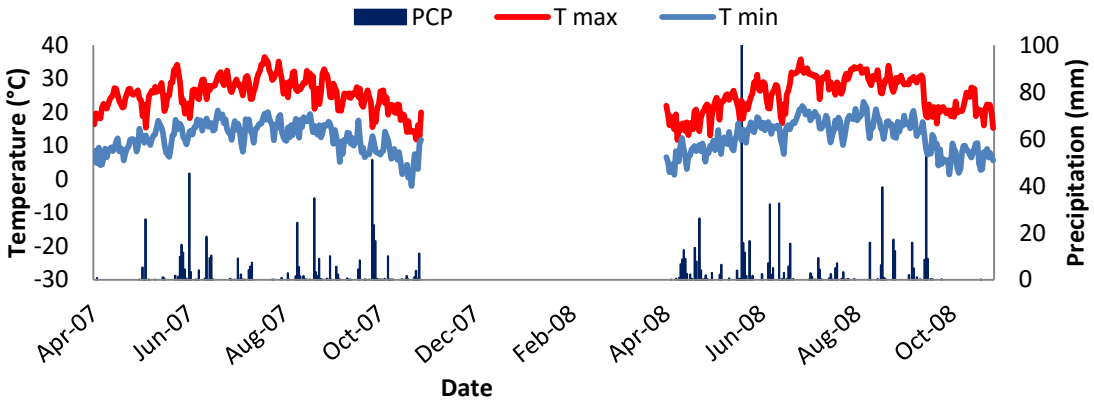

Fig. 77. Trend of daily maximum temperature (Tmax), minimum temperature (Tmin), mean temperature (Tmean), and precipitation (PCP), in Negrisia, in 2007 and 2008.

Reference evapotranspiration

The cumulative value of ETo_PM and ETo_HS were 757 mm and 772 mm in 2007, 719 mm and 770 mm in 2008. The maximum value, considering both years and both equations was around 6 mm (Figure 78). ETo_HS overestimation was observed in correspondence with rainy days. ETo_PM values followed the same trend of T, VPD, WS, and RN, high vales of ETo_PM were found in correspondence with high values of T, VPD and RN, and low WS values.

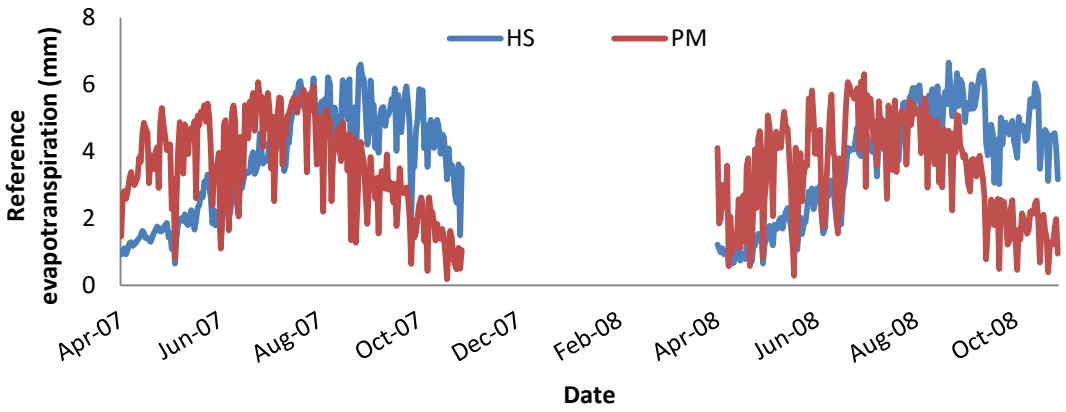

Fig. 78. Trend of daily reference evapotranspiration, in Negrisia, in 2007 and 2008.

Model results evaluation

Negrisia, grape 2007

The crop under study was irrigated, hence water supply did not come only from precipitation. No water deficit was defined according to the model because the net water application totally supplied the crop water requirement, in fact Ks was always equal to 1 (Figure 79). During the mid-season the crop coefficient values were adjusted depending on the local climate and conditions, and the IKc was 0.90 instead than 0.80, i.e. 0.10 higher than SIMETAW_R default value.

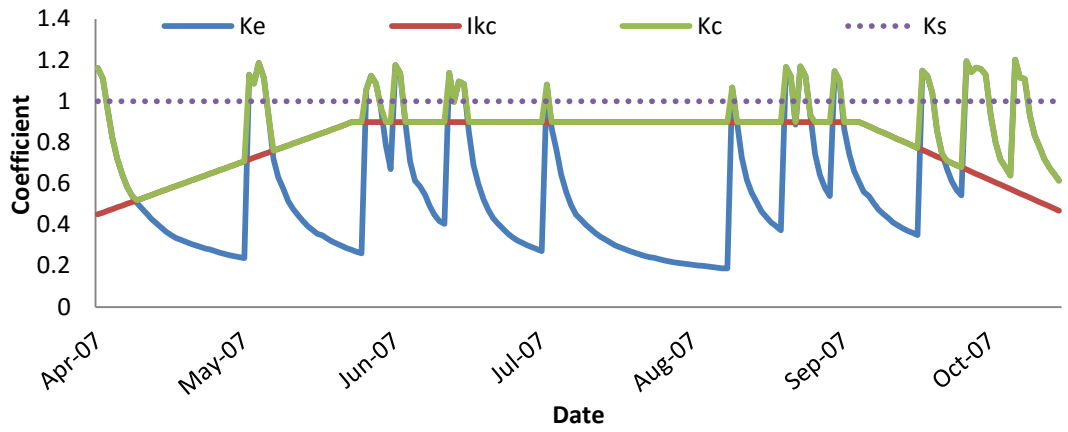

Fig.79. Daily trend of the crop coefficient for the bare soil (Ke), the generalized crop coefficient (IKc), the crop coefficient (Kc), and the stress coefficient (Ks) during grape growing season, in Negrisia, in 2007.

ETa was equal to ETc because no water deficit was computed in this experimental field due to irrigation applications (Figure 80).

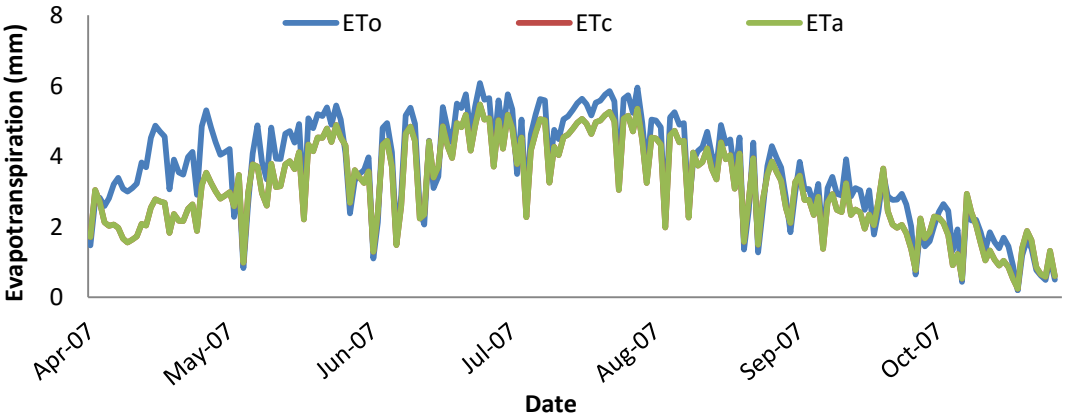

Fig. 80. Daily trend of reference, crop, and actual evapotranspiration, in Negrisia, in 2007.

The cumulated ETa observed values was 940 mm and the modeled 692 mm. Considering that the cumulative precipitation was 439 mm, crop water requirement was satisfied thanks to the water application. Figure 81 shows the trend of ETa observed and measured in Negrisia in 2007.

SIMETAW_R model provided an estimation of the number and the net water application for each event equal to 6 mm and 56.97 mm, respectively. The irrigations events were distributed during the growing season differently (2 in stage BC, 3 in CD,

and 1 in DE). The comparison with observed data was not possible because any information on water application was available for this vineyard.

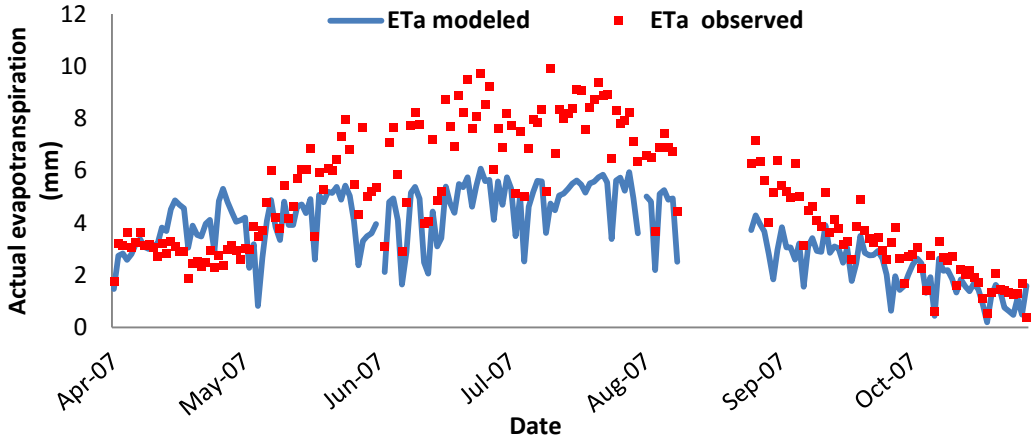

Fig. 81. Daily trend of modeled and observed actual evapotranspiration, in Negrisia, in 2007.

The Pearson's coefficient value was equal to 0.83, and it was significant for $P \leq 0.001$. The high RE is related to the high RMSE. The SIMETAW_R model overestimation was computed equal to 1.30 mm.

The index of agreement (77%) confirmed the good SIMETAW_R model performance for the assessment of grape ETa in Negrisia (Table 30) even though measured ETa values during the midseason were much more higher than the simulated ones, and this could be due to the accuracy of the measured data which is in turn explained by the low energy balance closure value: a value higher than 1 was measured for the slope and a percentage lower than 50 for the R^2.

Tab. 30. Statistical indices used to assess SIMETAW_R performance, in Negrisia, in 2007.

SITE	YEAR	CROP	r	RMSE	MBA	MBE	IA	RE	R^2	a	b
				mm	mm	mm	%	%	%		
Negrisia	07	GRAPE	0.83***	1.91	1.60	1.30	0.77	20.44	69	1.09	0.51

*P ≤ 0.05; **P ≤ 0.01; ***P ≤ 0.001

Wind speed, sensible heat flux, and latent heat flux were the only variables gap filled for a percentage showed in Table 31.

Tab. 31. Percentage of gap filled data in the original dataset, in Negrisia, in 2007.

SITE	YEAR	CROP	CO_2	Rn	Ta	WS	H	LE	VPD	PCP
			%	%	%	%	%	%	%	%
Negrisia	07	GRAPE	0.00	0.00	0.00	10.77	10.78	12.05	0.00	0.00

Negrisia, grape 2008

Grape was irrigated in 2008. The crop water requirement was supplied by the net water applications, thus any water deficit occurred (Figure 82).

Any difference was found between ETc and ETa thanks to the absence of water deficit conditions (Figure 83).

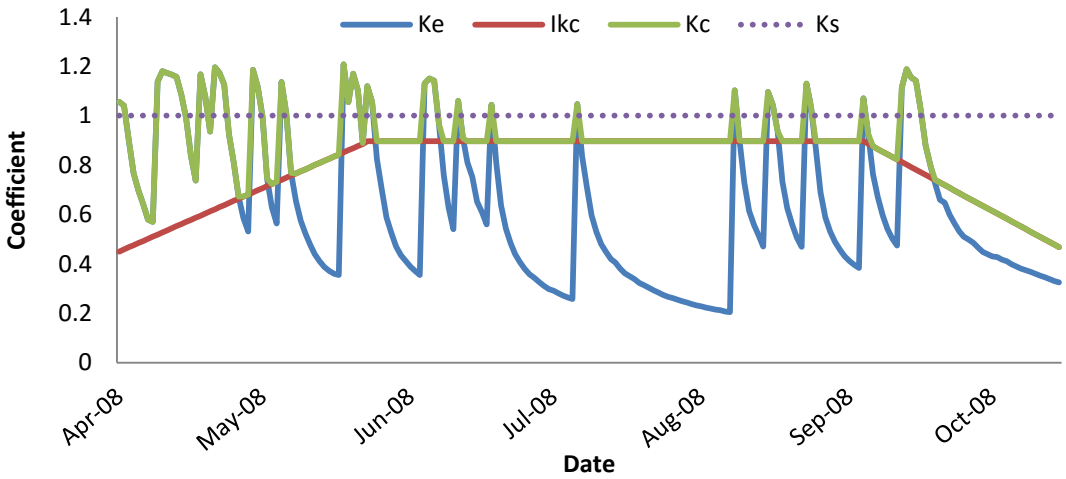

Fig. 82. Daily trend of the crop coefficient for the bare soil (Ke), the generalized crop coefficient (IKc), the crop coefficient (Kc), and the stress coefficient (Ks) during grape growing season, in Negrisia, in 2008.

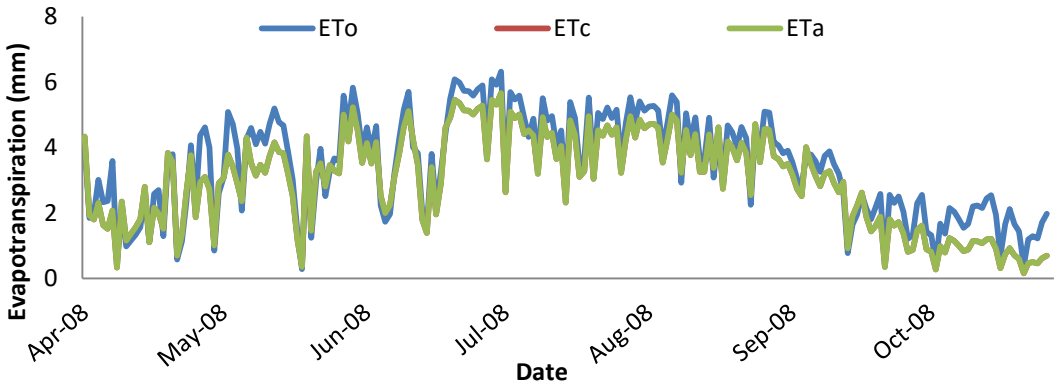

Fig. 83. Daily trend of reference, crop, and actual evapotranspiration, in Negrisia, in 2008.

The accuracy of SIMETAW_R in modeling ETa was assessed by comparing modeled and observed actual evapotranspiration (Figure 84). High values of ETa measured by the EC station were found mainly from the beginning of the crop season to the end of the growing season. The difference between cumulated observed ETa values (990 mm) and the modeled ones (719 mm) was high, and this is more noticeable during the midseason, when modeled values were understimated. Crop water requirement was satisfied thanks to the irrigation events.

The number of irrigation events estimated by the model was 4 (1 in step BC and 3 in CD). Each net water application provided 53.89 mm. Since any information on irrigation was available, the comparison between observed and measured data was not possible.

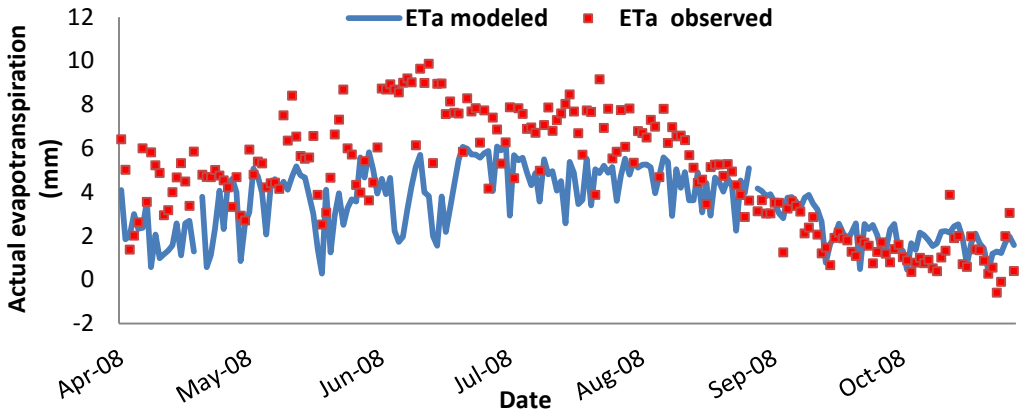

Fig. 84. Daily trend of modeled and observed actual evapotranspiration, in Negrisia, in 2008.

The Pearson's coefficient value and the coefficient of determination were equal to 0.58 and 33%, respectively (Table 32). The index of agreement was 67%. Differences between model and measured data could be explained by the accuracy of measured data assessed by the energy balance closure. The investigation of inputs accuracy showed a dispersion of the data equal to 53% and a slope of the regression line close to 1 (0.99).

Tab. 32. Statistical indices used to assess SIMETAW_R performance, in Negrisia, in 2008.

SITE	YEAR	CROP	r	RMSE	MBA	MBE	IA	RE	R^2	a	b
				mm	mm	mm	%	%	%		
Negrisia	08	GRAPE	0.58***	2.45	1.88	1.31	67	23.48	33	1.80	0.34

*P ≤ 0.05; **P ≤ 0.01; ***P ≤ 0.001

Percentage of data gap filled are repored in Table 33.

Tab. 33. Percentage of gap filled data in the original dataset, in Negrisia, in 2008.

SITE	YEAR	CROP	CO_2	Rn	Ta	WS	H	LE	VPD	PCP
			%	%	%	%	%	%	%	%
Negrisia	2008	GRAPE	8.60	0.00	0.00	0.26	0.28	1.76	0.00	0.00

1.3.9 Valle dell'Adige (IT-VdA)

Meteorological characterization

Climate and fluxes data were elaborated for grape growing season, from April 15th 2009 to September 5th, 2005.

Köppen climate classification indicates Valle dell'Adige climate as "snow, fully humid, warm summer".

The mean temperature in Valle dell'Adige was 19.94 °C during the grape growing season. The maximum and minimum mean temperature were 33.72 °C and -1.28 °C (Figure 85). The cumulative precipitation values was 140 mm. The mean saturation vapor pressure was 0.59 kPa. The maximum precipitation value measured was 30 mm in August.

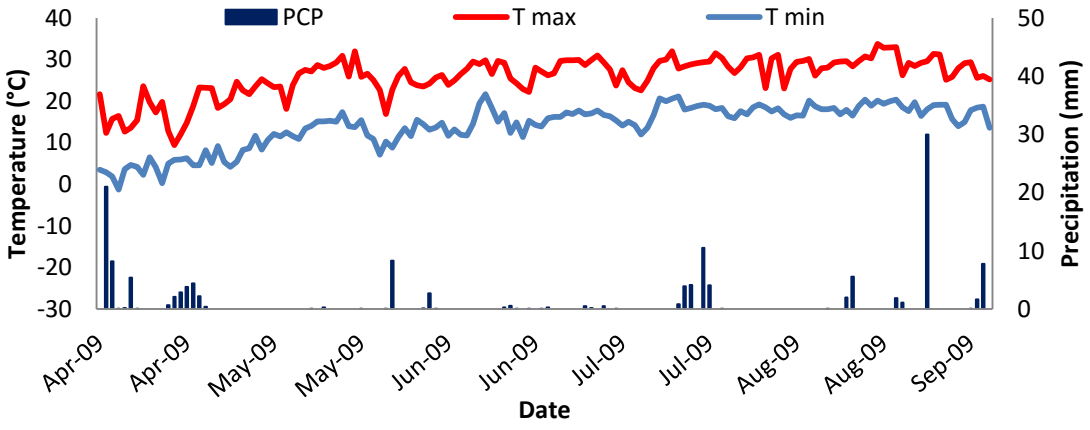

Fig. 85. Trend of daily maximum temperature (Tmax), minimum temperature (Tmin), mean temperature (Tmean), and precipitation (PCP), in Valle dell'Adige, in 2009.

The cumulated net radiation was 1548 MJ m^{-2}, with a maximum daily value of 18.35 MJ m^{-2} d^{-1} in June. The mean wind speed was 2.01 m s^{-1} with a maximum value equal to 5.31 m s^{-1} in June.

Reference evapotranspiration

The cumulative value of ETo_PM and ETo_HS were 509 mm and 433 mm in 2009 season. The maximum ETo_PM value was equal to 6.79 mm (Figure 86). ETo_HS tended to be .lower for the almost the entire grape growing season, and it may be due to the almost complete absence of precipitation events. The ETo_PM followed the same trend of the temperature, net radiation and saturation vapor pressure; minimum and maximum peaks of ETo were observed in correspondence with their minimum and maximum peaks.

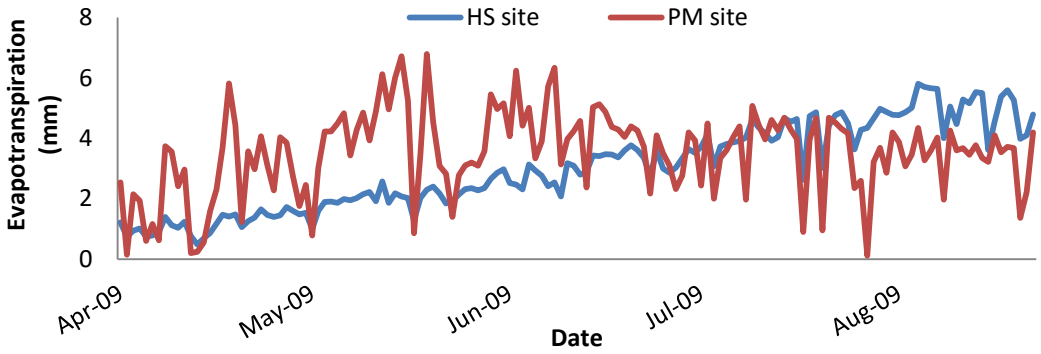

Fig. 86. Trend of daily reference evapotranspiration, in Valle dell'Adige, in 2009.

Model results evaluation

The vineyard cultivated in Valle dell'Adige site was irrigated, and any water deficit was measured during the growing season. Ks was always equal to 1 because precipitation and irrigation satisfied the crop water requirement (Figure 87). During the mid-season, the IKc values were adjusted depending on the local climate and conditions, in fact the value was 0.11 higher than the model default value (0.80).

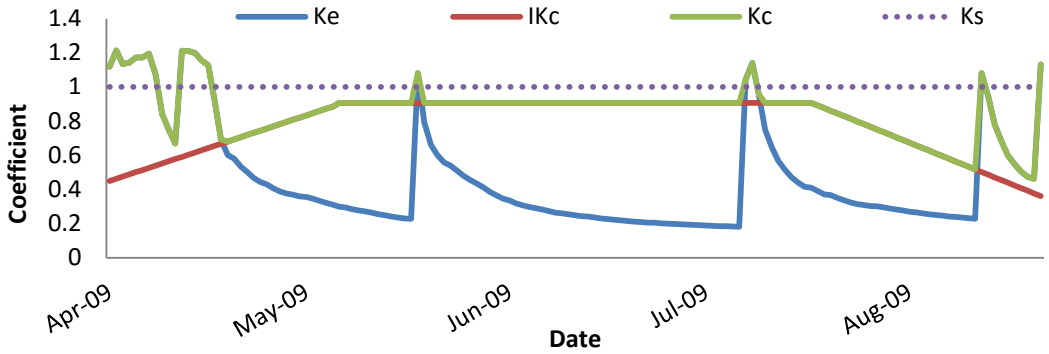

Fig. 87. Daily trend of the crop coefficient for the bare soil (Ke), the generalized crop coefficient (IKc), the crop coefficient (Kc), and the stress coefficient (Ks) during grape growing season, in Valle dell'Adige, in 2009.

In Figure 88, the daily values of ETo, ETc, and ETa referred to grape growing season are shown. ETa was equal to ETc because no water deficit was observed in this experimental field (Figure 84).

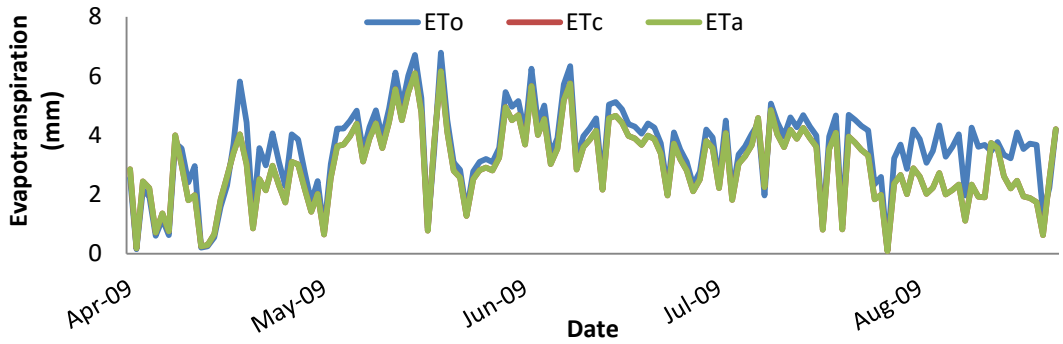

Fig. 88. Daily trend of reference, crop, and actual evapotranspiration, in Valle dell'Adige, in 2009.

The cumulated ETa observed values was 523 mm and the modeled one totaled 410 mm (Figure 89).

SIMETAW_R estimated 6 irrigations to supply crop water requirement was 6. The total amount of water allocated was 322 mm, i.e. 53.58 mm for each event. The information related to the net water application in the vineyard indicated a higher value (400-700 mm season^{-1}, 150-200 mm month^{-1}) than the simulated one.

According to SIMETAW_R model estimation, the total amount of water needed to satisfy the crop water requirement is lower than the observed water application, thus in this site, under the specific management practices applied, the crop and soil characteristics, the grape growth could be allowed using 78-378 mm of water less.

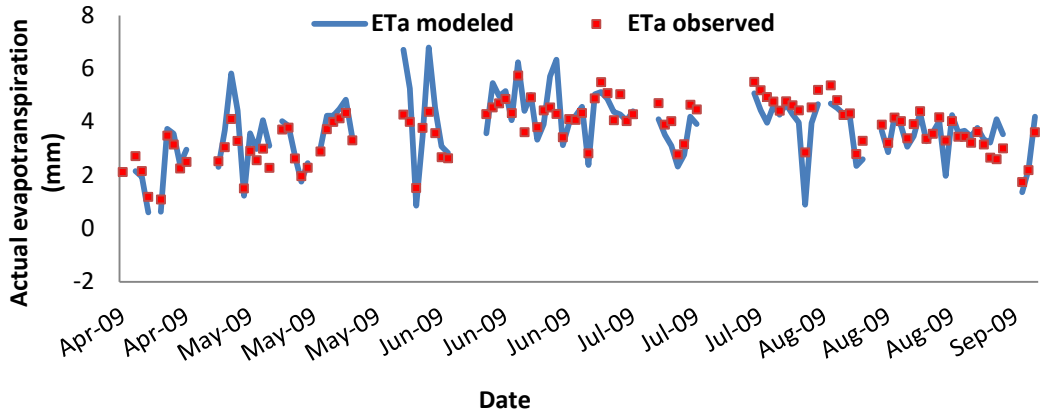

Fig. 89. Daily trend of modeled and observed actual evapotranspiration, in Valle dell'Adige, in 2009.

Observed and simulated ETa values were highly and significantly correlated (r=0.82, P ≤ 0.001) (Table 34). The good SIMETAW_R performance were confirmed also by the high slope (0.99) and the low intercept (0.08) values of the 1:1 line.

Tab. 34. Statistical indices used to assess SIMETAW_R performance, in Valle dell'Adige, in 2009.

SITE	YEAR	CROP	r	RMSE	MBA	MBE	IA	RE	R^2	a	b
				mm	mm	mm	%	%	%		
Valle dell'Adige	09	GRAPE	0.82***	0.68	0.50	0.06	90	14.67	68	0.08	0.99

*P ≤ 0.05; **P ≤ 0.01; ***P ≤ 0.001

Differences between measured and observed data could be determined by the high percentage of gap filled data, particularly LE values (23.42%) (Table 35). The R^2 and the slope of the regression between R-G and H+LE was equal to 75% and 0.60, respectively, and it explained the good accuracy of the data, thus the performance of SIMETAW_R.

Table 35 reports the percentage of gap filled data.

Tab. 35. Percentage of gap filled data in the original dataset, in Valle dell'Adige, in 2009.

SITE	YEAR	CROP	CO_2	Rn	Ta	WS	H	LE	VPD	PCP
			%	%	%	%	%	%	%	%
Valle dell'Adige	09	GRAPE	8.26	3.83	8.26	17.04	23.34	23.42	0.00	11.11

1.3.10 Gebesee (De-Geb)

Meteorological characterization

Climate and fluxes data were elaborated for wheat growing season, from November 9th 2006 to August 7th 2007.

Köppen classification indicates Gebesee climate as "Warm temperate, fully humid with warm summer" (https://fluxnet.ornl.gov/).

During plant growth, the site was characterized by a maximum, minimum, and mean temperature value equal to 36.04 °C, -9.15 °C, and 10.45 °C, respectively in 2006-2007. The cumulative value equal to 325 mm (Figure 90).

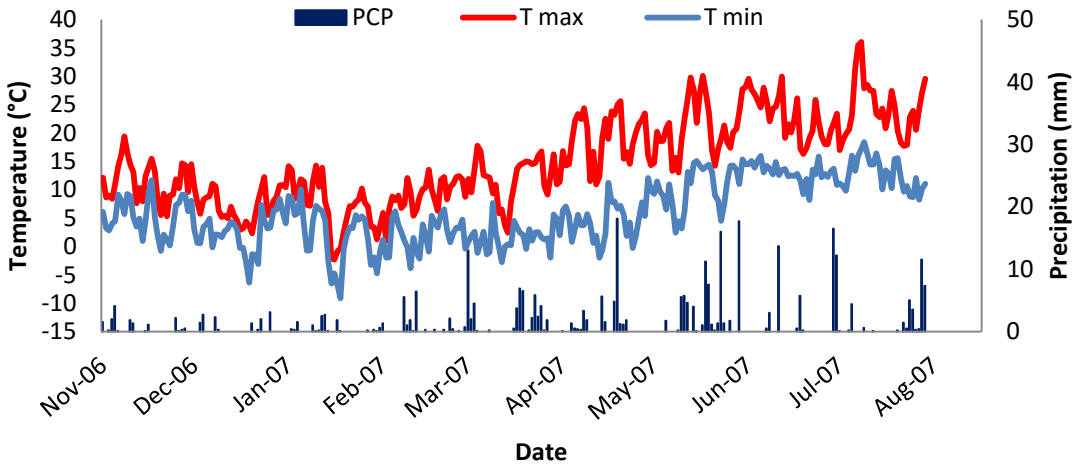

Fig. 90. Trend of daily maximum temperature (Tmax), minimum temperature (Tmin), mean temperature (Tmean), and precipitation (PCP), in Gebesee, in 2006-2007.

The cumulative value of net radiation was 1183 MJ m^{-2} in season 2006-2007. The mean wind speed value was the same in both seasons (3.43 m s^{-1}).

Reference evapotranspiration

The cumulative value of ETo_PM and ETo_HS were 534 mm and 651 mm in 2006-2007 season.The maximum ETo value was computed in 2007 using ETo_PM, and it was equal to 7.44 mm. ETo_HS maximum value was 6.27 mm and the mean saturation vapor pressure value was 0.17 kPa (Figure 91). The frequency and the intensity of precipitation influenced the ETo_HS values which tended to be higher than ETo_PM

equation until June, where instead, in correspondence with VPD, peaks higher values of ETo_PM were observed.

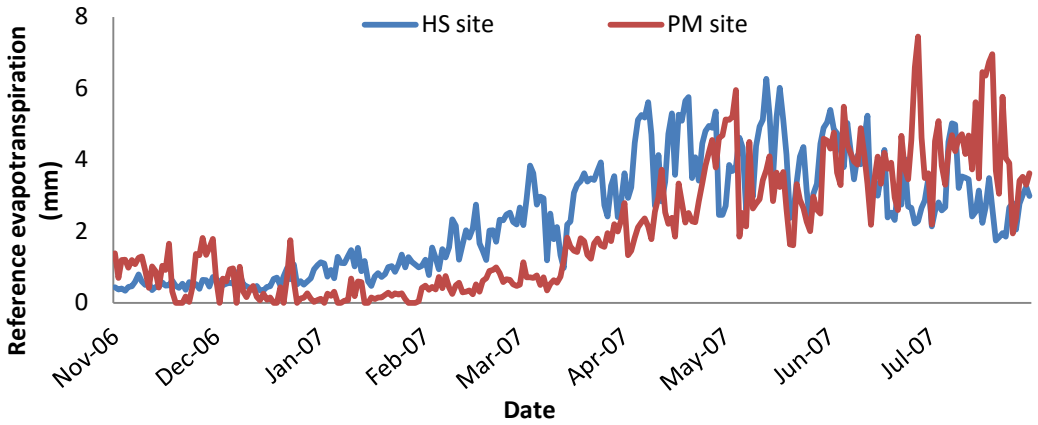

Fig. 91. Trend of daily reference evapotranspiration, in Gebesee, in 2006-2007.

Model results evaluation

Gebesee, wheat, 2006-2007

The crop under study was not irrigated, hence water supply came only from precipitation. Water deficit was measured during the late season and this was confirmed by the lower values of Ks. During the mid-season IKc values were adjusted depending on the local climate and conditions (Figure 92).

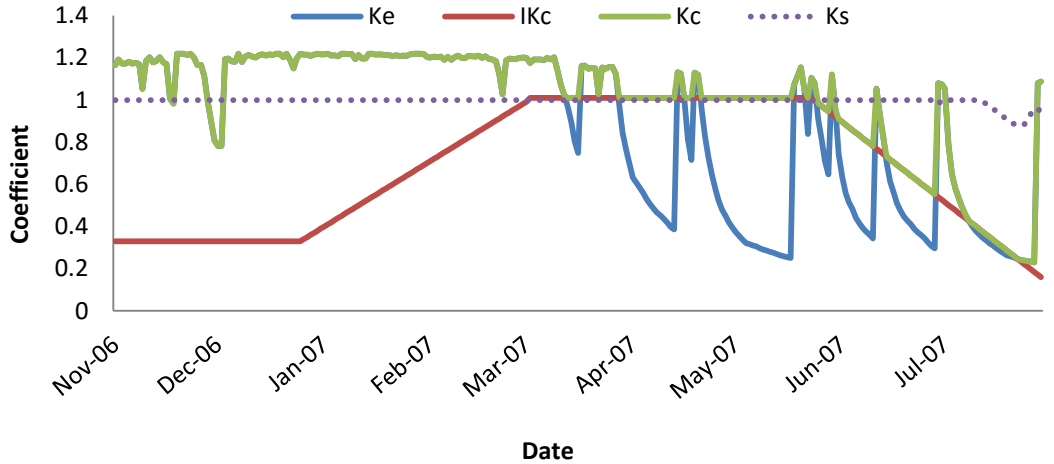

Fig. 92. Daily trend of reference, crop, and actual evapotranspiration, in Gebesee, in 2006-2007.

ETo, ETc, and ETa trend are shown in Figure 93, where ETa values were lower than ETc values in the late season probably due to a reduced amount of available water.

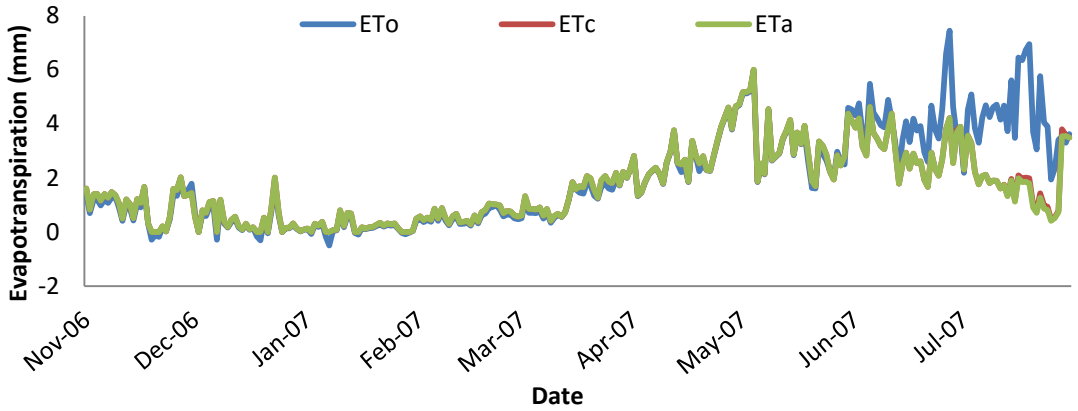

Fig. 93. Daily trend of reference, crop, and actual evapotranspiration (ETo, ETc, and ETa, respectively), in Gebesee, in 2006-2007.

Modeled cumulated ETa value were equal to 376 mm, about 231 mm higher than the observed one (Figure 94). The model well matched the observed values in almost the entire wheat growing season. Simulated values were a bit higher than the observed ones in particular in March, May, and in the first weeks of July.

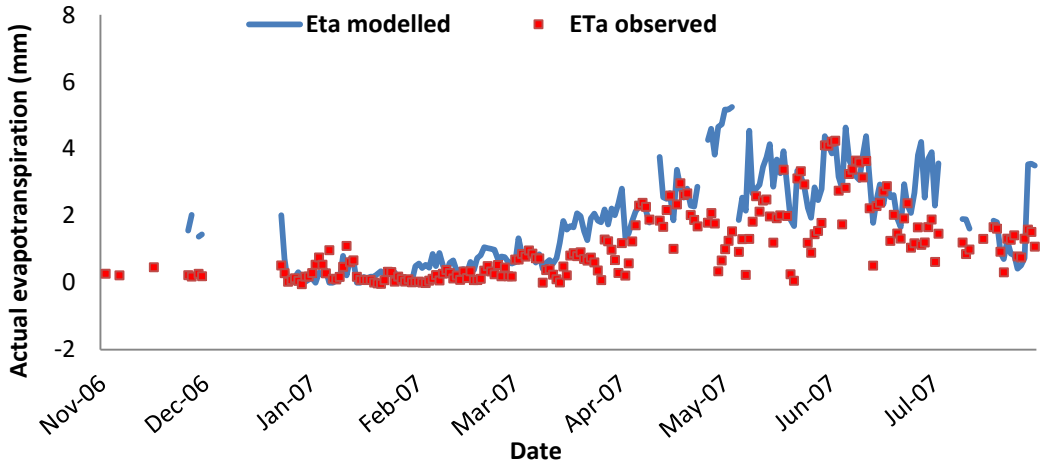

Fig. 94. Daily trend of modeled and observed actual evapotranspiration, in Gebesee, in 2006-2007.

The Pearson's coeffient value was significan for $P \leq 0.001$. The high dispersion of the data was indicated by the R^2 equal to 56% (Table 36). The index of agreement was equal to 78%. The model tended to overestimate mostly in May and July when several LE measurements were gap filled (Table 37).

Tab. 36. Statistical indices used to assess SIMETAW_R performance, in Gebesee, in 2006-2007.

SITE	YEAR	CROP	r	RMSE	MBA	MBE	IA	RE	R^2	a	b
				mm	mm	mm	%	%	%		
Gebesee	06-07	WHEAT	0.75***	1.14	0.78	0.69	78	26.56	56	0.71	0.99

*P ≤ 0.05; **P ≤ 0.01; ***P ≤ 0.001

The energy balance closure showed a high coefficient of determination (81%), thus a low data dispersion around the 1:1 line, but an angular coefficient which was closed to the threshold of acceptability (b=0.70).

Tab. 37. Percentage of gap filled data in the original dataset, in Gebesee, in 2006-2007.

SITE	YEAR	CROP	CO_2	Rn	Ta	WS	H	LE	VPD	PCP
			%	%	%	%	%	%	%	%
Gebesee	06-07	WHEAT	5.76	0.00	0.00	0.08	6.79	13.00	0.00	0.00

1.4 DISCUSSIONS AND CONCLUSIONS

The analysis of the original database led to state that the differences between measured and modeled data were mainly concentrated during rainy days. Even if the Eddy Covariance data are subjected to quality checks, still some influence of the rain in measuring LE fluxes could occur. Since most of the sites are located in the North Europe, where cloudy and rainy days characterized the growing season, the low value of the energy balance closure calculated in the measured fluxes, could be partly explained by the meteorological conditions in these sites. Measured data were closed to the simulated one mainly during period characterized by low or absent precipitation. According to the literature (Twine et al., 2000; Wilson et al., 2002) a deviation equal to 20-30% is normal when surface energy balance closure is computed. However, in some sites (Negrisia, Valle dell'Adige, Borgo Cioffi) these values were under the acceptable standard threshold, and it may explain the differences between measured and simulated ETa values.

The model performance were also probably influenced by the percentage of gap filled data. Even if only days with less than 30% of half-hour measurements were kept in order to perform the model evaluation, still in some sites, the amount of ETa, as well as meteorological missing data, could affect model performance.

The best SIMETAW_R performance were reached in sites where wheat was cultivated: the correlation between modeled and measured data ranged from 92% (Oensingen) to 82% (Lamasquère). Values lower than 70% were found in Gebesee and Lonzee (2006-2007) where the frequency and the intensity of the precipitation influenced probably the measurements. In addition, in the Gebesee database the percentage of gap filled data was high (Table 35 and 36).

The best correlation found in the comparison between simulated and observed maize data was found in Klingenberg, where LE data were gap filled only for about 1%. The good performance in Grignon, in both growing seasons, were explained also by the high coefficient of determination of the energy balance equal to 78% and 80%, in 2005 and 2005-2006 periods. High RMSE (1.22) and a low R^2 (37%) values were computed during maize growth in Lamasquère, and this could be related to the 37% of gap filled

data and the low accuracy of original data, which was expressed by a 1:1 energy balance closure line characterized by a slope of 0.57 and a R^2 of 57%.

Root mean square error higher than 1 were calculated, in each season, in Borgo Cioffi, where the R^2 value was equal to 41%. The performance in this site is maybe influenced by the high percentage of gap filled data in a few months.

SIMETAW_R was validated also in two sites in Italy where wine grape was cultivated. The performance of the model were good in Valle dell'Adige and in Negrisia (2007) where a correlation higher than the 80% was computed.

In this work reference evapotranspiration was computed using Hargreaves Samani equation and the standardized reference evapotranspiration equation, and as already observed by other authors (Allen et al., 1998; Temesgen et al., 1999; Droogers and Allen., 2002; Martinez-Cob and Tejero, 2004; Alexandris et al, 2008; de Sousa Lima et al., 2013) an overestimation of ETo computed using HS equation was noticed in sites (Klingenberg, Grignon, Oensingen) characterized by high humidity sites, and thus in correspondence to rainy days.

REFERENCES

Alexandris, S., Stricevic, R., Petkovic, S., 2008. Comparative analysis of reference evapotranspiration from the surface of rainfed grass in central Serbia, calculated by six empirical methods against the Penman-Monteith formula. European Water Publications, 21/22: 17-28.

Allen, R.G., Pereira, L. S., Raes, D., & Smith, M., 1998. Crop evapotranspiration: Guidelines for computing crop requirements. Irrigation and Drainage Paper No. 56, FAO, (56), 300, https://doi.org/10.1016/j.eja.2010.12.001.

Allen, R.G., Walter, I.A., Elliott, R.L., Howell, T.A., Itenfisu, D., Jensen, M.E., Snyder, R.L., 2005a. The ASCE Standardized Reference Evapotranspiration Equation. American Society of Civil Engeneers, Reston, VA.

Allen, R.G., Pereira, L.S., Smith, M., Raes, D., Wright, J.L., 2005b. FAO-56 dual crop coefficient method for estimating evaporation from soil and application extensions. Journal of Irrigation and Drainage Engineering 131 (1), 2–13.

Allen, R.G., Pruitt, W.O., Wright, J.L., Howell, T.A., Ventura, F., Snyder, R.L., Itenfisu, D., Steduto, P., Berengena, J., Yrisarry, J.B., Smith, M., Pereira, L.S., Raes, D., Perrier, A., Alves, I., Walter, I., Elliott, R.A., 2006. Recommendation on standardized surface resistance for hourly calculation of reference ETo by the FAO56 Penman–Monteith method. Agricultural Water Management 81 (1–2), 1–22.

Baldocchi, D., Hicks, B.B., Meyers, T.P., 1988. Measuring biosphere-atmosphere exchanges of biologically related gases with micrometeorological methods. Ecology 69, 1331-1340.

Bates, B.C., Kundzewicz, Z.W., Wu, S., Palutikof, J.P., 2008. Climate change and water. Technical Paper of the Intergovernmental Panel on Climate Change, IPCC Secretariat, Geneva, 210 pp.

Beziat, P., Ceschia, E., Dedieu, G., 2009. Carbon balance of a three crop succession over two cropland sites in South West France. Agricultural and Forest Meteorology 149, 1628–1645.

Braud, I., Tilmant, F., Samie, R., Le Goff, I., 2013. Assessment of the SiSPAT SVAT model for irrigation estimation in south-east France. Four Decades of Progress in Monitoring and Modeling of Processes in the Soil-PlantAtmosphere System: Applications and Challenges. Procedia Environmental Sciences 19, 747 – 756. Elsevier.

Brisson, N., Gary, C., Justes, E., Roche, R., Mary, B., Ripoche, D., Zimmer, D., Sierra, J., Bertuzzi, P., Burger, P., Bussière, F., Cabidoche, Y. M., Cellier, P., Debaeke, P., Gaudillère, J.P., Hénault, C., Maraux, F., Seguin, B., and Sinoquet, H., 2003. An overview of the crop model STICS. European Journal of Agronomy 18 (3-4), 309-332.

Camp, C.R., Christenbury, G.D., Doty, C.W., 1988. Scheduling irrigation for corn and soybeans in the southern coastal plains. Transaction of ASAE 31, 513-518.

Campi, P., Modugno, F., Mastrorilli, M., Tomei, F., Villani, G., Marletto, V., 2014. Evapotranspiration of tomato simulated with the CRITERIA model. Italian Journal of Agronomy 9, No. 2.

Ceschia, E., Béziat, P., Dejoux, J.F., Aubinet, M., Buchmann, N., Carrara, A., Cellier, P., Di Tomasi, P., Elbers, J., Eugster, W., Jacob, C., Jans, W., Jones, M., Kutsch, W., Lanigan, G., Moors, E.C.M., Olioso, A., Osborne, B., Saunders, M., Smith, P., Soegaard, H., Wattenbach, M., 2010. Management effects on NBP and global warming potential at European crop sites Agriculture. Ecosystems and Environment.

de Sousa Lima, J., Antonino, A., Souza, E., Hammecker, C., Montenegro, S., Lira, C., 2013. Calibration of Hargreaves-Samani equation for estimating reference evapotranspiration in the sub-humid region of Brazil. Journal of Water Resource and Protection, 5, No. 12A.

Doorenbos, J., Pruitt, W.O., 1977. Guidelines for predicting crop water requirements. FAO Irrigation and Drainage Paper 24, 144.

Droogers, P., Allen, R.G., 2002. Estimating reference evapotranspiration under inaccurate data condition. Irrigation and Drainage Systems 16 (1), 33–45.

Eurostat, 2014. Statistical book on agriculture, forestry and fishery. Facts and figures on agriculture in the European Union. Eurostat new realease.

Fader, M., von Bloh, W., Shi, S., Bondeau, A., Cramer, W., 2015. Modelling Mediterranean agro-ecosystems by including agricultural trees in the LPJmL model. Geoscientific Model Development 8, 3545–3561, doi:10.5194/gmd-8-3545-2015.

Falge E., Baldocchi D., Olson R.J., Anthoni P., Aubinet M., Bernhofer C., Burba G., Ceulemans R., Clement R., Dolman H., Granier A., Gross P., Grunwald T., Hollinger D., Jensen N.O., Katul G., Keronen P., Kowalski A., Lai C.T., Law B.E., Meyers T., Moncrieff J., Moors E., Suyker A., Tenhunen J., Tu K., Verma S., Vesala T., Wilson K And Wofsy S., 2001. Gap filling strategies for long term energy flux data sets. Agricultural and Forest Meteorology 107, 71–77.

FAO, IIASA, ISRIC, ISS-CAS, JRC, 2008. Harmonized world soil database (version 1.0). FAO, Rome, Italy and IIASA, Laxenburg, Austria.

Feddes, R.A., Bresler, E., Neuman, S.P., 1974. Field test of a modified numerical model for water uptake by root systems. Water Resources Research 10, 1199-1206.

Foroud, N., Hobbs, E.H., Riewe, R., Entz, T., 1992. Field verification of a micro computer irrigation model. Agricultural Water Management 21, 215-234.

George, B.A., Shende, S.A., Raghuwanshi, N.S., 2000. Development and testing of an irrigation scheduling model. Agricultural Water Management 46, 121-136.

Gosain, A.K., Sandhya Rao, R., Srinivasan, 2005. Return-flow assessment for irrigation command in the Palleru river basin using SWAT model. Hydrological Processes 19, 673–682.

Guerra, E., Ventura, F., Spano, D., Snyder, R.L., 2014. Correcting midseason crop coefficients for climate. Journal of Irrigation and Drainage Engineering, doi:10.1061/(ASCE)IR.1943-4774.0000839.

Hargreaves, G.H., & Samani, Z.A., 1985. Reference crop evapotranspiration from temperature. Applied Engineering in Agriculture 1 (2), 96–99, https://doi.org/10.13031/2013.26773.

Hastings, A.F., Wattenbach, M., Eugster, W., Li, C., Buchmann, N., Smith, P., 2010. Uncertainty propagation in soil greenhouse gas emission models: an experiment using the DNDC model and at the Oensingen cropland site. Agriculture, ecosystems & environment 136, 1, 97-110. Elsevier.

IPCC, 2013. Summary for Policymakers. In: Climate Change 2013: The Physical Science Basis. Contribution of Working Group I to the Fifth Assessment Report of the Intergovernmental Panel on Climate Change Stocker, T.F., D. Qin, G.-K. Plattner, M. Tignor, S. K. Allen, J. Boschung, A. Nauels, Y. Xia, V. Bex and P.M. Midgley. Cambridge University Press, Cambridge, United Kingdom and New York, NY, USA.

Jones, J.W., Hoogenboom, G., Porter, C.H., Boote, K.J., Batchelor, W.D., Hunt, L.A., Wilkens, P.W., Singh, U., Gijsman, A.J., Ritchie, J.T., 2003. The DSSAT cropping system model. European Journal Of Agronomy No.18, 235-265.

Jones, C.A., Kiniry, J.R., 1986. CERES-Maize: A Simulation Model of Maize Growth and Development. Texas A & M University Press, College Station, Texas, 1-194.

Khandelwal, S.S., Dhiman, S.D., 2015. Irrigation water requirements of different crops in Limbasi branch canal command area of Gujarat. Journal of Agrometeorology 17 (1), 114-117.

Kotsopoulos, S., Kalfountzos, D., Alexiou, I., Zerva, G., Karamaligas, C., Vyrlas, P., 2003. Actual evapotranspiration and soil moisture studies in irrigated cotton fields. European Water 3/4, 25-31, E.W. Publications.

Kroes, J.G., van Dam, J.C., 2003. Reference Manual SWAP version 3.0.3. Alterra-Report 773. Alterra, Green World Research, Wageningen, The Netherlands.

Kutsch, W.L., Aubinet, M., Buchmann, N., Smith, P.,Osborne, B., Eugster, W., Wattenbach, M., Schrumpf, M., Schulze, E.D., Tomelleri, E., Ceschia, E., Bernhofer, C., Béziat, P., Carrara, A., Di Tommasi, P., Grünwald, T., Jones, M., Magliulo, V., Marloie, O., Moureaux, C., Olioso, A., Sanz, M.J., Saunders, M., Søgaard, H., Ziegler, W., 2010. The net biome production of full crop rotations in Europe. Agriculture, Ecosystems & Environment 139, Issue 3, 336–345.

Li, L., Vuichard, N., Viovy, N., Ciais, P., Wang, T., Ceschia, E., Jans, W., Wattenbach, M., Beziat, P., Gruenwald, T., Lehuger, S., Bernhofer, C., 2011. Importance of crop varieties and management practices: evaluation of a process-based model for simulating CO_2 and H_2O fluxes at five European maize (Zea mays L.) sites. Biogeosciences 8, 1721–1736, doi:10.5194/bg-8-1721-2011.

Longobardi, A., Villani, P., 2013. Four Decades of Progress in Monitoring and Modeling of Processes in the Soil-Plant-Atmosphere System: Applications and Challenges The use of micrometeorological data to identify significant variables in evapotranspiration modeling. Procedia Environmental Sciences 19, 267 – 274. Elsevier.

Marletto, V., Zinoni, F., 1998. The Criteria project: integration of satellite, radar, and traditional agroclimatic data in a GIS-supported water balance modelling environment. In: EUR 18328, Dalezios N.R. (ed.), 1998. Proc. COST 77, 79, 711 Int. Symp. on Applied Agrometeorology and Agroclimatology, Volos, Grecia, 24-26 april 1996, ISBN 92-828-4137-5, 173-178.

Marletto, V., Zinoni, F., Botarelli, L., Alessandrini, C., 2005. Studio dei fenomeni siccitosi in Emilia-Romagna con il modello di bilancio idrico Criteria (extended

abstract). RIAM 9: 32-33. Quaderno dei riassunti Convegno AIAM Vasto/Caramanico 3-5/5/2005.

Martinez-Cob, A., Tejero-Juste, M., 2004. A wind-based qualitative calibration of the Hargreaves ET0 estimation equation in semiarid region. Agricultural Water Management 64 (3), 251–264.

Mancosu, N., 2013. Agricultural water demand assessment using the SIMETAW# model. Ph.D. thesis. University of Sassari.

Mancosu, N., Snyder, R.L., Spano, D., 2014. Procedures to Develop a Standardized Reference Evapotranspiration Zone Map. Journal of Irrigation and Drainage Engineering 140, doi:10.1061/(ASCE)IR.1943-4774.0000697.

Mancosu, N., Spano, D., Orang, M., Sarreshteh, S., Snyder, R.L., 2015. SIMETAW# - a Model for Agricultural Water Demand Planning. Water Resources Management, doi:10.1007/s11269-015-1176-7.

Moors, E.J., Jacobs, C., Jans, W., Supit, I., Kutschf, W.L., Bernhoferb, C., Béziate, P., Buchmann, N., Carrarad, A., Ceschiae, E., Elbersa, J., Eugsterc, W., Kruijta, B., Loubetg, B., Magliuloh, E., Moureauxi, C., Oliosoj, A., Saundersk, M., Soegaard H., 2010. Variability in carbon exchange of European croplands. Agriculture, Ecosystems and Environment 139 (3), 325–335, https://doi.org/10.1016/j.agee.2010.04.013.

Najafi, P., Asgari, K., 2008. Forecasting crop water requirement by et-hs model for arid and semi arid region of iran. Computer and Computing Technologies in Agriculture II, Volume 1. IFIP Advances in Information and Communication Technology 293. Springer, Boston, MA.

Papale, D., Migliavacca, M., Cremonese, E., Cescatti, A., Alberti, G., Balzarolo, M., Belelli Marchesini, L., Canfora, E., Casa, R., Duce, P., Facini, O., Galvagno, M., Genesio, L., Gianelle, D.,Magliulo, V., Matteucci, G., Montagnani, L., Petrella, F., Pitacco, A., Seufert, G., Spano, D., Stefani, P., Vaccari, F.P., Valentini, R., 2015. Carbon, Water and Energy Fluxes of Terrestrial Ecosystems in Italy.

Environmental Science and Engineering, doi:10.1007/978-3-642-32424-6_2. Springer-Verlag Berlin Heidelberg.

Pereira, L.S., Allen, R.G., Smith, M., Raes, D., 2015. Crop evapotranspiration estimation with FAO56: Past and future. Agricultural Water Management 147, 4–20. Elsevier.

Popova, Z., Kercheva, M., Pereira, L.S., 2006. Validation of the FAO methodology for computing ETo with missing climatic data application to South Bulgaria. Irrigation Drainage 55, 201–215.

Raes, D., 2002. BUDGET: a soil water and salt balance model. Reference Manual, Version, 5 (June).

Raes, D., Steduto, P., Hsiao, T.C., Fereres, E., 2012. AquaCrop Version 4.0. Reference Manual, Chapter 2. FAO, Land and Water Division Rome, Italy.

Rana, G., Katerji, N., Lazzara, P., Ferrara, R.M., 2012. Operational determination of daily actual evapotranspiration of irrigated tomato crops under Mediterranean conditions by one-step and two step models: Multiannual and local evaluations. Agricultural Water Management 115, 285–296. Elsevier.

Ranucci, S., Bertolini, T., Vitale, L., Di Tommasi, P., Ottaiano, L., Oliva, M., Amato, U., Fierro, A., Magliulo, V., 2011. The influence of management and environmental variables on soil N_2O emissions in a crop system in Southern Italy. Springer Science.

Revill, A., Sus, O., Barrett, B., Williams, M., 2013. Carbon cycling of European croplands: A framework for the assimilation of optical and microwave Earth observation data. Remote Sensing of Environment 137, 84–93. Elsevier.

Ritchie, J.R. and Otter, S., 1985. Description and performance of CERES-Wheat: a user-oriented wheat yield model. In: ARS Wheat Yield Project. ARS-38. National Technical Information Service, Springfield, Missouri, 159-175.

Rowse, H.R., Mason, W.K., Taylor, H.M., 1983. A microcomputer simulation model of soil water extraction by soybeans. Soil Science 136, 218-225.

Saadi, S., Todorovic, M., Tanasijevic, L., Pereira, L.S., Pizzigalli, C., Lionello, P., 2014. Climate change and Mediterranean agriculture: Impacts on winter wheat and tomato crop evapotranspiration, irrigation requirements and yield. Agricultural Water Management. Elsevier.

Santhi, C., Muttiah, R.S., Arnold, J.G., Srinivasan, R., 2005. A GIS-based regional planning tool for irrigation demand assessment and saving using SWAT. American Society of Agricultural Engineers 48 (1), 137–147.

Sheikh, V., Mohammadi, M., 2013. Evaluation of Reference Evapotranspiration Equations in Semi-arid Regions of Northeast of Iran. International Journal of Agriculture and Crop Sciences. IJACS/2013/5-5/450-456, ISSN 2227-670X.

Siebert, S., Portmann, F.T., Döll, P., 2010. Global Patterns of Cropland Use Intensity. Remote Sensing 2, 1625-1643, doi:10.3390/rs2071625.

Šimůnek, J., Šejna, M., Saito, H., Sakai, M., van Genuchten, M. Th., 2009. The HYDRUS-1D Software Package for Simulating the One-Dimensional Movement of Water, Heat, and Multiple Solutes in Variably-Saturated Media. Version 4.08. Department of environmental sciences university of California Riverside.

Smith, M., 1991. CROPWAT: a computer program for irrigation planning and management. FAO Land and Water Development Division, FAO, Rome, Italy.

Snyder, R.L., Bali, K.M., Ventura, F., Gomez-MacPherson, H., 2000. Estimating evaporation from bare or nearly bare soil. Journal of Irrigation and Drainage Engineering 126 (6), 399-403.

Snyder, R.L., Geng, S., Orang, M.N., Matyac, J.S., Sarreshteh, S., 2004. A simulation model for ET of applied water. Acta Horticulturae 664, 623–629.

Snyder, R.L., Orang, M., Geng, S., Matyac, S., Sarreshteh, S., 2005. SIMETAW (Simulation of Evapotranspiration of Applied Water). California water plan update 4, 211–226.

Snyder, R.L., Moratiel, R., Song, Z., Swelam, A., Jomaa, I., Shapland, T., 2011. Evapotranspiration response to climate change. Acta Horticulturae, doi:10.17660/ActaHortic.2011.922.11.

Snyder, R.L., Geng, S., Orang, M., Sarreshteh, S., 2012. Calculation and Simulation of Evapotranspiration of Applied Water. Journal of Integrative Agriculture 11 (3), 489–501, https://doi.org/10.1016/S2095-3119(12)60035-5.

Stöckle, C.O., Donatelli, M., Nelson, R., 2003. CropSyst, a cropping systems simulation model. European Journal of Agronomy No.18, 289-307.

Stroosnijder, L., 1987. Soil evaporation: test of a practical approach under semi-arid conditions. Netherlands. Journal of Agricultural Science 35, 417-426.

Taiz, L., Zeiger, E., 2008. Fisiologia Vegetale, Piccin, Padova.

Temesgen, B., Allen, R.G., Jensen, D.T., 1999. Adjusting temperature parameters to reflect well-water conditions. Journal of Irrigation and Drainage Engineering 125, 26–33.

Todorovic, M., Karic, B., Pereira, L.S., 2013. Reference evapotranspiration estimate with limited weather data across a range of Mediterranean climates. Journal of Hydrology 481, 166–176.

Twine T.E., Kustas W.P., Norman J.M., Cook D.R., Houser P.R., Meyer T.P., Pruege, J.H., Starks P.J., Wesely M.L., 2000. Correcting eddy-covariance flux underestimates over a grassland. Agricultural and Forest Meteorology 103, 279-300.

Van den Hoof, C., Hanert, E., Vidale, P.L., 2010. Simulating Dynamic Crop Growth with an Adapted Land Surface Model - JULES SUCROS: Model Development and Validation. Elsevier.

Wattenbach, M., Sus, O., Vuichard, N., Lehuger, S., Gottschalk, P., Li, L., Leip, A., Williams, M., Tomelleri, E., Kutsch, W.L., Buchmann, N., Eugster, W., Dietiker, D., Aubinet, M., Ceschia, E., Béziat, P., Grünwald, T., Hastings, A., Osborne, B., Ciais, P., Cellier, P., Smith, P., 2010. The carbon balance of European croplands: a cross-site comparison of simulation models. Agriculture, ecosystems & environment 139, No.3, 419-453 Elsevier.

Williams, J.R., Jones, C.A., Dyke, P.T., 1984. A modeling approach to determining the relationship between erosion and soil productivity. Transactions of the American Society of Agricultural Engineers 27 (1), 129-144.

Wilson K., Goldstein A, Falge E., Aubinet M., Baldocchi D., Berbigier P., Bernhofer C., Ceulemans R., Dolman H., Field C., Grelle A., Ibrom A., Law B.E., Kowalski A., Meyers T., Moncrieff J., Monson R., Oechel W., Tenhunen J., Valentini R., Verma S., 2002. Energy balance closure at FLUXNET sites. Agricultural and Forest Meteorology 113, 223-243.

Zheng, J., Li, G., Han, Z., Meng, G., 2010. Hydrological cycle simulation of an irrigation district based on a SWAT model. Mathematical and Computer Modelling 51, 1312–1318. Elsevier.

Website

http://analyticstrainings.com/?p=101

http://www.fao.org/docrep/t7202e/t7202e06.htm

https://fluxnet.ornl.gov/

PART 2. Regional assessment of climate change impact on crop evapotranspiration and irrigation demand in Euro-Mediterranean Countries

2.1 INTRODUCTION

Climate change, quick demographic growth, socio-economic development, the increasing demand for raw materials, all together have a strong impact on available water resources. Water crises are becoming more and more exacerbated with the extension of residential centers, and the improvement to quality of life (UNRIC, 2015).

The IPCC states that there won't be uniform changes in the global water cycle since the differences in rainfall between regions are expected to be variable in general, but also across Europe (IPCC, 2013). In particular, according to climate models forecasts, there may be a general increase in rainfall in Northern Europe and a reduction in the Southern. In central and Northern parts of Europe, winters will be characterized by a strong increase in precipitation, while the South will witness drier summers (IPCC, 2013). In addition, climate model may predict, on average over Mediterranean areas, a slight decrease in total seasonal and annual rainfall, which will be associated to an increase in the frequency of extreme events (such as heavy precipitation events). The resulting risks associated with this tendency might be an increase in prolonged dry seasons and drought periods with extreme precipitation events. The intensity, the magnitude and distribution of the precipitation, as well as the soil water content and the atmospheric water vapor, may vary causing a consequent increase of events such as floods, landslides, and drought (Caciagli, 2012).

In Mediterranean areas, agriculture is one of the sectors which mainly contributes to water use. In this context, it is worth considering the double role of agriculture, because if it is true that it is one of the most responsible for water consuming, it is also true that its products are basic to guarantee a food supply to the stated population growth. Irrigation is a basic practice in the arid and semi-arid Euro-Mediterranenan regions,

where the total amount of water withdrawal for crop water requirements is expected to increase due to climate change, thus improvements in water use efficiency are needed.

Given the predicted impact of climate change on crop available water in many Mediterranean Countries, especially in semi-arid or arid areas, the application of crop models in agriculture has great utility to represent potential changes in crop growth as a function of the increasing temperature and the variability of precipitation intensity and frequency. Many models have been developed and applied for this purpouse since 1965 (Part 1), to simulate interactions between plants, climate and soil. Several studies investigated on crop water consumption and irrigation requirement using models at different scales and at different resolutions, and considering different scenarios. They investigated on different crops, and keeping a focus on Mediterranean irrigated agriculture, they all agree with an increasing crop water needs due to a more severe drought risk which is expected to characterize Southern Countries in the next future (Rodriguez-Diaz et al., 2007; Saadi et al., 2014; Tanasijevic et al., 2014; Fader et al., 2015; Fader at al., 2016). The first step to cope with this issue is to increase knowledge about the water consumption and irrigation requirement of Mediterranean crops.

For this purpose this work aims to implement the SIMETAW-R modelling scheme, using GIS libraries available in R, to construct a spatial platform (named SIMETAW_GIS) that can interact with large geodatasets of climate variables, environmental conditions and agronomic practices, to provide regional simulation of water consumption and net water application for grape, maize, and wheat at Euro-Mediterranean scale under past (1976-2005) and future (2036-2065) climate conditions.

The Era-Interim climatic data for historical conditions (1981-2010) have been firstly used to compare model results against observation for each European site described in Part 1. In addition, a calculation and validation of reference evapotranspiration computed using the Standardized reference evapotranpiration (Penmann Monteith) and the Hargreaves Samani equations has been carried on in order to define the input data to use for the calculation of actual evapotranspiration at regional scale for the SIMETAW_GIS platform.

2.2 MATERIALS AND METHODS

2.2.1 The SIMETAW_GIS platform

The impact of climate change on crop evapotranspiration at Euro-Mediterranean scale was assessed through an implementation of the irrigation modelling scheme SIMETAW-R, in association with GIS libraries, statistical and validation procedures, developed under "R", which provides a soil water balance for crop species simulated under particular conditions of irrigation management. The SIMETAW_GIS platform couples and automathizes interaction for climate and environmental input data to process the soil water balance for multiple years and pixels across regional and continental assessments (Figure 95). The climate data are integrated and processed from ncdf format files, typical output of climate models, for climate variables needed to process ETo with Penman-Monteith (minimum and maximum temperature, relative humidity, wind speed, and net radiation) or Hargreaves Samani (minimum and maximum temperature) equations, that are then used with precipitation to run soil water balance in association with crop growth development. Environmental soil data, either as ncdf or other GIS files, are also used to define spatial distribution of both soil depth (m) and available water content (mm/m) needed to define the maximum available water content for crops and maximum rooting depth achievable during crop development. Additional crop management options can be specified as input raster to define several agronomic conditions needed to assess crop development (e.g. planting and harvest dates). The platform processes simulation on a pixel per pixel basis and calculates spatial distribution of yearly crop water requirements, and the amount and number of net applications. These results are saved on a year by year basis as rasters (i.e. ncdf format) for presentation or further raster analyses, and as tables aggregated by administrative boundaries for tabula presentation and validation against statistical agriculture accounting.

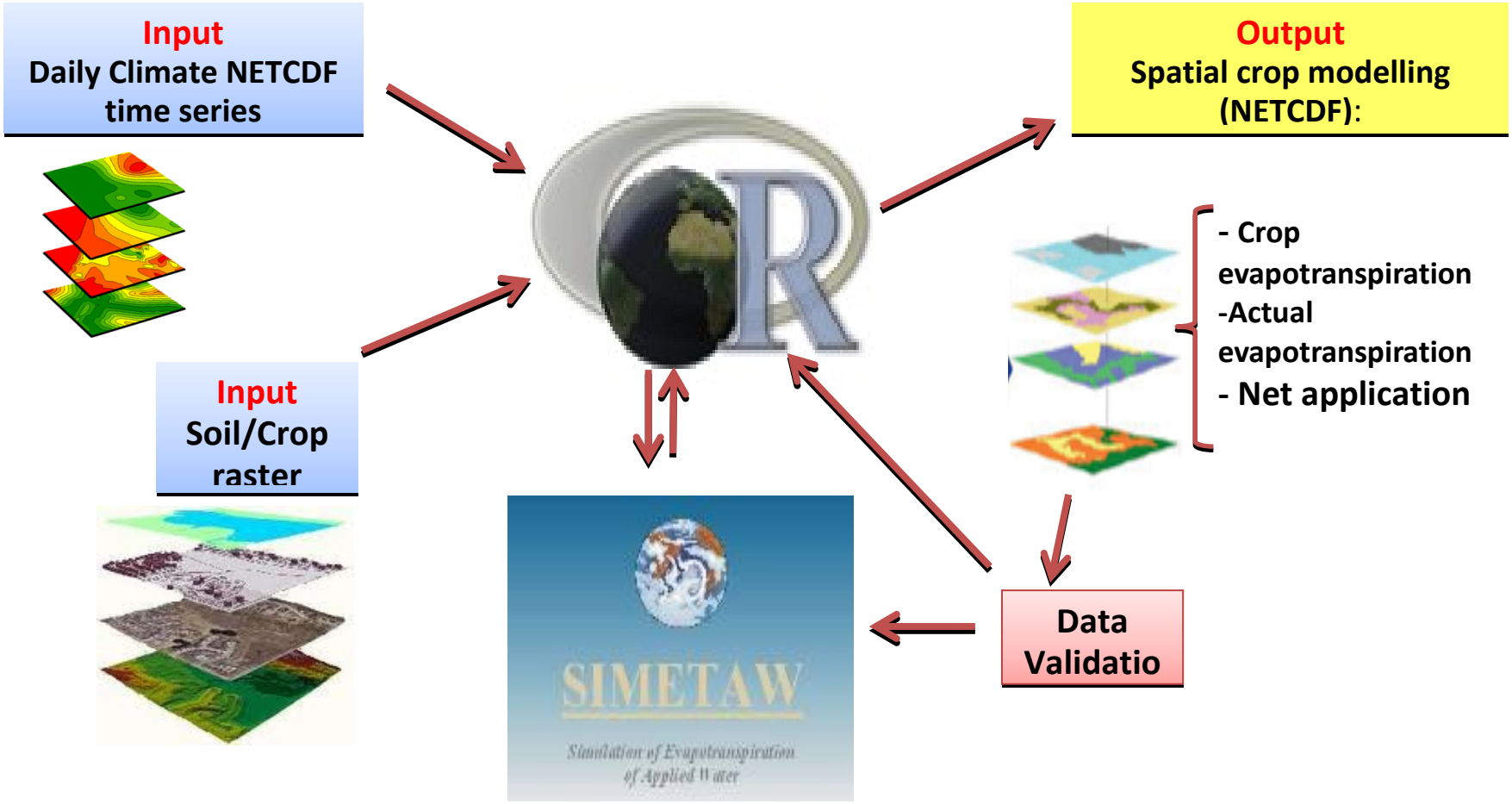

Fig. 95. Scheme of SIMETAW_GIS platform.

The domain under investigation extended from 9.6W to 30.7E, and from 40.6S to 55N. The Northern boundary extends until Germany, Poland, a part of United Kingdom, Belarus and Russia. It does not encompasses Denmark, the Scandinavian Peninsula and the Baltic Countries. The Southern extends until the Northern Africa, and a small area of the Near East Countries, such as Israel, Jordan, Syria, Lebanon, Saudi Arabia, and, Iraq. In the Eastern part of the domain are included almost the entire Turkey and a small area of Georgia The Mediterranean basin Countries (Correia, 1999) investigated in this work are highlighted in orange in Figure 96.

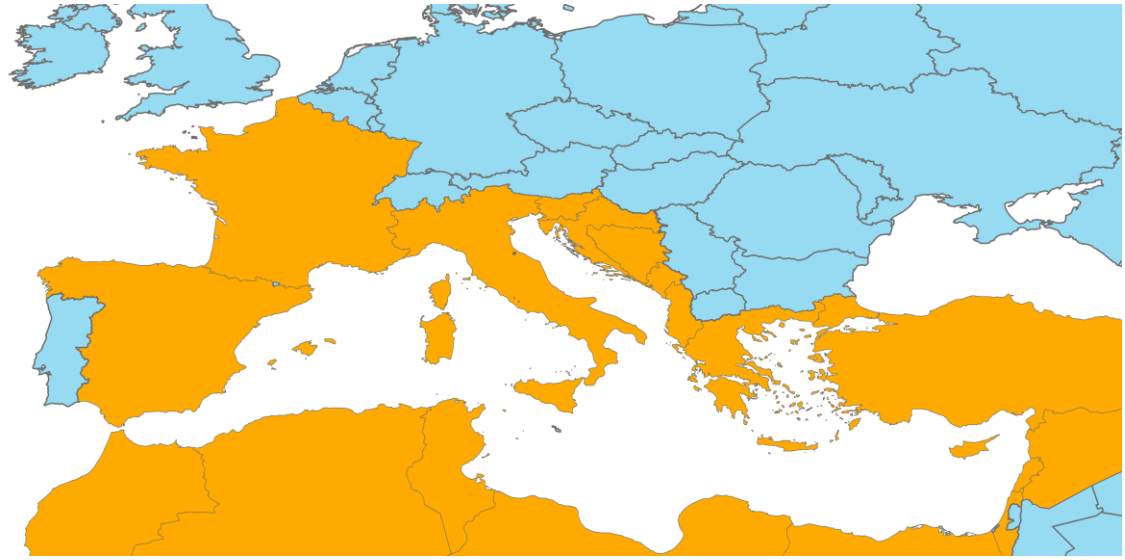

Fig. 96. Euro-Mediterranean domain (light blue) and focus on Mediterranean Countries under investigation (orange).

2.2.1.1 Input data

Climate input data

Daily climate variables (minimum and maximum temperature, net radiation, wind speed, relative humidity) from the Global Circulation Model (GCM) CMCC-MED (Gualdi et al. 2011; Scoccimarro et al. 2011), downscaled to a spatial resolution of 14 Km with the regional climate model COSMO-CLM (Rockel et al, 2008), were used to estimate daily reference evapotranspiration (ETo) (Part 1) at Euro-Mediterranean scale for the baseline (1976-2005) and the intermediate future (2036-2065) period,. The climate Representative Concentration Pathway (RCP) 4.5 and 8.5 scenarios, with

projected radiative forcing for the future as from the CMIP5 (Taylor et al., 2012), were used. In addition, both COSMO-CLM RCM forced by Era-Interim reanalysis (EI) produced by ECMWF (Dee et al., 2011) and the European high-resolution gridded (E-OBS) data (Haylock et al., 2008) for the past climate (1979-2011) were used in this work. EI data downscaled with COSMO-CLM RCM have a resolution of 14 km, while E-OBS have a resolution of about 21 km. E-OBS data are the result of the interpolation of several meteorological stations over Europe. This dataset is known as the daily historical climate gridded dataset with the largest resolution for Europe (Hofstra et al., 2009).

Soil and crop input data

Soil data were included in the soil water budget to compute actual evapotranspiration (ETa) and the irrigation requirement (NA). The soil water holding capacity from the Global Data Set of Derived Soil Properties, 5 Minutes Grid (ISRIC-WISE) (Batjes, 2000) database (Figure 97), as well as the maximum soil depth from the 30 arc-second raster Harmonized World Soil Database (HWSD) v1.2 (Figure 98) (Wieder et al., 2014) were included into the SIMETAW_GIS platform.

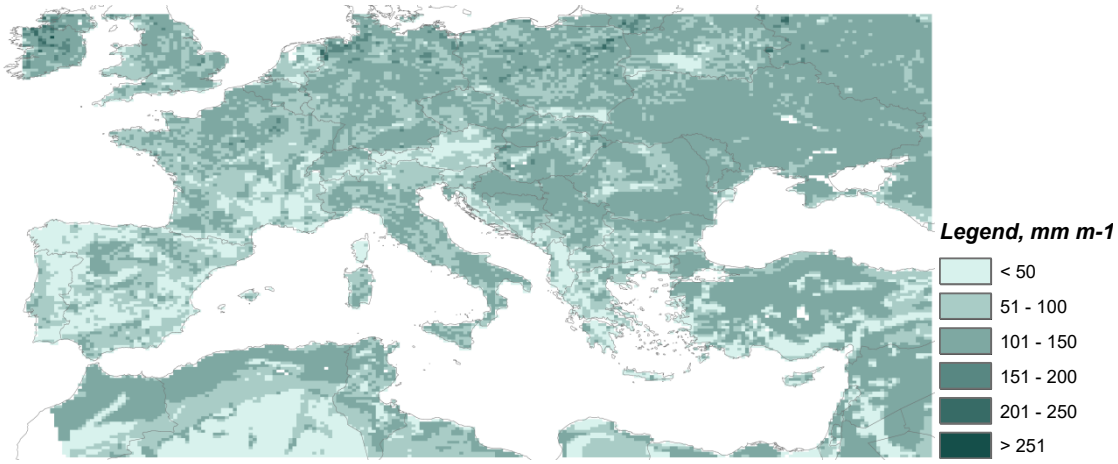

Fig. 97. Gridded soil water holding capacity from the ISRIC-WISE database.

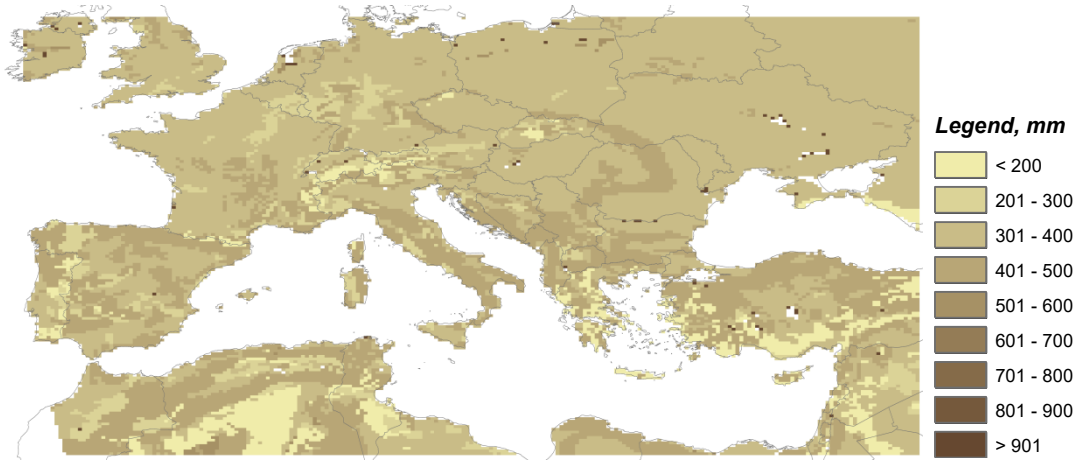

Fig. 98. Maximum soil depth from the HWSD database.

The sowing and harvest date for maize (Figure 99 and 100, respectively) and wheat, both under irrigated conditions (Figure 101 and 102, respectively) and rainfed (Figure 103 and 104, respectively), were obtained from the Agricultural Model Intercomparison and Improvement Project (AgMiP) database (Elliott et al., 2015).

Since grape phenological data were not available in Elliott et al. (2015) database, a NetCDF file containing the mean grape bud break and harvest Julian day (JD) was created in this work. The mean values were obtained from literature and through the PEP725 database (http://www.pep725.eu/). Some assumptions were made: the mean date is referred to the average for the available *Vitis vinifera* data without differences between grape varieties, and the mean value is kept uniform within any Country. The Countries included in the new gridded layer were selected considering a grape production area higher than 10,000 hectares according to the FAOSTAT (http://www.fao.org/faostat/en/#data/QC) data, and the availability of bud break and harvest data from literature and from PEP725 database. Table 38 shows the bud break/harvest Julian day (JD) for the selected Countries following the above mentioned criteria. The literature taken into account to obtain the mean bud break and harvest dates per each Country is reported in Appendix 1.

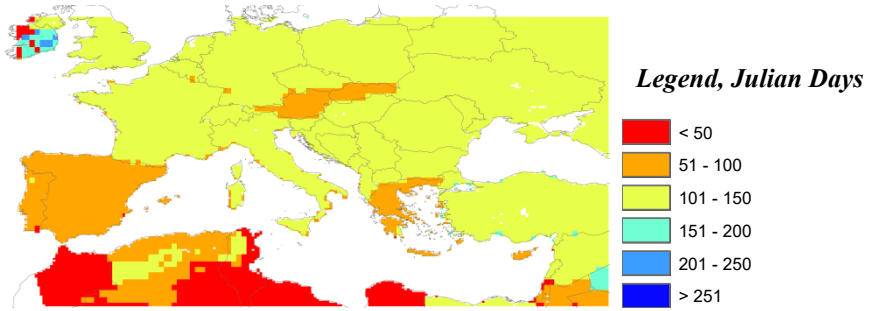

Fig. 99. Sowing dates of maize according to AgMIP database.

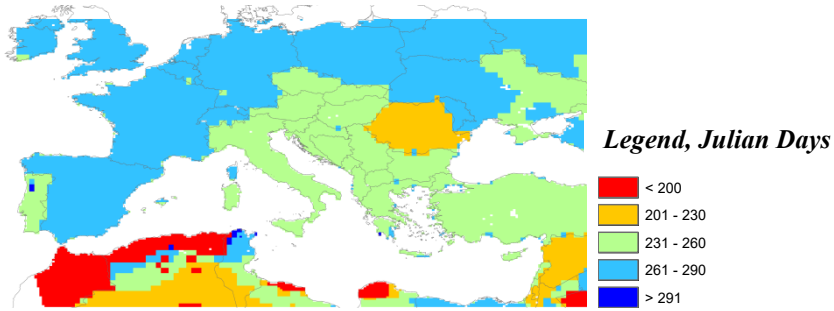

Fig. 100. Harvest dates of maize according to AgMIP database.

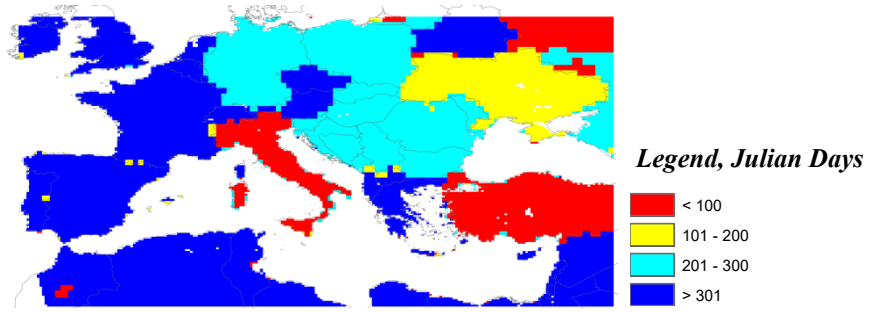

Fig. 101. Sowing dates of irrigated wheat according to AgMIP database.

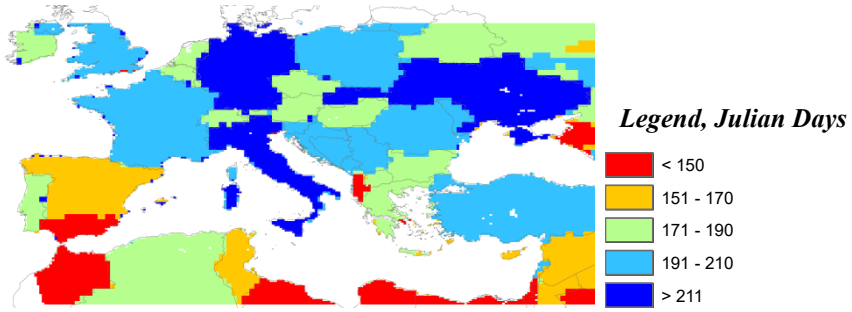

Fig. 102. Harvest dates of irrigated wheat according to AgMIP database.

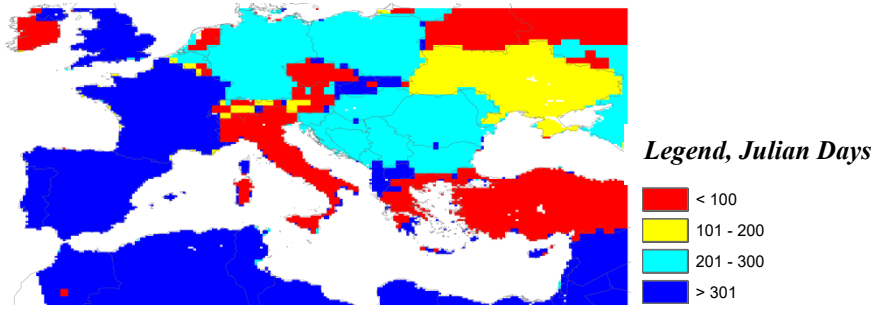

Fig. 103. Sowing dates of rainfed wheat according to AgMIP database.

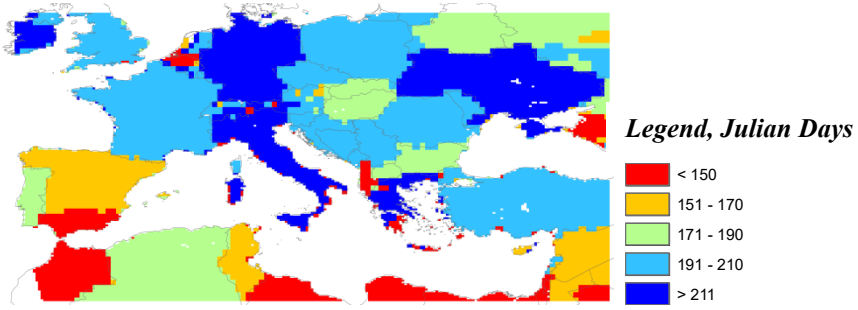

Fig. 104. Harvest dates of rainfed wheat according to AgMIP database.

Tab. 38. Julian day referred to bud break and harvest dates for Vitis vinifera per Country.

Zone	Zone_Name	Bud break Julian day	Harvest Julian day
5	Algeria	90	210
15	Austria	115	278
35	Bulgaria	102	291
66	Egypt	90	210
74	Czechia	113	278
83	France	95	261
93	Germany	115	281
97	Greece	91	304
106	Croatia	98	263
107	Hungary	113	278
116	Italy	99	264
140	Slovakia	113	278
156	Morocco	90	210
189	Portugal	91	255
196	Romania	102	291
213	Spain	91	255
214	Serbia	107	244
221	Switzerland	115	281
231	Tunisia	90	210
232	Turkey	91	304
208	Slovenia	98	263
220	Syria	91	304
153	Macedonia	91	304

The mean Julian day of bud break and harvest dates are shown in Figure 105 and 106, respectively, for the selected Countries.

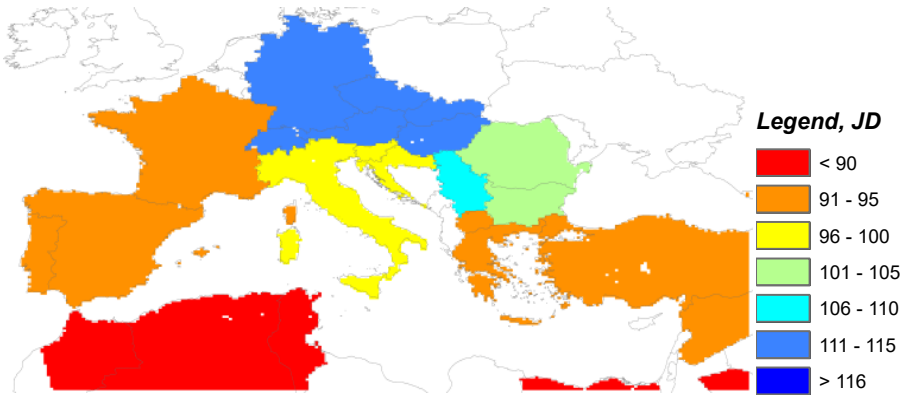

Fig. 105. Bud break date for grape. JD = Julian Days

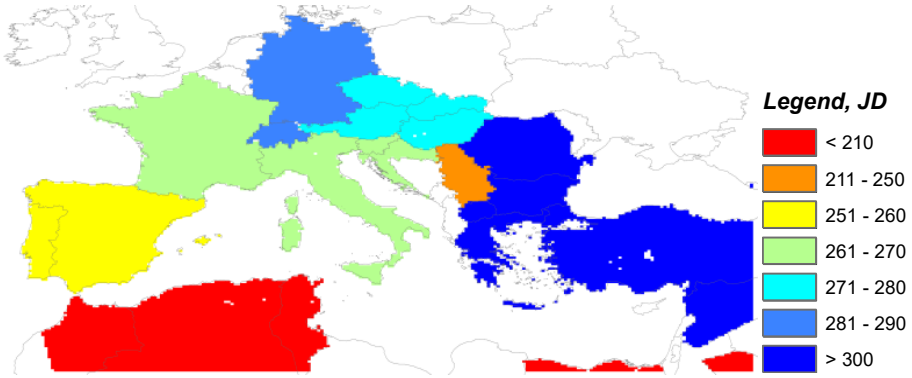

Fig. 106. Harvest date for grape. JD = Julian Days

The maximum rooting depth suggested by the FAO Irrigation and drainage paper 56 (Allen et al., 1998) was used for crop at maturity and scaled down for the other stages. Specifically the maximum rooting depths of 1350 mm (maize), 1650 mm (winter wheat), and 1500 mm (grape) were used. The maximum rooting depth value of 1800 mm was instead considered to run simulations for wheat under rainfed condition as suggested by Allen et al. (1998). During the first step of the growing season, i.e. the stage AB of the growth curve (Figure 14), the effective rooting depth was considered equal to one-third of the depth during the midseason.

In this work, SPAM database (You et al., 2014), was used to define the actual crops spatial distribution (Figure 107, 108, and 109). The spatial crops allocation is expressed in hectares, and the resolution is 5 minutes. The spatial allocation is provided by the database for irrigated and rainfed crops. Since any grape distribution was available in the SPAM database, it was rather obtained from the novel global data set of monthly irrigated and rainfed crop areas at the year 2000 (MIRCA 2000) (Portmann et al., 2010).

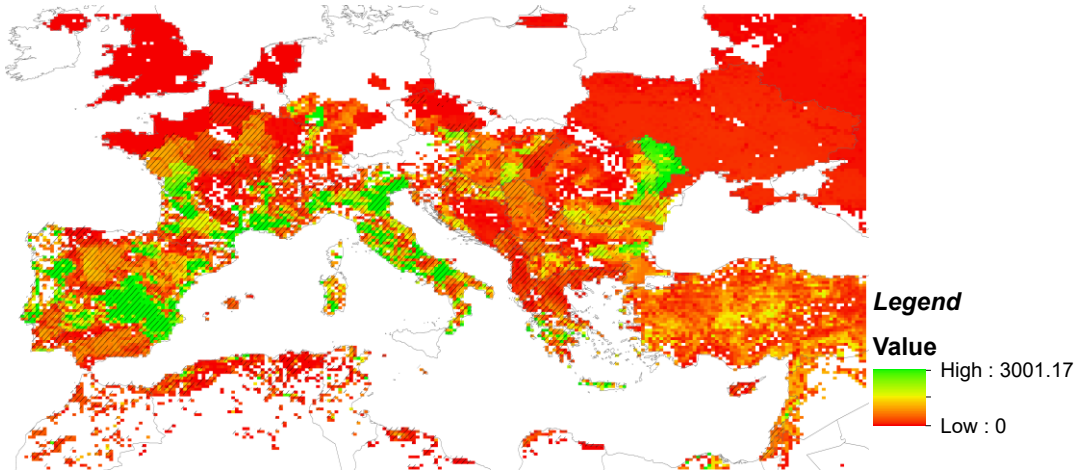

Fig. 107. Actual grape distribution according to SPAM database. The irrigated areas are distinguished by diagonal solid lines.

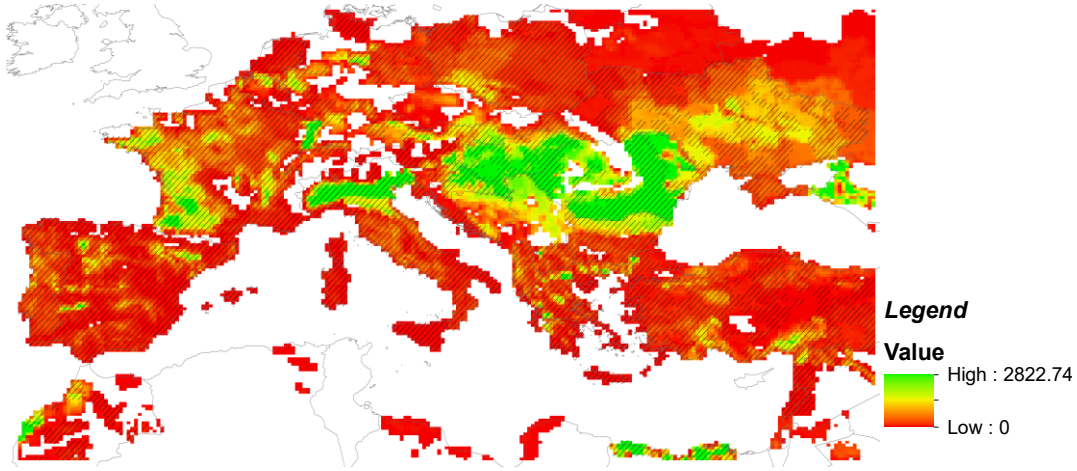

Fig. 108. Actual maize distribution according to SPAM database. The irrigated areas are distinguished by diagonal solid lines.

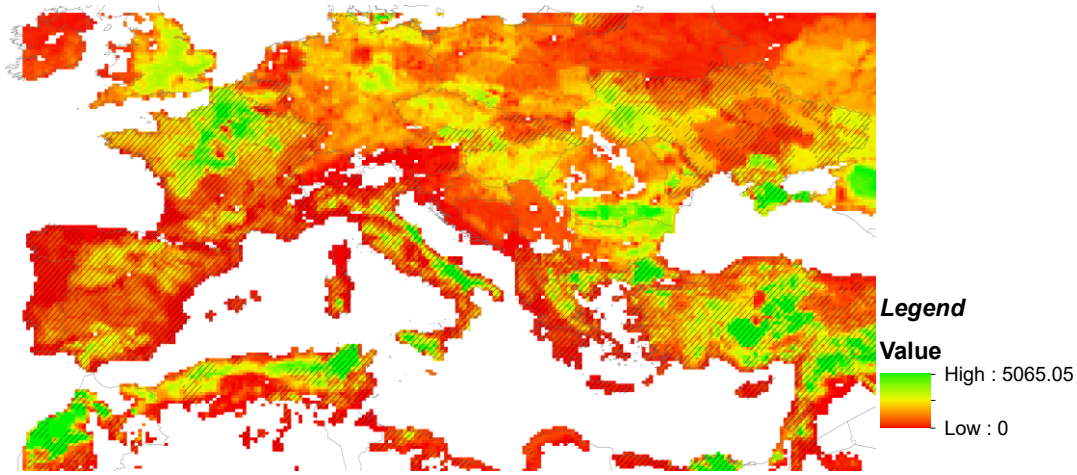

Fig. 109. Actual wheat distribution according to SPAM database. The irrigated areas are distinguished by diagonal solid lines.

Crop management data

The crops under investigation were not pre-irrigated, i.e. any water application occurred during the initial growth stage, thus the soil water depletion (SWD) value at the beginning of simulations was predetermined by the soil water balance for the offseason before the first crop growing season (i.e. between end of the season and the leaf out).

Any reduction of the planted land was taken into account, and the water application percentage, i.e. the percentage of full water application for the specific crop allocated for the crop growing season (WAP) was set equal to 100% for irrigated crop. The allowable depletion (AD) was set equal to 50%, thus the yield threshold depletion (YTD), when irrigation is applied, was equal to half of the plant available water (PAW). WAP was set equal to zero to simulate the actual evapotranspiration of wheat in rainfed conditions.

The sprinkler irrigation method with a distribution uniformity (DU) of 75%, and an application rate efficiency (AE) of 3.2 mm h^{-1} was applied to run simulation for maize and irrigated wheat at Euro-Mediterranean scale.

The drip method was chosen to simulate grape water consumption and the related water net applications. In this case, DU and AE were set equal to 85% and 0.7 mm h^{-1}, respectively.

The runoff was set equal to zero in this study.

Assessment of regional standardized reference evapotranspiration for short canopies and Hargreaves-Samani equation

The reliability of the modeled climate variables used to compute ETo was assessed by comparing them with the observed climatic data measured in the FLUXNET sites (Part 1). In addition, a comparison between the two ETo values simulated with the standardized Penman-Monteith equation and the Hargreaves Samani equations was perfomed, by using the ETo values calculated with measured data from the Fluxnet sites, in order to verify the best one method to be included into the SIMETAW_GIS platform.

Hargreaves Samani ETo (ETo_HS) was calculated using both EI and E-OBS data for the past climate (1979-2011). Since in the E-OBS dataset only daily precipitation and

temperature values are currenly available, the standardized Penman-Monteith ETo (ETo_PM) was computed only using the EI.

ETo_PM and ETo_HS were computed at Euro-Mediterranean scale with a final spatial resolution of 14 km using COSMO-CLM RCM model for the baseline (1976-2006) and the intermediate future (2036-2065), under RCP 4.5 and 8.5 scenarios. Their difference anomalies was then calculated to assess the impact of climate change on ETo values.

2.2.2 Data processing and simulations

Crop growth was assumed to be allowed everywhere in order to asses crop water consumption and water application also in new hypothetical zones that due to climate change may be cultivated with maize, wheat, and grape. Extreme areas, such as the ones close to the Sahara desert and mountain ranges were considered.

However, simulation results were mostly associated to the existing total cultivated distribution (irrigated and rainfed areas) for maize and wheat in each grid cell. The crop distribution indicates the percentage of the pixel that is cultivated with the specific crop.

The global NetCDF files of climatic variables (minimum and maximum temperature, net radiation, wind speed, relative humidity), as well as soil and crop data were elaborated with the Climate Data Operators (CDO, 2013) software in order to pre-process them as input in the SIMETAW-GIS platform.

Firstly, each global NetCDF input file was subset for the domain under investigation, and remapped from curvilinear to geographic projection performing a nearest neighbor remapping.

Secondly, each variable was grouped in packages of 30 years and then their unit of measurement was converted to compute evapotranspiration at regional scale: temperature was converted from Kelvin to Celsius degrees by removing a constant value of 273.15.

Net radiation was obtained by adding the longwave and shortwave radiation components, and then converted from W m^{-2} to MJ m^{-2} d^{-1} by multiplying a conversion factor of 0.0864.

The product of the two orthogonal wind components (u and v) resulted in the wind speed variable, which was then converted from the height of 10 to 2 meters using the conversion factor of 0.75.

The computation of the actual vapor pressure at the dew point temperature was established using the percentage of relative humidity. Since the platform runs daily simulations, the ground heat flux was considered equal to zero.

The input variables loaded in R were used to compute water consumption and irrigation requirement through the equations described in Part 1, which were included into a loop in order to simulate variables for each point of the studied domain, and for each day of years. The simulation of the crop coefficient curve was based on the percentage of stage advancement during the crop growing season (Figure 14 and 15, Part 1).

Once computations were finalized, new NetCDF files containing the specific variable were created. Units, dimensions as well as the long name of the variable were defined for the NetCDF header.

Thirty, climate data for two period 1976-2005 and 2036-2065 were aggregated to estimate the average for the thirty years period and per each Country.

2.2.3 Statistical analysis

Climatic variables from the Era-Interim driven by COSMO_CLM model were compared to the observed variables assessed in Part 1, for each specific site in order to assess the accuracy of the climate model input.

The indeces Root Mean Square Error (RMSE), Mean Absolute Error (MAE), Mean Bias Error (MBE), Pearson's Coefficient (r), coefficient of determination (R^2), Relative Error (RE), and Index of agreement (IA) were used to assess model performance. The statistical indices are described in Part 1.

2.3 RESULTS

The application of SIMETAW_GIS platform allowed to estimate the reference (ETo), crop (ETc), and actual evapotranspiration (ETa), at regional scale, and net water application (NA) for maize, wheat and grape for past and future (2036-2065) climate, under RCP 4.5 and 8.5 climate scenarios, at a spatial resolution of 14 km.

In this section, first results for reference evapotranspiration are presented both using the Hargreaves Samani (ETo_HS) and the standardized Penman Monteith equations (ETo_PM) using historical gridded climate observations (COSMO-CLM RCM driven by ERA-INTERIM; E-OBS. Then, the difference of ETo between future and present climate conditions, for climate projections (COSMO-CLM RCM driven by CDMCC_MED GCM), are shown across the selected domain and aggregated for each Country. The results obtained by the comparison between ETo_HS and ETo_PM allowed to select the PM equations to be used for the estimation of regional crop (ETc) and actual (ETa) evapotranspiration, and irrigation requirement (NA) in the Euro-Mediterranean domain.

The simulation results of ETc and ETa evapotranspiration, and NA are reported for irrigated maize, wheat and grape as well as rainfed wheat.

Results are showed for the potential crops distribution (i.e. crops are allowed to grow in each pixel of the domain). However, since maize, wheat, and grape are not currently cultivated everywhere, in this work the actual crops spatial distribution was taken into account in order to show the impact of global warming on crop water consumption and irrigation demand in areas currently cultivated.

In addition, for the top producer Countries (i.e. Maize > ~ 27,500 ha, irrigated wheat ~ 14,000, rainfed wheat ~ 886,000 ha, and grape ~ 10,000 hectars cultivated), results are reported considering the total irrigated areas and the rainfed areas.

2.3.1 Regional ETo estimation for past climate conditions

Figure 110 and 111 show the ETo_HS and ETo_PM values at Euro-Mediterranean scale for the baseline period (1976-2005) using the climate scenario from the COSMO-CLM RCM driven by the CMCC-MED GCM.

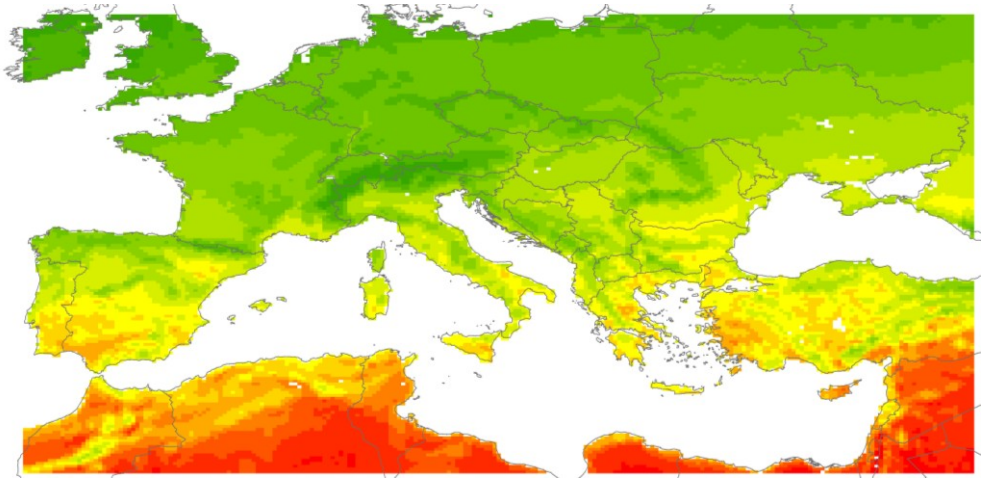

Fig. 110. Average yearly ETo_HS at Euro-Mediterranean scale for the baseline period (1976-2005).

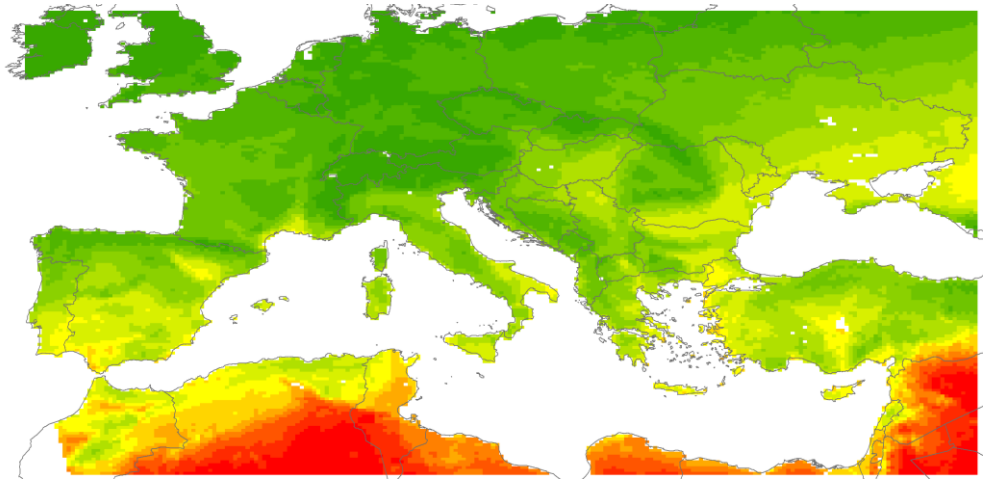

Fig. 111. Average yearly ETo_PM at Euro-Mediterranean scale for baseline period (1976-2005).

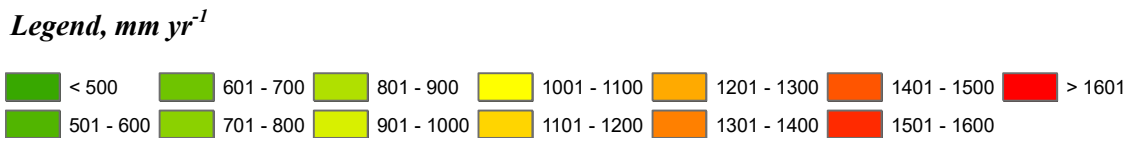

In Figure 110 the yearly average ETo values using HS equation were higher than the ones obtained using PM equation (Figure 111) in most of the Euro-Mediterranean domain. The highest ETo values was estimated in the eastern part of the domain using the standardized PM equation (1600 mm yr^{-1}). Yearly values of ETo_HS higher than 700 mm yr^{-1} were obtained in all Mediterranean Countries, in Moldava, Portugal, and Romania. In these Countries the difference between ETo_HS and ETo_PM was never lower than 100 mm yr^{-1} except for Tunisia (69 mm yr^{-1}), Syria (23 mm yr^{-1}), Algeria (37 mm yr^{-1}), and Moldava (20 mm yr^{-1}). Since ETo is strictly related to temperature, wind speed, net radiation, and relative humidity, the lowest values were estimated at the highest latitude, with wetter and colder climate conditions, such as Denmark, Ireland, Lithuania, Liechtenstein, Switzerland, and United Kingdom. However, the Hargreaves Samani equation is a method based on temperature, and it does not consider the influence of wind speed, relative humidity, and solar radiation on the evapotranspiration process. For this reason an overestimation of ETo with HS in Countries characterized by a high percentage of relative humidity and low wind speed is expected. Several studies, in fact, reported the overestimation in humid areas (Droogers and Allen 2002; Alexandris et al., 2008; de Sousa Lima et al., 2013). On the contrary, the underestimation of ETo by HS equation was stated in case of high wind speed values and dry regions (Allen et al., 1998; Temesgen et al., 1999; Martinez-Cob and Tejero-Juste, 2004). This work is in line with studies found in literature.

Figure 112 shows the average of ETo_HS and ETo_PM values per each Mediterranean Country, for the baseline period (from 1976 to 2005). In addition, differences between ETo_HS and ETo_PM (%), mean relative humidity (%), as well as mean wind speed (m s^{-1}) for the same time series are included (Figure 112 and 113). In Figure 114 and 115 are reported the same variables but for all the other Countries that belong to the domain under investigation.

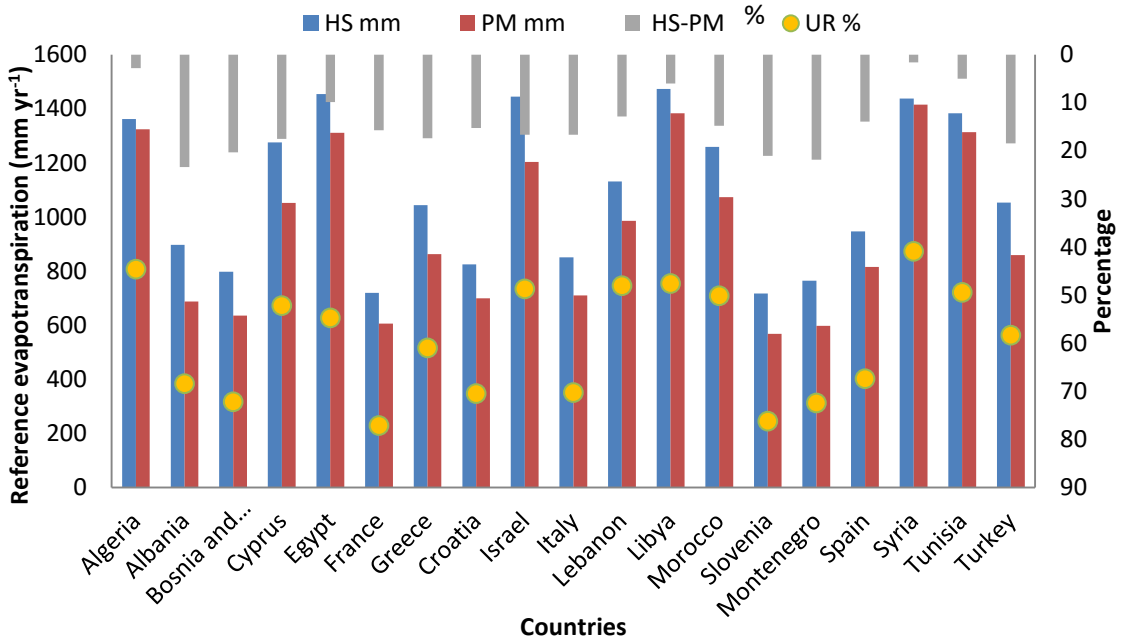

Fig. 112. Mean annual ETo_HS and ETo_PM values and differences of their values, and mean annual relative humidity in Mediterranean basin Countries for the period 1976-2005.

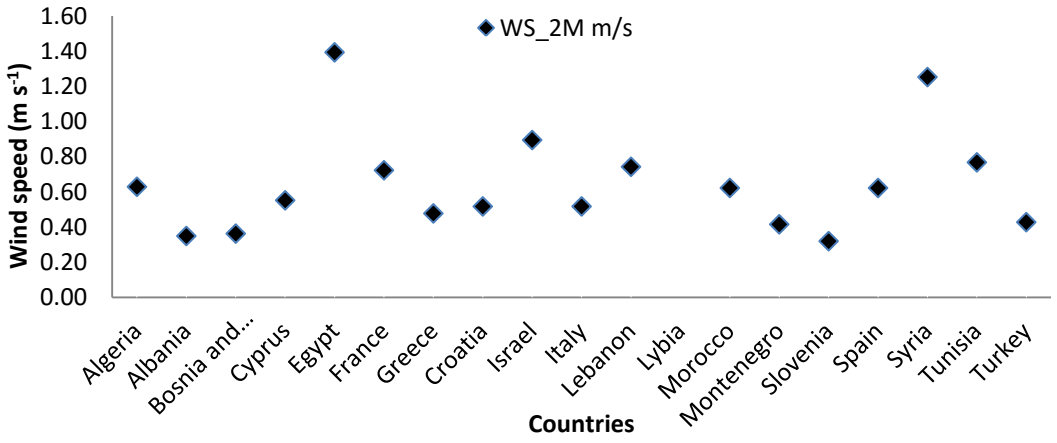

Fig. 113. Mean annual wind speed in the Mediterranean basin Countries for the period 1976-2005.

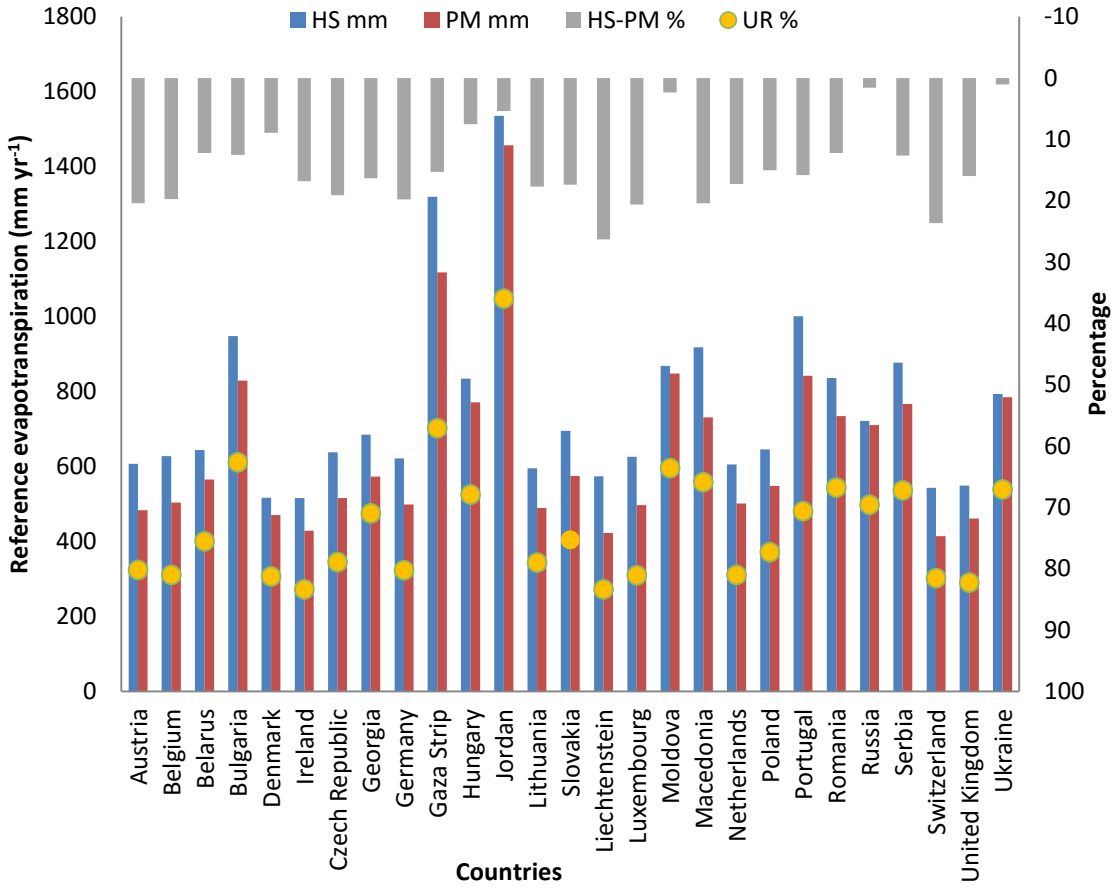

Fig. 114. Mean annual ETo_HS and ETo_PM values and differences of their values, and mean annual relative humidity in Countries which belong to the domain under study for period 1976-2005.

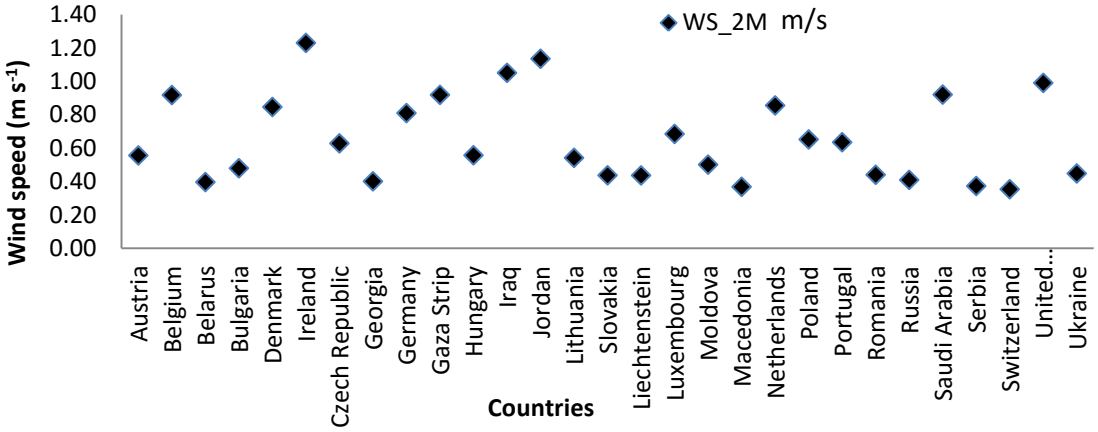

Fig. 115. Mean annual wind speed in Countries which belong to the domain under study for period 1976-2005.

Excluding the Mediterranean Countries, a value of mean relative humidity (RH) higher than 70% was found in Austria, Belgium, Belarus, Denmark, Ireland, Czech Republic,

Germany, Lithuania, Slovakia, Liechtenstein, Luxemburg, The Netherlands, Poland, Slovenia, Switzerland, and United Kingdom. These Countries also showed the higher differences between HS and PM equations. Differences between the two methods higher than 100 mm yr^{-1} were also found in Countries characterized by low mean wind speed (WS) such as Switzerland, Serbia, Slovenia, and Macedonia where WS was never higher than 0.38 m s^{-1}. The lowest mean RH values were estimated in very dry and windy Countries such as Jordan (RH=36% and WS=1.13 m s^{-1}). The underestimation in ETo_HS compared to ETo_PM computed in dry Countries was in line with Nandagiri and Kovoor (2006) and Rahimi Khoob (2008).

In Mediterranean Countries, and specifically Tunisia, Syria, and Algeria, the lowest differences between ETo_HS and ETo_PM were found, in correspondence with the lowest values of mean RH. WS values lower than 0.4 m s^{-1} were found in Turkey, Montenegro, Greece, Bosnia and Herzegovina, as well as in Albania where the highest overestimation, i.e. differences between HS and PM, was found.

The correlation between mean annual ETo_HS and ETo_PM in Mediterranean Countries was equal to 98%, and 99% in the other Countries of the domain.

2.3.1.1 Validation of ETo regional estimates

The accuracy of the modeled climatic variables used to compute ETo at regional scale was assessed by comparing observed daily climate data (i.e. TMAX, TMIN, RN, PCP, and WS site) obtained at the FLUXNET sites (Part 1), E-OBS gridded observation climate data interpolated at 21 km (i.e. TMAX and TMIN E-OBS) and the climate variables simulated by the COSMO-CLM RCM forced by Era-Interim reanalysis with a final spatial resolution of about 14 km (TMAX, TMIN, RN, PCP, and WS EI). Simulated variables performance was assessed for each FLUXNET site for the specific crop growing seasons (Table 39).

Tab. 39. Assessment of modeled variables performance by comparing the observed (site) and modeled (E-OBS and EI) variables. TMAX EI, TMIN EI, RN EI, PCP EI, WS EI=maximum and minimum temperature, net radiation, precipitation, and wind speed simulated by COSMO-CLM RCM forced by Era-Interim reanalysis. TMAX EOBS and TMIN EOBS= E-OBS gridded maximum and minimum temperature obtained by the interpolation of station data. TMAX site, TMIN site, RN site, PCP site, and WS site= maximum and minimum temperature, net radiation, precipitation, and wind speed measured by the Eddy Covariance station.

			TMAX EI TMAX site		TMAX EOBS TMAX site		TMIN EI TMIN site		TMIN EOBS TMIN site		RN EI RN site		PCP EI PCP site		WS EI WS site	
SITE	YEAR	CROP	r	R^2	r	R^2	r	R^2	r	R^2	r	R^2	r	R^2	r	R^2
Grignon	05	MAIZE	0.94	0.88	0.99	0.98	0.86	0.73	0.92	0.84	0.72	0.52	0.45	0.20	0.66	0.43
Grignon	05-06	WHEAT	0.97	0.95	0.99	0.98	0.95	0.90	0.98	0.96	0.9	0.80	0.59	0.35	0.80	0.61
Gebesee	06-07	WHEAT	0.97	0.95	0.99	0.99	0.93	0.86	0.99	0.98	0.90	0.82	-0.07	0.005	0.87	0.78
Klingenberg	05-06	WHEAT	0.99	0.97	0.99	0.99	0.97	0.94	0.99	0.98	0.92	0.84	0.46	0.21	0.67	0.45
Klingenberg	07	MAIZE	0.91	0.83	0.99	0.99	0.91	0.82	0.96	0.91	0.75	0.57	0.52	0.27	0.67	0.45
Oensingen	06-07	WHEAT	0.93	0.86	0.93	0.86	0.88	0.77	0.89	0.79	0.90	0.81	0.61	0.37	0.81	0.66
Dijagraaf	07	MAIZE	0.83	0.68	0.89	0.80	0.81	0.65	0.90	0.82	0.59	0.35	0.15	0.02	0.04	0.00
Lamasquere	06	MAIZE	0.93	0.86	0.96	0.92	0.77	0.60	0.86	0.74	0.55	0.30	0.25	0.06	0.45	0.20
Lamasquere	06-07	WHEAT	0.95	0.89	0.98	0.96	0.93	0.87	0.96	0.93	0.87	0.75	0.66	0.44	0.76	0.60
Lonzee	04-05	WHEAT	0.98	0.95	0.99	0.97	0.95	0.89	0.95	0.89	0.9	0.82	0.62	0.39	0.86	0.74
Lonzee	06-07	WHEAT	0.7	0.49	0.72	0.51	0.63	0.39	0.68	0.46	0.78	0.61	0.5	0.26	0.58	0.33
Borgo Cioffi	05	MAIZE	0.73	0.53	0.88	0.78	0.66	0.43	0.78	0.60	0.58	0.34	0.26	0.07	0.44	0.20
Borgo Cioffi	06	MAIZE	0.75	0.56	0.74	0.55	0.81	0.66	0.91	0.83	0.30	0.09	0.22	0.05	0.22	0.05
Borgo Cioffi	07	MAIZE	0.78	0.62	0.92	0.86	0.78	0.61	0.88	0.78	0.43	0.18	0.13	0.016	0.44	0.20
Borgo Cioffi	09	MAIZE	0.74	0.54	0.86	0.74	0.68	0.46	0.82	0.66	0.24	0.06	0.04	0,00	0.25	0.06
Valle dell'Adige	09	GRAPE	0.84	0.70	0.93	0.87	0.84	0.70	0.93	0.87	0.40	0.15	0.11	0.01	0.45	0.20
Negrisia	07	GRAPE	0.91	0.83	0.98	0.96	0.88	0.78	0.94	0.88	0.80	0.64	0.47	0.22	0.45	0.20
Negrisia	08	GRAPE	0.92	0.85	0.99	0.97	0.89	0.79	0.96	0.92	0.74	0.55	0.14	0.02	0.04	0.00

Although the differences in resolution between observed (point for weather station and 21 km for gridded observations) and modeled (14 km) variables, a good correlation was observed for temperature between site observation and both gridded interpolated and simulated temperature. Correlation values of TMAX site were consistenly higher when compared with TMAX EOBS. In the same sites also the determination coefficient (R^2) between Era Interim (TMIN EI) minimum temperature and the observation (TMIN site) was high, even if the best performance were reached using E-OBS temperature, as expected. A Pearson's coefficient lower than 0.70 was observed in Borgo Cioffi (Campania region), and this could confirm lower performances for climate models due to the low number of weather stations for E-OBS in South Italy (Haylock et al., 2008; Bucchignani et al., 2013). The low performance of E-OBS in South Italy is also confirmed for all the other variables.

The low agreement obtained between modeled and observed precipitation, could be attributed to COSMO precipitation missrepresentation, particularly in winter and spring, with differences up to 8 mm day^{-1}. In areas characterized by the presence of mountains, and in general by a high orography, the low performance obtained between modeled and observed precipitation is easily explained by the general interaction between climate and landform at a much higher scale than the one represented by the climate model. In addition, the percentage of filled gap data in each site (Part 1) could influence the correct variable representation. Good correlation between measured and simulated net radiation were observed with limited lack of data, such as for instance in Klingenberg 2005-2006, Oensingen, Negrisia 2007, and in Gebesee. The best wind speed performance ($r > 0.80$) were computed in Grignon 2006, Gebesee 2006-2007, Oensingen, and Lonzee 2004-2005. The lower performance could be explained by the site location, as many studies stated the scarce ability of RCMs in predicting wind speed as the one carried on by Geyer et al. (2015), where a high variability of this variable was noticed (e.g. in North Europe).

The assessment of the modeled ETo performance was based on the comparison between reference evapotranspiration computed using HS and PM equation on gridded datset (E-OBS and EI), and using the measured variables in the Fluxnet sites. Both the modeled ETo with E-OBS and Era Interim gridded datasets were used for the comparison (Table 40).

Tab. 40. Validation assessment of modeled of ETo with Hargreaves (E-OBS and EI gridded data) and Penman Monteith (EI gridded data) methods against site observations (FLUXNET sites) and modeled ones.

SITE	YEAR	CROP	HS site		HS site		PM site	
			HS E OBS		**HS Era Interim**		**PM EI**	
			r	**R^2**	**r**	**R^2**	**r**	**R^2**
Grignon	2005	MAIZE	-0.095	0.009	-0.17	0.029	0.7	0.49
Grignon	2005-2006	WHEAT	0.92	0.85	0.9	0.8	0.9	0.81
Gebesee	2006-2007	WHEAT	0.89	0.79	0.89	0.79	0.8	0.64
Klingenberg	2005-2006	WHEAT	0.64	0.41	0.6	0.36	0.93	0.87
Klingenberg	2007	MAIZE	-0.04	0.001	-0.112	0.012	0.83	0.69
Oensingen	2006-2007	WHEAT	0.79	0.62	0.79	0.62	0.91	0.82
Dijagraaf	2007	MAIZE	-0.33	0.11	-0.3	0.09	0.59	0.35
Lamasquere	2006	MAIZE	0.38	0.15	0.41	0.17	0.67	0.45
Lamasquere	2006-2007	WHEAT	0.79	0.62	0.75	0.56	0.88	0.78
Lonzee	2004-2005	WHEAT	0.81	0.66	0.79	0.62	0.93	0.87
Lonzee	2006-2007	WHEAT	0.67	0.45	0.68	0.46	0.81	0.66
Borgo Cioffi	2005	MAIZE	0.17	0.03	0.05	0.003	0.46	0.21
Borgo Cioffi	2006	MAIZE	0.31	0.09	0.34	0.12	0.59	0.35
Borgo Cioffi	2007	MAIZE	0.57	0.33	0.47	0.22	0.52	0.27
Borgo Cioffi	2009	MAIZE	-0.11	0.012	-0.05	0	0.38	0.15
Valle dell'Adige	2009	GRAPE	0.39	0.15	0.66	0.43	0.41	0.16
Negrisia	2007	GRAPE	0.17	0.03	0.21	0.04	0.77	0.6
Negrisia	2008	GRAPE	0.22	0.05	0.38	0.14	0.75	0.56

Even though modeled gridded temperatures reach a high levels of agreement compared with observations, still the greatest level of reliability of ETo was observed using PM. Correlation values higher than 0.80 were computed by comparing gridded PM estimated using Era Interim data with observations in almost all sites. The best correlations for HS and PM were obtained for longer time series (longer growing season) as these integrate largest range of values, reducing the relevance of data noise. In Grignon 2005-2006, Gebesee 2006-2007, and Lonzee 2004-2005, cultivated by wheat and where a longer crop growing period is on place, a correlation higher than 0.80 was observed both considering outcomes with the HS and PM equations and using the EOBS and EI datasets (Table 40). The accuracy was also confirmed by a low RE and RMSE, as well as by an index of agreement close to 90%.

Correlation coefficient under 0.50 were found instead for HS computed using both climatic models and on site measurements for maize and grape, which have a shorter

growing season, mainly concentrated in summer months. In addition, a negative correlation coefficient was verified for these crops comparing HS site and HS E-OBS and HS EI in Klingenberg 2007, Dijagraaf 2007, Borgo Cioffi 2009, and Grignon 2005, where high values of RE, RMSE, an index of agreement lower than 40% and an overestimation of the modeled HS (MBE) were also computed (Table 41). A ETo_HS overestimation higher than 1 mm day^{-1} was also found in each season in Borgo Cioffi and in Valle dell'Adige, in correspondence with an underestimation of site ETo_PM. The systematic HS overestimation of climate gridded products in summer months may be related to the site location, specifically to the high humidity that characterized the sites located in the Northern Europe (precipitation of 172 mm, 310 mm, and 299 mm were measured in Grignon 2005, Klingenberg 2007, and Dijagraaf). The highest ETo_HS overestimation values in the Southern sites were measured where temperature values were high. In Table 41, statistical indices define the performance of the modeled ETo_HS and ETo_PM in each European site and for each available crop growing season.

Tab. 41. Comparison between modeled ETo_HS and ETo_PM with the observed ones in each European site and for each available year.

SITE YEAR	CROP	HS site EOBS	HS site EI	PM site EI	HS_OBS vs HS_site	HS_EI vs HS_site	PM_EI vs PM_site	HS_OBS vs HS_site	HS_EI vs HS_site	PM_EI vs PM_site	HS_OBS vs HS_site	HS_EI vs HS_site	PM_EI vs PM_site	HS_OBS vs HS_site	HS_EI vs HS site	PM_EI vs PM site
		RE	RE	RE	RMSE	RMSE	RMSE	MAE	MAE	MAE	MBE	MBE	MBE	IA	IA	IA
		%	%	%	mm	mm	mm	mm	mm	mm	mm	mm	mm	%	%	%
Grignon 05	MAIZE	43.3	46.6	18.7	2.24	2.42	1.15	1.95	2.1	0.92	1.38	1.6	0.6	0.32	0.3	0.79
Grignon 05-06	WHEAT	15.7	18.7	14.3	0.77	0.91	0.89	0.64	0.74	0.64	-0.17	-0.15	0.04	0.94	0.92	0.93
Gebesee 06-07	WHEAT	14.7	14.3	14.5	0.87	0.85	1.08	0.71	0.69	0.74	-0.04	-0.32	-0.2	0.93	0.93	0.89
Klingenberg 05-06	WHEAT	43.2	41.5	11.4	1.59	1.53	0.7	1.15	1.13	1.15	0.71	0.6	0.21	0.63	0.63	0.96
Klingenberg 07	CORN	54.7	48.6	12.4	2.24	1.99	0.78	1.89	1.68	0.55	1.51	1.11	0.06	0.36	0.33	0.91
Oensingen 06-07	WHEAT	16.4	17.8	14.4	1.31	1.42	0.84	0.98	1.07	0.59	-0.63	-0.83	-0.35	0.85	0.82	0.93
Dijagraaf 07	MAIZE	49.8	46.0	21.5	2.2	2.03	0.94	1.88	1.75	0.75	1.44	1.06	-0.02	0.3	0.27	0.76
Lamasquere 06	MAIZE	52.3	62.6	33.8	2.26	2.71	1.68	2.01	2.39	1.36	1.9	2.36	1.32	0.48	0.45	0.65
Lamasquere 06-07	WHEAT	16.8	19.6	15.9	0.96	1.12	0.87	0.8	0.92	0.58	-0.22	-0.4	0.32	0.87	0.83	0.92
Lonzee 04-05	WHEAT	19.4	20.0	10.4	1.02	1.05	0.63	0.81	0.85	0.47	-0.01	0	0.02	0.86	0.85	0.96
Lonzee 06-07	WHEAT	23.1	22.6	18.5	1.17	1.15	0.91	0.88	0.88	0.64	0.1	0	-0.04	0.79	0.79	0.89
Borgo Cioffi 05	MAIZE	66.7	83.8	18.0	2.26	2.85	0.9	2.05	2.59	0.69	2.04	2.56	-0.19	0.4	0.34	0.67
Borgo Cioffi 06	MAIZE	33.4	38.6	23.5	2.29	2.65	1.06	1.9	2.29	0.81	1.77	2.15	-0.21	0.51	0.59	0.72
Borgo Cioffi 07	MAIZE	42.8	48.0	19.6	2.26	2.54	1.01	2.1	2.32	0.74	2.07	2.29	-0.32	0.47	0.44	0.69
Borgo Cioffi 09	MAIZE	92.4	73.0	26.2	2.4	3.08	1.11	2.21	2.8	0.79	2.19	2.8	-0.46	0.33	0.27	0.55
Valle dell'Adige 09	GRAPE	33.8	24.4	21.8	1.79	1.29	1.46	1.55	1.12	1.11	1.19	0.72	-0.44	0.55	0.72	0.61
Negrisia 07	GRAPE	30.8	33.1	17.8	1.83	1.97	1.05	1.67	1.78	0.83	0.19	0.45	-0.38	0.48	0.52	0.86
Negrisia 08	GRAPE	30.6	28.5	19.5	1.86	1.74	1.18	1.68	1.5	0.93	0.08	0.09	-0.47	0.51	0.63	0.84

2.3.2 Regional ETo estimation for future climate conditions

In this section the behavior of ETo under future climate conditions is presented following the two climate scenarios (RCP 4.5 and RCP 8.5) (Figures 116 and 118). The impact of climate change on ETo is also analyzed through the calculation of the climate anomalies (i.e. the difference between the future climate, in the period 2036-2065, and the baseline period, 1976-2005 (Figures 117 and 119).

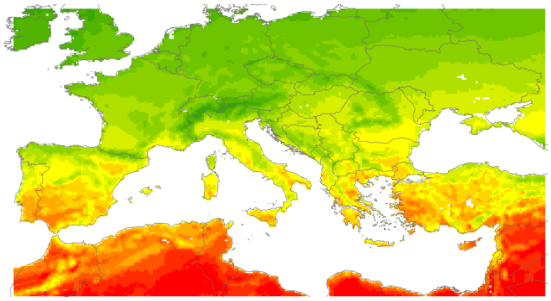

Fig. 116. Regional estimates of mean annual ETo_HS for the future period (2036-2065) under the RCP 4.5 scenario.

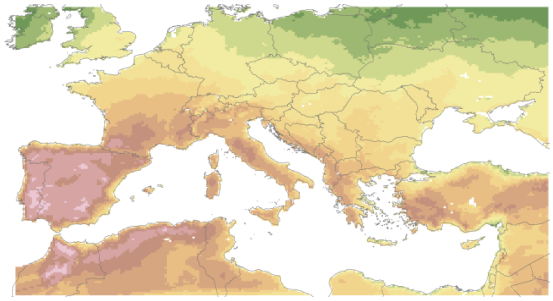

Fig. 117. Climate anomalies for ETo_HS regional estimates.

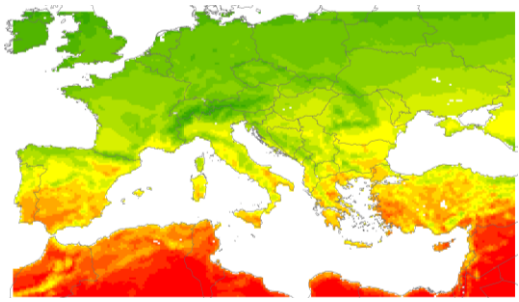

Fig. 118. Regional estimates of mean annual ETo_HS for the future period (2036-2065) under the RCP 8.5 scenario.

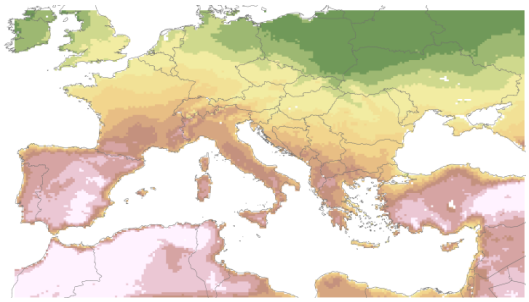

Fig. 119. Climate anomalies for ETo_HS regional estimates.

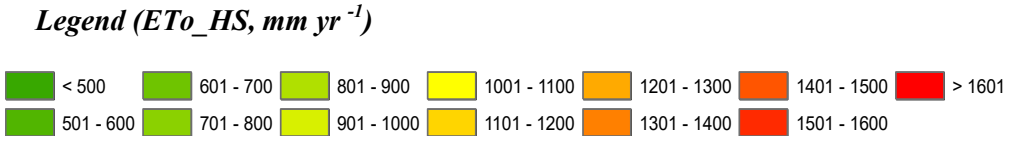

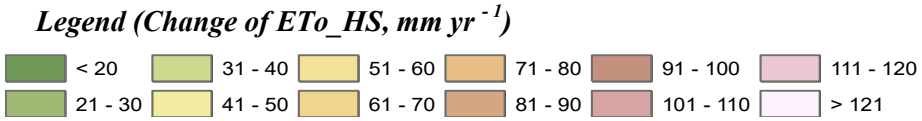

Results showed increasing ETo_HS values along the entire domain from the baseline to the future. The highest values of ETo_HS under both RCPs were estimated in most of the Mediterranean Countries, specifically values from about 1000 mm yr^{-1} (Spain) to 1600 mm yr^{-1} (Libya) were estimated in the Northern Africa, Syria, Israel, Cyprus, Lebanon, Turkey, and Greece. Values about 100 mm yr^{-1} higher than in Libya were computed in Jordan, while values close to the ones estimated in Spain were found in Portugal (~ 1100 mm yr^{-1}) and Bulgaria (~1015 mm yr^{-1}).

A range between 1000 mm yr^{-1} and 900 mm yr^{-1} was computed in Albania, Serbia, and Italy with maximum and minimum values in Macedonia (1006 mm yr^{-1}) and Moldova (915 mm yr^{-1}). In Croatia, Bosnia and Herzegovina, France, as well as in Romania values from 900 mm yr^{-1} (Romania) to 800 mm yr^{-1} (Ukraine) were computed in the intermediate future. In all the other Countries, ETo_HS values were lower than 800 mm yr^{-1}, and the lowest values were found in the Northern Countries such as Ireland and United Kingdom (540 mm yr^{-1}) under both RCPs.

In Figure 117 and 119 are reported the climate anomalies, expressed in millimeters for the entire domain investigation. It is worth notincing that the highest differences (100-140 mm yr^{-1}) were estimated in the Southern regions, such as Morocco, Algeria, Tunisia, Spain, Jordan, Syria, Portugal, and Turkey and that they were more evident under RCP 8.5. Differences from about 90 mm yr^{-1} to 80 mm yr^{-1} were estimated in Macedonia, Lebanon, Italy, Montenegro, Greece, and Cyprus.

In Figure 120 and 121, the climate anomalies are reported in percentage. In general, differences between future period and baseline were higher under RCP 8.5 except in Belgium, Netherlands, Czech Republic, Slovakia, Moldova, Denmark, Unkraine, Poland, Belarus, Russia, and Lithuania. Any difference between ETo_HS computed under RCP 8.5 and 4.5 was found in several Countries, such as in Portugal, France, Austria, Croatia, Germany, United Kingdom, Hungary, Romania, and Ireland.

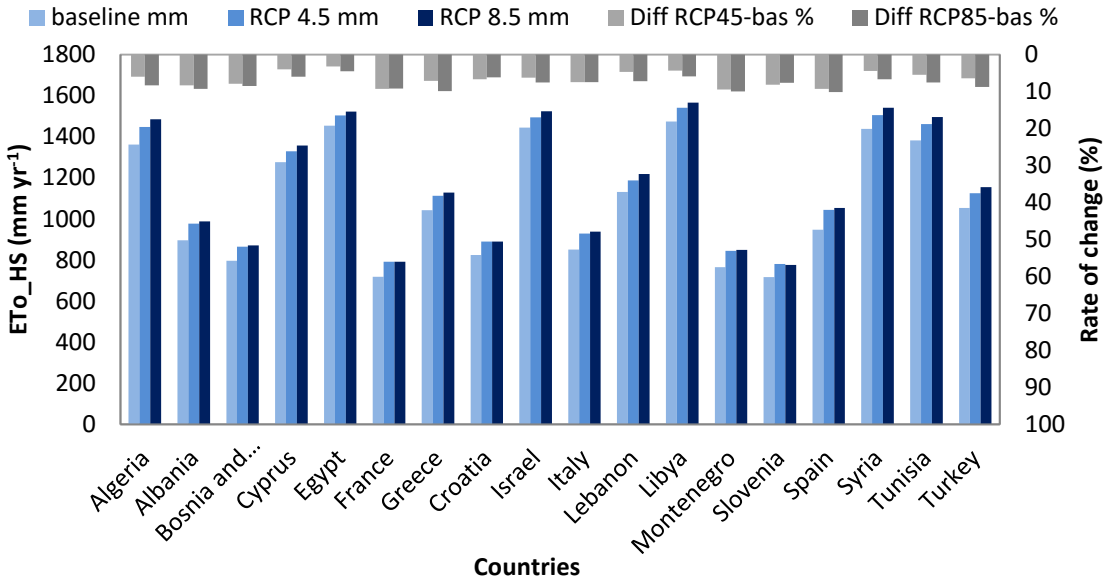

Fig. 120. Mean annual ETo_HS values estimated for baseline and future climate scenarios, and climate anomalies per each Mediterranean Country.

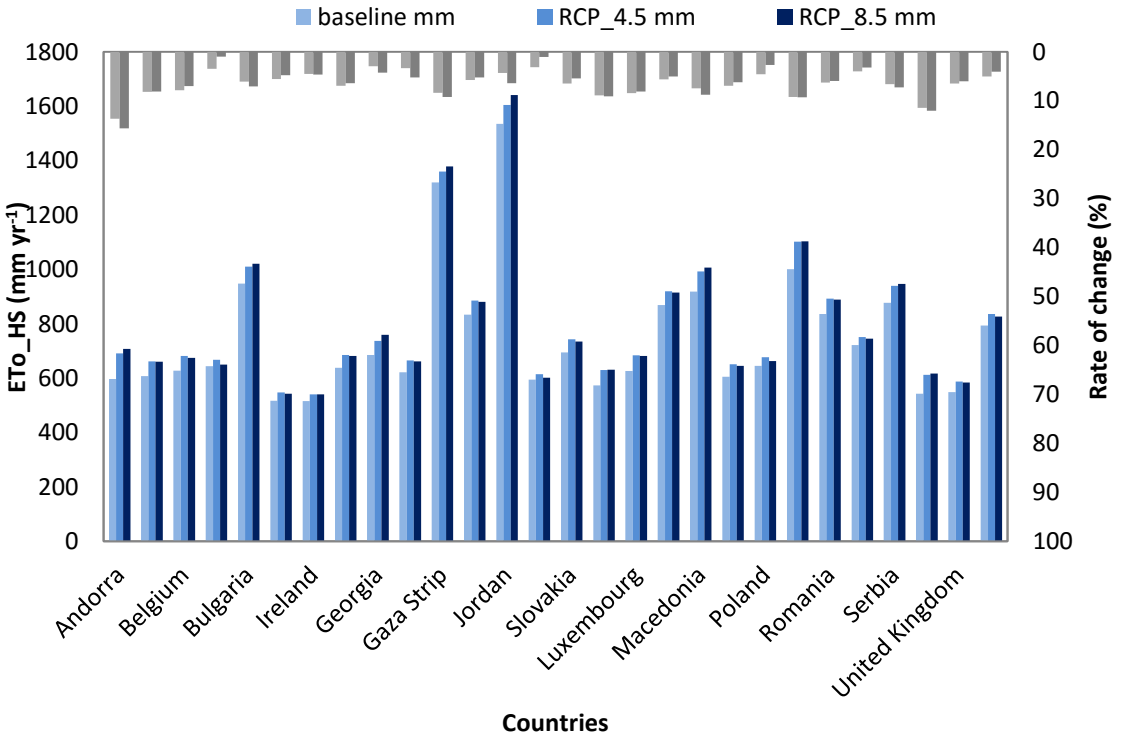

Fig. 121. Mean annual ETo_HS values estimated for baseline and future climate scenarios, and climate anomalies per each Countries which belong to the studied domain.

Regional estimates of ETo_PM for future climate (2036-2065) are reported in this section (Figures 122 and 124). Climate anomalies are also reported in Figure 123 and 125.

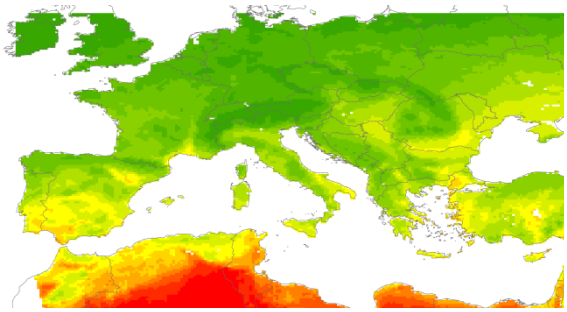

Fig. 122. Regional estimates of mean annual average of ETo_PM values for the future (2036-2065), RCP 4.5 scenario.

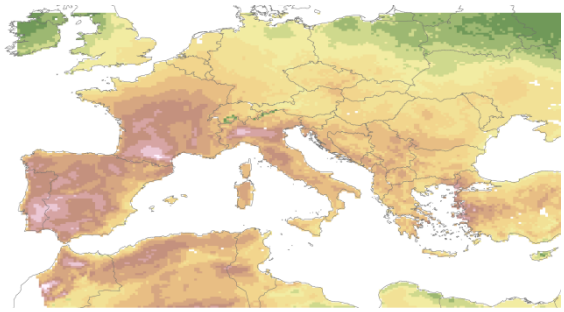

Fig. 123. Climate anomalies for ETo_PM regional estimates.

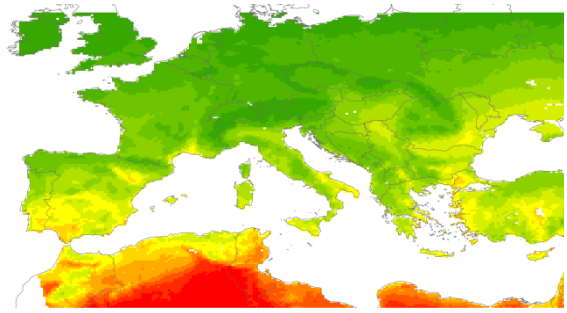

Fig. 124. Regional estimates of mean annual average of ETo_PM values for the future (2036-2065), RCP 8.5 scenario.

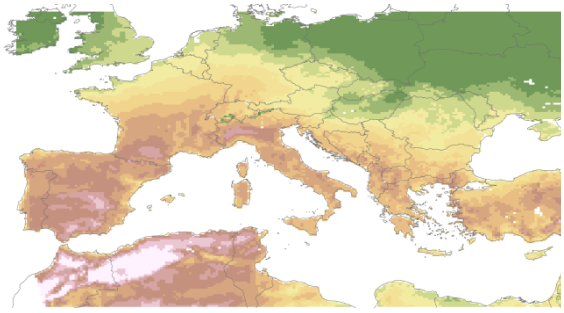

Fig. 125. Climate anomalies for ETo_PM regional estimates.

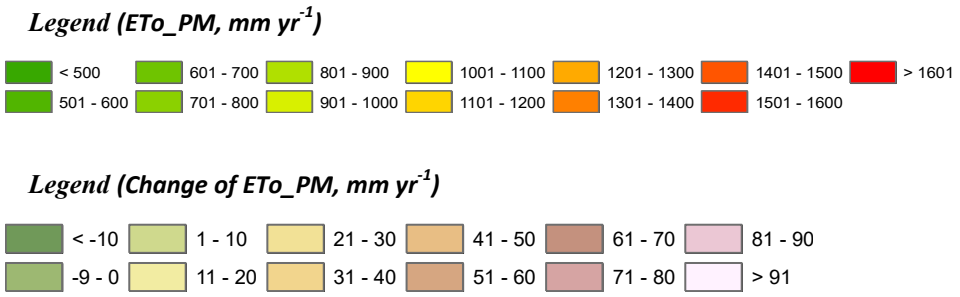

Regional annual mean ETo_PM (Figure 122 and 124) estimates followed the same trend as observed for the ETo_HS values (Figure 116 and 118). ETo_PM was projected to grow in each Country with a greater difference in the Mediterranean Countries where mean values ranged from ~ 60 to 40 mm yr^{-1} under RCP 4.5. Under the same scenario, values lower than 22 mm yr^{-1} were computed in Syria, Libya, Israel, Lebanon, Egypt, and Cyprus. The same trend was found also under RCP 8.5, with differences only in Libya and Slovenia, where a reverse condition occurred, i.e. higher differences were estimated in Syria (41 mm yr^{-1}) and lower in Slovenia (27 mm yr^{-1}). In general the highest differences were estimated under RCP 8.5 except for Northern and Northern

Eastern Countries, such as Denmark, Poland, Germany, Slovakia and so on. It is noticeable that the areas characterized by mean ETo_PM values highest than 90 mm yr^{-1} are located in the Northern Africa, specifically in Morocco and Algeria.

In Figure 126 and 127 the mean annual ETo_PM per each Mediterranean Country and for the other Countries of the domain, respectively, are shown.

ETo_PM tended to be lower than the ETo_HS. Values higher than 1000 mm yr^{-1} were estimated in Algeria, Egypt, Gaza strip, Israel, Jordan, Lebanon, Libya, Morocco, Syria, and Tunisia were the high temperature, the strong wind speed and low humidity are the main features of these areas affecting ETo values. This is expected to be exacerbated under both RCPs for the future. In Mediterranean Regions, values were up to 700 mm yr^{-1} except for France, Bosnia and Herzegovina, and Slovenia. Low values of ETo_PM (< 500 mm yr^{-1}) were found in Austria, Denmark, Ireland, Lithuania, Slovakia, Liechtenstein, Luxemburg, The Netherlands, Poland, Switzerland, as well as United Kingdom, i.e. in Northern European Countries, where a general slightly increase of relative humidity is expected, even though it is important to consider that the differences between the relative humidity estimated in the future under both RCPs was never greater than 3%.

Differences between RCPs scenarios and baseline (Figure 126 and 127) ranged from 1 to 7% and from 1 to 8% under RCP 4.5 and 8.5, respectively, in Mediterranean Countries. Negative values were estimated in the other Countries which belong to the studied domain where differences ranged from -1 to 9 under RCP 4.5, and from -8 to 10 under RCP 8.5. Negative values were estimated in Belarus, Lithuania, Russia, Poland, Ireland, Ukraine, Denmark, and United Kingdom under RCP 8.5, and in Ireland, Lithuania, Belarus, and Russia under RCP 4.5. Negative percentages may be due to the low temperature values, and the high relative humidity and wind speed values that characterized this Countries. The greatest RH differences were expected in Mediterranean basin, specifically by 1.3% under RCP 4.5 and 1.4% under RCP 8.5, while the difference between RCP 8.5 and 4.5 in Mediterranean Countries was equal to -0.13%. An average of -0.01 m s^{-1} was expected as the difference of future WS under RCP 4.5 and the baseline.

Regarding to the remaining Countries, an average difference of 0.04 m s^{-1} between future climate (under RCP 4.5) and the baseline, was computed for WS, and 0.02 m s^{-1}

under RCP 8.5. The difference between RCP 8.5 and 4.5 was equal to -0.02 m s^{-1}. The difference between the projected RH (under RCP 4.5) and the baseline was -0.63%, while under RCP 8.5 it was lower (-0.09%). The difference between WS estimated under RCP 8.5 and 4.5 was equal to 0.54%.

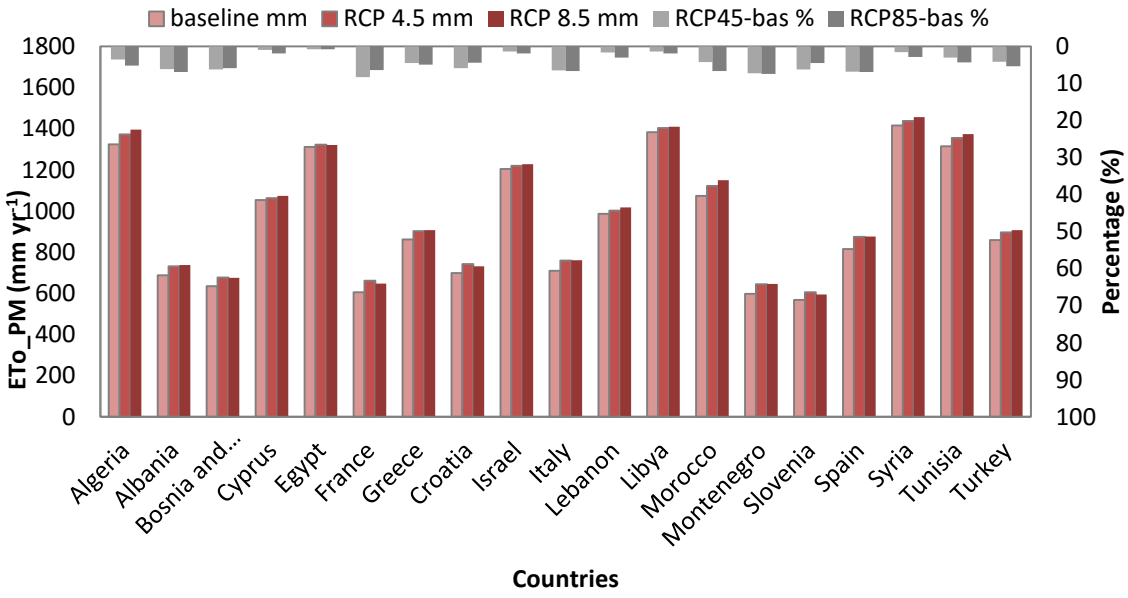

Fig. 126. Mean annual ETo_PM values estimated for baseline and future climate scenarios, and climate anomalies per each Mediterranean Country.

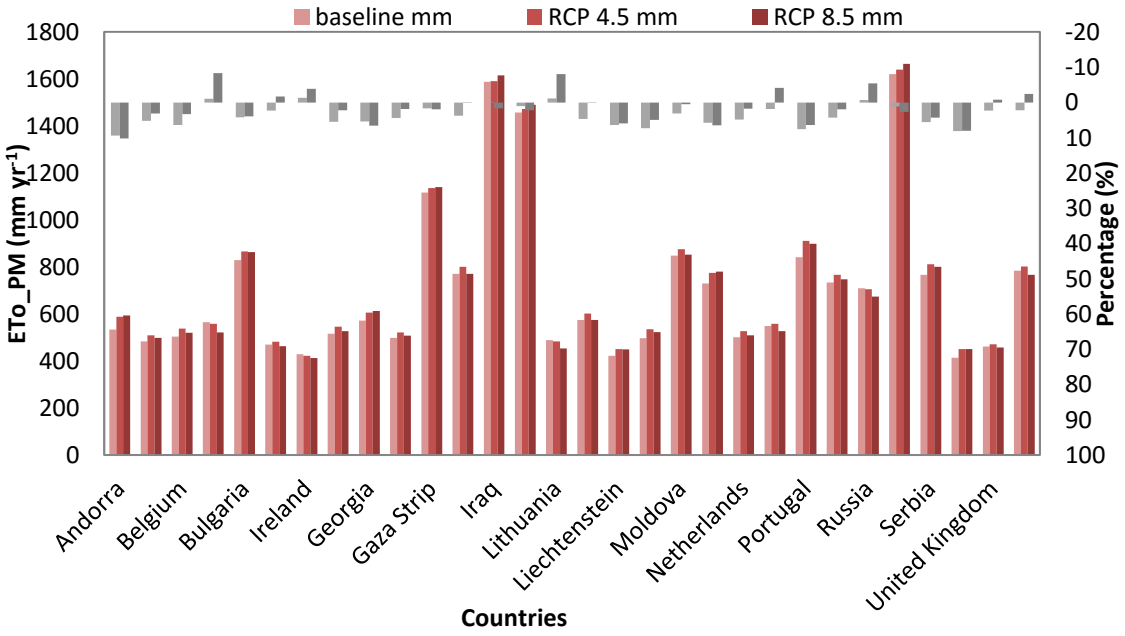

Fig. 127. Mean annual ETo_PM values estimated for baseline and future climate scenarios, and climate anomalies per each Countries which belong to the studied domain.

2.3.3 Impact of climate change on crop evapotranspiration and irrigation demand

Several studies stated that climate change is affecting crop productivity (Harrison and Butterfield, 1996; Alexandrov, 1999; Harrison and Butterfield, 2000). Nevertheless, Kenny et al. (1993), Carter et al. (1996) and Harrison and Butterfield (1996) stated that cereals growth areas, and specifically maize and wheat cultivated areas, should enlarge areas northward due to climate change.

The impact of climate change on crop and actual evapotranspiration, and irrigation requirement was assessed considering wheat cultivated in rainfed conditions, maize and wheat irrigated using sprinkler irrigation methods, and grape irrigated using drip method. Values of ETc, ETa, and NA, for the entire domain and weighted by the area where the crops are actually cultivated, are reported for the top productive Countries at Euro-Mediterranean scale. No-weighted values describe the water consumption and requirement assuming that crop is allowed to grow up everywhere inside the domain (i.e. values were not weighted for the percentage of cultivated area per each Country). Weighted values emphasize where the crop is currently cultivated in irrigated and rainfed conditions. In addition values were weighted for irrigated areas as reported in the SPAM database.

Actual evapotranspiration (ETa) was estimated by making soil, crop, and management assumptions previously mentioned, i.e. the allowable depletion of 50%, the maximum soil depth and soil water holding capacity characteristic of the area under investigation, the sowing, bud break, and harvest date, and the maximum rooting depth of the specific crop. Sprinkler irrigation method was considered for maize and wheat, while drip system for grape.

2.3.3.1 Maize

The regional mean estimates of crop (ETc) and actual (ETa) evapotranspiration, and their differences, are reported for the baseline (1976-2005) (Figure 128, 129, and 130), and the intermediate future (2036-2065) under RCP 4.5 (Figure 131, 132, and 133), and

RCP 8.5 scenarios (Figure 134, 135, and 136). The irrigated areas shown in the maps are distinguished using solid diagonal lines.

Results show increasing values of ETc and ETa from the past to the future in the Euro-Mediterranean area. Assuming all the simulated domain, the highest ETc values were estimated in the Mediterranean Countries, particularly in Northern Africa regions such as Tunisia, Libya, and Algeria where values ranged from 800 mm yr^{-1} and 900 mm yr^{-1} close to the Sahara desert, while lower values (500-700 mm yr^{-1}) were estimated closer to the coast. High values of ETc characterized also Spain, Italy, Turkey, Lebanon, and Greece, where ETc values were never lower than 600 mm yr^{-1}. The lowest crop water consumption from around 400 mm yr^{-1} to 500 mm yr^{-1} was obtained in Ireland, Switzerland, United Kingdom, Germany, Netherlands, Czech Republic, Austria, and Poland. Despite water applications (NA) applied in the model at specific soil water deficit thresholds, the estimated actual evapotranspiration was lower than crop evapotranspiration denoting a general suboptimal efficiency of intermitting applications to fulfill crop water requirements. The highest ETc values correspond to areas where ETa could be substantially very low, with differences reaching values up to around 800 mm yr^{-1}. This could be explained considering areas in north Africa with very low soil depth (140 mm) and a soil water holding capacity near zero, limiting the effectiveness of irrigation to reduce high water stress. The lowest ETa values were also estimated in other Mediterranean Countries where a stress coefficient (Ks) between 0.50 and 0.90 was computed. Large amount of precipitation and irrigation, and deep soils, contribute to reduce water stress, and obtain high ETa values, in Northern European Countries.

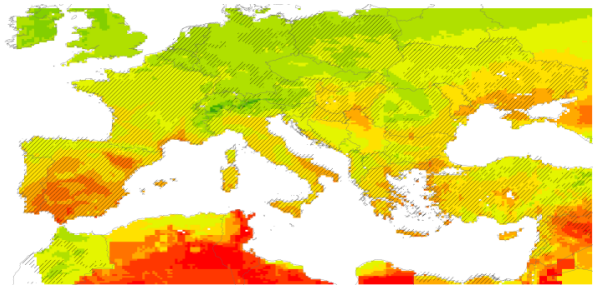

Fig. 128. Regional mean values of ETc for maize (1976-2005), considering crop growth in the entire domain. The irrigated areas are distinguished using solid diagonal lines

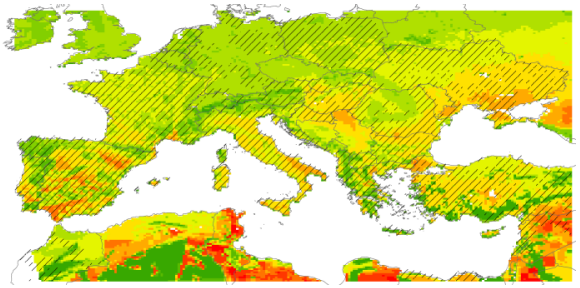

Fig. 129. Regional mean values of ETa, maize, 1976-2005, considering crop growth in the entire domain. The irrigated areas are distinguished using solid diagonal lines

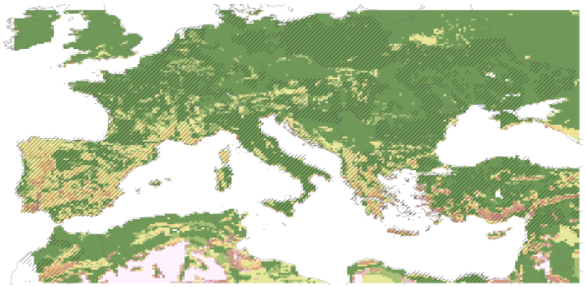

Fig. 130. Regional mean values of differences between ETc and ETa in the period 1976-2005, for maize, considering crop growth in the entire domain. The irrigated areas are distinguished using solid diagonal lines

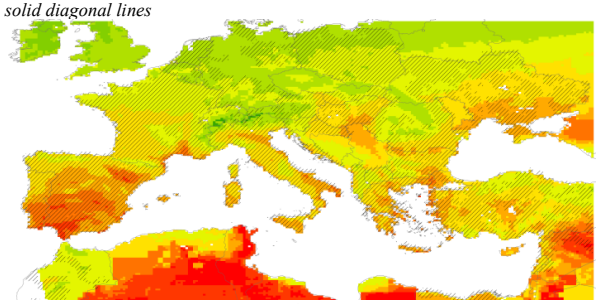

Fig. 131. Regional mean values of ETc, maize, 2036-2065, RCP 4.5, considering crop growth in the entire domain. The irrigated areas are distinguished using solid diagonal lines

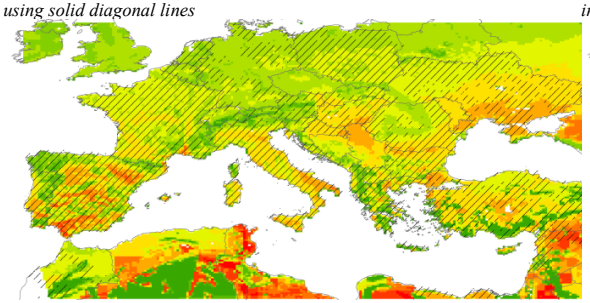

Fig. 132. Regional mean values of ETa, maize, 2036-2065, RCP 4.5, considering crop growth in the entire domain. The irrigated areas are distinguished using solid diagonal lines

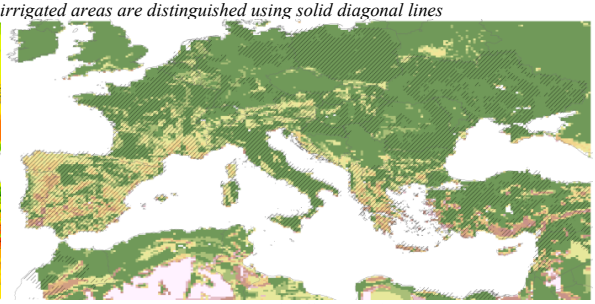

Fig. 133. Regional mean values of differences between ETc and ETa in the period 2036-2065 under RCP 4.5, for maize, considering crop growth in the entire domain. The irrigated areas are distinguished using solid diagonal lines

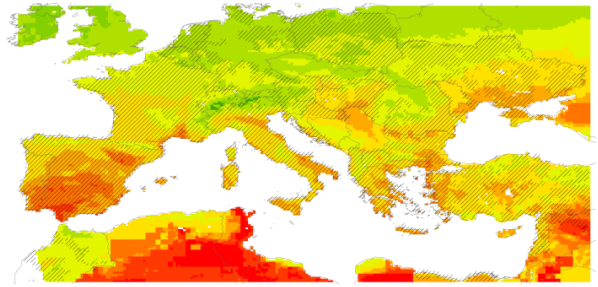

Fig. 134. Regional mean values of ETc, maize, 2036-2065, RCP 8.5, considering crop growth in the entire domain. The irrigated areas are distinguished using solid diagonal lines

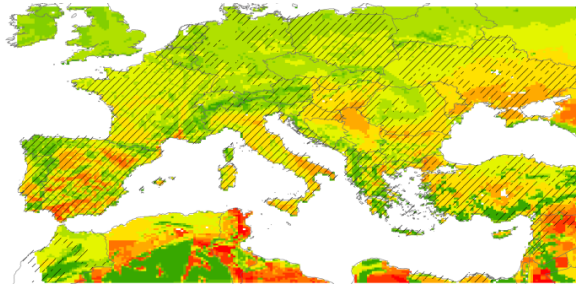

Fig. 135. Regional mean values of ETa, maize, 2036-2065, RCP 8.5, considering crop growth in the entire domain. The irrigated areas are distinguished using solid diagonal lines

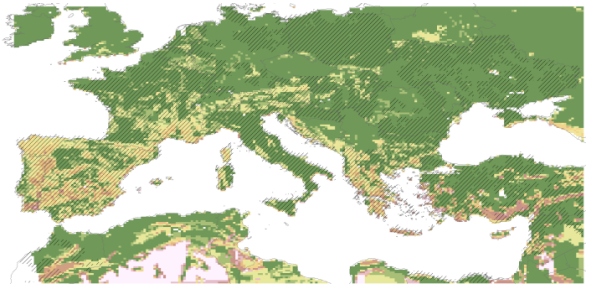

Fig. 136. Regional mean values of differences between ETc and ETa in the period 2036-2065 under RCP 8.5, for maize, considering crop growth in the entire domain. The irrigated areas are distinguished using solid diagonal lines

Legend (ETc and ETa mm yr $^{-1}$)

Legend (differences between ETc and ETa mm yr $^{-1}$)

Almost all agriculture areas under maize are irrigated at Euro-Mediterranean scale. Maize is grown as rainfed condition mostly in the Northern Europe (Belarus, Russia, Czech Republic, and a few areas in Germany) where crop water needs can be satisfied by precipitation. Crop and actual evapotranspiration are expected to increase under both climate scenarios. The highest differences between future and past ETc values were estimated in France, Italy, Portugal, Serbia, and Spain where the difference ranged from 4 to 7% (from 30 to 45 mm yr^{-1}), respectively, while a difference no higher than 2% was found between RCP 4.5 and 8.5 scenarios. The future values mostly close to the baseline were obtained in Egypt and Israel with a difference no higher than 1% (from 4 to 5 mm yr^{-1}). The highest differences of the mean ETa values were estimated around 38 mm yr^{-1} (6%) for Italy and 29 mm yr^{-1}(4%) for Spain.

Assuming maize growth along the entire domain, regional estimates of the mean water net application (NA) for the baseline (1976-2005) (Figure 137) and future climate (2036-2065) under the RCP 4.5 (Figure 138) and 8.5 scenarios (Figure 140) are shown below. In addition, differences of NA related to the climate anomalies are shown in Figure 139 and 141.

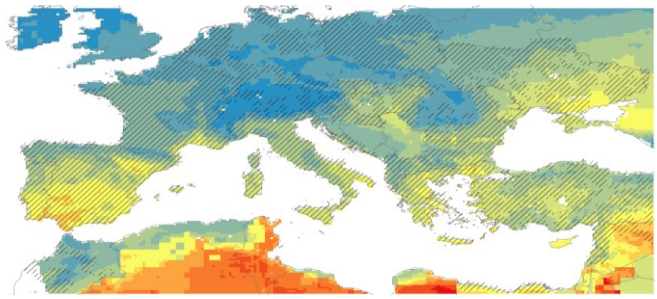

Fig. 137. Regional mean NA values for maize (1976-2005), considering crop growth in the entire domain. The irrigated areas are distinguished using solid diagonal lines.

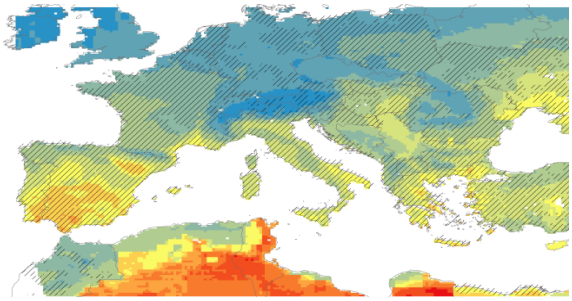

Fig. 138. Regional ,mean NA values for maize for the future (2036-2065) under RCP 4.5, considering crop growth in the entire domain. The irrigated areas are distinguished using solid diagonal lines.

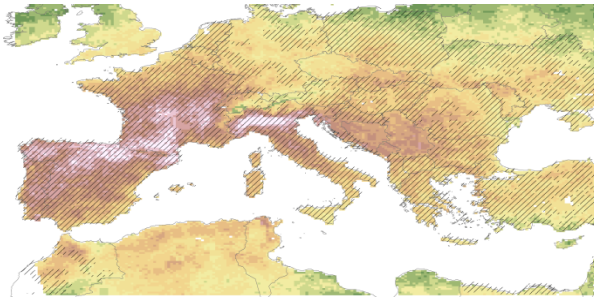

Fig. 139. Climate anomalies for Na regional estimates, considering crop growth in the entire domain. The irrigated areas are distinguished using solid diagonal lines.

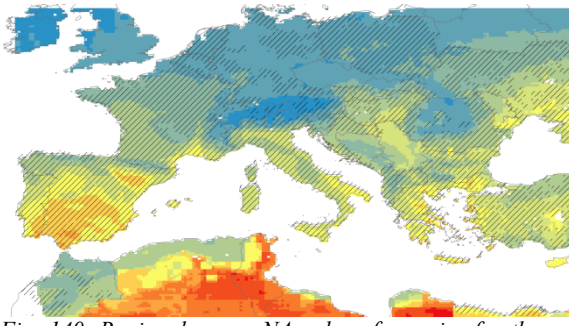

Fig. 140. Regional ,mean NA values for maize for the future (2036-2065) under RCP 8.5, considering crop growth in the entire domain.. The irrigated areas are distinguished using solid diagonal lines.

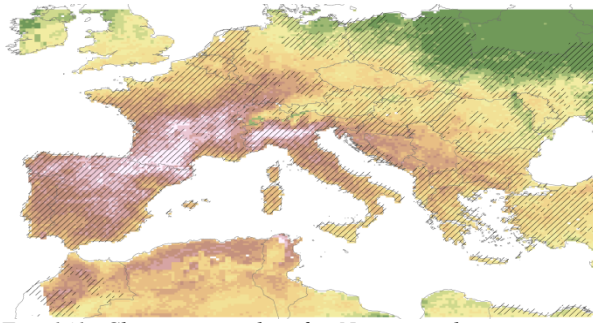

Fig. 141. Climate anomalies for Na regional estimates, considering crop growth in the entire domain. The irrigated areas are distinguished using solid diagonal lines

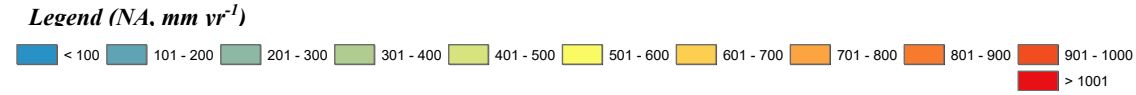

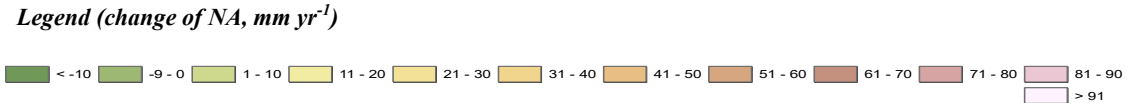

The irrigation requirement is expected to increase in the future under both RCP 4.5 and 8.5 scenarios, in each Country of the Euro-Mediterranean domain. The highest net water application were accounted for in the Sahara desert were values of NA were around 900

mm yr^{-1}. The greater irrigation demand for maize was computed in Libya, Tunisia, and Jordan where NA values were around 750 mm yr^{-1}. NA values around 400 mm yr^{-1} characterized the Northern part of Algeria. Greece, Portugal, Spain, Lebanon, and Turkey showed NA values ranging from 400 mm yr^{-1} to 500 mm yr^{-1}. The highest values of NA were simulated in areas where the total amount of precipitation was not higher than 200 mm yr^{-1}.

NA differences ranged from around 60 mm yr^{-1} to 80 mm yr^{-1} in Italy, Spain, France, Portugal, and Montenegro. In general, all Mediterranean Countries were characterized by a decreasing amount of precipitation that was more noticeable under RCP 4.5 scenario. This results in a higher irrigation requirement. Differences lower than -10 mm yr^{-1} were accounted for in the irrigated areas of the Northern East Countries, such as Russia, Belarus, Ukraine, and Poland under RCP 8.5 scenario, while in the same Countries positive differences were computed under RCP 4.5 scenario. Negative anomalies values mean higher values of NA in the baseline than in the future, due to higher values of future precipitation, specifically under the RCP 8.5 scenario.

The ETc, ETa and NA values for maize irrigated using sprinkler method over the entire domain and weighted for the total maize distribution estimated per Country, for past and future climate, under both 4.5 and 8.5 RCPs, are reported in Table 42.

Tab. 42. ETc, ETa and NA values for maize estimated per Country for the baseline (bas) and future climate conditions, under both 4.5 and 8.5 RCPs scenarios. NW = no-weighted by existing crop distribution and I+R = weighted values for the total (irrigated and rainfed areas) maize distribution.

	NW	*I+R*	*NW*	*I+R*	*NW*	*I+R*	*NW*	*I+R*	*NW*	*I+R*	*NW*	*I+R*	*NW*	*I+R*	*NW*	*I+R*	*NW*	*I+R*
	ETC	**ETC**	**ETC**	**ETC**	**ETC**	**ETC**	**ETA**	**ETA**	**ETA**	**ETA**	**ETA**	**ETA**	**NA**	**NA**	**NA**	**NA**	**NA**	**NA**
	bas	**bas**	**RCP 4.5**	**RCP 4.5**	**RCP 8.5**	**RCP 8.5**	**bas**	**bas**	**RCP 4.5**	**RCP 4.5**	**RCP 8.5**	**RCP 8.5**	**bas**	**bas**	**RCP 4.5**	**RCP 4.5**	**RCP 8.5**	**RCP 85**
Countries	**mm**	**mm**	**mm**	**mm**	**mm**	**mm**	**mm**	**mm**	**mm**	**mm**	**mm**	**mm**	**mm**	**mm**	**mm**	**mm**	**mm**	**mm**
Albania	566	584	585	602	595	613	375	450	376	456	385	466	275	288	316	329	316	328
Belgium	475	476	488	490	487	488	441	455	446	464	446	463	134	144	173	179	173	180
Bulgaria	624	653	647	674	652	679	567	622	585	641	590	645	346	373	388	413	385	406
Egypt	708	710	718	715	717	715	525	627	530	629	530	630	563	558	577	571	577	571
France	560	575	588	605	588	607	502	541	519	565	519	567	217	230	279	295	280	297
Germany	465	480	478	495	477	495	451	471	462	485	460	485	120	124	146	154	150	161
Greece	698	693	719	719	720	720	438	569	445	586	446	587	484	473	519	511	519	514
Italy	609	599	638	642	638	644	552	569	573	606	573	608	316	280	370	360	372	358
Morocco	532	516	548	544	551	541	422	493	433	520	433	517	265	240	293	282	311	294
Portugal	710	685	751	725	742	717	478	510	494	529	487	522	456	426	519	489	516	487
Romania	551	584	565	598	565	598	535	574	546	587	546	587	229	273	265	307	252	293
Spain	717	749	755	791	752	786	551	649	570	681	567	676	448	485	512	553	518	556
Syria	807	856	823	881	820	873	668	827	682	852	678	844	593	633	606	651	610	655
Turkey	629	637	649	654	653	657	511	504	526	517	529	519	395	394	419	414	422	418
Ukraine	619	642	633	658	619	644	606	632	619	647	606	634	358	390	379	414	355	390

Finally, the ETc, ETa, and NA weighted for the only irrigated areas are reported for the baseline and the intermediate future under RCP 4.5 and RCP 8.5 scenarios in order to assess the impact of climate change on this variables for the main productive Countries (Table 43). Values related to climate anomalies are reported in Figure 142.

In Tables 43 were reported also the increasing values of future reference evapotranspiration (ETo) computed using the standardized reference evapotranspiration (Allen et al., 1998) compared to the values estimated for the baseline, and that was due to the expected increasing temperature from the past to the future climate conditions. The highest ETo values were computed in Egypt, Morocco, and Syria where a crop coefficient (Kc) of around 0.55 was estimated. Each Country was characterized by increasing crop evapotranspiration, and consequently actual evapotranspiration, under future climate conditions. Despite maize was irrigated, ETa values were always lower

than ETc values, since irrigation application can not perfectly fulfill crop water requirements unless applied continuously, and this water stress, measured by a stress coefficient (Ks), is exacherbated by pedo-climatic conditions. The stress coefficient tended to be lower for the baseline than for the future in Albania, Belgium, Portugal, and Spain, while it remained the same in Italy, Egypt, Greece, and Morocco. The highest water stress for the baseline was computed in Portugal and Albania (Ks ~ 0.77) which corresponded to the highest loss of yield, more noticeable under both RCP scenarios. The highest Ks values were found in Germany, Romania, and Ukraine (Ks ~ 0.98) where the lowest loss of yield was found. The highest water net application was estimated in Egypt, Greece, Spain, and Syria while the lowest values were found in Belgium and Germany. Albania, Bulgaria, Egypt, Portugal, Ukraine, and Romania are characterized by a lower NA value under RCP 8.5 than 4.5 scenario because the larger amount of projected precipitation. Egypt, France, Greece, Italy, and Spain are the Countries where the highest amount of water applied by irrigation is estimated. Despite the number of irrigated hectares was lower in Egypt than in France, the larger irrigation amount was estimated in the first one, due to the lowest total amount of precipitation. The higher precipitation amount estimated in Italy led to use less water to irrigate maize than in Spain, despite the similar number of cultivated hectares.

Tab. 43. ETc, ETa and NA values weighted for the maize irrigated areas, for the climate baseline period (1976-2005), and for the climate future period (2036-2065), under both RCP 4.5 and 8.5. bas = baseline, 45 = RCP 4.5, and 85 = RCP 8.5, VNa= volume of water applied, and Irr=irrigated.

	bas	RCP 45	RCP 85	bas	RCP 45	RCP 85	bas	RCP 45	RCP 85	bas	RCP 45	RCP 85	bas	RCP 45	RCP 85	bas	RCP 45	RCP 85	bas	RCP 45	RCP 85	bas	RCP 45	RCP 85	bas	RCP 45	RCP 85	bas	RCP 45	RCP 85
	ETo	ETo	ETo	ETC	ETC	ETC	ETA	ETA	ETA	NA	NA	NA	PCP	PCP	PCP	Kc	Kc	Kc	Ks	Ks	Ks	Ya/Yc	Ya/Yc	Ya/Yc	Irr Area	Irr area	Irr area	VNa	V NA	VNa
Irrigated Country	mm	mm	mm	mm	mm	mm	mm	mm	mm	mm	mm	mm	mm	mm								%	%	%	ha	ha	ha	Mm^3	Mm^3	Mm^3
Albania	687	732	739	590	609	620	469	476	486	293	335	333	1095	990	1025	0.86	0.83	0.84	0.79	0.78	0.78	0.26	0.27	0.27	28530	28530	28530	84	96	95
Belgium	504	538	521	474	487	486	451	460	459	144	178	180	831	810	836	0.94	0.91	0.93	0.95	0.94	0.95	0.06	0.07	0.07	45241	45241	45241	65	80	81
Bulgaria	829	866	863	643	668	671	598	619	622	368	409	405	490	447	457	0.78	0.77	0.78	0.93	0.93	0.93	0.09	0.09	0.09	27525	27525	27525	101	113	111
Egypt	1312	1322	1321	709	714	715	594	597	598	554	567	566	38	38	40	0.54	0.54	0.54	0.84	0.84	0.84	0.2	0.21	0.2	694120	694120	694120	3842	3933	3931
France	606	661	648	577	607	609	544	568	570	234	298	300	882	856	883	0.95	0.92	0.94	0.94	0.94	0.94	0.07	0.08	0.08	802139	802139	802139	1875	2394	2410
Germany	498	521	508	485	502	503	476	491	493	130	164	172	807	806	808	0.97	0.96	0.99	0.98	0.98	0.98	0.02	0.03	0.03	65159	65159	65159	85	107	112
Greece	863	903	907	693	719	720	569	587	588	474	511	514	521	425	436	0.8	0.8	0.79	0.82	0.82	0.82	0.22	0.23	0.23	240226	240226	240226	1138	1228	1236
Italy	710	759	761	608	653	654	578	618	619	290	372	370	834	772	771	0.86	0.86	0.86	0.95	0.95	0.95	0.06	0.07	0.07	485966	485966	485966	1407	1806	1798
Morocco	1074	1122	1150	533	556	556	460	481	479	273	306	320	352	285	256	0.5	0.5	0.48	0.86	0.86	0.86	0.17	0.17	0.17	42821	42821	42821	117	131	137
Portugal	842	911	899	671	710	703	507	525	518	410	473	471	924	848	938	0.8	0.78	0.78	0.76	0.74	0.74	0.31	0.33	0.33	99675	99675	99675	408	471	470
Romania	734	767	748	637	652	654	626	641	642	351	381	369	604	572	601	0.87	0.85	0.87	0.98	0.98	0.98	0.02	0.02	0.02	191042	191042	191042	670	728	704
Spain	816	875	876	749	791	786	649	681	676	485	553	556	711	637	669	0.92	0.9	0.9	0.87	0.86	0.86	0.17	0.17	0.18	412830	412830	412830	2001	2283	2294
Syria	1416	1438	1457	871	897	889	842	866	858	648	667	671	146	152	137	0.62	0.62	0.61	0.97	0.97	0.97	0.04	0.04	0.04	50877	50877	50877	330	339	341
Turkey	860	897	908	657	676	678	581	598	599	413	433	437	479	449	438	0.76	0.75	0.75	0.88	0.88	0.88	0.14	0.15	0.15	113635	113635	113635	469	492	497
Ukraine	785	802	766	681	694	685	666	678	669	445	467	447	456	452	478	0.87	0.87	0.89	0.98	0.98	0.98	0.03	0.03	0.03	85379	85379	85379	380	399	382

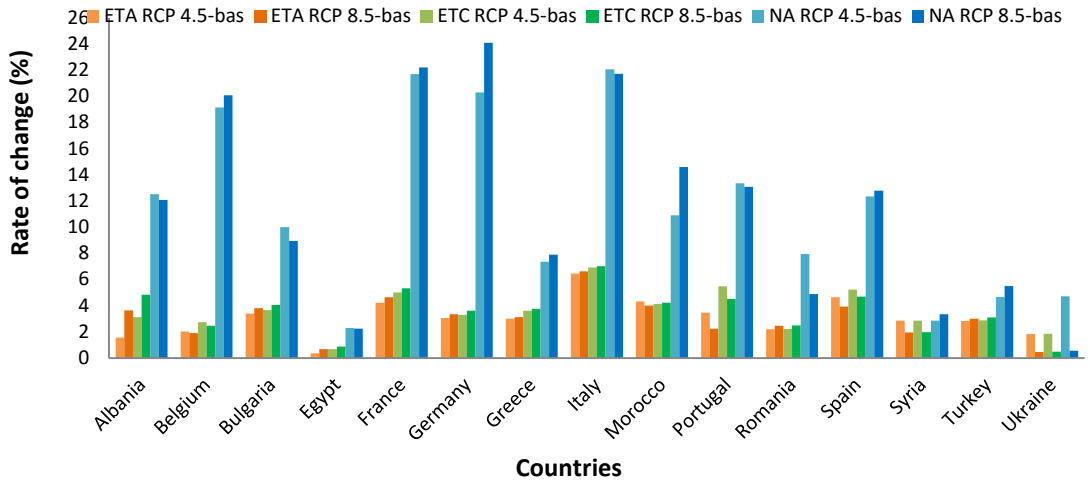

Fig. 142. Rate of change of ETc, ETa, NA values, weighted for the irrigated maize distribution, between the future climate conditions (2036-2065), under both RCPs 4.5 and 8.5 scenarios, and the baseline (1976-2005).

The highest differences between future and past ETc were computed in Italy (around 7%) with a very low difference between the RCP 4.5 and 8.5 scenarios, while the lowest was computed in Egypt (around 1%). The more noticeable difference between ETc estimated under RCP 4.5 and 8.5 scenario was found in Albania and Ukraine (around 1.5%) where the highest values were observed under RCP 8.5 (Albania) and RCP 4.5 (Ukraine). ETa values followed the same trend of ETc. The difference between the past and the future water application is around 22% in Germania, France and Italy. In Ukraine, Romania, Albania, Bulgaria, Egypt, Italy, and Portugal the difference between the future NA under RCP 8.5 was lower than under RCP 4.5 due to the higher projected precipitation under the worst scenario.

2.3.3.2 Wheat

2.3.3.2.1 Irrigated wheat

ETc, ETa, and their differences were reported for the baseline (1976-2005) (Figure 143, 144, and 145), and the intermediate future (2036-2065) under RCP 4.5 (Figure 146, 147, and 148), and RCP 8.5 (Figure 149, 150, and 151).

The areas where wheat is not currently cultivated at Euro-Mediterranean scale are mainly located in Northern Africa. Despite wheat is generally cultivated in rainfed

conditions, there are areas where it is irrigated, and they are concentrated mostly in the Mediterranean basin.

The highest mean ETc values were estimated in the Northern Africa Countries, particularly in Algeria, Ukraine, Tunisia, Jordan, Moldova, Syria, Turkey, Italy, and Lebanon were values ranged from about 500 to 700 mm yr^{-1}. Except for Ireland, Lithuania, and Belarus, where mean ETc values ranged from about 300 to 400 mm yr^{-1}, in all the other Countries, mean values from 400 to 500 mm yr^{-1} were estimated. In some Countries such as Albania, Belarus, Bulgaria, Ireland, Georgia, Hungary, Moldova, Libya, Macedonia, Poland, Romania, Russia, mean ETc values tended to be equal or slightly lower in the intermediate future, under both RCPs, than in the baseline. Maps showed increasing mean values of ETc in France, Czech Republic, Denmark, Germany, Croatia, Israel, Ukraine under RCP 4.5, and a slightly decrease under RCP 8.5 when comparared with the baseline. On the contrary, the increasing mean ETc values were higher under RCP 8.5 than RCP 4.5 in Montenegro, Lebanon, and Greece. This could be explained considering the variability of mean ETo values under both RCPs in these Countries. The highest mean values of ETc were shown in Algeria where in correspondence with high ETo value.

Mean ETa values were always lower than ETc. The lowest ETa values were mainly noticeable in areas characterized by a stress coefficient close to zero.

The highest differences between the past and the future ETc and ETa values were computed in the Mediterranean basin, with peaks up to 600 mm yr^{-1} in North Africa, in particular in the Southern Algeria.

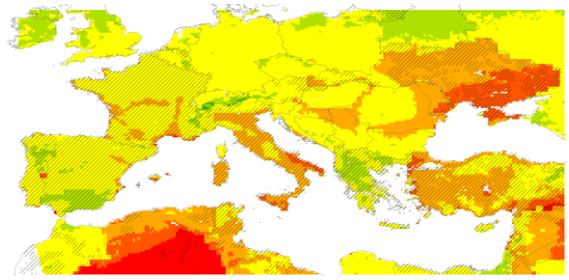

Fig. 143. Regional mean values of ETc for irrigated wheat (1976-2005), considering crop growth in the entire domain. The irrigated areas are distinguished using solid diagonal lines

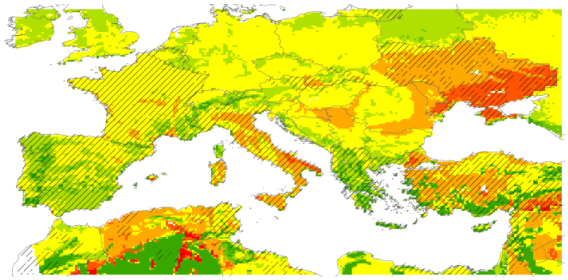

Fig. 144. Regional mean values of ETa for irrigated wheat, (1976-2005), considering crop growth in the entire domain. The irrigated areas are distinguished using solid diagonal lines

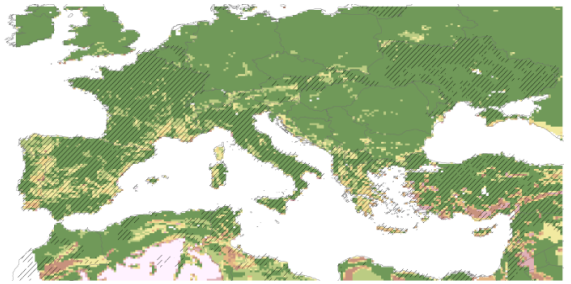

Fig. 145. Regional mean differences between ETc and ETa (1976-2005), for irrigated wheat, considering crop growth in the entire domain. The irrigated areas are distinguished using solid diagonal lines

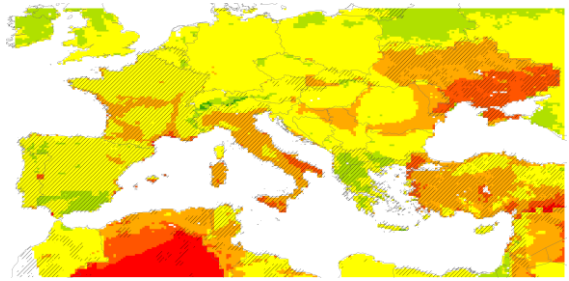

Fig. 146. Regional mean values of ETc for irrigated wheat, (2036-2065), under RCP 4.5, considering crop growth in the entire domain. The irrigated areas are distinguished using solid diagonal lines

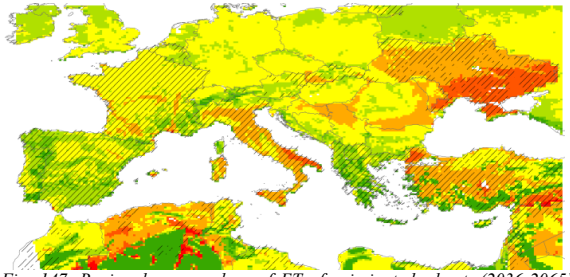

Fig. 147. Regional mean values of ETa for irrigated wheat, (2036-2065) under RCP 4.5, considering crop growth in the entire domain. The irrigated areas are distinguished using solid diagonal lines

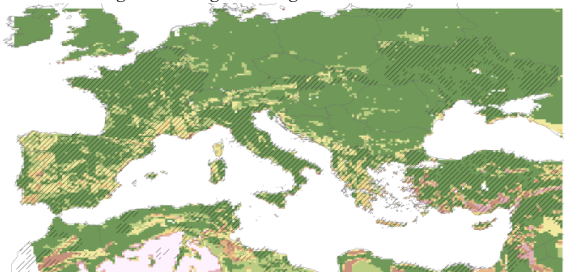

Fig. 148. Regional mean differences between ETc and ETa (2036-2065), for irrigated wheat under RCP 4.5, considering crop growth in the entire domain. The irrigated areas are distinguished using solid diagonal lines

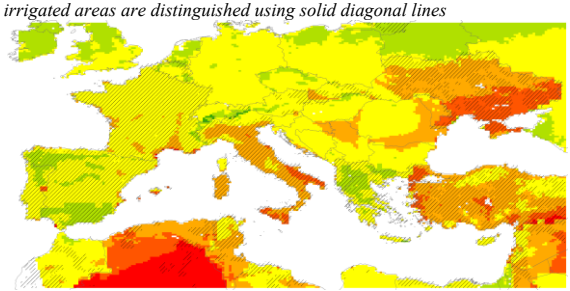

Fig. 149. Regional mean values of ETc for irrigated wheat (2036-2065), under RCP 4.5, considering crop growth in the entire domain. The irrigated areas are distinguished using solid diagonal line

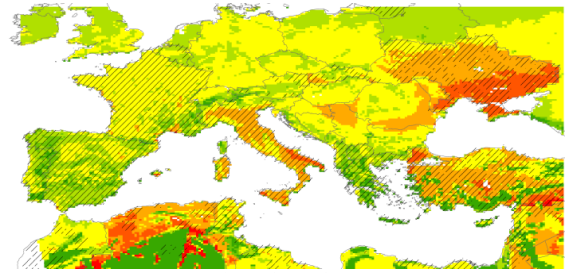

Fig. 150. Regional mean values of ETa for irrigated wheat, (2036-2065) under RCP 8.5, considering crop growth in the entire domain. The irrigated areas are distinguished using solid diagonal lines

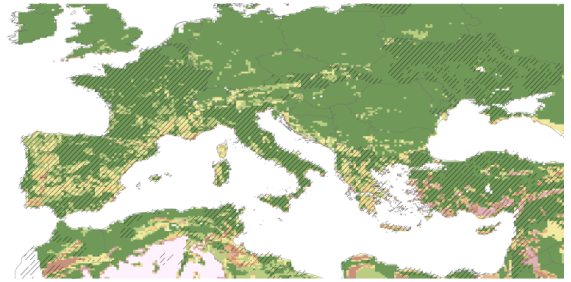

Fig. 151. Regional mean differences between ETc and ETa (2036-2065), for irrigated wheat under RCP 8.5, considering crop growth in the entire domain. The irrigated areas are distinguished using solid diagonal lines

Legend, ETc and ETa, mm yr^{-1}

< 200 | 201 - 300 | 301 - 400 | 401 - 500 | 501 - 600 | 601 - 700 | > 701

Legend (Differences between ETc and ETa, mm

< 50 | 51 - 100 | 101 - 200 | 201 - 300 | 301 - 400 | 401 - 500 | 501 - 600 | > 601

NA estimations for the baseline (1976-2005) (Figure 152) and the future climate (2036-2065) under the RCP 4.5 (Figure 153) and 8.5 (Figure 155) were shown in maps. The irrigated areas were distinguished using diagonal solid lines. Differences between past and future water net application amount were computed (Figure 154 and 156).

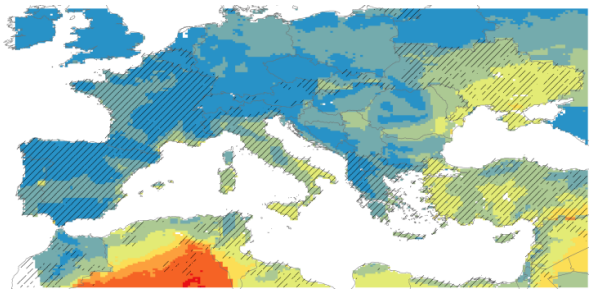

Fig. 152. Regional mean NA values for irrigated wheat (1976-2005), considering crop growth in the entire domain. The irrigated areas are distinguished using solid diagonal lines.

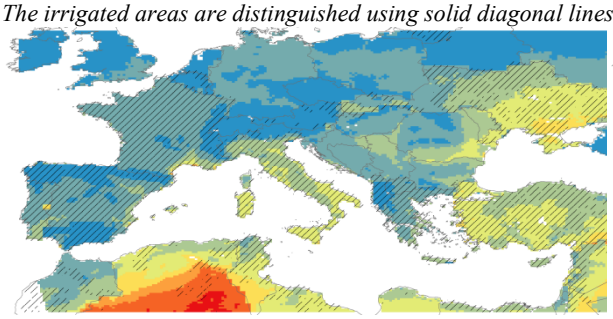

Fig. 153. Regional mean NA values for irrigated wheat for the future (2036-2065) under RCP 4.5, considering crop growth in the entire domain. The irrigated areas are distinguished using solid diagonal lines.

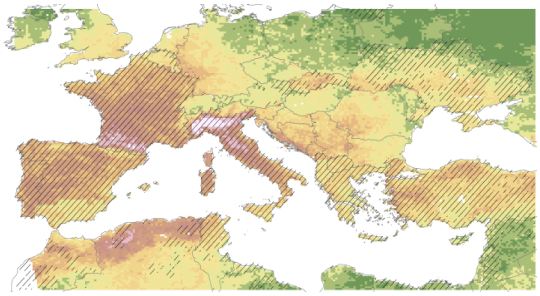

Fig. 154. Climate anomalies for Na values for irrigated wheat regional estimates, considering crop growth in the entire domain. The irrigated areas are distinguished using solid diagonal lines.

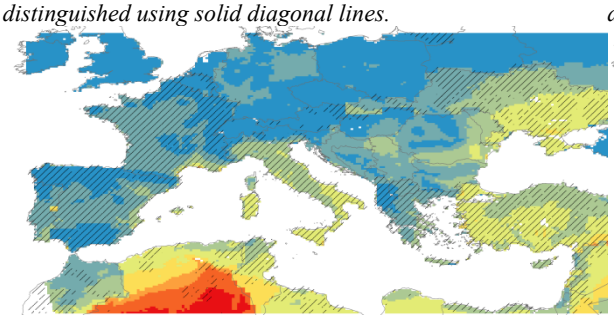

Fig. 155. Regional mean NA values for irrigated wheat for the future (2036-2065) under RCP 8.5, considering crop growth in the entire domain. The irrigated areas are distinguished using solid diagonal lines.

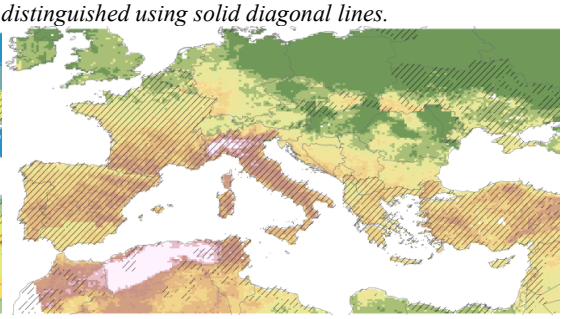

Fig. 156. Climate anomalies for Na values for irrigated wheat regional estimates, considering crop growth in the entire domain. The irrigated areas are distinguished using solid diagonal lines.

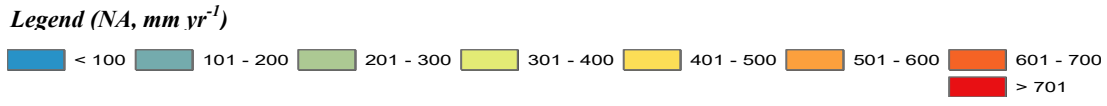

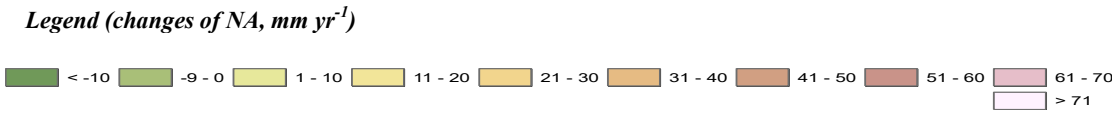

The aim was to investigate about the mean wheat irrigation requirement using sprinkler method in Euro-Mediterranean regions. Results showed increasing values of water use for wheat irrigation in France, Spain, Germany, Croatia, Bosnia and Herzegovina, and Greece. Italian regions were also influenced by climate change where NA reached values up to 300-400 mm yr^{-1} in the future. A lower amount of NA was estimated under both scenarios (mainly under RCP 4.5) for Countries located in the North of Europe, such as The Netherland, Poland, and United Kingdom where higher precipitation amount is expected in the intermediate future. The highest values were estimated in Northern Africa, Lebanon, Turkey, Jordan, Syria, and Ukraine.

The highest differences betweenirrigation requirement values were computed in the Mediterranean regions as a direct consequences of the precipitation reduction.

Table 44 reports ETc, ETa, and NA values for the baseline and the future climate by considering the crop potential and total (irrigated and rainfed) actual distribution.

Tab. 44. ETc, ETa and NA values for irrigated wheat estimated per Country for the baseline (bas) and future climate conditions, under both 4.5 and 8.5 RCPs scenarios. NW = no-weighted by existing crop distribution and I+R = weighted values for the total (irrigated and rainfed areas) irrigated wheat distribution.

	NW	**I+R**	***NW***	**I+R**	***NW***	**I+R**	***NW***	**I+R**	***NW***	**I+R**	***NW***	**I+R**	***NW***	**I+R**	***NW***	**I+R**	***NW***	**I+R**
	ETC	**ETC**	**ETC**	**ETC**	**ETC**	**ETC**	**ETA**	**ETA**	**ETA**	**ETA**	**ETA**	**ETA**	**NA**	**NA**	**NA**	**NA**	**NA**	**NA**
	bas	**bas**	**RCP 45**	**RCP 45**	**RCP 85**	**RCP 85**	**bas**	**bas**	**RCP 45**	**RCP 45**	**RCP 85**	**RCP 85**	**bas**	**bas**	**RCP 45**	**RCP 45**	**RCP 85**	**RCP 85**
Countries	**mm**	**mm**	**mm**	**mm**	**mm**	**mm**	**mm**	**mm**	**mm**	**mm**	**mm**	**mm**	**mm**	**mm**	**mm**	**mm**	**mm**	**mm**
Algeria	675	557	682	566	695	578	343	521	346	527	353	539	476	265	505	312	529	338
Belgium	417	422	421	425	408	411	398	408	396	407	387	397	48	49	68	68	48	46
Denmark	420	421	424	425	413	414	372	377	377	380	368	372	116	117	115	115	98	99
Egypt	419	417	416	419	416	416	304	397	302	399	301	395	291	295	283	289	288	294
France	474	472	482	481	466	463	439	452	438	455	425	440	98	100	140	140	119	113
Greece	415	409	415	412	417	412	277	330	268	326	269	325	154	146	173	165	176	168
Italy	515	563	533	581	532	581	473	534	484	549	484	549	201	270	245	314	245	314
Lebanon	507	482	509	487	518	497	315	318	312	318	314	320	303	286	302	285	320	305
Libya	484	485	475	475	477	475	380	380	371	371	372	369	324	294	321	295	332	305
Morocco	446	441	456	456	456	451	354	408	359	420	358	415	172	149	198	184	218	200
Portugal	433	448	442	460	432	452	325	336	316	331	308	326	116	144	157	187	147	177
Spain	431	427	435	433	423	419	374	391	364	387	353	374	86	80	120	115	116	109
Syria	530	520	531	528	540	534	430	473	431	479	438	484	335	307	329	304	352	328
Tunisia	549	497	543	493	548	495	421	452	413	444	415	445	336	203	352	233	372	251
Turkey	521	538	533	551	542	559	423	458	432	468	438	474	281	302	305	323	312	331
Ukraine	565	568	569	573	560	565	555	557	558	561	550	554	283	286	293	295	274	277

Past and future ETc, ETa, and NA values only in irrigated areas are shown in Table 45. A focus on the main productive Countries was set in order to assess the impact of global warming. Differences in percentage between the future and the past values are reported in Figure 157.

The highest total average crop water consumption were found in Algeria, Italy, Lebanon, Syria, Turkey, and Ukraine where ETc values were between 500 an 600 mm, and values estimated under RCP 8.5 were slightly lower in Italy and Ukraine. The crop coefficients computed in this Countries ranged from 0.37 in Syria under RCP 8.5 to 0.79 in Ukraine. The lowest Kc values were computed in North Africa and precisely in Egypt, Libya, and Tunisia in correspondence with high ETo values. The lowest ETa value was computed in Lebanon in correspondence with the lowest stress coefficient. Ks tended to be lower, i.e. closer to zero, in areas where the pedo-climatic condition were not optimal and reverse. Ks values played a basic role in the percentage of yield reduction, in fact the lowest losses were found in correspondence with the high Ks values, such as in Belgium, Denmark, Egypt, Italy, Spain and Ukraine.

Considering that the irrigated ares are mostly concentrated in the Mediterranean regions, the highest mean volume used for irrigation were computed in Turkey, Egypt, Syria, Morocco, Algeria, and Libya. The mean volume followed the same trend of NA from the past to the intermediate future under both RCP 4.5 and 8.5 (Table 45).

Tab. 45. ETc, ETa and NA values weighted for the irrigated wheat areas for the climate baseline period (1976-2005), and for the climate future period (2036-2065), under both RCP 4.5 and 8.5. bas = baseline, 45 = RCP 4.5, and 85 = RCP 8.5, VNa= volume of water applied, and Irr=irrigated.

	bas	RCP 45	RCP 85	bas	RCP 45	RCP 85	bas	RCP 45	RCP 85	bas	RCP 45	RCP 85	bas	RCP 45	RCP 85	bas	RCP 45	RCP 85	bas	RCP 45	RCP 85	bas	RCP 45	RCP 85	bas	RCP 45	RCP 85
	ETo	ETo	ETo	ETC	ETC	ETC	ETA	ETA	ETA	NA	NA	NA	PCP	PCP	PCP	Kc	Kc	Kc	Ks	Ks	Ks	Ya/Yc	Ya/Yc	Ya/Yc	Irr areas	Irr areas	Irr areas	VNA	VNA	VNA
Irrigated Countries	mm	mm		mm	mm	mm	mm	mm	mm	mm	mm	mm	mm	mm	mm							%	%	%	ha	ha	ha	Mm^3	Mm3	Mm^3
Algeria	1324	1373	1397	631	637	645	543	547	554	411	442	461	185	156	137	0.48	0.46	0.46	0.86	0.86	0.86	0.15	0.16	0.16	110301	110301	110301	454	488	509
Belgium	504	538	521	417	421	405	405	406	394	49	65	47	831	810	836	0.83	0.78	0.78	0.97	0.96	0.97	0.03	0.04	0.03	5422.7	5422.7	5422.7	3	4	3
Denmark	471	482	463	409	415	399	398	403	388	98	101	82	663	675	685	0.87	0.86	0.86	0.97	0.97	0.97	0.03	0.03	0.03	63759	63759	63759	63	64	52
Egypt	1312	1322	1321	418	421	417	401	403	399	297	291	295	38	38	40	0.32	0.32	0.32	0.96	0.96	0.96	0.05	0.05	0.05	862779	862779	862779	2559	2510	2547
France	606	661	648	474	484	465	454	458	443	104	144	116	882	856	883	0.78	0.73	0.72	0.96	0.95	0.95	0.05	0.06	0.05	64102	64102	64102	67	92	75
Greece	863	903	907	419	424	422	361	361	359	156	176	179	521	425	436	0.49	0.47	0.47	0.86	0.85	0.85	0.15	0.16	0.17	38892.7	38892.7	38892.7	61	69	70
Italy	710	759	761	565	582	581	526	540	539	271	313	313	834	772	771	0.8	0.77	0.76	0.93	0.93	0.93	0.08	0.08	0.08	41913	41913	41913	113	131	131
Lebanon	986	1002	1017	509	512	520	330	329	330	312	309	329	397	385	340	0.52	0.51	0.51	0.65	0.64	0.63	0.39	0.39	0.4	16302.7	16302.7	16302.7	51	50	54
Libya	1384	1403	1410	481	474	470	413	406	401	285	288	298	76	66	59	0.35	0.34	0.33	0.86	0.86	0.85	0.15	0.16	0.16	81030	81030	81030	231	233	242
Morocco	1074	1122	1150	454	471	473	417	431	431	175	209	227	352	285	256	0.42	0.42	0.41	0.92	0.91	0.91	0.09	0.09	0.1	252720	252720	252720	443	527	575
Portugal	842	911	899	430	438	427	358	351	340	107	148	136	924	848	938	0.51	0.48	0.47	0.83	0.8	0.8	0.18	0.22	0.22	14492.9	14492.9	14492.9	16	21	20
Spain	816	875	876	428	434	421	396	394	381	86	120	115	711	637	669	0.52	0.5	0.48	0.92	0.91	0.9	0.08	0.1	0.11	66453	66453	66453	57	80	76
Syria	1416	1438	1457	524	531	537	492	498	503	315	313	335	146	152	137	0.37	0.37	0.37	0.94	0.94	0.94	0.07	0.07	0.07	686946	686946	686946	2167	2147	2302
Tunisia	1314	1355	1374	499	495	498	445	437	438	228	255	274	163	137	116	0.38	0.37	0.36	0.89	0.88	0.88	0.12	0.13	0.13	57807	57807	57807	132	147	158
Turkey	860	897	908	555	569	575	498	509	515	321	339	348	479	449	438	0.65	0.63	0.63	0.9	0.9	0.9	0.11	0.11	0.12	1827895	1827895	1827895	5859	6203	6363
Ukraine	785	802	766	607	612	606	596	600	594	346	359	343	456	452	478	0.77	0.76	0.79	0.98	0.98	0.98	0.02	0.02	0.02	39928	39928	39928	138	143	137

The climate anomalies in percentage of ETc, ETa, and NA, for irrigated wheat distribution are shown in Figure 157.

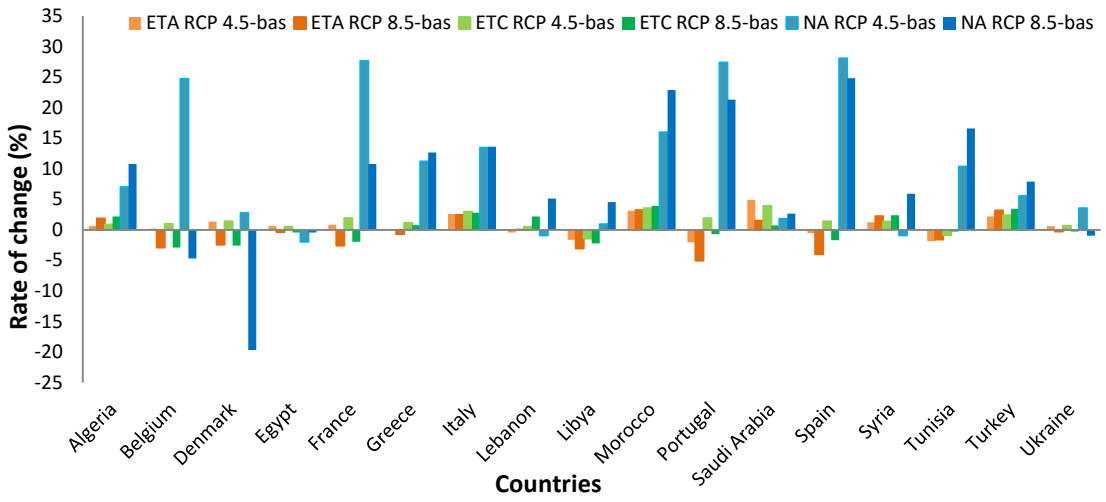

Fig. 157. Rate of change of ETc, ETa, and NA values weighet for the irrigated wheat distribution estimated between the future climate conditions (2036-2065), under both RCP 4.5 and 8.5 scenarios, and the baseline (1976-2005).

The higher ETc difference was 4% in Morocco under both RCPs. ETc values estimated in the baseline were higher than the ones estimated under RCP 4.5 in Libya and RCP 8.5 in Belgium, Lybia, Portugal, and Spain. The lowest difference of ETa (-5.2%) was found between the RCP 8.5 and the baseline in Portugal, while the higher in Morocco under the same scenario. Negative values of ETa were estimated in Belgium, Denmark, France, Libya, and Spain. A difference equal to a percentage of around 20 was computed between future and past NA values in Denmark under RCP 8.5 due to an increase of projected precipitation. Difference close to the about 30% were found in Spain, France, and Portugal under RCP 4.5, while in the same Countries differences were lower under RCP 8.5 due to a precipitation reduction.

2.3.3.2.2 Rainfed wheat

Wheat is grown in rainfed conditions in all Euro-Mediterranean regions except for in a few areas in Northern Africa Countries. Figure 158, 161, and 164 are very similar to Figure 143, 146, and 149, i.e. the maps obtained running simulation for wheat cultivated in irrigated conditions. The differences that could be appreciated between maps were related to the differences in sowing and harvest day. This fact could affect in fact the length of the growing season, thus the total average ETc values. ETa values in rainfed wheat (Figure 159, 162, and 165) was lower than ETa values computed considering irrigated wheat (Figure 144, 147, and 150). Figure 159, 162, and 165 showed total average ETa values lower than ETc in each regions. ETa values tended to be lower from the baseline to the intermediate future under both RCPs, due to a crop water stress that was not satisfied by water applications. Higher values of ETa are in fact shown in Figure 144, 147, and 150 where wheat was irrigated using sprinkler method. The influence of climate change on rainfed wheat was more noticeable in Mediterranean coast where areas characterized by ETa values close to 200-300 mm yr^{-1} tend to be larger under both RCPs. France, Southern Germany, Switzerland, as well as the Northern Italy were characterized by ETa values around 400-500 mm yr^{-1} (Figure 159) which tended to be lower under both RCPs (Figure 162 and 165).

Northern Countries were characterized by the lowest differences between ETa and ETc, while the highest were shown in the South, specifically in Northern Africa, Turkey, Syria, and Greece (Figure 160, 163, and 166).

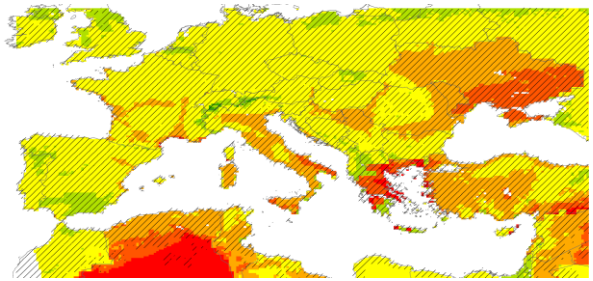

Fig. 158. Regional mean values of ETc for rainfed wheat (1976-2005) considering crop growth in the entire domain. The rainfed areas are distinguished using solid diagonal lines

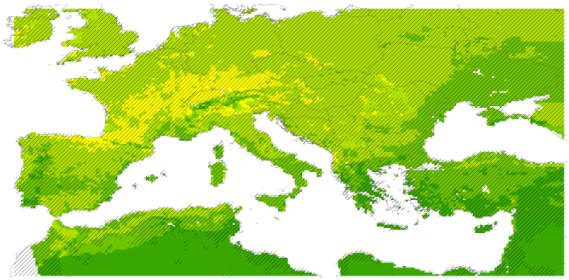

Fig. 159. Regional mean values of ETa for rainfed wheat (1976-2005) considering crop growth in the entire domain. The rainfed areas are distinguished using solid diagonal lines

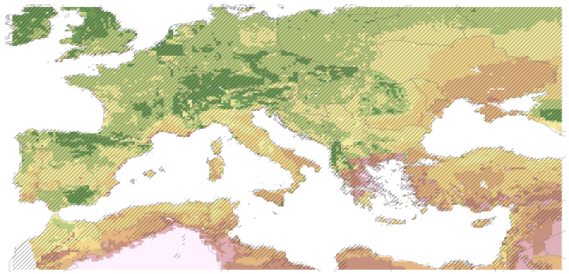

Fig. 160. Regional mean values of differences between ETc and ETa in the period 1976-2005, for rainfed wheat, considering crop growth in the entire domain. The rainfed areas are distinguished using solid diagonal lines

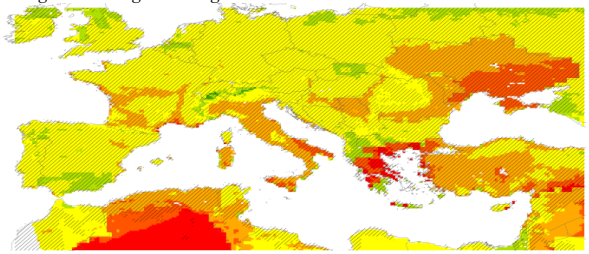

Fig. 161. Regional mean values of ETc for rainfed wheat (2036-2065), under RCP 4.5 considering crop growth in the entire domain. The rainfed areas are distinguished using solid diagonal lines

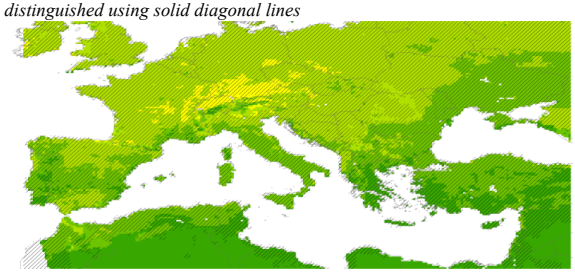

Fig. 162. Regional mean values of ETa for rainfed wheat (2036-2065), under RCP 4.5 considering crop growth in the entire domain. The rainfed areas are distinguished using solid diagonal lines

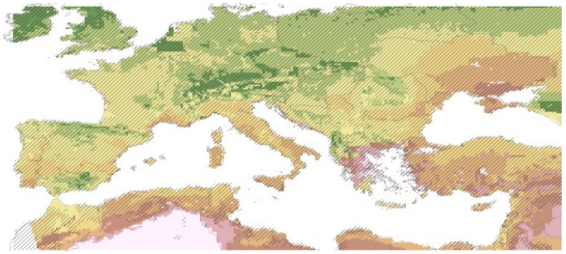

Fig. 163. Regional mean values of differences between ETc and ETa in the period 2036-2065, under RCP 4.5, for rainfed wheat, considering crop growth in the entire domain. The rainfed areas are distinguished using solid diagonal lines

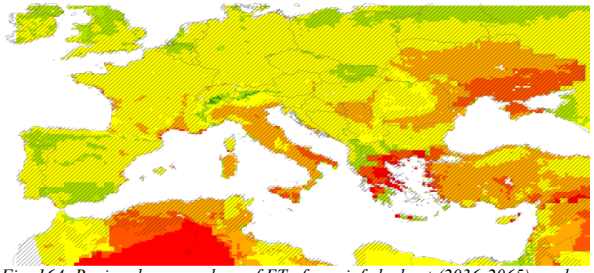

Fig. 164. Regional mean values of ETc for rainfed wheat (2036-2065), under RCP 8.5 considering crop growth in the entire domain. The rainfed areas are distinguished using solid diagonal lines

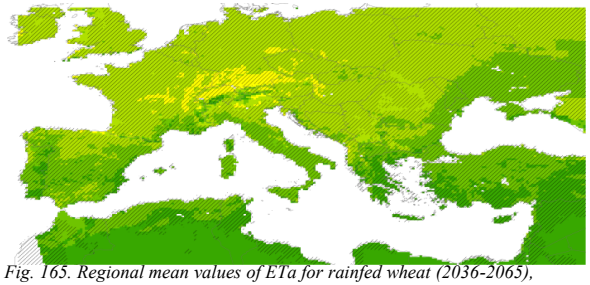

Fig. 165. Regional mean values of ETa for rainfed wheat (2036-2065), under RCP 8.5 considering crop growth in the entire domain. The rainfed areas are distinguished using solid diagonal lines

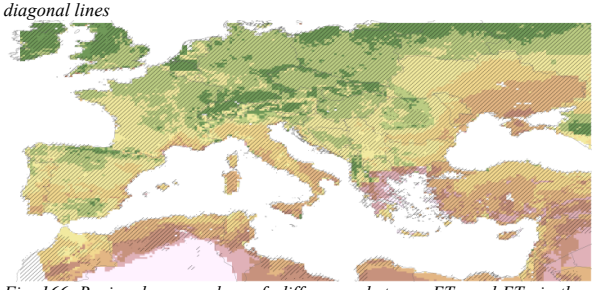

Fig. 166. Regional mean values of differences between ETc and ETa in the period 2036-2065, under RCP 8.5, for rainfed wheat, considering crop growth in the entire domain. The rainfed areas are distinguished using solid diagonal lines

Legend (ETc and ETa, mm yr^{-1})

< 200 | 201 - 300 | 301 - 400 | 401 - 500 | 501 - 600 | 601 - 700 | > 701

Legend, Differences between ETc and ETa, mm yr^{-1}

< 50 | 51 - 100 | 101 - 200 | 201 - 300 | 301 - 400 | 401 - 500 | 501 - 600 | > 601

Wheat cultivated in Northern Africa, close to the Sahara desert and to the mountain ranges, is characterized by the highest values of ETc because of the pedo-climatic conditions.

In Table 46 are shown the mean ETc and ETa values (no-weighted by existing crop distribution) for wheat growth in rainfed conditions and the average of ETc and ETa values weighted for the irrigated and rainfed distribution. Values are shown per Country for the past and future climate conditions.

Tab.46. ETc, ETa and NA values for rainfed wheat estimated per Country for the baseline (bas) and future climate conditions, under both 4.5 and 8.5 RCPs scenarios. NW = no-weighted by existing crop distribution and I+R = weighted values for the total (irrigated and rainfed areas) *rainfed wheat* distribution.

	NW	*I+R*	*NW*	*I+R*	*NW*	*I+R*	*NW*	*I+R*	*NW*	*I+R*	*NW*	*I+R*
	ETC	**ETC**	**ETC**	**ETC**	**ETC**	**ETC**	**ETA**	**ETA**	**ETA**	**ETA**	**ETA**	**ETA**
	bas	**bas**	**RCP 45**	**RCP 45**	**RCP 85**	**RCP 85**	**bas**	**bas**	**RCP 45**	**RCP_45**	**RCP 85**	**RCP 85**
Countries	**mm**	**mm**	**mm**	**mm**	**mm**	**mm**	**mm**	**mm**	**mm**	**mm**	**mm**	**mm**
Algeria	675	556	681	566	695	578	133	284	113	242	103	227
Bulgaria	470	481	464	475	468	480	305	300	268	265	282	280
France	474	472	483	481	467	463	384	391	348	359	350	364
Germany	447	448	453	454	438	438	378	376	373	372	371	370
Hungary	456	457	447	449	436	437	370	370	347	348	354	354
Italy	508	558	524	575	523	575	310	293	281	265	279	262
Morocco	446	441	456	456	456	451	210	249	190	227	165	197
Poland	433	438	433	438	418	423	352	356	356	360	360	364
Romania	490	511	484	506	480	503	340	323	313	295	330	316
Russia	431	441	424	433	418	430	307	302	312	304	321	314
Spain	429	426	433	432	420	418	322	337	285	301	274	289
Syria	530	520	531	527	540	533	117	152	121	158	109	141
Tunisia	546	496	541	492	545	494	153	272	122	222	108	207
Turkey	520	537	533	550	541	558	198	199	188	191	188	189
United Kingdom	411	418	412	421	397	405	354	359	347	350	344	348
Ukraine	565	568	569	573	560	565	297	297	287	288	298	298

Past and future crop and actual evapotranspiration values weighted for the rainfed areas are reported for the in Table 47 for the baseline, the future under RCP 4.5 and 8.5 respectively. A focus on the most productive Countries was set. Differences in percentage between the future and the past values are reported in Figure 167.

Values of ETc higher than 500 mm yr^{-1} were estimated in Algeria, Italy, Romania, Syria, Turkey, and Ukraine, and values tended to increase in correspondence with the increasing ETo. Bulgaria, Hungary, Romania, and Tunisia were characterized by a ETa estimated in the baseline higher than the one estimated in the future, and that could be explained by the higher ETo values and the lower precipitation values projection in the future. Differences between ETc and ETa were high in Syria and Turkey where the lowest Ks (0.27) was computed. The average ETa values were strictly related to the stress coefficient value under 0.50 in Algeria, Italy, Morocco, and Tunisia, having an impact on the relative yield reduction that was about the 50%. The lowest yield losses due to the water stress condition were found in wetter Countries such as France, Germany, Poland, Russia, Ukraine, Spain and United Kingdom. Since in this Countries the amount of precipitation projected under RCP 8.5 will be higher, the loss of yield will be a bit lower. A reverse situation will happen in Northen Africa regions, and in most of the Mediterranean Countries due to a precipitation reduction under the RCP 8.5. An increase of the allowable depletion may reduce yield losses.

Tab. 47. ETc, ETa and NA values weighted for the rainfed wheat areas for the climate baseline period (1976-2005), and for the climate future period (2036-2065), under both RCP 4.5 and 8.5. bas = baseline, 45 = RCP 4.5, and 85 = RCP 8.5.

		RCP	RCP		RCP	RCP		RCP	RCP		RCP	RCP		RCP	RCP		RCP	RCP		RCP	RCP		RCP	RCP
	bas	45	85	bas	45	85	bas	45	85	bas	45	85	bas	45	85	bas	45	85	bas	45	85	bas	45	85
Rainfed	**ETo**	**ETo**	**ETo**	**ETC**	**ETC**	**ETC**	**ETa**	**ETa**	**ETa**	**PCP**	**PCP**	**PCP**	**Ks**	**Ks**	**Ks**	**Kc**	**Kc**	**Kc**	**Ya/Yc**	**Ya/Yc**	**Ya/Yc**	**Area**	**Area**	**Area**
Countries	**mm**	**mm**	**mm**	**mm**	**mm**	**mm**	**mm**	**mm**	**mm**	**mm**	**mm**	**mm**							**%**	**%**	**%**	**ha**	**ha**	**ha**
Algeria	1324	1373	1397	556	566	578	290	247	232	185	156	137	0.52	0.44	0.4	0.42	0.41	0.41	0.53	0.62	0.66	1689089	1689089	1689089
Bulgaria	829	866	863	481	475	480	300	265	280	490	447	457	0.62	0.56	0.58	0.58	0.55	0.56	0.41	0.49	0.46	1037291	1037291	1037291
France	606	661	648	472	481	463	391	359	364	882	856	883	0.83	0.75	0.79	0.78	0.73	0.72	0.19	0.28	0.24	5190462	5190462	5190462
Germany	498	521	508	448	454	438	376	372	370	807	806	808	0.84	0.82	0.84	0.9	0.87	0.86	0.18	0.2	0.17	3132353	3132353	3132353
Hungary	771	801	771	457	449	437	370	348	354	518	505	541	0.81	0.78	0.81	0.59	0.56	0.57	0.21	0.25	0.21	1126419	1126419	1126419
Italy	710	759	761	558	575	575	293	265	262	834	772	771	0.52	0.46	0.46	0.79	0.76	0.76	0.52	0.59	0.6	2092227	2092227	2092227
Morocco	1074	1122	1150	441	456	451	250	228	198	352	285	256	0.57	0.5	0.44	0.41	0.41	0.39	0.48	0.55	0.62	2792646	2792646	2792646
Poland	548	559	527	438	438	423	356	360	364	619	630	654	0.81	0.82	0.86	0.8	0.78	0.8	0.21	0.2	0.15	2234908	2234908	2234908
Romania	734	767	748	511	506	503	323	295	316	604	572	601	0.63	0.58	0.63	0.7	0.66	0.67	0.4	0.46	0.41	2228995	2228995	2228995
Russia	710	705	674	441	433	430	302	304	314	503	531	556	0.69	0.7	0.73	0.62	0.61	0.64	0.35	0.33	0.3	23550308	23550308	23550308
Spain	816	875	876	426	432	418	337	301	289	711	637	669	0.79	0.7	0.69	0.52	0.49	0.48	0.23	0.33	0.34	2056648	2056648	2056648
Syria	1416	1438	1457	520	527	533	152	159	141	146	152	137	0.29	0.3	0.27	0.37	0.37	0.37	0.78	0.77	0.81	1153745	1153745	1153745
Tunisia	1314	1355	1374	496	492	494	274	224	208	163	137	116	0.55	0.46	0.42	0.38	0.36	0.36	0.49	0.6	0.64	886758	886758	886758
Turkey	860	897	908	537	550	558	197	188	187	479	449	438	0.37	0.34	0.34	0.62	0.61	0.61	0.7	0.72	0.73	7185431	7185431	7185431
United Kingdom	461	472	458	418	421	405	359	350	348	909	925	949	0.86	0.83	0.86	0.91	0.89	0.88	0.16	0.19	0.15	1897333	1897333	1897333
Ukraine	785	802	766	568	573	565	297	288	298	456	452	478	0.52	0.5	0.53	0.72	0.71	0.74	0.52	0.55	0.52	5831974	5831974	5831974

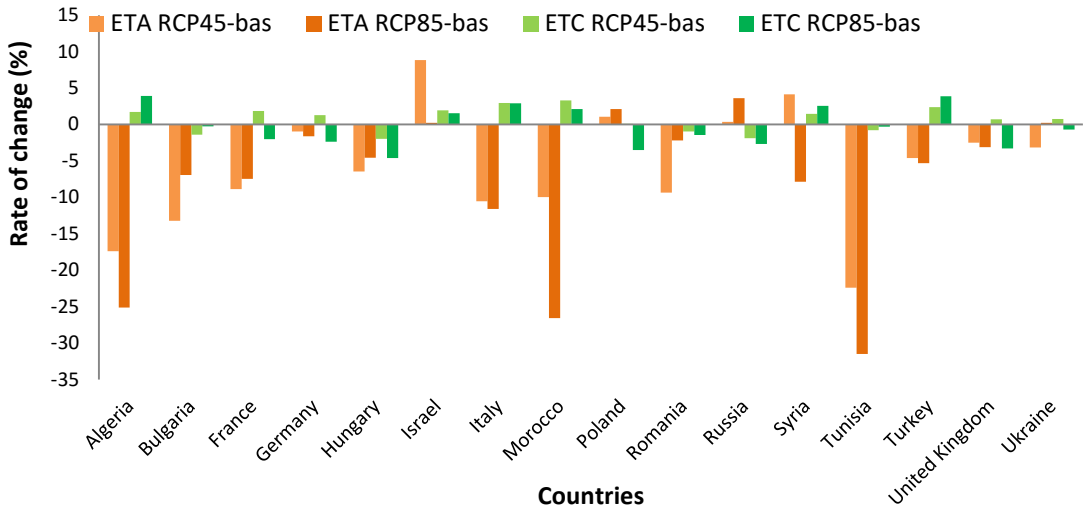

Fig. 167. Rate of change of ETc and ETa values weighted for the rainfed wheat distribution, between the future climate conditions (2036-2065), under both RCPs 4.5 and 8.5 scenarios, and the baseline (1976-2005).

In general, no so many differences were found between the ETc values simulated under RCP 4.5 and 8.5 and the baseline (Figure 167). The highest values were found in Hungary (-5%) and Turkey (+4%) with a ETc decrease and increase, respectively. The rate of change estimated under both RCPs was almost the same in Italy, Israel, Romania, and Tunisia. The highest difference between RCPs was found in France, Germany, Poland, and United Kingdom where the value was about 4%. Great ETa differences were found between the future scenarios and the baseline, particularly under RCP 8.5 in Algeria, Morocco, and Tunisia due to a great precipitation reduction. Lower precipitation values under future RCP led to negative ETa differences of the actual crop evapotranspiration in almost all Countries except for Israel, Poland, and Russia.

2.3.3.3 Grape

The areas where grape is irrigated are mostly concentrated in the Mediterranean basin where the highest values of crop water consumption were found, particularly in Syria, Greece, Turkey (ETc higher than 700 mm yr^{-1}) (Figure 168, 171, and 174). Grape water consumption in optimal water condition is expected to increase under both RCPs, and this is more evident in Mediterranean Countries, especially under RCP 4.5 (Figure 171).

ETc maps showed increasing areas in France, Spain, and Italy where values rised from about 500 (baseline) to 700 (future) mm yr^{-1}. The lower ETc was found in Switzerland, Austria, Germany, Czech Republic, because of the pedo-climatic conditions. Due to the maximum soil depth and the soil water holding capacity, ETa values were always lower than ETc (Figure 169, 172, and 175). It was worth noticing that the lower ETa values were located in areas where the soil holding capacity was under than 150 mm yr^{-1}.

Differences between the regional average ETc and ETa were mainly estimated in Mediterranean Countries. Great differences were also estimated in Greece, Tunisia, Portugal, Turkey, Syria, and Morocco. Particularly low were instead the differences in the Northern Countries, with values lower than 20 mm yr^{-1} where the precipitation were more plentiful (Figure 170, 173, and 176).

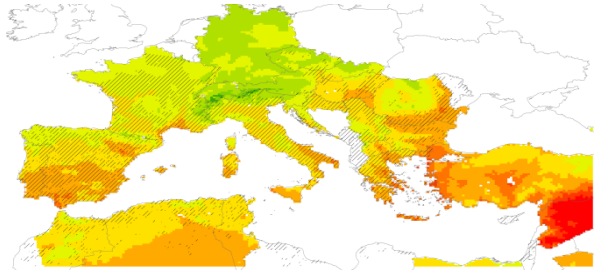

Fig. 168. Regional mean ETc values for grape (1976-2005), considering its actual distribution. The irrigated areas are distinguished using solid diagonal lines.

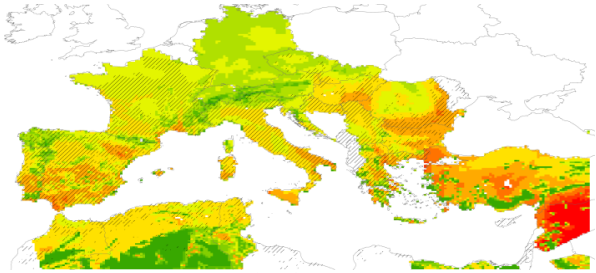

Fig. 169. Regional mean ETa values for grape (1976-2005), considering its actual distribution. The irrigated rinfed areas are distinguished using solid diagonal lines.

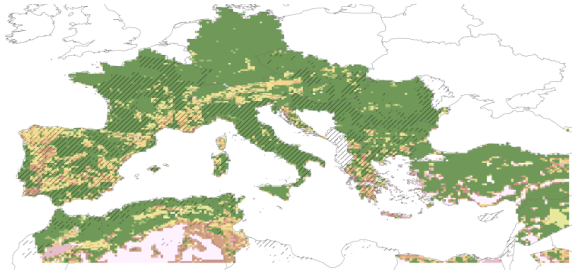

Fig. 170. Regional mean ETa values for grape (1976-2005), considering its actual distribution. The rinfed areas are distinguished using solid diagonal lines.

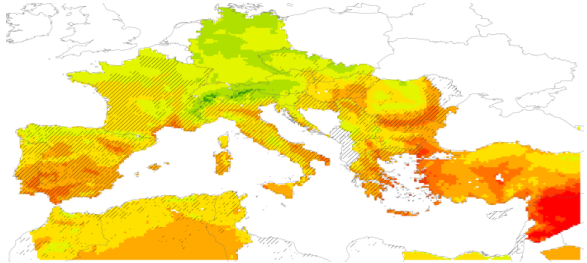

Fig. 171. Regional mean ETc values for grape (2036-2065) under RCP 4.5, considering its actual distribution. The irrigated rinfed areas are distinguished using solid diagonal lines.

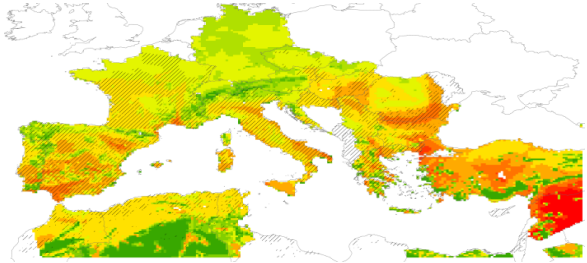

Fig. 172. Regional mean ETa values for grape (2036-2065) under RCP 4.5, considering its actual distribution. The irrigated areas are distinguished using solid diagonal lines.

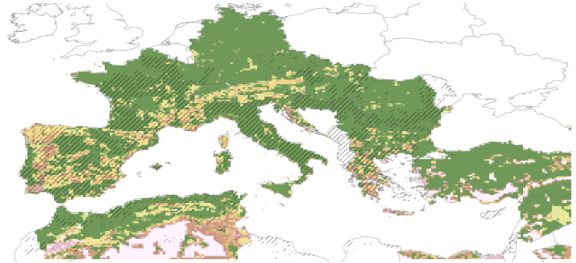

Fig. 173. Regional mean values of differences between ETc and ETa in the period 2036-2065, under RCP 4.5, for grape, considering crop growth in the entire domain. The irrigated areas are distinguished using solid diagonal lines.

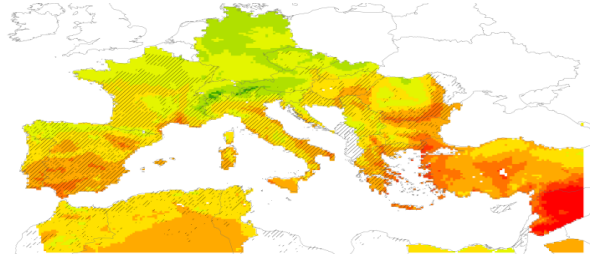

Fig. 174. Regional mean ETc values for grape (2036-2065) under RCP 8.5, considering its actual distribution. The irrigated rinfed areas are distinguished using solid diagonal lines.

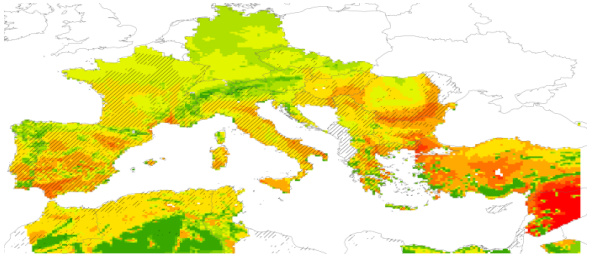

Fig. 175. Regional mean ETc values for grape (2036-2065) under RCP 8.5, considering its actual distribution. The irrigated rinfed areas are distinguished using solid diagonal lines.

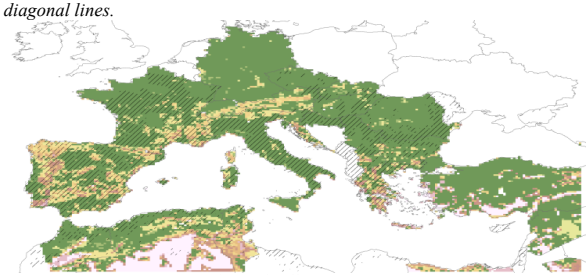

Fig. 176. Regional mean values of differences between ETc and ETa in the period 2036-2065, under RCP 8.5, for grape, considering crop growth in the entire domain. The irrigated areas are distinguished using solid diagonal lines.

Legend (ETc and ETa, mm yr^{-1})

< 200 | 201 - 300 | 301 - 400 | 401 - 500 | 501 - 600 | 601 - 700 | 701 - 800 | 801 - 900 | 901 - 1000 | > 1001

Legend (differences between ETc and ETa, mm yr^{-1})

0 - 10 | 11 - 20 | 21 - 30 | 31 - 100 | 101 - 200 | 201 - 300 | 301 - 400 | 401 - 500 | 501 - 600 | > 601

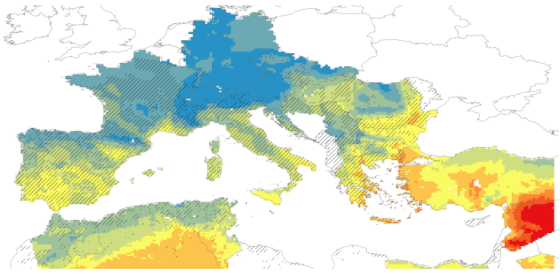

Fig. 177. Regional mean NA values for grape (1976-2005 considering its actual distribution. The irrigated areas are distinguished using solid diagonal lines.

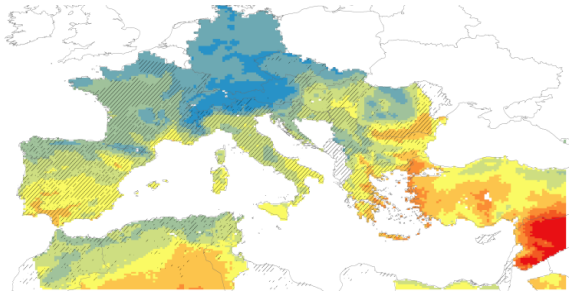

Fig. 178. Regional mean NA values for grape for the future (2036-2065) under RCP 4.5, considering crop growth in the entire domain. The irrigated areas are distinguished using solid diagonal lines

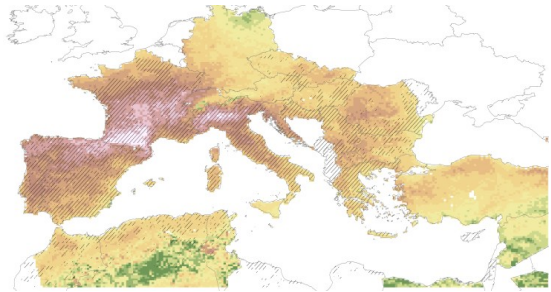

Fig. 179 Climate anomalies for Na values for grape regional estimates, considering crop growth in the entire domain. The irrigated areas are distinguished using solid diagonal lines

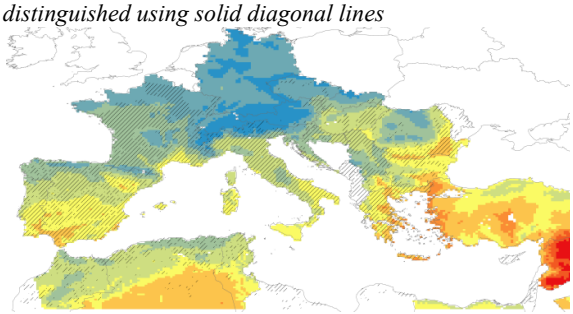

Fig. 180. Regional mean NA values for irrigated wheat for the future (2036-2065) under RCP 8.5, considering crop growth in the entire domain. The irrigated areas are distinguished using solid diagonal lines

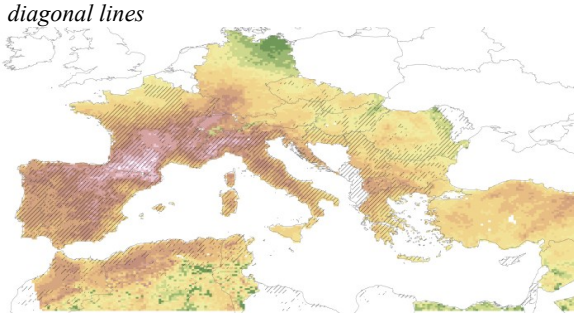

Fig. 181. Climate anomalies for Na values for grape regional estimates, considering crop growth in the entire domain. The irrigated areas are distinguished using solid diagonal lines

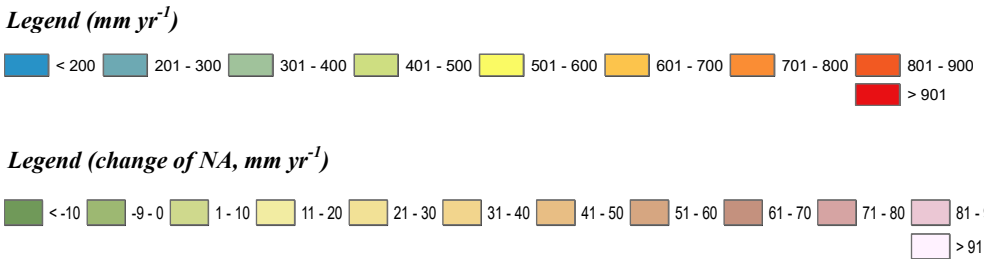

Regional average of irrigation requirement (NA) were higher in correspondence with the higher crop water consumption (Figure 177, 178, and 180). NA values were expected to be higher in the future than in the past, and this was particularly evident in Mediterranean Countries where the total average precipitation amount was expected to

reduce (Figure 178 and 179). In Spain, France, and Italy was shown a great difference between future and past values even if the highest values were estimated in Switzerland (Figure 179 and 181). The lower irrigation requirement were estimated in wetter Countries, even if due to climate change the total average NA amount will be negatively affected in the future under both scenarios.

The mean of ETc, ETa and NA values no-weighted and weighted for the total (irrigated and raifed areas) grape distribution values of estimated per Country for the past and future climate conditions are shown in Table 48.

Tab. 48. ETc, ETa and NA values for grape estimated per Country for the baseline (bas) and future climate conditions, under both 4.5 and 8.5 RCPs scenarios. NW = no-weighted by existing crop distribution and I+R = weighted values for the total (irrigated and rainfed areas) grape distribution.

	NW	I+R	NW	I+R	NW	I+R	NW	I+R	NW	I+R	NW	I+R	NW	I+R	NW	I+R	NW	I+R
	ETC	ETC	ETC	ETC	ETC	ETC	ETA	ETA	ETA	ETA	ETA	ETA	NA	NA	NA	NA	NA	NA
	bas	bas	RCP 45	RCP 45	RCP 85	RCP 85	bas	bas	RCP 45	RCP 45	RCP 85	RCP 85	bas	bas	RCP 45	RCP 45	RCP 85	RCP 85
Countries	mm	mm	mm	mm	mm	mm	mm	mm	mm	mm	mm	mm	mm	mm	mm	mm	mm	mm
Algeria	694	648	699	655	699	659	377	605	381	609	390	612	512	394	530	421	545	434
Austria	482	565	500	588	495	575	440	551	451	573	445	560	145	272	175	305	177	294
Bulgaria	713	741	734	761	735	762	695	733	716	753	716	753	502	541	541	576	535	570
Egypt	613	611	609	606	612	611	363	405	325	494	342	397	506	502	507	499	508	505
Czech Republic	497	517	517	540	507	530	496	517	516	539	507	530	202	218	234	250	225	241
France	566	626	595	663	588	656	545	593	572	627	564	619	261	336	327	409	315	399
Georgia	564	537	585	562	593	571	479	374	488	376	491	375	295	260	349	321	353	328
Germany	488	508	501	528	495	530	486	505	499	525	493	526	188	206	215	249	210	257
Greece	748	769	769	788	772	790	574	538	587	547	589	548	574	599	609	631	610	631
Croatia	621	633	646	658	643	655	580	619	601	643	599	640	354	368	402	415	394	407
Hungary	663	670	679	686	666	673	658	668	674	683	661	671	412	420	446	454	429	438
Italy	618	638	647	671	645	668	593	631	620	662	618	660	365	388	418	446	417	443
Slovakia	533	600	550	620	536	603	524	598	540	618	527	602	268	344	308	381	289	361
Macedonia	668	675	694	702	699	707	620	634	643	659	647	663	464	473	513	522	517	526
Morocco	627	624	646	643	648	644	519	567	525	578	540	588	401	400	429	427	443	441
Portugal	678	662	716	700	706	690	557	555	584	581	576	574	448	431	506	490	502	485
Romania	650	726	671	746	663	739	647	726	667	746	660	739	414	518	455	552	434	533
Slovenia	536	553	559	574	555	568	516	525	535	541	532	537	247	268	296	310	285	298
Spain	669	706	701	738	699	736	604	647	630	675	628	673	419	464	477	519	480	526
Serbia	617	634	639	657	638	655	608	631	630	653	629	651	347	364	390	405	381	396
Syria	1027	980	1037	993	1043	997	915	934	923	947	929	951	885	824	894	837	904	846
Switzerland	435	481	459	505	461	509	412	475	428	498	430	502	96	124	146	182	156	189
Tunisia	698	664	695	664	693	665	535	614	518	588	541	592	502	439	522	460	527	467
Turkey	745	765	767	788	774	794	633	694	651	714	656	719	575	596	605	625	612	632

ETc, ETa and NA values weighted only for the irrigated grape distribution are reported in Table 49 for Country.

The highest mean crop consumption value was simulated in Turkey (923 mm yr^{-1}) under RCP 4.5 while the lowest one in Switzerland (512 mm yr^{-1}) for the baseline. Due to climate change, all ETc values are expected to increase, and this is more evident under RCP 4.5 than 8.5. Higher values of ETc were strictly linked to the increasing ETo under both scenarios. However, values of ETo are lower under RCP 8.5 in some Countries such as Austria, Bulgaria, Czech Republic, Croatia, Hungary, Portugal, Macedonia, Romania, Slovenia, Serbia, and Switzerland, where precipitation is expected to increase.

Since the pedo-climatic condition were optimal to allow grape growth, any water stress was simulated in Austria, Czech Republic, Hungary, Slovakia, Romania, Slovenia, and Switzerland in the baseline, even if the stress coefficient was a bit lower in Austria, Czech Republic, and Hungary due to a future precipitation reduction. The average stress coefficient from 1976 to 2005 was never lower than 0.80 (Greece). ETa values were in line with the ETc values. The lowest amount of water applied by irrigation is computed in Austria, Czech Republic, Slovenia, and Switzerland, were high precipitation are projected. The higher crop coefficient values were found in the past, and rarely they are under 0.80 (Algeria, Tunisia). The highest crop coefficients (around 0.20) were estimated in Austria, Switzerland, where the humidity is higher. Any grape yield loss was estimated where any water stress was computed. The highest yield loss under this pedo-climatic conditions is estimated for the grape growth in Greece (19%), in Morocco, Spain, and Tunisia (about 10%) (Table 49).

Tab. 49. ETc, ETa and NA values weighted for the irrigated grape areas for the climate baseline period (1976-2005), and for the climate future period (2036-2065), under both RCP 4.5 and 8.5. bas = baseline, 45 = RCP 4.5, and 85 = RCP 8.5.

	bas	RCP 45	RCP 85	bas	RCP 45	RCP 85	bas	RCP 45	RCP 85	bas	RCP 45	RCP 85	bas	RCP 45	RCP 85	bas	RCP 45	RCP 85	bas	RCP 45	RCP 85
	ETo	ETo	ETo	ETC	ETC	ETC	ETA	ETA	ETA	NA	NA	NA	PCP	PCP	PCP	Ks	Ks	Ks	Kc	Kc	Kc	Ya/Yc	Ya/Yc	Ya/Yc
Irrigated Countries	mm	mm	mm	mm	mm	mm	mm	mm	mm	mm	mm	mm	mm	mm	mm							%	%	
Algeria	1324	1373	1397	649	655	660	604	609	611	395	422	435	185	156	137	0.93	0.93	0.93	0.49	0.48	0.47	0.07	0.07	0.07
Austria	483	510	499	601	625	609	599	624	607	320	355	339	1273	1238	1260	1	1	1	1.24	1.23	1.22	0	0	0
Bulgaria	829	866	863	739	760	760	734	754	754	541	576	570	490	447	457	0.99	0.99	0.99	0.89	0.88	0.88	0.01	0.01	0.01
Czech Republic	516	546	527	522	543	534	522	544	534	229	261	252	759	729	737	1	1	1	1.01	1	1.01	0	0	0
France	606	661	648	649	688	681	622	659	651	362	436	426	882	856	883	0.96	0.96	0.96	1.07	1.04	1.05	0.04	0.04	0.04
Greece	863	903	907	774	793	795	626	639	641	605	637	638	521	425	436	0.81	0.81	0.81	0.9	0.88	0.88	0.19	0.19	0.19
Croatia	699	743	731	637	661	656	632	655	650	371	413	404	895	853	905	0.99	0.99	0.99	0.91	0.89	0.9	0.01	0.01	0.01
Hungary	771	801	771	683	698	686	681	697	684	432	465	449	518	505	541	1	1	1	0.89	0.87	0.89	0	0	0
Italy	710	759	761	649	686	683	645	682	678	397	461	455	834	772	771	0.99	0.99	0.99	0.91	0.90	0.90	0.01	0.01	0.01
Slovakia	574	602	575	625	645	628	625	646	628	363	399	380	724	701	745	1	1	1	1.09	1.07	1.09	0	0	0
Macedonia	731	775	781	674	701	707	655	681	686	476	524	529	626	548	558	0.97	0.97	0.97	0.92	0.9	0.9	0.03	0.03	0.03
Morocco	1074	1122	1150	624	643	644	567	578	588	400	427	441	352	285	256	0.91	0.9	0.91	0.58	0.57	0.56	0.09	0.1	0.09
Portugal	842	911	899	679	716	705	638	671	660	448	506	501	924	848	938	0.94	0.94	0.94	0.81	0.79	0.78	0.06	0.06	0.06
Romania	734	767	748	772	793	787	772	793	787	575	607	589	604	572	601	1	1	1	1.05	1.03	1.05	0	0	0
Slovenia	568	606	595	570	588	582	568	586	579	289	328	315	1084	1056	1144	1	1	1	1	0.97	0.98	0	0	0
Spain	816	875	876	721	752	751	646	673	671	484	536	543	711	637	669	0.9	0.89	0.89	0.88	0.86	0.86	0.1	0.11	0.11
Serbia	767	812	801	623	646	646	619	642	641	356	399	391	623	584	590	0.99	0.99	0.99	0.81	0.80	0.81	0.01	0.01	0.01
Switzerland	414	451	450	512	539	540	512	540	540	170	241	238	1712	1617	1635	1	1	1	1.24	1.20	1.20	0	0	0
Tunisia	1314	1355	1374	664	663	665	614	588	592	439	460	467	163	137	116	0.92	0.89	0.89	0.51	0.49	0.48	0.08	0.11	0.11
Turkey	860	897	908	888	923	922	888	924	922	707	751	747	479	449	438	1	1	1	1.03	1.03	1.02	0	0	0

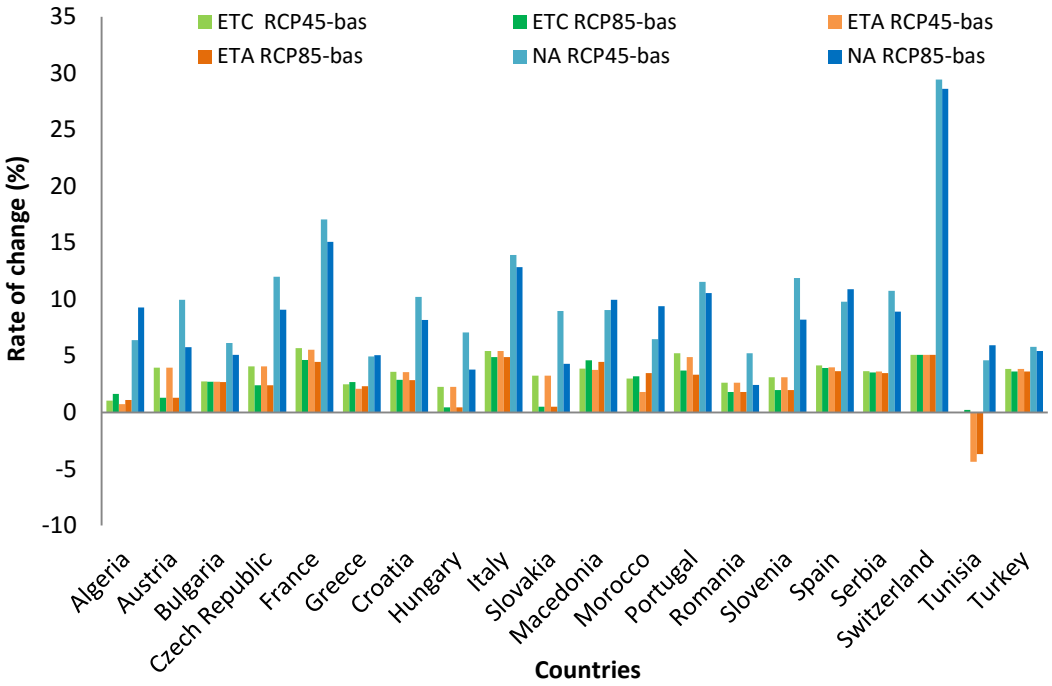

Fig. 182. Rate of change of ETc, ETa, NA values weighted for the irrigated grape distribution estimated between the future climate conditions (2036-2065), under both RCPs 4.5 and 8.5 scenarios, and the baseline (1976-2005).

The higher difference between future and past ETc values were estimated in Czech Republic, Italy, Portugal, Spain, as well as in Switzerland (about 5%) under RCP 4.5 (Figure 182). Any difference was found instead in Tunisia. It was worth to notice that the differences between the two RCPs are never higher than 3 mm. ETc values were equal to ETa values under all RCPs in Bulgaria, Turkey, and Spain.

Differences between future and past ETc and ETa values were higher under RCP 4.5 than 8.5 in France, Italy Austria, Croatia, Hungary, Portugal, Romania, and Slovenia in correspondence with increased values of precipitation. A great difference was estimated for the amount of water applied by irrigation in Switzerland under both RCPs where a great precipitation reduction was projected. Differences of NA higher than 10% under both RCPs were estimated in France, Italy, and Portugal.

2.4 DISCUSSIONS AND CONCLUSIONS

In this research, the impact of climate change on maize, wheat, and grape water consumption and irrigation requirement was assessed using the SIMETAW_GIS platform at Euro-Mediterranean scale with a resolution of 14 km, for the baseline (1976-2005) and the future climate conditions (2036-2065), under RCP 4.5 and 8.5 scenarios.

Cultivated area, sowing, bud break, and harvest date, and crop management were assumed not changing in future.

Results about the accuracy of the climatic modeled variables, by comparing variables simulated by the climate model and measured at the selected FLUXNET sites, showed that the best performance was obtained for temperatures (correlation values higher than 85% in almost all sites). ETo calculation were the most accurate, when compared with site measurements, using the Penman Monteith method in combination of climate data dynamically downscaled by Era-Interim.

In line with several studies (Allen et al., 1998; Temesgen et al., 1999; Droogers and Allen., 2002; Martinez-Cob and Tejero, 2004; Alexandris et al, 2008; de Sousa Lima et al., 2013), the differences between ETo_HS and ETo_PM were due to an overestimation of ETo_HS in areas characterized by a high relative humidity (%) and low wind speed (m s^{-1}), reversely to an underestimation in areas where the percentage of relative humidity was low and wind speed was high. Despite the different data source and resolution, in general, the trend of ETo_PM values estimated in this work was in line with other works. In this work, Northern France and Italy showed ETo_PM values lower than 750 mm yr^{-1}, as well as in most of the areas in Slovenia and Northern-Eastern part of Bosnia and Herzegovina. The spatial trend in Mediterranean regions was similar to Todorovic et al. (2013), where long-term monthly average climatic data from 3262 metereological stations in 144 different regions were used to compute ETo. In this work as well as in Todorovic et al. (2013), higher values in Northern Africa, particularly in the desert zones, were estimated, even though the ETo_PM values computed in this one were about 500 mm lower than in Todorovic et al. (2013).

Due to the increasing CO_2 concentration values (ppm) in the atmosphere, and therefore the increasing temperature, higher values of ETo, were simulated for future climate. In general, the highest differences between future and past values were estimated using HS equation.

The largest differences between future and past ETo, according to ETo_HS and ETo_PM, were found in Mediterranean Countries, where it was equal to 35 mm yr^{-1} under RCP 4.5 and 48 mm yr^{-1} under RCP 8.5, while in all the other Countries it was equal to 29 mm yr^{-1} and 43 mm yr^{-1} under RCP 4.5 and 8.5, respectively. Specifically, in the Mediterranean regions, under RCP 4.5, the highest difference (~ 45 mm yr^{-1}) was found in Libya, Morocco, Syria, and Cyprus while the lowest in France (~ 22 mm yr^{-1}). In the same Countries, under RCP 8.5, differences were higher in Lybia (~ 51 mm yr^{-1}) and Cyprus (~ 61 mm yr^{-1}), and lower in Syria (~ 40 mm yr^{-1}), and Morocco (33 mm yr^{-1}). In France ETo values 35 mm higher were estimate. The highest differences (between ~ 66 and 56 mm yr^{-1}) were estimated, under the worst scenario, in Israel, Bosnia and Herzegovina, Cyprus, Montenegro, Lebanon, Turkey, and Spain.

The trend related to the increasing ETo values in Euro-Mediterranean regions showed by Saadi et al. (2014) is in line with the one found in this study, even though the percentage climate change impact on ETo_PM was about 3% higher than what estimated in this work in Spain, Morocco, Portugal, and Algeria, and 1.3% lower in Croatia, Slovenia, and France, considering the average of both RPCs. Differences between the two works may be due to the different scenario, resolution and climate data input.

In view of the obtained results, the ETo calculated with the standardized reference evapotranspiration equation (ETo_PM) gave the best performances ($r > 70\%$ in almost all sites), and was used in the computation of ETc, ETa and NA for maize, wheat, and grape.

In general, the climate change impact would increase the values of these variables for all crops in the Mediterranean basin where temperature is expected to increase and precipitation events to decrease, with greater differences under RCP 4.5 than 8.5 most of the times.

In this work the assumed allowable depletion of 50%, the maximum soil depth, the soil water holding capacity, the maximum rooting depth, as well as the irrigation

system led to a water stress condition for each crop under investigation, i.e. thus values of actual evapotranspiration (ETa) lower than ETc were estimated. The lowest stress coefficient value was estimated in Portugal (~ 0.74) and the highest in Germany, Ukraine, Romania (~ 0.98) for maize irrigated using sprinkler system. The minimum and maximum Ks values were estimated in Lebanon (~ 0.63) and in Ukraine (~ 0.98), respectively for wheat irrigated using sprinkler methods, while lower values were computed for wheat grown in rainfed conditions, specifically the highest value was found in United Kingdom (~ 0.86) and the lowest in Algeria (~ 0.4). The lowest stress conditions were found for grape irrigated using drip method were Ks value was in almost all investigated Countries close to 1.

The impact of global warming on the **maize** water consumption (ETc) and irrigation requirement (NA) in the top productive Countries at Mediterranean scale is expected to be from 4% to 12% higher than in the baseline, under both RCPs. ETa values were about 3% higher in the past than in the future, thus 1% lower than ETc.

Keeping a focus only on Mediterranean Countries, already affected by water scarcity, the estimated maize irrigation requirement value is expected to be about 9.3% (40 mm yr^{-1}) higher in the future ,under both RCPs, than in the baseline where the total average values was about 398 mm yr^{-1}. Generally, NA values computed under RCP 8.5 were higher than RCP 4.5 except for Albania, Egypt, Italy, Slovenia, Bosnia and Herzegovina, Montenegro, and Croatia, where precipitation are projected to increase under the most extreme RCP scenario to compensate increasing Mazie water requirements.

The trend of the increasing maize water requirement along Italy, from Northern to Southern, under both RCP 4.5 and 8.5 scenarios is in line with Gallo et al. (2015).

An increasing water application of about 10% and 9% is expected under RCP 4.5 and 8.5, respectively for the **grape** growth in the top productive Countries of the domain under investigation, while, in the same Countries, an increasing grape water consumption of about 3% was estimated under both scenarios was estimated. A focus on the Mediterranean Countries showed a total average NA value of about 7.5% (525 mm yr^{-1}) higher in the future under both RCPs, i.e. about 40 mm yr^{-1} more, than in the baseline. ETc values were higher (~ 3%) under RCP 4.5 than 8.5 in France, Italy, and

Slovenia. In Sardinia region grape irrigation requirement values ranged from about 400-530 mm yr^{-1}, in agreement with Mancosu (2013).

Differences between the future and the past ETc and NA values ranged from about 1.4 to 10% under RCP 4.5, while from 0.3 to 8% under RCP 8.5 in the **irrigated wheat** top productive Countries. The ETa computed under the stress conditions assumed in this work were 0.70% higher in the future under RCP 4.5, values were 0.50% lower under RCP 8.5 than in past period.

In the Mediterranean basin, wheat total water application needs are expected to be about 9% (21 mm) higher in the future than in the past, when the value is equal to about 227 mm yr^{-1}. Negative values associated to an increasing precipitation were found under RCP 8.5 in France, Albania, Slovenia, Spain, and Montenegro.

The ETc range estimated in the South of Spain, in Turkey, and the Northern Africa in this work for the past period (394-631 mm yr^{-1}) was lower than the one found in Saadi et al. (2014) (303-864 mm yr^{-1}), which also indicated a decreasing range in the future (298-840 mm yr^{-1}) in contrast with what found in this work under RCP 4.5 (396-637 mm yr^{-1}) and RCP 8.5 (382-645 mm yr^{-1}). Differences between the two works could be due to the different time series, input data, and resolution. The negative impact of climate change on wheat evapotranspiration, thus net application, and yield was in agreement with others studies (Tubiello et al., 2000; Özdogan, 2011; Valizadeh et al., 2014).

Any difference between future and past ETc values under RCP 8.5 scenario was estimated for **rainfed wheat**, while an increase of about 1 percentage was found under RCP 4.5 considering the main productive Countries. The stress water condition expressed by the actual evapotranspiration (ETa) computed in the future and in the past was higher under RCP 8.5 (-8%) than under RCP 4.5 (-6%). In Mediterranean Countries, since the only water supply was given by precipitation, values of ETa lower than ETc were found in the entire basin. Precisely, the difference between ETc and ETa was equal to 234 mm yr^{-1} in the baseline, and it was expected to be about 10% (26 mm yr^{-1}) higher considering both RCPs. The range of actual evapotranpiration estimated by Saadi et al., (2014) (46-494 mm yr^{-1}) was higher than the one estimated using SIMETAW_GIS model (36-288 mm yr^{-1}) in the baseline. In the same study, future ETa range was lower (46-460 mm yr^{-1}) than in the past. The reverse was

obtained instead in this work under both RCP 4.5 (38-411 mm yr^{-1}) and RCP 8.5 (38-414 mm yr^{-1}), even though, ETa values were in general lower.

In this work, water applications were estimated on crop water consumption, i.e. the total amount of water consumed by a crop in well-water conditions, in absence of any water stress (full-irrigation, ETc). Most of the time, the crop growth in optimal conditions is not possible due to limiting physical and economic factors (Daccache et al., 2014).

Although to the applied irrigation practice, the actual evaporanspiration estimated in this work was always lower than the crop water consumption, and this is related to the pedoclimatic (weather, maximum soil depth, soil water holding capacity, as well as maximum rooting depth input gridded data), conditions and the management practices (both percentage of full water allocation applied and the planted area, irrigation system, and allowable depletion) assumed. Assuming any changes in input data, actual evapotranspiration values could increase changing the frequency and number of irrigation events (AD < 50%): this management strategy will reduce the water stress, thus increase actual evapotranspiration, that in turn allow to reduce the yield losses. It is worth to notice that, in this case much water will be applied for the crop growth, so an environmental-economic analysis should be made in order to achieve the best balance between the impact on water resources and yield losses. In addition, the price of water should also take into account, since it encumbers on farm business.

In this contex, in view of the quick increasing of demographic growth, and the consequent food security, it is necessary to cope with climate change through strategies targets to achieve agricultural sustainable productions.

This work provides a tool to evaluate the impact of climate change on crops water consumption and irrigation requirement at local and region scale. Water scarcity is expected to be more severe in Mediterranean regions where temperature will increase and precipitation events will decrease.

The best response to increasing CO_2, in terms of yield loss, was given by grape and wheat (C3 crops) than maize (C4). Reference, crop, and actual evapotranspiration, as well as irrigation requirement will increase under future climate, and most of the times differences are greater under the RCP 4.5 scenario.

Results are strictly related to the input gridded data resolution and uncertainty, and crop management assumptions.

In order to tackle climate change impact on agricultural sector, adaptation strategies should be developed and implemented at regional scale. In this context, crop breeding and new technologies, as well as shifts in sowing, bud break, and harvest date should be taken into account in order to investigate on crop physiological adaptation to different climate change conditions. In addition, changing in the percentage of cultivated areas should be assessed. A larger number of crops under several water management scenarios should be evaluated to reduce water losses, in particular in Mediterranean basin. Higher resolution input gridded data are needed in order to include more details in the outcomes at Euro-Mediterranean scale. An ensemble of climate models may reduce result uncertainties, and in this regard a reduction in climate model bias may have a key role.

REFERENCES

Alexandris, S., Stricevic, R., Petkovic, S., 2008. Comparative analysis of reference evapotranspiration from the surface of rainfed grass in central Serbia, calculated by six empirical methods against the Penman-Monteith formula. European Water Publications 21/22, 17-28.

Alexandrov, V., 1999. Vulnerability and adaptation of agronomic systems in Bulgaria. Climate Research 12, 161-173.

Allen, R.G., Pereira, L.S., Raes, D., Smith, M., 1998. Crop evapotranspiration: Guidelines for computing crop requirements. Irrigation and Drainage Paper No. 56, FAO 56, 300, https://doi.org/10.1016/j.eja.2010.12.001.

Anderson, J., Dimou, P., Jones, G.V., Kalivas, D., Koufos, G., Mavromatis, T., Koundouras, S., Fyllas, N.M., 2014. Harvest Dates, Climate, And Viticultural Region Zoning In Greece, https://inside.sou.edu/assets/bce/Anderson_etal_Greece_Terroir_Congress_2014.pdf.

Andreini, L., Viti, R., Scalabrelli, G., 2009. Study on the morphological evolution of bud break in Vitis vinifera L. Vitis 48, No.4, 153–158.

Batjes, N.H., 2000. Global Data Set of Derived Soil Properties, 0.5-Degree Grid (ISRIC-WISE). Global Data Set of Derived Soil Properties, 0.5-Degree Grid (International Soil Reference and Information Centre - World Inventory of Soil Emission Potentials). Data set. Available on-line http://www.daac.ornl.gov. From Oak Ridge National Laboratory Distributed Active Archive Center, Oak Ridge, Tennessee, U.S.A., doi:10.3334/ORNLDAAC/546.

Bucchignani, E., Mercogliano, P., Manzi, M.P., Montesarchio, M., Rillo, V., 2013. Assessment of ERA-Interim driven simulation over Italy with COSMO-CLM. Research Papers Issue RP0183. Centro Euro-Mediterraneo sui Cambiamenti Climatici, Impact on Soil and Coast Division (ISC).

Caciagli, L., 2012. Cambiamenti climatici e rischio idrogeologico nell'area mediterranea. Centro Euro-Mediterraneo sui Cambiamenti Climatici, CMCC. Italia.

Camps, J.O., Ramos, M.C., 2012. Grape harvest and yield responses to inter-annual changes in temperature and precipitation in an area of north-east Spain with a Mediterranean climate. International Journal of Biometeorology 56, 853–864, doi:10.1007/s00484-011-0489-3.

Carter, T.R., Parry, M., Nishioka, S., Harasawa, H., 1996. Technical Guidelines for assessing climate change impacts and adaptations. In: Climate Change 1995. Impacts, Adaptations and Mitigation of Climate Change: Scientific-Technical Analysis. Contribution of Working Group II to the Second Assessment Report of the Intergovernmental Panel on Climate Change [Watson, R.T., M.C. Zinyowere and R.H. Moss (eds.)]. Cambridge University Press, Cambridge, United Kingdom and New York, NY, USA, pp. 823-833.

CDO, 2013. Climate Data Operators: Release 1.6.1. Max-Planck-Institut für Meteorologie.

Christensen, J.H., Hewitson, B., Busuioc, A., Chen, A., Gao, X., Held, I., Jones, R., Kolli, R.K., Kwon, W.-T., Laprise, R., Magaña Rueda, V., Mearns, L., Menéndez, C.G., Räisänen, J., Rinke, A., Sarr, A., Whetton, P., 2007. Regional Climate Projections. In: Climate Change 2007: The Physical Science Basis. Contribution of Working Group I to the Fourth Assessment Report of the Intergovernmental Panel on Climate Change. Cambridge University Press, Cambridge, United Kingdom and New York, NY, USA.

Christoph, N., Rossmann, A., Voerkelius, S., 2003. Possibilities and limitations of wine authentication using stable isotope and meteorological data, data banks and statistical tests. Part 1: Wines from Franconia and lake Constance 1992 to 2001. Mitteilungen klosterneuburg 53, 23-40.

Correia, F.N. 1999. Water Resources in the Mediterranean region.Water International 24 (1), 22-30.

Cortesi, P., Bisiach, M., Ricciolini, M., Gadoury, D.M., 1997. Cleistothecia of Uncinula necator—An additional source of inoculum in Italian vineyards. Plant Disease 81, 922-926.

Daccache, A., Ciurana, J S., Rodriguez Diaz, J A., Knox, J W., 2014. Water and energy footprint of irrigated agriculture in the Mediterranean region. Environmental Research Letters 9, 12, doi:10.1088/1748-9326/9/12/124014.

de Sousa Lima, J., Antonino, A., Souza, E., Hammecker, C., Montenegro, S., Lira, C., 2013. Calibration of Hargreaves-Samani equation for estimating reference evapotranspiration in the sub-humid region of Brazil. Journal of Water Resource and Protection 5, 12A.

Dee, D., Uppala, SM., Simmons, A.J., Berrisford, P., Poli, P., Kobayashi, S., Andrae, U., Balmaseda, MA., Balsamo, G., Bauer, P., Bechtold, P., Beljaars, ACM., van de Berg, L., Bidlot, J., Bormann, N., Delsol, C., Dragani, R., Fuentes, M., Geer, A.J., Haimberger, L., Healy, S.B., Hers-bach, H., Holm, E.V., Isaksen, L., Kallberg, P., Kohler, M., Matricardi, M., McNally, A.P., Monge-Sanz, B.M., Morcrette, J.J., Park, B.K. Peubey, C., de Rosnay, P., Tavolato, C., Thepaut, J.N., Vitart, F., 2011. The era-interim re-analysis: configuration and performanceof the data assimilation system. Quarterly Journal of Royal Meteorological Society 137, 553–597.

Droogers, P., Allen, R.G., 2002. Estimating reference evapotranspiration under inaccurate data conditions. Irrigation and Drainage Systems 16, 33–45. Kluwer Academic Publishers. Printed in the Netherlands.

Elliott, J., Müller, C., Deryng, D., Chryssanthacopoulos, J., Boote, K.J., Büchner, M., Foster, I., Glotter, M., Heinke, J., Iizumi, T., Izaurralde, R.C., Mueller, N.D., Ray, D.K., Rosenzweig, C., Ruane, A.C., Sheffield, J., 2015. The Global Gridded Crop Model Intercomparison: data and modeling protocols for Phase 1 (v1.0). Geoscientific Model Development 8, 261–277, doi:10.5194/gmd-8-261-2015. www.geosci-model dev.net/8/261/2015/

Ezzhaouani, A., Valancogne, C., Pieri, P., Amalak, T., Gaudillère, J., 2007. Water economy by Italia grapevines under different irrigation treatments in a Mediterranean climate. International Journal of Vine and Wine Sciences 41 (3), 131-139.

Fader, M., von Bloh, W., Shi, S., Bondeau, A., Cramer, W., 2015. Modelling Mediterranean agro-ecosystems by including agricultural trees in the LPJmL model. Geoscientific Model Development 8, 3545–3561, doi:10.5194/gmd-8-3545-2015.

Fader, M., Shi, S., von Bloh, W., Bondeau, A., Cramer, W., 2016. Mediterranean irrigation under climate change: more efficient irrigation needed to compensate for increases in irrigation water requirements. Hydrology and Earth System Sciences 20, 953–973, doi:10.5194/hess-20-953-2016.

Gallo, A., 2015. Assessment of the Climate Change Impact and Adaptation Strategies on Italian Cereal Production using High Resolution Climate Data. Ph.D. thesis. University of Sassari.

Geyer, B., Weisse, R., Bisling, P., Winterfeldt, J., 2015. Climatology of North Sea wind energy derived from a model hindcast for 1958-2012. Journal of Wind Engineering and Industrial Aerodynamics 147, 18-29. Elsevier.

Gualdi, S., Scoccimarro, E., Bellucci, A., Oddo, P., Sanna, A., Fogli, P.G., Vichi, M., Manzini, E., Navarra, A., 2011. Regional climate simulations with a global high resolution coupled model: the euro-mediterranean case. Submitted to Clim Dyn.

Harrison, P.A., Butterfield, R.E., 1996. Effects of climate change on Europe-wide winter wheat and sunflower productivity. Climate Research 7, 225-241.

Harrison, P.A., Butterfield, R.E., 2000. Modelling climate change impacts on wheat, potato and grapevine in Europe, in: Downing, T.E., Harrison, P. A., Butterfield, R. E. and Lonsdale, K. G. (eds.), Climate Change, Climate

Variability and Agriculture in Europe: An Integrated Assessment, Research, Report 21, Environmental Change Unit, University of Oxford, 367–390.0.

Haylock, M.R., Hofstra, N., Klein Tank, A.M.G., Klok, E.J., Jones, P.D., New, M., 2008. A European daily high resolution gridded data set of surface temperature and precipitation for 1950–2006. Journal of Geophysical Research 113, D20119, doi:10.1029/2008JD010201.

Hofstra, N., Haylock, M., New, M., Jones, P.D., 2009. Testing E-OBS European high-resolution gridded data set of daily precipitation and surface temperature. Journal of geophysical research, atmospheres 114, Issue D21, doi: 10.1029/2009JD011799.

IPCC, 2013. Summary for Policymakers. In: Climate Change 2013: The Physical Science Basis.Contribution of Working Group I to the Fifth Assessment Report of the Intergovernmental Panel on Climate Change Stocker, T.F., D. Qin, G.-K. Plattner, M. Tignor, S.K. Allen, J. Boschung, A. Nauels, Y. Xia, V. Bex and P.M. Midgley. Cambridge University Press, Cambridge, United Kingdom and New York, NY, USA.

Jones, G.V., Davis, R.E., 2000. Climate Influences on Grapevine Phenology, Grape Composition, and Wine Production and Quality for Bordeaux, France. American Journal of Enology and Viticulture 51, No. 3.

Kenny, G.J., Harrison, P.A., Olesen, J.E., Parry, M.J., 1993. The effects of climate change on land suitability of grain maize, winter wheat and cauliflower in Europe. European Journal of Agronomy 2, 325-338.

López-Urrea, R., Montoro, A., Manas, F., López-Fuster, P., Fereres, E., 2012. Evapotranspiration and crop coefficients from lysimeter measurements of mature ‘Tempranillo’ wine grapes. Agricultural Water Management 112, 13-20.

Mancosu, N., 2013. Agricultural water demand assessment using the SIMETAW# model. Ph.D. thesis. University of Sassari.

Martinez-Cob, A., Tejero-Juste, M., 2004. A wind-based qualitative calibration of the Hargreaves ET0 estimation equation in semiarid region. Agricultural Water Management 64 (3), 251–264.

Meier, N., Rutishauser, T., Pfister, C., Wanner, H., Luterbacher, J., 2007. Grape harvest dates as a proxy for Swiss April to August temperature reconstructions back to AD 1480. Geophysical Research Letters 34, L20705, doi:10.1029/2007GL031381.

Nandagiri, L., Kovoor, G.M., 2006. Performance Evaluation of Reference Evapotranspiration Equations across a Range of Indian Climates. Journal of Irrigation and Drainage Engineering 132 (3), doi:10.1061/(ASCE)0733-9437(2006)132:3(238).

Nendel, C., 2010. Grapevine bud break prediction for cool winter climates. International Journal of Biometeorology 54, 231–241, doi:10.1007/s00484-009-0274-8. Springer.

Novello, V., de Palma, L., 2008. Growing grapes under cover. Acta horticulturae May 2008, doi:10.17660/ActaHortic.2008.785.44.

Ozdogan, M., 2011. Modeling the impacts of climate change on wheat yields in Northwestern Turkey. Agriculture, Ecosystems and Environment 141, 1–12.

Picòn-Toro, J., Gonzàlez-Dugo, V., Uriarte, D., Mancha, L.A., Testi, L., 2012. Effects of canopy size and water stress over the crop coefficient of a ‘‘Tempranillo’’ vineyard in south-western Spain. Irrigation Science 30, 419–432 doi:10.1007/s00271-012-0351-3.

Portmann, F.T., Siebert, S., Döll, P., 2010. MIRCA2000—Global monthly irrigated and rainfed crop areas around the year 2000: A new high resolution data set for agricultural and hydrological modeling. Global biogeochemical cycles, 24, GB1011, doi:10.1029/2008GB003435.

Rahimi Khoob, A., 2008. Comparative study of Hargreaves's and artificial neural network's methodologies in estimating reference evapotranspiration in a semiarid environment. Irrigation Science 26, 253–259.

Rockel, B., Will, A., Hense, A., 2008. The regional Climate Model COSMO-CLM (CCLM). Meteorologische Zeitschrift 17 (4), 347-348.

Rodriguez-Diaz, J.A., Weatherhead, E.K., Knox, J.W., Camacho, E., 2007. Climate change impacts on irrigation water requirements in the Guadalquivir river basinin Spain. Regional Environment Change 7, 149–159.

Saadi, S., Todorovic, M., Tanasijevic, L., Pereira, L.S., Pizzigalli, C., Lionello, P., 2014. Climate change and Mediterranean agriculture: Impacts on winter wheat and tomato crop evapotranspiration, irrigation requirements and yield. Agricultural Water Management. Elsevier.

Schwab, A.L., Knott, R., Schottdorf, W., 2000. Results from new fungus-tolerant grapevine varieties for Organic Viticulture. Beitrag präsentiert bei der Konferenz: 6th International Congress on Organic Viticulture, Basel, Switzerland, 25.08. - 26.08.2000; Veröffentlicht in Willer, Helga und Meier, Urs, (Hrsg.) Proceedings 6th International Congress on Organic Viticulture, Seite(n) 225-227. SÖL-Sonderausgabe 77. Stiftung Ökologie & Landbau, Bad Dürkheim.

Scoccimarro, E., Gualdi, S., Bellucci, A., Sanna, A., Fogli, P.G., Manzini, E., Vichi, M., Oddo, P., Navarra, A., 2011. Effects of tropical cyclones on ocean heat transport in a high resolution coupled general circulation model. Journal of climate 24 (16), 4368–4384.

Tanasijevic, L., Todorovic, M., Pereira, L.S., Pizzigalli, C., Lionello, P., 2014. Impacts of climate change on olive crop evapotranspiration and irrigation requirements in the Mediterranean region. Agricultural Water Management 144, 54–68. Elsevier.

Taylor, K.E., Stouffer, R.J., Meehl, G.A., 2012. An overview of CMIP5 and the experiment design. Bulletin of the American Meteorological Society 93 (4), 485-498.

Temesgen, B., Allen, R.G., Jensen, D.T., 1999. Adjusting temperature parameters to reflect well-water conditions. Journal of Irrigation and Drainage Engineering 125 (1), 26–33.

Todorovic, M., Karic, B., Pereira, L.S., 2013. Reference evapotranspiration estimate with limited weather data across a range of Mediterranean climates. Journal of Hydrology 481, 166–176.

Tomasi, D., Jones, G.V., Giust, M., Lovat, L., Gaiotti, F., 2011. Grapevine Phenology and Climate Change: Relationships and Trends in the Veneto Region of Italy for 1964-2009. American Journal of Enology and Viticulture (AJEV), doi: 10.5344/ajev.2011.10108.

Tubiello, F.N., Donatelli, M., Rosenzweig, C., Stockle, C.O., 2000. Effects of climate change and elevated CO_2 on cropping systems: Model predictions at two Italian locations. European Journal of Agronomy 13, 179–189.

UNRIC, 2015. Il nuovo rapporto dell' onu avverte: l'aumento della popolazione mondiale si somma alla crisi acqua. Centro Regionale d'Informazione delle Nazioni Unite, Brussels.

Valdés-Gómez, H., Celette, F., de Cortázar-Atauri, I.G., Jara-Rojas, F., Ortega-Farías, S., Gary, C., 2009. Modelling Soil Water Content And Grapevine Growth And Development With The Stics Crop-Soil Model Under Two Different Water Management Strategies. Journal International des Sciences de la Vigne et du Vin 43, No.1, 13-28.

Valizadeh, J., Ziaei, S.M., Mazloumzadeh, S.M., 2014. Assessing climate change impacts on wheat production (a case study). Journal of the Saudi Society of Agricultural Sciences 13, 107-115.

Wieder, W.R., Boehnert, J., Bonan, G.B., Langseth, M., 2014. Regridded Harmonized World Soil Database v1.2. Data set. Available on-line [http://daac.ornl.gov] from Oak Ridge National Laboratory Distributed Active Archive Center, Oak Ridge, Tennessee, USA, http://dx.doi.org/10.3334/ORNLDAAC/1247 .

You, L., Wood-Sichra, U., Fritz, S., Guo, Z., See, L., Koo., J., 2014. Spatial Production Allocation Model (SPAM) 2005 v2.0. March 7, 2017. Available from http://mapspam.info.

Websites

http://www.pep725.eu/

http://www.fao.org/faostat/en/#data/QC

PART 3. Vulnerability assessment of Euro-Mediterranean irrigated agriculture under climate change

3.1 INTRODUCTION

"Food security exists when all people, at all times, have physical and economic access to sufficient, safe and nutritious food that meets their dietary needs and food preferences for an active and healthy life" (World Food Summit, 1996).

In the last few decades, the number of areas, over the world, where food is becoming an emergency is rising. At European level, the impact of climate change on food production has been critical in many Countries, particularly in the Eastern and Southern Mediterranean regions (Paciello, 2015). The increasing population growth, urbanization and the consumers changing behaviour lead to larger requirements of freshwater (Harrison et al., 2014; McDonald et al., 2011; McDonald et al., 2014), as well as increasing request of food quantity and quality (Paciello, 2015). The biggest challenge is to feed a rising number of people and guarantee the sustainable use of natural resources at the same time.

The relevance of agriculture in the Southern regions is supported by the cultivated area extension which accounts for about 186 Mha in the Euro-Mediterranean regions, where 112 Mha are located in the Countries bordering the Mediterranean Sea. Specifically, the 92% of the total irrigated crop area (about 26 Mha) is estimated in the Southern Countries. In addition, the area equipped for irrigation and actually irrigated is about 18 Mha, i.e. about the 95% of the total at Euro-Mediterranean level, and the water withdrawal for irrigation is about the 89% of the total. The area equipped for surface irrigation (13 Mha) is larger than the one equipped for sprinkler (5 Mha) and localized (2 Mha) systems (see Table 2 and 3).

(http://www.fao.org/nr/water/aquastat/data/query/index.html?lang=en).

The total irrigated crops in Mediterranean basin is accounted for 16.3 Mha, and the main crop types are cereals (about 6.23 Mha), vegetables (1.78 Mha), fruit (2.68Mha), and fodder and pastures (2.24 Mha) (http://www.fao.org/3/a-bc824e.pdf).

Mediterranean Countries are coping with several physical and socio-political water crises, which are deeply exacerbated by climate unpredictability and variability of precipitation events. Since agricultural production in Mediterranean basin is mostly dependent on water, its availability is a key factor for food security in these areas (Paciello, 2015).

The increasing irrigation water requirement due to changing climate for Mediterranean crops was stated by several studies (Tubiello et al., 2000; Kapur et al., 2007; Rodriguez Diaz et al., 2007; Yano et al., 2007; Mancosu et al., 2013; Saadi et al., 2014; Tanasijevic et al., 2014; Gallo et al., 2015).

The first step to face with the expected irrigation demand increase is to improve water use efficiency. In this contest, strategies should be target to move from the lowest distribution uniformity system, such as surface and sprinkler, to the highest one as drip.

As a result of the exacerbated water shortages, studies focused on the vulnerability of irrigated agriculture systems are becoming crucial (Nam and Choi, 2014). A significant change in precipitation patterns, which is expected to characterize these areas by more frequent extreme events and prolonged drought periods, will lead to marked hydrological imbalances (IPCC, 2014). Furthermore, future risks of water shortage in arid and semi-arid climate will also depend on increasing water demand to supply tourism, industrial, commercial, and civil use requests, in addition to irrigated agriculture. However, the impact of a severe drought on infrastructure and services for human wellbeing is mostly related to the vulnerability of the sector under investigation (Cancelliere and Rossi, 2011). When a pluviometric deficit becomes quite permanent, it is associated to high temperatures, low relative humidity, and strong insolation and evapotranspiration (Gabriels, 2007), leading to semi-arid conditions (where annual precipitation is 100-250 mm) characterized by ecosystems with low productivity, or arid conditions (where annual precipitation is lower than 100 mm) characterized by desert (IPCC, 2001).

Crop production located in arid and semi-arid areas require a supplement of irrigation to sustain crop growth and farming activities (IPCC, 2014). In this contest, the role of dams and reservoirs, used totally or partially to supply water for irrigation, is essential for a sustainable agriculture. The water demand of irrigated agriculture will be affected by climate change, and its fulfilment conditioned by available freshwater. Thus, the evaluation of the reservoirs water storage levels respect to the crops water demand should be considered together to evaluate future risk and vulnerability for irrigated agriculture under climate change (Nam and Choi, 2014). The risk of water scarcity in water supply systems is related to drought intensity, infrastructure capacity and adaptation policies in case of drought events. This environmental and socio-economic issue is particularly relevant in the Mediterranean Countries (Cancelliere and Rossi, 2011), and the understanding of its implications are fundamental to support scientific bases for optimal development policies.

Garrote et al. (2015) analyzed more than sixty basins in Southern Europe, and they showed great differences in irrigation systems vulnerability across Europe, highlighting particularly significant vulnerabilities in the Iberian peninsula and in some parts of Italy and Greece.

This work aims to contribute in assessing the vulnerability of Euro-Mediterranean irrigated agriculture systems under climate change. The simultaneous impact of climate change on both crop water demand and water inflows to reservoirs, granting water supplies needed for irrigation, are assessed to define future level of adequacy of reservoir infrastructures to sustain irrigated agriculture and food security. Crop water requirements were estimated through the SIMETAW_GIS platform for a representative basket of crop types relevant for Euro-Mediterranean agriculture: maize, wheat, grape, tomato (as representative of horticultural crops), and peach (as representative of fruit trees). Specific reservoirs and associated irrigation systems in the Euro-Mediterranean were selected to aggregate simultaneous changes in crop water demand and water levels in reservoirs, and vulnerability to irrigated agriculture. Water inflow to reservoirs was assessed by defining upstream area contributing hydrologically to specific reservoirs, and analysing both runoff partitioning and precipitation changing patterns for the selected reservoir upstream watersheds in the Euro-Mediterranean. Climate projections downscaled at high resolution (spatial

resolution of 14 km) were used to represent underlying climate conditions for our baseline (1976-2005) and future (period 2036-2065), under Representative Concentration Pathways scenarios 4.5 and 8.5, and determine specific changes in crop water demand and water inflow to reservoirs.

3.2 MATERIALS AND METHODS

This research analyses the impact of climate and climate change on both irrigation requirements for the most representative crops in the Euro-Mediterranean irrigated agriculture, while assessing the physical characteristics of reservoirs granting water supplies (and resilience to climate variability) to irrigated agriculture. First, the location and physical characteristics of principal dams, and associated reservoirs, with main use for irrigation purposes is selected for the study domain. From this list, a smaller subset is selected to apply a vulnerability assessment under climate change. To this purpose, climate change projections are applied, for the selected reservoir systems, to calculate both changes in the water inflow from the upstream catchment areas and in the irrigation requirements of the most relevant crops distributed in the associated irrigation scheme.

3.2.1 Study domain

The domain extends from the Northern Africa to the Southern Denmark, and from Spain to Turkey (Figure 96). This domain is particularly connected to irrigated agriculture, and especially in its Southern part where freshwater abstractions for agriculture is very high (up to 80% of total abstraction) and vulnerability to droughts under climate change is projected to worsen.

3.2.2. Climate database

Climate daily data from COSMO-CLM regional model (Rockel et al., 2008) were used to estimate reference and crop evapotranspiration for the baseline (1976-2005) and the intermediate future (2036-2065), with a final spatial resolution of 14x14 km.

The Representative Concentration Pathways (RCP) climate scenarios 4.5 and 8.5 were considered for future projections.

3.2.3 Principal dams for irrigation use over the Euro-Mediterranean domain

3.2.3.1 Dam (GranD) database

The Global Reservoir and Dam (GranD) database, version 1.1, is a spatially explicit open source global dataset developed by Lehener et al. (2011), which aims to consolidate and reduce inconsistencies of existing available dataset. The GranD database is the result of the Global Water System project (GWSP) and several other collaborations and partnership with institutes and organizations whose main effort is to provide to the scientific community a single, large, and clear collection of available reservoirs and dam information worldwide. The database includes reservoirs characterized by a capacity higher than 0.1 km^3. The current version includes 6862 reservoirs and the associated dams, with a total storage capacity equal to 6197 km^3. In order to include a larger number of details, such as elevation, catchment area, and discharge, the GranD dataset is combined with the HydroSHEDS, i.e. a near global digital river network with a spatial resolution of ~ 500 m, developed by Lehener et al. (2008). Specifically, the global water balance model (waterGAP) is used to provide the runoff (from 1961 to 1990) to compute the discharge value indicated in the GranD database. Data are available in ESRI geographic projection shapefile format, referenced to the WGS84 datum. Several attributes are provided by the dataset to allow its application in different scientific fields.

Actually, the GranD database is divided into two GIS layers: (i) a point layer where dams and their information are included (GranD dams), (ii) a polygon layer which includes information of reservoirs (GranD reservoir).

- Grand_dams

The point layer of the GranD_dams provides a unique ID for each point, representing a dam and its related reservoir, the name of the water body and dam structure, the main basin and sub-basin name, the nearest city, as well as the administrative unit and Country. Technical information such as year of construction, dam height, and length,

representative surface area, capacity, depth of the reservoir, long term mean discharge, as well as elevation and area of upstream catchment are also reported. The database characterizes also the dams by their main use or second use (irrigation, hydroelectricity production, fisheries, water supply, flood control, and so on).

- GranD reservoirs

The attribute table of the GranD_reservoirs shapefile includes the ID for each polygon, representing the reservoir surface, the surface area, as well as the data source.

3.2.3.2 Main reservoir systems used for irrigation over the Euro-Mediterranean domain

Dams were located mainly along the Mediterranean basin, where irrigation practice is widely used to supply crop water requirement. In these areas, only the dams with irrigation practice as main use were selected for this study (Figure 183). Spain, France, Turkey, and Italy accounted for the highest number of dams used for this purpose, and specifically 124, 28, 14, and 20, respectively. In Northern Africa, 3 dams are located in Libya, 33 in Algeria, 21 both in Tunisia and Morocco. Less than 3 dams are reported in Greece, Syria, and Libya. Dam storage capacity higher than 10000Mm^3 were built in Turkey and Syria. The largest capacity (~ 48700 Mm^3) is reported for Ataturk dam, in Turkey. In Italy dam's representative capacity ranged from 11 (Rubino, in Sicily) to 530 Mm^3 (Monte Cotugno, in Basilicata). In Spain the lowest capacity was reported equal to 9.5 Mm^3 (San Lorenzo Mongay, in Lerida), and the highest 3231.8 Mm^3 (La Serena, in Badajoz). The dams capacity ranged from 0.8 Mm^3 (Tahouna, in Nabeul) to 807 Mm^3 (Oued el Makhazin, in Nord Ouest) (Lehener et al., 2011)

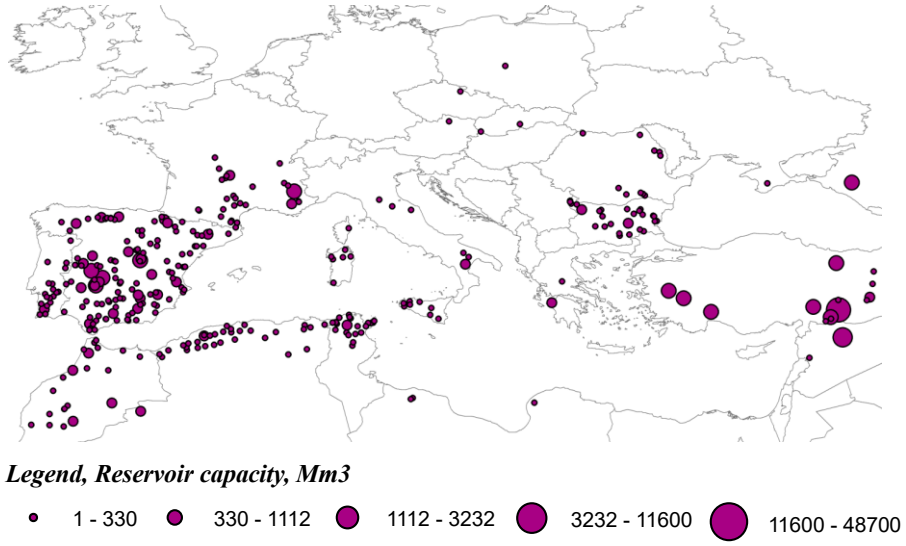

Fig. 183. Dams selected by irrigation as main use through the GranD database.

3.2.4 Physical characteristics of the reservoir systems - Aridity index

Zones more prone to drought are identified along the domain by the aridity index (eq. 53), and are shown in Figure 184, 185, and 186. The aridity index was used to quantify the moisture deficit, and consequently it was used as an indicator of the typical vegetation of a specific area. It is calculated as:

$$AI = \frac{P}{ETo} \qquad \text{eq. 53}$$

where P is the precipitation obtained by the regional climate model COSMO-CLM, and ETo is the reference evapotranspiration computed using the standardized Penman-Monteith equation by the SIMETAW_R model. Both variables are expressed in millimeters.

The aridity index classification was based on UNEP (1992) classification (Table 50).

Tab.50. Aridity index classification (UNEP, 1992)

Classification	Aridity Index
Hyperarid	AI < 0.03
Arid	0.03 < AI < 0.20
Semi-arid	0.20 < AI < 0.50
Dry subhumid	0.50 < AI < 0.65

Climatologists recognized four aridity index classes: hyperarid, arid, semi-arid, and sub-humid zones. A hyperarid zone is characterized by an aridity index lower than 0.03. In addition, a desert climate with irregular precipitation (interannual rainfall variability of 100% is possible) is typical of this areas. Vegetation is mainly composed by annual crops and bushes, and perennial plants are almost completely absent. Agriculture and pasture practice is hard and almost impossible. Annual precipitation, ranging from 80-150 mm and 200-350 mm, with an interannual variability of about 50-100%, is typical of arid zones where scattered vegetation of small woody, bushes, and succulent shrubs with thorns and without leaves is characteristic of the landscape. In this areas it is only possible a light grazing. Pasture and rainfed agriculture are possible in semi-arid zone (steppe) where precipitation values range from 300-400 mm and 700-800 mm in summer, and 200-250 mm and 450-500 mm in winter. Interannual precipitation variability ranges from 25 to 50%. Agriculture is a common practice in sub-humid zones where interannual precipitation variability is no higher than 25%. The typical vegetation is composed by savannah plants, steppe, and chaparral and maquis in Mediterranean climate (UNESCO, 1979).

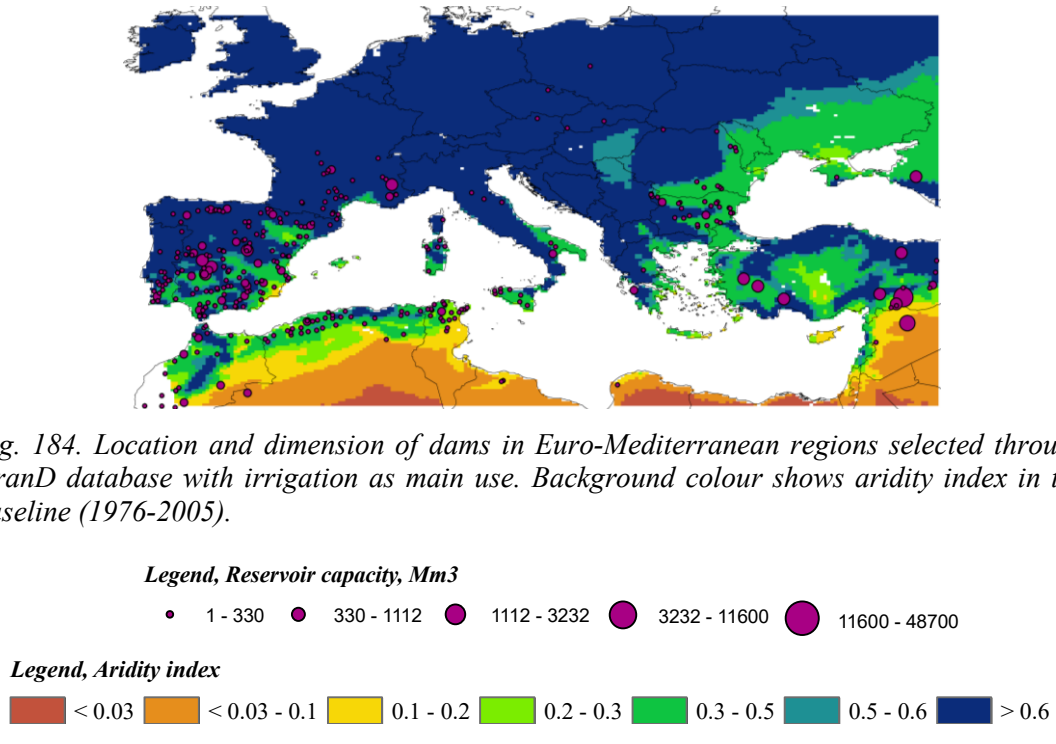

Fig. 184. Location and dimension of dams in Euro-Mediterranean regions selected through GranD database with irrigation as main use. Background colour shows aridity index in the baseline (1976-2005).

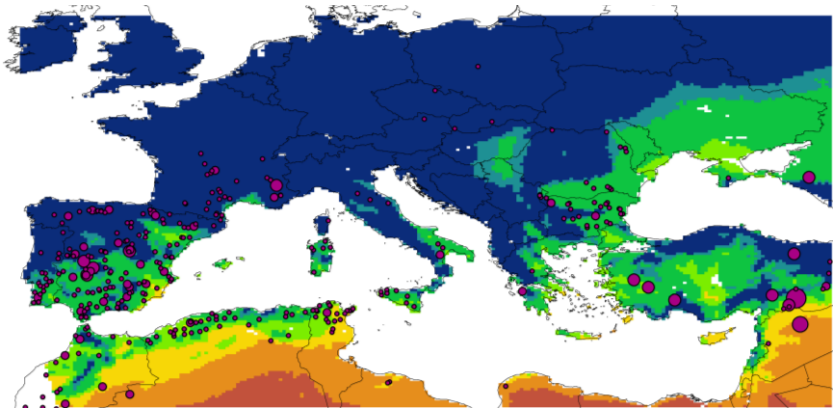

Fig. 185. Location and dimension of dams in Euro-Mediterranean regions selected through GranD database with irrigation as main use. Background colour shows aridity index in the future (2036-2065) under RCP 4.5.

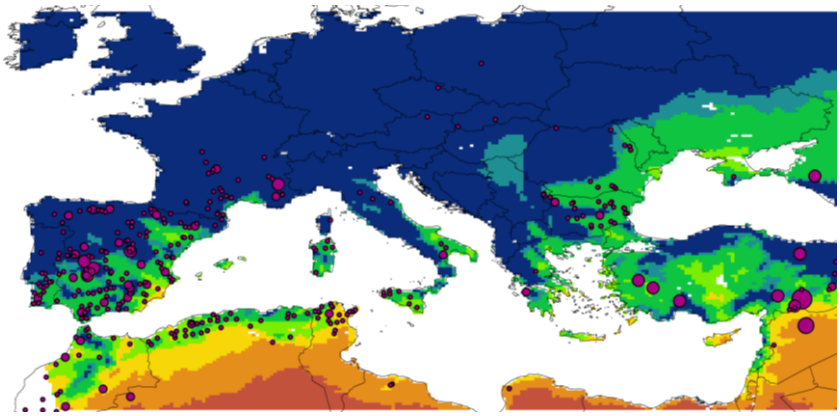

Fig. 186. Location and dimension of dams in Euro-Mediterranean regions selected through GranD database with irrigation as main use. Background colour shows aridity index in the future (2036-2065) under RCP 8.5.

3.2.5 Reservoirs upstream basin area and change of runoff flow in the reservoirs

The distribution of reservoir upstream basins areas, combined with present and future distribution of precipitation, were used to indicate changes in water inflow from the basins upstream of the reservoirs supplying water to irrigation. Such water inflow is estimated by the product of basin area, mean annual precipitation falling over the basin and a basin runoff coefficient.

3.2.5.1 Reservoirs upstream basin area

The reservoir upstream basin, i.e. the area collecting rainfall flowing into the reservoirs, was computed in ArcGIS software by using a digital elevation model (DEM). The DEM was developed by the SRTM (Shuttle Radar Topographic mission) and gap filled from CSI-CGIAR, and it is available globally at 90 meters resolution The procedure of calculating the watershed area over specific collector points, in our case the reservoirs, is available and used as part of the ESRI ARCGIS hydro-tools. Firstly, the original DEM input raster were gap-filled for Digital approximation of elevation, resulting in artifacts with no continuity in water flow with holes, where streamflow is collected without outflow. These are corrected with the FILL command using the minimum cell value from a weight raster along zone boundary. Secondly, the raster of flow direction for any specific cell to its steepest downslope neighbour was created using the FLOWDIRECTION command and the previously calculated filled DEM (Figure 187).

Fig.187. Scheme to obtain a flow direction raster (Flow_Dir) from DEM (Elev_Ras).

Then the flow direction grid is used to create a raster of flow accumulation, i.e. a raster counting the number of accumulated contributing pixels flowing into each cell.

Cell with undefined flow direction did not contribute to any downstream flow. Generally, the cells characterized by a high flowed accumulation were the ones located close to stream channels (Figure 188).

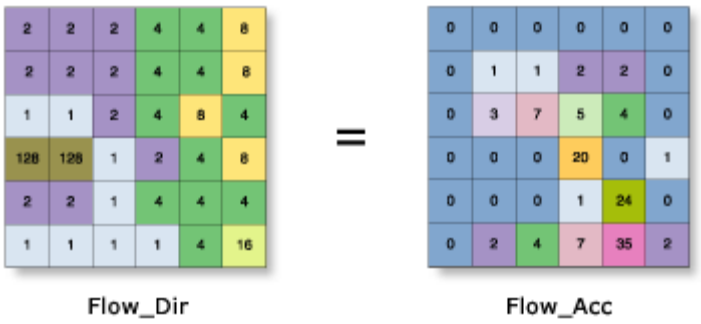

Fig.188. Scheme to obtain a flow accumulation raster (Flow_Acc) from Flow Direction raster (Flow_Dir).

Finally, the upstream catchment area was calculated as the contributed area above a set of cell in the raster, i.e. the reservoirs (Figure 189).

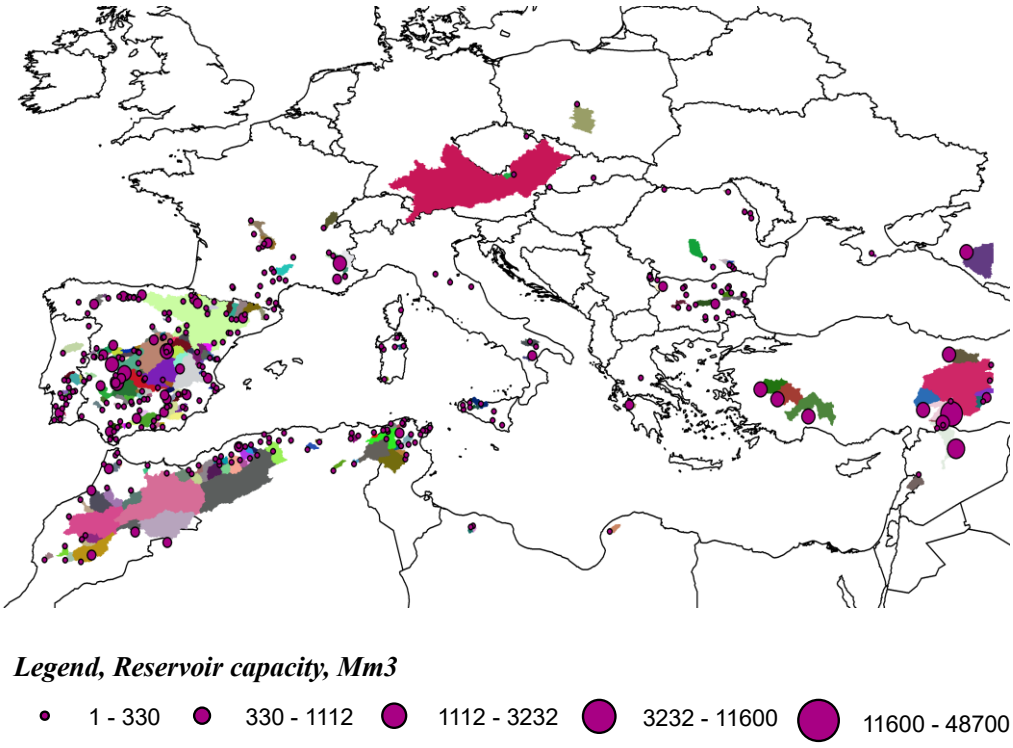

Fig.189. Map of reservoir upstream recharging basin, with plot size indicating maximum capacity of reservoirs.

3.2.6 Runoff coefficient

The runoff coefficient determines the relative amount of water falling on a catchment area that is converted into runoff, flowing through the stream network to the watershed outlet. It implicitly depends on specific environmental characteristics of the watershed, such as vegetation cover (i.e. distribution of vegetation types affecting evapotranspiration) and soil types (Table 51) (i.e. soil water holding capacity and infiltration rates, affecting soil water retention for vegetation use).

Tab.51. Description of the runoff classes as a function of soil type obtained by following the Soil Conservation Service Curve Number (SCS-CN) Methodology (Modified by Autorità di bacino regionale della Sardegna, https://www.regione.sardegna.it/documenti/1_470_20161129104147.pdf)

Low potential runoff	The soil of this group, when are fully saturated, have a low potential runoff, and high permeability. They are characterized by having less than 10% of clay and over 90% of sand and or gravel, and the texture is sandy or pebble. The hydraulic conductivity is greater than 14.4 cm/h throughout the depth. The horizon waterproof and shallow surface depth is greater than 50 cm and 60 cm, respectively. In addition, rocks with high permeability for fracturing or karstism belong to this group.
Moderately low potential runoff	The soils of this group, when fully saturated, have a moderately low potential runoff, and the water crosses the ground without any hindrance. They are characterized by having between 10% and 20% of clay and between 50 and 90% of sand, and the texture is sandy-frank, frank-sandy. The hydraulic conductivity changes between 3.6 and 14.4 cm/h throughout the depth. The depth of the waterproof horizon is greater than 50 cm, and the depth of the shallow surface is greater than 60 cm. In addition, rocks with medium-high and medium permeability for fracturing or karstism belong to this group.
Moderately high potential runoff	The soils of this group, when fully saturated, have a moderately high potential runoff, and the water crosses the ground with some limitation. They are characterized by having between 20% and 40% of clay and less than 50% of sand, and the texture is predominantly free, franco-limo, franco-clayey-sandy, franco-clayey, and franco-clay-lime. The hydraulic conductivity changes from 0.36 to 3.6 cm /h throughout the depth. The depth of the waterproof horizon is greater than 50 cm, and the depth of the shallow surface is greater than 60 cm. In addition, rocks with low and medium-low permeability for fracturing or karstism belong to this group.
High potential runoff	The soils of this group, when fully saturated, have a high potential runoff, and the water crosses the ground with strong limitation. They are characterized by having over 40% of clay and less than 50% of sand and the texture is clayey. The hydraulic conductivity is ≤ 0.36 cm /h throughout the depth. The depth of the waterproof horizon is between 50 cm and 100 cm, and the depth of the shallow surface is within 60 cm. In addition rocks with very low permeability, waterproof rocks, and unrecognized or unclassified areas belong to this group.

The runoff coefficient was computed as the ratio between the mean annual runoff and the mean annual precipitation values, both computed over the 1950 to 2000 period:

$$Rc = \frac{Total\ runoff}{Total\ precipitation} \quad \text{eq. 54}$$

Specifically, in this study the total runoff was obtained following Fekete et al. (2000), i.e. using a global composite runoff field dataset obtained through the combination of observed river discharge with simulated Water Balance. The gridded mean composite runoff field has a monthly time step and a final spatial resolution of 30 minutes.

Precipitation data were obtained from Willmott and Matsuura (2001) database, consistently with climate data used to generate the extrapolated composite runoff field. The proportion of annual runoff over annual precipitation over the historical period is shown in Figure 190. Runoff coefficient values range from 0 to 1, where low values (close to zero) are specific of permeable, flat and/or vegetated areas, reversely high values are found in areas with low infiltration, such as steep slope and pavement, (http://www.waterboards.ca.gov/water_issues/programs/swamp/docs/cwt/guidance/513.pdf).

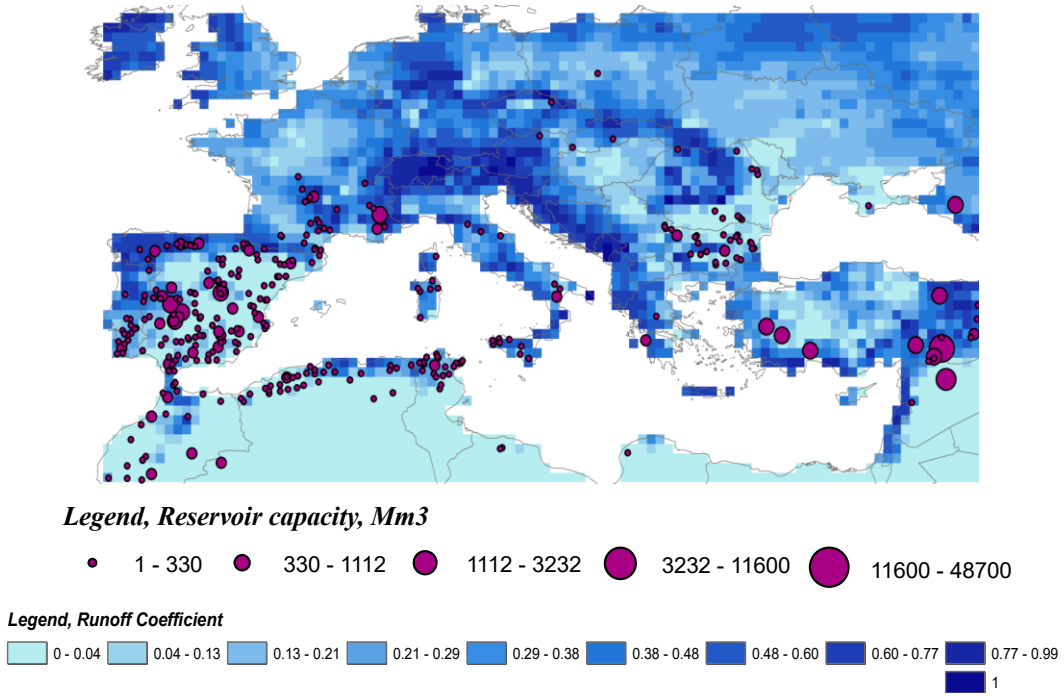

Fig. 190. Map of runoff coefficient obtained as the ratio of total runoff to total precipitation values with plot size indicating maximum capacity of reservoirs.

Values were validated by comparing measured and modelled data (Table 52). Observed data were obtained from the literature.

Tab. 52. Comparison of observed (Rc_obs) and simulated (Rc_mod) runoff coefficient in several Euro-Mediterranean reservoirs.

Basin	Country	Lon	Lat	Rc_obs	Rc_mod	Literature
Pedra'E Othoni	Italy	40.32	9.54	**0.40**	**0.46**	Mereu et al., 2016
Coghinas	Italy			**0.25**	**0.26**	RAS, 2002
Tirso	Italy	40.05	8.86	**0.18**	**0.42**	RAS, 2002
Flumendosa	Italy	39.43	9.61	**0.32**	**0.34**	RAS, 2002
Darlik	Turkey	41.06	29.35	**0.59**	**0.36**	Kadioglu and Sen., 2001
Alibaykou	Turkey	41.11	28.91	**0.40**	**0.36**	Kadioglu and Sen., 2001
Emarli	Turkey	41.07	29.11	**0.51**	**0.36**	Kadioglu and Sen., 2001
Omerli	Turkey	41.05	29.38	**0.45**	**0.36**	Kadioglu and Sen., 2001
Durusu	Turkey	41.30	28.67	**0.35**	**0.36**	Kadioglu and Sen., 2001

3.2.7 Irrigation requirements

The maize, grape, and wheat mean irrigation requirement (NA), previously estimated with the SIMETAW_GIS platform at Euro-Mediterranenean scale (Part 2), was used to assess the impact of climate change in the areas served by the dams under investigation for the baseline (1976-2005) and future (2036-2065) conditions, under RCP 4.5. Given its very high economic relevance (17.6 millions of tonnes in 2015 produced in Europe (Eurostat, 2017)), tomato was included in this study. Tomato was selected also as representative item for vegetable crops. Simulations of water application for this crop were run considering sowing and harvest date from literature (Appendix 2). Date were converted in Julian Days (JD) (Table 53) and used as an input in SIMETAW_GIS platform.

Tomato water requirement simulations were run for tomato cropping distribution with a resolution of 5 minutes (Monfreda et al. 2008).

The distribution of peaches reached 200,000 ha at European level, in 2012. This crop is considered the most important after apple and citrus with the largest production in Spain, Italy and Greece

(http://appsso.eurostat.ec.europa.eu/nui/show.do?dataset=orch_total&lang=en). In this contest, peaches (nectarines included) water requirement for the baseline and the future climate condition were computed. Simulation were run considering the same bud break and harvest date of grape, while the distribution area was obtained by Monfreda et al. (2008). Furthermore, simulations for peach are considered as representative for fruit trees representatives.

Tab. 53. Julian day referred to bud break and harvest dates for Tomato per Country.

Zone	Zone_Name	Sowing Julian day	Harvest Julian day
5	Algeria	196	334
7	Albania	121	243
26	Bosnia and Herzegovina	102	229
35	Bulgaria	127	258
66	Egypt	196	334
83	France	102	229
97	Greece	121	243
106	Croatia	102	229
107	Hungary	95	230
115	Israel	121	243
116	Italy	102	229
123	Jordan	15	120
136	Lebanon	121	243
148	Moldava	152	304
153	Macedonia	121	243
156	Morocco	196	334
163	Montenegro	121	243
189	Portugal	105	227
196	Romania	95	230
208	Slovenia	81	227
213	Spain	105	222
214	Serbia	102	229
220	Syria	46	166
231	Tunisia	196	334
232	Turkey	109	241

3.2.8 Irrigation systems vulnerability indicator:

The change in irrigation requirement and water inflow to the reservoir over its maximum capacity is computed in this work as:

$$\text{Vulnerability indicator (VI)} = \frac{\Delta Qinflow - \Delta Qirr}{Cap\ MCM} \qquad (Mm^3) \qquad \text{eq. 55}$$

where *ΔQinflow* is the change in water entering in the reservoir between future and baseline, *ΔQirr* is the change in water used for irrigation between future climate and baseline for a combination of representative crops, and Cap MCM is the dam capacity. For a greater cumulated water change for irrigation demand and reservoir water inflow, a greater stress is presented to irrigation system. Reservoirs with larger capacity are generally considered more resilient to adsorb (relatively) smaller water budget changes. High vulnerability index shows a high reservoir vulnerability to future climate changes, reversely low VI values show low vulnerability. Vulnerability tends to increase as a function of water deficit; where resilience is mostly related to storing capacity, but also to water use efficiency in the irrigation system and system management capacity.

3.3 RESULTS

Specific reservoirs with irrigation practice as main use are selected as case studies along the Euro-Mediterranean area. In this work, the vulnerability of irrigated agriculture systems is estimated for six reclamation consortia and associated reservoirs located in Italy, specifically four in Sardinia, one in Basilicata and one in Sicily (Table 54). Vulnerability is assessed by comparing estimates for the baseline (1976-2005) and the future period (2036-2065), under RCP 4.5 and 8.5.

The changes in reservoir water inflow as a function of annual precipitation, basin area, and runoff coefficient are reported for each basin in this section. Maize, wheat, grape, vegetable, and fruit trees irrigation requirements are estimated through SIMETAW_GIS platform. Tomato and peach are used as representative of vegetable and fruit trees in the Mediterranean basin. Water distribution volumes used to irrigate field in each consortium are computed considering both the cultivated area by crops and the crop irrigation requirement. Specifically, water distribution volumes of the abovementioned crops constitute a relatively majority of irrigated crop distribution, and are divided by the fraction of their distribution over the total irrigated area in the consortium to estimate the total irrigation abstraction for the baseline and the future scenarios. Reservoir capacity is crucial to determine the irrigation system vulnerability index under climate change condition for each case study. Values for future period are mostly driven by climatic changes over the basin draining on the reservoir and irrigated area in the reclamation consortium, and neglecting changes in runoff coefficient and crop distribution.

Tab. 54. Italian reservoirs selected as irrigation main use (Lehner et al., 2011).

River	Dam	Near city	Admistrative unit	Dam height (m)	Capacity (Mmc)	Elevation (mslm)	Longitude (dd)	Latitude (dd)
Liscia	Stretta di Calamaiu	Sassari	Sardinia	69	105.2	170	9.27	41.01
Cuga	Cuga	Sassari	Sardinia	53	31.7	101	8.45	40.61
Temo	Alto Temo	Sassari	Sardinia	58	95.7	242	8.56	40.47
Rio Palmas	Monte Pranu	Cagliari	Sardinia	55	62.0	42	8.59	39.09
Rosamarina	San Leonardo	Palermo	Sicily	93	100.0	153	13.64	37.95
San Giuliano	Bradano	Matera	Basilicata	79	107.0	100	16.53	40.60

3.3.1 Stretta di Calamaiu

Stretta di Calamaiu dam (170 m.s.l.m, 41.01 latitude, 9.27 longitude) is located in the municipality of Luras, in the Northern-Eastern part of Sardinia (Figure 191a) (ENAS, 2017). The dam was completed on the Liscia river in 1962, and it is mainly used for irrigation. The 57 km long river has its head water at 731 m.s.l.m. in the San Giorgio mountain, and it flows out into the Maddalena Arcipelago. Liscia's reservoir maximum storage capacity is equal to 105.2 Mm^3 (Lehner et al., 2011). It supplies water to the Gallura consortium, which includes seventeen municipalities: Aggius, Arzachena, Calangianus, la Maddalena, Luogosanto, Olbia, San'Antonio di Gallura, Telti, Trinità d'Agultu, Aglientu, Bortigiadas, Golfo Aranci, Loiri Porto San Paolo, Luras, Palau, Santa Teresa di Gallura, and Tempio Pausania (Figure 191b). Currently, the irrigation service is divided into two districts: Arzachena and Olbia. Liscia is the main irrigation water supply source in the consortium where the main irrigation systems are sprinkler (88%) and drip (12%) (CBGallura, 2017).

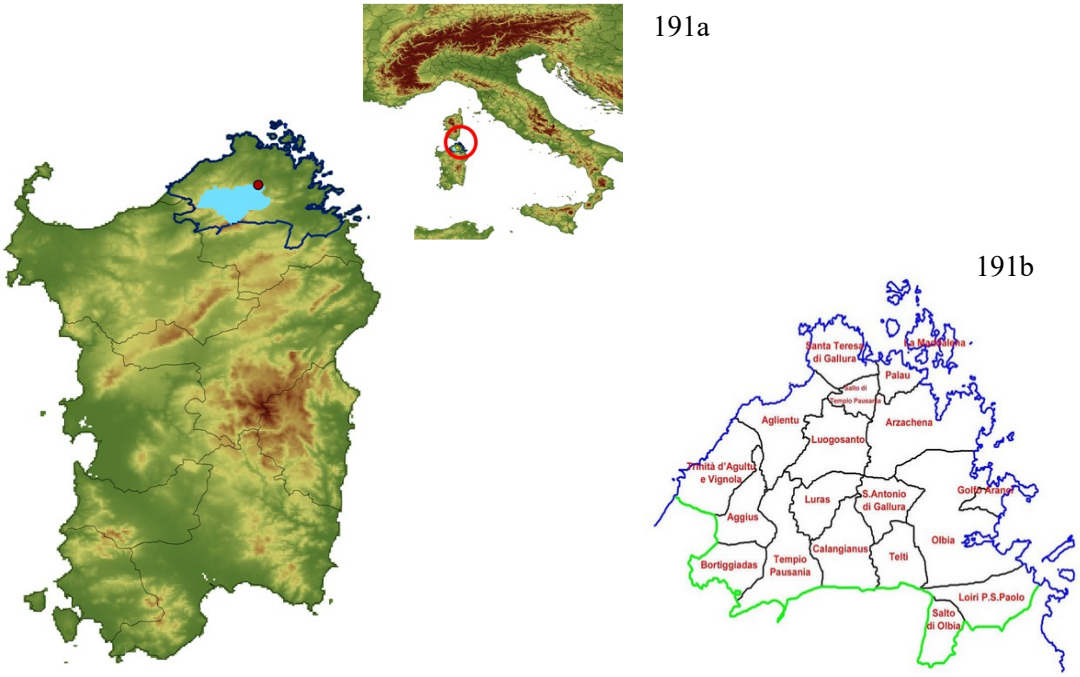

Fig. 191a. Reclamation consortium of Gallura (dark blue perimeter), and Stretta di Calamaiu dam (red point) and reservoir upstream watershed (light blue area). Fig.191b. Municipalities of the Gallura consortium (CBGallura, 2017).

- ***Reservoir water inflow***

The reservoir water volume depends on the effective precipitation. The average annual precipitation estimated in Liscia basin, upstream the reservoir, in the period 1976-2005 is 492 mm. The mean precipitation value is estimated to be lower for the future (2036-2065), and specifically 69 mm and 85 mm lower under RCP 4.5 and 8.5 emission scenarios, respectively. The water inflow for different periods and scenarios is computed by multiplying the basin average precipitation by the basin area (i.e. 339 km^2) and the runoff coefficient (i.e. 0.45). The mean annual inflow into the reservoir is reported in Table 55.

Tab. 55. Mean annual precipitation (mm yr^{-1}), basin area (km^2), runoff coefficient, and reservoir water inflow (Mm^3) in Liscia reservoir for the baseline (1976-2005) and future (2036-2065), under RCP 4.5 and 8.5 scenarios.

Basin annual precipitation			***Basin area***	***Runoff coefficient***	***Reservoir water inflow***		
baseline	**RCP 45**	**RCP 85**			**baseline**	**RCP 45**	**RCP 85**
mm	**mm**	**mm**	**km^2**		**Mm^3**	**Mm^3**	**Mm^3**
492	423	407	339	0.45	75.05	64.53	62.09

Water inflow into the reservoir in the intermediate future was about 10 Mm^3 lower under RCP 4.5 and about the 13 Mm^3 under RCP 8.5, compared to the baseline period, and this is due to the strong decrease in precipitation that was expected to characterize the basin for the future under both RCP.

The Aridity Index (AI) value indicated the Gallura consortium as a semi-arid area, with mean AI values that range from about 0.40 to 0.50. AI values are lower on average in the future (~ 0.43) than in the baseline (~ 0.49), and it highlights local future climate subject to increasing timing and frequency of drought events. According to Kosmas et al. (1999) the consortium is considered under desertification risk.

- ***Irrigation Water Demand (water outflow)***

Maize, wheat, grape, vegetables, and fruit trees all together account for the 36% of the total irrigated crop production (1402 ha) in the consortium of Gallura. Their total distribution is estimated equal to 501 hectares (ISTAT, 2010). Grape is the most

relevant irrigated crop in this area (327 ha), while the cultivation of the others crops together covered about 150 ha. The total crop irrigation requirement (IR, mm) tends to be about 215 mm and 212 mm higher in the intermediate future, respectively under RCP 4.5 and 8.5 scenarios. The highest mean IR values was computed for grape (~ 480-520 mm) and fruit trees (~ 600-660 mm). The total water volume used to satisfy crop water needs is abstracted from the reservoir, and their estimates for the baseline and future periods are shown in Table 56.

The total water demand for irrigated area is higher in the future than in the baseline, and considering the total irrigated area in the Gallura consortium the crop water demand is expected to be about 0.52 Mm^3 higher under both RCPs. The difference between the two scenarios is negligible (0.02).

Tab. 56. Irrigation requirement (mm yr^{-1}), cultivated area (ha), and water abstraction (Mm^3) for maize, grape, wheat, vegetable, fruit trees, and adjusted total irrigation volumes for all cultivated crops (i.e. total irrigated area) in Gallura consortium. Values are shown for the baseline and future period, under RCP 4.5 and 8.5 scenarios.

Crop	***Irrigation requirement***			***Cultivated area***	***Irrigation Water volumes***		
	baseline	**RCP 4.5**	**RCP 8.5**		**baseline**	**RCP 4.5**	**RCP 8.5**
	mm	**mm**	**mm**	**ha**	**Mm^3**	**Mm^3**	**Mm^3**
Maize	432	470	470	25	0.11	0.12	0.12
Grape	479	522	521	327	1.57	1.71	1.70
Fruit trees	606	663	659	12	0.07	0.08	0.08
Vegetables	410	452	452	84	0.34	0.38	0.38
Wheat	290	335	327	53	0.15	0.18	0.17
Total				**501**	**2.25**	**2.46**	**2.45**
Total Irrigated Area				**1402**	**5.77**	**6.30**	**6.28**

- ***Vulnerability Index***

The index of vulnerability (VI) was computed considering the simultaneous changes in both total reservoir water inflow and outflow for irrigation between baseline and future climate conditions as showed in Table 57, i.e. the effective precipitation

entering (Mm^3) into the Liscia reservoir and the total amount of water used to irrigate the crop fields (Mm^3) located in the Gallura consortium.

Tab. 57. Differences of annual water inflow, outflow, and Cumulated Water Shortage between baseline (1976-2005) and future (2036-2065) scenarios, under RCP 4.5 and 8.5, and Index of Vulnerability, in Liscia reservoir.

	RCP 4.5-baseline **Mm^3**	**RCP 8.5-baseline** **Mm^3**
Δ Inflow	-10.53	-12.97
Δ Outflow	0.53	0.51
Cumulated Water Shortage (Δ Inflow + Δ Outflow)	-10.86	-13.29
Vulnerability Index (Cumulated Water Shortage / Reservoir Maximum Capacity)	-0.10	-0.13

The total water entering into the reservoir tends to be lower in the future than in the baseline, and the strongest decrease was computed equal to 12.97 Mm^3 under RCP 8.5 scenario. At the same time, the total crop water demand in the consortium is higher in the future reaching values closed to about 0.52 Mm^3 under both scenarios. The cumulated water shortage due to climate change from variations in basin inflow and outflow for irrigation in the reservoir was expected to account to 11-13 Mm^3, and the most relevant impact was found under RCP 8.5 scenario. In this context, the irrigated agriculture in the Gallura consortium was considered partially vulnerable to climate change with vulnerability index (VI) values ranging from -0.10 to -0.13. The value is higher under RCP 8.5 than 4.5, and this is mostly related to the lowest mean precipitation value (407 mm), which characterizes the basin under the worst scenario. Thus, the risk of reservoir vulnerability was higher under RCP 8.5. Despite the water inflow tended to decrease under both scenarios, and water outflow to increase, the Liscia reservoir was considered rather resilient under global warming because the large reservoir capacity together with water entering the reservoir compensate the largely increasing crop water requirements.

3.3.2 Cuga and Alto Temo

The Nurra consortium was created in 1963, and it is located in the Northern–Western part of Sardinia region in the Provence of Sassari (Figure 192a). One of the main reservoir system developed by this consortium is the Temo-Cuga system, i.e. a great complex mostly used for irrigation which serves about 3000 users, and about 25000 hectares. The Temo river is about 55 km long, and it is the only river navigable in Sardinia for about 6 km. The dam was built in the period 1971-1984. Its head water is at 473 m.s.l.m. on the Monte Calarighe in the Province of Sassari. The Temo lake is a reservoir created by the dam on the homonymous river located in the Monteleone Rocca Doria municipality (242 m.s.l.m, 40.47 latitude, 8.56 longitude) (Lehner et al., 2011; ENAS, 2017). The Alto Temo reservoir has a water capacity of 95.5 Mm^3 (Lehner et al., 2011). In the same consortium, the Cuga dam was built from 1956 to 1974 in the Uri municipality (101 m.s.l.m, 40.61 latitude, 8.45 longitude) (Lehner et al., 2011; ENAS, 2017). The Cuga reservoir water capacity is 63.8 Mm^3, about two thirds lower than the previous reservoir. Alto Temo and Cuga dams are both used mainly for irrigation purposes (Lehner et al., 2011). They supply water for five municipalities in this consortium: Sassari, Alghero, Porto Torres, Olmedo, Stintino, and Uri CBNurra, 2017 (Figure 192b).

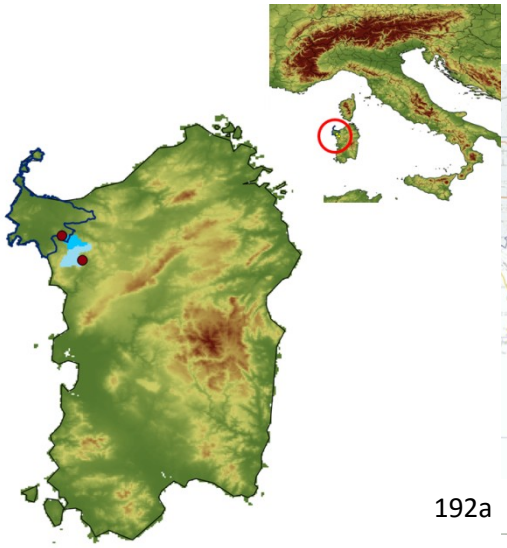

192a

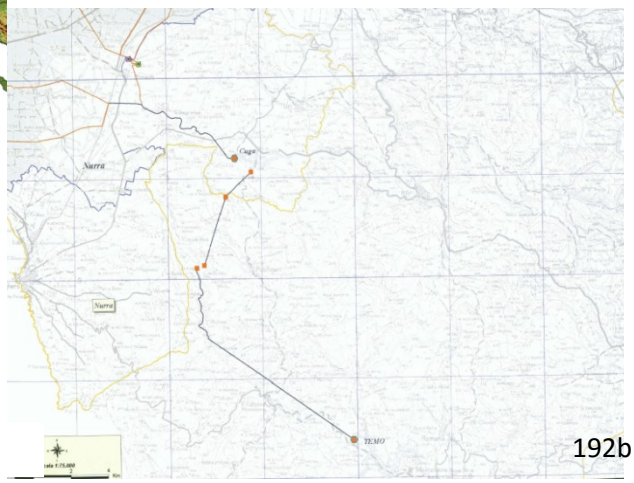

192b

Fig. 192a. Reclamation consortium of Nurra (dark blue perimeter), and Cuga and Alto Temo dams (red points) and reservoir upstream watersheds (light blue areas). Fig.192b. The Temo-Cuga system (CBNurra 2017).

- ***Reservoir water inflow***

The mean precipitation is higher for the Alto-Temo upstream watershed than for Cuga in both baseline and future period. However, differences between future and baseline values are almost double in the Cuga than in Alto-Temo watersheds. The highest difference (- 43 mm) is computed under RCP 4.5 for the Cuga reservoir, while the Alto Temo upstream watershed is projected to witness small changes in precipitation. Since both dams contribute to supply water for irrigation practice, the total water inflow is cumulated for the whole Cuga-Alto Temo system, considering for both watersheds (total area equal to 197 km^2) a runoff coefficient of 0.42 (Table 58).

Tab. 58. Mean annual precipitation (mm yr^{-1}), basin area (km^2), runoff coefficient, and reservoir water inflow (Mm^3) for both Cuga and Alto Temo reservoirs, and cumulated (Cuga-Alto Temo system) for the baseline (1976-2005) and future (2036-2065), under RCP 4.5 and 8.5 scenarios.

	Basin annual precipitation			***Basin area***	***Runoff coefficient***	***Reservoir water inflow***		
	baseline	**RCP 4.5**	**RCP 8.5**			**baseline**	**RCP 4.5**	**RCP 8.5**
	mm	**mm**	**mm**	**km^2**		**Mm^3**	**Mm^3**	**Mm^3**
Cuga	436	393	412	73	0.42	13.37	12.05	12.63
Alto Temo	476	447	464	124	0.42	24.82	23.28	24.17
Cuga-Alto Temo system				197	0.42	38.18	35.33	36.80

The largest water inflow is estimated for the Alto-Temo reservoir because of the more abundant precipitation and the largest catchment area under investigation. The total mean water inflow in Cuga-Alto Temo system is equal to 38.18 Mm^3 in the baseline, which is projected to decrease by 2.85 Mm^3 and 1.38 Mm^3 under climate change condition, for RCP 4.5 and 8.5 emission scenarios, respectively.

The patterns of total precipitation, together with total reference evapotranspiration characterized the Nurra consortium climate as semi-arid with a range of aridity index from about 0.35 to 0.50, thus this area is considered under desertification risk (Kosmas et al., 1999).

- ***Irrigation Water Demand (water outflow)***

The 55% of the total irrigated crops cultivated in the Nurra consortium (total irrigated area) is composed by maize, wheat, vegetables, grapes, and fruit trees. According to ISTAT (2010) the five crops together covered an area of 2591 ha. Grape, vegetable, and maize are the most abundant crops cultivated in that area. Irrigation requirement (IR) of each crop is always higher for the future under climate change. In line with IR, also the irrigation total water volumes are higher for the intermediate future, and it is expected that in the period 2036-2065 the total water amount used to satisfy crop water needs for the total irrigated area in the Nurra will be about 1.7 Mm^3 higher than for the period 1975-2005 (Table 59).

Tab. 59. Irrigation requirement (mm yr^{-1}), cultivated area (ha), and water abstraction (Mm^3) for maize, grape, wheat, vegetables, fruit trees, and adjusted to total irrigation volumes for all crops cultivated (i.e. total irrigated area) in Nurra consortium. Values are shown for the baseline and future period, under RCP 4.5 and 8.5 scenarios.

Crop	***Irrigation requirement***			***Cultivated area***	***Irrigation Water volumes***		
	baseline	**RCP 4.5**	**RPC 8.5**		**baseline**	**RCP 4.5**	**RCP 8.5**
	mm	**mm**	**mm**	**ha**	**Mm^3**	**Mm^3**	**Mm^3**
Maize	409	446	447	466	1.91	2.08	2.08
Grape	469	506	507	1160	5.44	5.87	5.88
Fruit trees	577	630	630	66	0.38	0.42	0.42
Vegetables	392	429	426	697	2.73	2.99	2.97
Wheat	287	322	318	202	0.58	0.65	0.64
Total				**2591**	**11.04**	**12.01**	**11.99**
Total Irrigated Area				**4704**	**20.07**	**21.84**	**21.80**

- ***Vulnerability index***

In the Alto Temo catchment area, the mean annual runoff/streamflow entering into the reservoir is expected to be 1.54 Mm^3 lower under RCP 8.5 than for the baseline. Likewise, the water requirements for irrigated areas in the Nurra consortium is expected to increase in the future under both RCP (~ 1.75 Mm^3).

The vulnerability of this irrigated agriculture system is estimated to be higher under RCP 4.5. It is worth noticing that even if both basins are characterized by almost the same changes in inflow and outflow values, the impact of climate change is more evident in Cuga reservoir, and this is due to its lower dam capacity. A future water deficit condition is expected to characterize the Cuga-Alto Temo irrigation system, with an impact on irrigated agriculture under climate change. The system is in fact estimated to store (or to accumulate) a water shortage in the intermediate future of about 6 Mm^3 less than in the baseline. In this context, the system is considered vulnerable to climate change, and its resilience to changes in the period 2036-2065 is shown to be lower under RCP 4.5 than 8.5 (Table 60).

Tab. 60. Differences of annual water inflow, outflow, and Cumulated Water Shortage between baseline (1976-2005) and future (2036-2065) scenarios, under RCP 4.5 and 8.5, and Index of Vulnerability, in Cuga-Alto Temo system.

		RCP 4.5-baseline Mm^3	**RCP 8.5-baseline Mm^3**
Cuga	Δ Inflow	-1.32	-0.74
	Δ Outflow	1.76	1.73
	Cumulated Water Shortage (Δ Inflow + Δ Outflow)	-3.08	-2.46
	Vulnerability Index (Cumulated Water Shortage / Reservoir Maximum Capacity)	-0.10	-0.08
Alto Temo	Δ Inflow	-1.54	-0.65
	Δ Outflow	1.76	1.73
	Cumulated Water Shortage (Δ Inflow + Δ Outflow)	-3.30	-2.38
	Vulnerability Index (Cumulated Water Shortage / Reservoir Maximum Capacity)	-0.03	-0.02
Cuga Alto Temo system	Δ Inflow	-2.86	-1.39
	Δ Outflow	3.52	3.46
	Cumulated Water Shortage (Δ Inflow + Δ Outflow)	-6.38	-4.84
	Vulnerability Index (Cumulated Water Shortage / Reservoir Maximum Capacity)	-0.13	-0.10

3.3.3 Monte Pranu

Monte Pranu dam (42 m.s.l.m., 39.09 latitude, 8.59 longitude) was built between 1947 and 1951 on the Palmas river (Figure 193a) (Lehner et al., 2011) in Tratalias municipality, in the province of Carbonia-Iglesias, in the South of Sardinia (ENAS, 2017). The dam is owned by the Sardinia Autonomous Region and with a maximum capacity of 62 Mm^3. It mainly supplies water for irrigation. The reservoir specifically serves irrigation requirements of six municipalities: Tratalias, San Giovanni Suergiu, Giba, Masainos, and Sant'Anna Arresi. Specifically, the Basso Sulcis irrigation district is divided into two others sub-districts limited by the Palmas river (Figure 193b). The one located on the right side of the river serves Tratalias and San Giovanni Suergiu, while the one on the left side serves all the others municipalities.

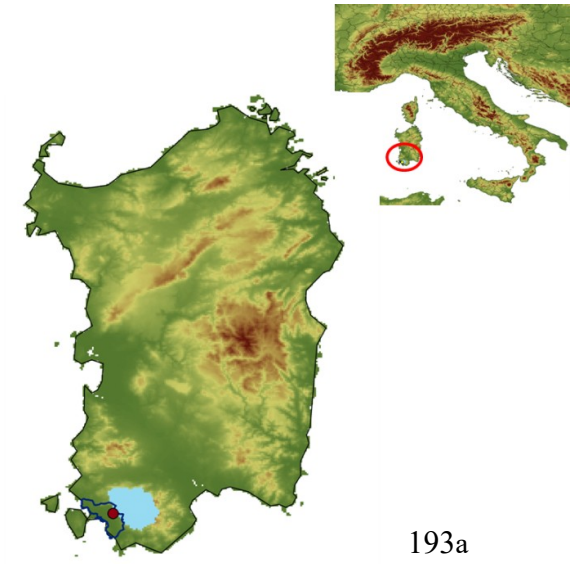

193a

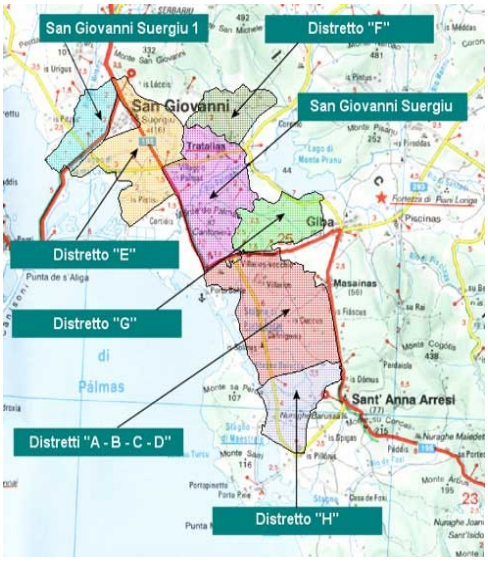

193b

Fig. 193a. Reclamation consortium of the Basso Sulcis (dark blue perimeter), and Monte Pranu dam (red point) and reservoir upstream watershed (light blue area). Fig. 193b. Scheme of the irrigation sub-districts in the Basso Sulcis district (CBBasso-Sulcis).

- ***Reservoir water inflow***

The mean precipitation over the upstream watershed is expected to decrease by 29 mm and 60 mm in the future under RCP 4.5 and RCP 8.5, respectively. The upstream basin area is equal to 420 km^2 and the runoff coefficient for the basin 0.32. The mean total precipitation entering on the watershed and runoff to reservoir, assuming no change in runoff coefficient for future, tends to decrease for future climate conditions, compared to baseline (Table 61).

Tab. 61. Mean annual precipitation (mm yr^{-1}), basin area (km^2), runoff coefficient, and reservoir water inflow (Mm^3) in Monte Pranu reservoir for the baseline (1976-2005) and future (2036-2065), under RCP 4.5 and 8.5 scenarios.

Basin annual precipitation			***Basin area***	***Runoff coefficient***	***Reservoir water inflow***		
baseline	**RCP 4.5**	**RCP 8.5**			**baseline**	**RCP 4.5**	**RCP 8.5**
mm	**mm**	**mm**	**km^2**		**Mm^3**	**Mm^3**	**Mm^3**
378	349	318	420	0.32	50.80	46.90	42.73

In line with the precipitation trend, also the water inflow to reservoir under future climate condition is lower, and differences between future and baseline are almost double under RCP 8.5 than under RCP 4.5.

The ratio of annual precipitation over annual reference evapotranspiration (AI) ranges from 0.40 to 0.36 in Basso Sulcis consortium, thus the area under investigation is considered under desertification risk (Kosmas et al., 1999).

- ***Irrigation Water Demand (water outflow)***

The percentage of maize, wheat, vegetable, grape, and fruit trees accounts for the 82% of the total irrigated crop area in the Basso Sulcis consortium. The main crops produced are vegetables, followed by wheat and grape. A limited distribution was estimated by ISTAT (2010) for fruit trees (5.7 ha) and maize (12.2 ha). The irrigation requirements (IR) of these two crops are affected by climate change here more than for the others study sites. Maize and fruit trees IR are in fact about 60 mm higher under both RCPs. Assuming no future changes in crop distribution, compared to baseline, the annual reservoir water outflow to irrigate agriculture areas in this

consortium tends to increase under both scenarios. In the intermediate future the water amount required to irrigate the entire area is expected to be about 0.5 Mm^3 higher than in the period 1976-2005 (Table 62).

Tab. 62. Irrigation requirement (mm yr^{-1}), cultivated area (ha), and water abstraction (Mm^3) for maize, grape, wheat, vegetables, fruit trees, and adjusted to total irrigation volumes for all cultivated crops (i.e. total irrigated area) in Basso Sulcis consortium. Values are shown for the baseline and future period, under RCP 4.5 and 8.5 scenarios.

Crop	***Irrigation requirement***			***Cultivated area***	***Irrigation Water volumes***		
	baseline	**RCP 4.5**	**RPC 8.5**		**baseline**	**RCP 4.5**	**RPC 8.5**
	mm	**mm**	**mm**	**ha**	**Mm^3**	**Mm^3**	**Mm^3**
Maize	454	519	514	12.2	0.06	0.06	0.06
Grape	486	528	521.5	96.66	0.47	0.51	0.5
Fruit trees	605	666.5	658.5	5.72	0.03	0.04	0.04
Vegetables	413.5	452.5	447	911.9	3.77	4.13	4.08
Wheat	257	303	261	104.69	0.27	0.32	0.27
Total				**1131.17**	**4.60**	**5.06**	**4.95**
Total irrigated Area				**1382**	**5.62**	**6.18**	**6.05**

- ***Vulnerability index***

Differences in annual water storage between future and baseline are estimated equal to -4.47 Mm^3 under RCP4.5 and -8.49 Mm^3 under RCP 8.5. The consortium is expected to undergone a water deficit in future that is more relevant under the worst scenario. The reservoir is more vulnerable to climate change under RCP 8.5 (VI = -0.14) than under RCP 4.5 (VI = -0.07) scenarios (Table 63). Considering precipitation the only water inflow source for the basin, the system is expected to be water stressed under future changes. The capacity (62 Mm^3) of Monte Pranu reservoir strongly contributes to reduce the resilience of the dam to global warming. The reservoir, thus the irrigated agriculture in Basso Sulcis consortium, is under vulnerable risk, but it is still resilient (Table 63).

Tab.63. Differences of annual water inflow, outflow, and Cumulated Water Shortage between baseline (1976-2005) and future (2036-2065) scenarios, under RCP 4.5 and 8.5, and Index of Vulnerability, in Monte Pranu reservoir.

	RCP 4.5-baseline	**RCP 8.5-baseline**
	Mm^3	**Mm^3**
Δ Inflow	-3.90	-8.06
Δ Outflow	0.56	0.43
Cumulated Water Shortage (Δ Inflow + Δ Outflow)	-4.46	-8.49
Vulnerability Index (Cumulated Water Shortage / Reservoir Maximum Capacity)	-0.07	-0.14

3.3.4 Rosamarina

Rosamarina dam (153 m.s.l.m, 37.95° latitude, 13.64° longitude) is located in the province of Palermo, in the Northern-Western part of Sicily (Lehner et al., 2011) (Figure 194). The dam was built on the San Leonardo river between 1972 and 1992, and it is used mainly to provide water for irrigation in the Palermo 2 consortium. The reservoir capacity is 100 Mm^3 (Lehner et al., 2011). The municipalities served by Rosamarina for irrigation requirements are: Palermo, Caccamo, Termini Imerese, Trabia, Altavilla, Casteldaccia, Villabate, Santa Flavia, Misilmeri, Bagheria, Ficarazzi, Sciara, Cerda, Collesano, Campofelice e Lascari, (http://adpaloha.altervista.org/wp-content/uploads/2012/10/ROSAMARINA.pdf).

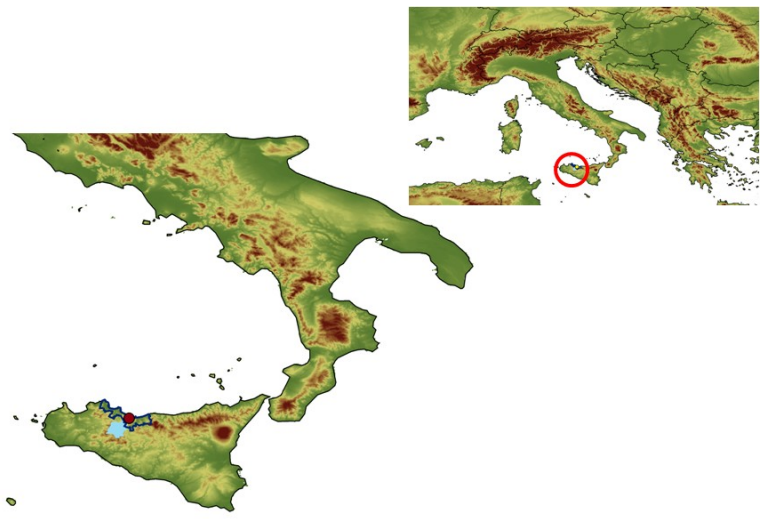

Fig. 194. Reclamation consortium of the Palermo 2 (dark blue perimeter), and Rosamarina dam (red point) and reservoir upstream watershed (light blue area).

- ***Reservoir water inflow***

Mean annual precipitation in Rosamarina reservoir watershed is projected to decrease by 36 mm/yr and 62 mm/yr for future scenarios RCP 4.5 and 8.5, respectively, compared to the baseline. Precipitation, upstream basin area, and runoff coefficient determine the total volume of water inflow to the reservoir that, in line with future reductions of total precipitation, may expect a decrease of 10 and 16 Mm^3 in the intermediate future, from total water inflow volumes of 102 Mm^3 for the period 1976-2005 (Table 64).

Tab. 64. Mean annual precipitation (mm yr^{-1}), basin area (km^2), runoff coefficient and water inflow in Rosamarina reservoir for the baseline (1976-2005) and future (2036-2065), under RCP 4.5 and 8.5 scenarios.

Basin annual precipitation			***Basin area***	***Runoff coefficient***	***Reservoir water inflow***		
baseline	**RCP 4.5**	**RCP 8.5**			**baseline**	**RCP 4.5**	**RCP 8.5**
mm	**mm**	**mm**	**km^2**		Mm^3	Mm^3	Mm^3
386	350	324	529	0.5	102	93	86

The Aridity Index (AI) value estimated in Palermo 2 consortium indicated the area as semi-arid, with mean values that range from about 0.33 to 0.43, thus following Kosmas et al. (1999) the area is defined under desertification risk.

- ***Irrigation Water Demand (water outflow)***

Maize, wheat, vegetables, grape, and fruit trees cover the 29% of the total distribution of irrigated area (1125 ha; ISTAT, 2010) in the consortium. Vegetables are the irrigated crops type predominant in this area, followed by fruit trees (Table 65). The total water volume used for the whole irrigated area in the consortium tends to be 0.88 Mm^3 and 0.95 Mm^3 higher under RCP 4.5 and 8.5, respectively (Table 66).

Tab. 65. Irrigation requirement (mm yr^{-1}), cultivated area (ha), and water abstraction (Mm^3) for maize, grape, wheat, vegetables, fruit trees, and adjusted to total irrigation volumes for all cultivated crops (i.e. total irrigated area) in Palermo 2 consortium. Values are shown for the baseline and future period, under RCP 4.5 and 8.5 scenarios.

Crop	***Irrigation requirement***			***Cultivated area***	***Irrigation Water volumes***		
	baseline	**RCP 4.5**	**RPC 8.5**		**baseline**	**RCP 4.5**	**RPC 8.5**
	mm	**mm**	**mm**	**ha**	**Mm^3**	**Mm^3**	**Mm^3**
Maize	422	439	448	0.05	0.0002	0.0002	0.0002
Grape	493	515	521	49.49	0.24	0.25	0.26
Fruit trees	602	631	640	130.39	0.78	0.82	0.83
Vegetables	410	432	432	909.90	3.73	3.93	3.93
Wheat	310	329	340	35.31	0.11	0.12	0.12
Total				**1125.14**	**4.87**	**5.12**	**5.14**
Total irrigated Area				**3825.74**	**16.79**	**17.67**	**17.73**

- ***Vulnerability Index***

The largest reduction of water inflow to the reservoir is estimated under RCP 8.5 (-16 Mm^3) for the period 2036-2065. Over the same period, and under the same emission scenario, the whole irrigated area in the consortium will require about 0.95 Mm^3 more than in the baseline. In this context, the reservoir is considered vulnerable to future change, thus the irrigated system is under risk of water deficit. Vulnerability of Rosamarina irrigation system is lower under RCP 4.5, where relatively higher precipitation are projected, with extremely high value of vulnerability for RCP 8.5 (Table 66).

Tab. 66. Differences of annual water inflow, outflow, and Cumulated Water Shortage between baseline (1976-2005) and future (2036-2065) under RCP 4.5 and 8.5, and Index of Vulnerability, in Rosamarina reservoir.

	RCP 4.5-baseline	**RCP 8.5-baseline**
	Mm^3	**Mm^3**
Δ Inflow	-9.52	-16.4
Δ Outflow	0.88	0.95
Cumulated Water Shortage (Δ Inflow + Δ Outflow)	-8.64	-15.45
Vulnerability Index (Cumulated Water Shortage / Reservoir Maximum Capacity)	-0.086	-0.15

3.3.5 San Giuliano

San Giuliano dam (100 m.s.l.m, 41.60° latitude, 16.53° longitude) is located in the province of Matera, in Basilicata region, in the Southern of Italy (Figure 195a) (Lehner et al., 2011). The massive infrastructure was built in the period 1950-1958 (http://www.bradanometaponto.it/SanGiuliano.html). The dam was created on the Bradano river, which is about 120 km long, and managed by the Basin Authority of Basilicata (Figure 195b) (Basilicata, 2017). San Giuliano's reservoir water storage capacity is equal to 107 Mm^3 (Lehner et al., 2011). It supplies water to the Bradano-Metaponto consortium, i.e. to the 31 municipalities of Matera Provence: Accettura, Aliano, Bernalda, Calciano, Cirigliano, Colobraro, Craco Ferrandina, Garaguso, Gorgoglione, Grassano, Grottole, Irsina, Matera, Miglionico, Montalbano Jonico, Montescaglioso, Nova Siri, Oliveto Lucano, Pisticci, Policoro, Pomarico, Rotondella, Salandra, San Giorgio Lucano, San Mauro Forte, Scanzano Jonico, Stigliano, Tricarico, Tursi e Valsinni
(http://www.bradanometaponto.it/PianoClassifica.html).

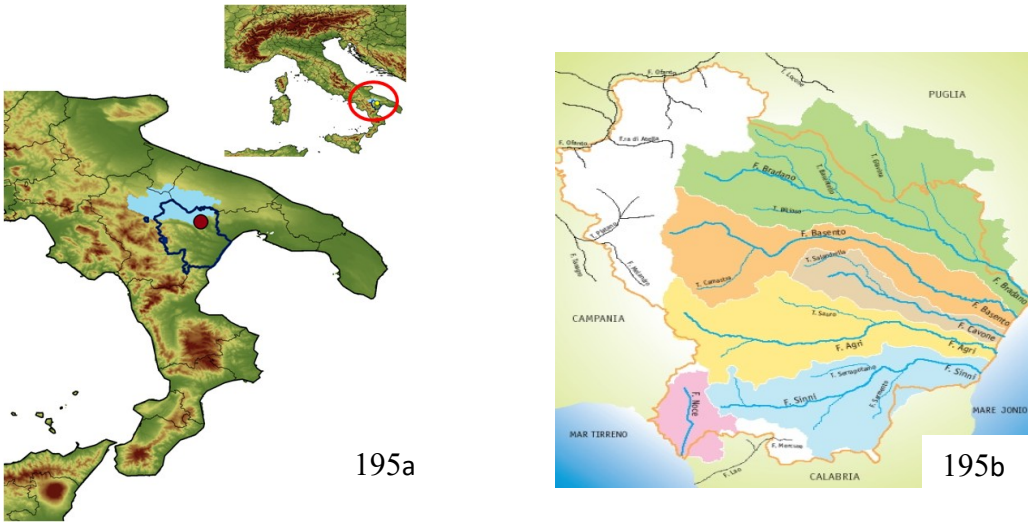

Fig. 195a. Reclamation consortium of Bradano-Metaponto (dark blue perimeter), and San Giuliano dam (red point) and reservoir upstream watershed (light blue area). Fig. 195b. Hydrografic basins in Basilicata region (Basilicata, 2017).

- ***Reservoir water inflow***

A great reduction of the mean annual precipitation is estimated under future climate condition in San Giuliano upstream watershed (69 mm and 96 mm lower under RCP 4.5 and 8.5, respectively). The consortium area and the runoff coefficient are estimated equal to 2490 km^2 and 0.35, respectively. The product of all these variables for the baseline and future climate define a reduction of the mean total water inflow to the reservoir equal to about 60 Mm^3 and 83 Mm^3, under RCP 4.5 and 8.5, respectively in the basin under study. A difference of about 23 Mm^3 is estimated between the two RCP scenarios (Table 67).

Tab. 67. Mean annual precipitation (mm yr^{-1}), basin area (km^2), runoff coefficient, and water inflow (Mm^3) in San Giuliano reservoir for the baseline (1976-2005) and future (2036-2065) under RCP 4.5 and 8.5 scenarios.

Basin annual precipitation			***Basin area***	***Runoff coefficient***	***Reservoir water inflow***		
baseline	**RCP 4.5**	**RCP 8.5**			**baseline**	**RCP 4.5**	**RCP 8.5**
mm	**mm**	**mm**	**km^2**		**Mm^3**	**Mm^3**	**Mm^3**
448	379	352	2490	0.35	390.43	330.30	306.77

The consortium is characterized by an aridity index value which ranges from 0.30 to 0.50, thus following Kosmas et al. (1999) the Bradano-Metaponto is defined as an area under desertification risk.

- ***Irrigation Water Demand (water outflow)***

The highest seasonal irrigation requirements (IR) are estimated for fruit trees and grape under RCP 8.5. The seasonal IR of maize, grape, vegetables, wheat, and fruit trees (56% of the total crop distribution) is estimated to be larger in the future under both RCP scenarios. The total hectares cultivated with the representative crops under study are 14188, over a total irrigated area for the consortium of 25202 ha (ISTAT, 2010). The water outflow computed considering the total crop distribution in the consortium shows an increased value of 4.26 Mm^3 in future under RCP 4.5 and a value about 11 Mm^3 higher under RCP 8.5 (Table 68).

Tab. 68. Irrigation requirement (mm yr^{-1}), cultivated area (ha), and water abstraction (Mm^3) for maize, grape, wheat, vegetables, fruit trees, and all the other crops cultivated in Bradano-Metaponto consortium. Values are shown for the baseline and future period, under RCP 4.5 and 8.5 scenarios.

Crop	***Irrigation requirement***			***Cultivated area***	***Irrigation Water volumes***		
	baseline	**RCP 4.5**	**RPC 8.5**		**baseline**	**RCP 4.5**	**RPC 8.5**
	mm	**mm**	**mm**	**ha**	**Mm^3**	**Mm^3**	**Mm^3**
Maize	466	493	500	392	1.83	1.93	1.96
Grape	505	544	549	1368	6.9	7.44	7.51
Fruit trees	665	665	707	8075	53.7	53.7	57.09
Vegetables	438	480	485	2704	11.84	12.98	13.11
Wheat	313	350	354	1649	5.16	5.77	5.84
Total				**14188**	**79.43**	**81.82**	**85.51**
Total irrigated Area				**25202**	**141.83**	**146.10**	**152.69**

- ***Vulnerability index***

The largest reduction of the total water volume entering into the reservoir is observed under RCP 8.5, where the water volume decreases by -83.67 Mm^3 compared to volumes of the baseline. This is explained by the relevant precipitation reduction (-96 mm) under the worst scenario. In turn, the total water outflow to supply irrigated area in the Bradano-Metaponto consortium is expected to increase of about 11 Mm^3, under RCP 8.5, in respect to the baseline. The cumulated water deficit in future climate for the reservoir is expected to be ~ 31 Mm^3 and 50 Mm^3 lower than in the baseline. Taking into account the dam capacity, the vulnerability of the irrigated agriculture is extremely high under RCP 8.5 (-0.46). A difference in vulnerability index of about 0.16 is in fact computed between the two scenarios (Table 69). Lastly, despite the increasing crop water demand and the decreasing water stored in the basins under future climate conditions, the San Giuliano reservoir is stated to be vulnerable to climate change but resilient under both scenarios; precipitation values are in fact enough to guarantee water for the dam main purpose.

Tab. 69. Differences of annual water inflow, outflow, and Cumulated Water Shortage between baseline (1976-2005) and future (2036-2065) under RCP 4.5 and 8.5, and Index of Vulnerability, in San Giuliano reservoir.

	RCP 4.5-baseline Mm^3	**RCP 8.5-baseline** Mm^3
Δ Inflow	-27.49	-38.25
Δ Outflow	4.27	10.86
Cumulated Water Shortage (Δ Inflow + Δ Outflow)	-31.76	-49.10
Vulnerability Index (Cumulated Water Shortage / Reservoir Maximum Capacity)	-0.30	-0.46

3.4 DISCUSSIONS AND CONCLUSIONS

The irrigated agriculture vulnerability under climate change conditions is assessed for five consortia located in the Mediterranean basin, and served by reservoirs whose main use is for irrigation.

The lowest precipitation values are accounted for in Monte Pranu and Rosamarina where the mean values considering both RCPs are 334 and 337 mm, respectively. The mean annual inflow into San Giuliano basin is the greatest, even if values tend to decrease under future climate of about 60 mm under RCP 4.5 and 84 mm under RCP 8.5. Compared to the other case studies, the water amount entering in this reservoir is larger because of the size of the basin (2490 km^2). Despite Rosamarina and Monte Pranu basins are characterized by almost the same area and precipitation values, the highest reservoir water inflow is estimated in Rosamarina, and this is due to the size (109 km^2 bigger than Monte Pranu), but mainly to the runoff coefficient which is 0.18 higher. The runoff coefficient and the basin area play a key role also in Stretta di Calamaiu basin where water inflow is higher than in Monte Pranu both in the baseline and in the intermediate future. In this case, the lowest precipitation estimated in the Basso Sulcis may be related to the climate which is known to be drier in the South than in the Northern of Sardinia. Changes in future effective precipitation are almost negligible in Cuga and Alto Temo where, in the future, the water reduction is expected to be about 1 Mm^3 lower. On the contrary, the strongest differences between RCPs emission scenarios are found in San Giuliano dam, where under the "best" scenario a total amount of 24 Mm^3 of water lower than in the baseline is expected to enter into the reservoir. However, precipitation values are higher under RCP 4.5 than 8.5, except in the Cuga and Alto Temo basins. Compared to the baseline, the strongest water inflow reduction is estimated in San Giuliano, specifically under RCP 8.5, where the mean amount of effective precipitation was about 38 Mm^3 lower. Reverse, the lowest reduction is expected in Cuga-Alto Temo system, specifically under RCP 8.5 (about 1.39 Mm^3). Water inflow changes under global worming are almost double in Monte Pranu basin than in Cuga-Alto Temo system, even if the trend is the opposite; in fact the highest water reductions are computed in Monte Pranu under RCP 8.5 (-8.06 Mm^3) and in the system under RCP 4.5 (-2.86 Mm^3). Almost the same future reductions are

accounted for in Stretta di Calamaiu and Rosamarina basin (10 Mm^3). It is estimated that the water quantity entering in the basin is related to the basin area, and that is greater in large areas. In this contest, it is worth noticing the water entering per km^2, in fact this assessment shows the highest value in Stretta di Calamaiu and Alto Temo (about 0.20 Mm^3), and in Rosamarina (about 0.18 Mm^3). These values are related to the runoff coefficient values (0.50-0.42). Slightly lower value of water inflow per km^2 (0.17 Mm^3) are estimated in Cuga basin, and this is explained by the lower mean annual precipitation. The lowest water volumes inflow are computed in reservoirs characterized by low runoff coefficient values that range from 0.32 to 0.35, i.e. in Monte Pranu (about 0.14 Mm^3) and San Giuliano (0.11 Mm^3).

The mean annual outflow is estimated for each reservoir taking into account the cultivated area and the crop irrigation requirement. The difference between future and baseline total water volume distribution used to irrigate maize, wheat, grape, vegetables, fruit trees, and all the other crops cultivated in the Basso Sulcis and Gallura consortium is almost the same (0.43-0.57 Mm^3), and this is due to the cultivated area. Despite maize, grape, vegetables, wheat, and fruit trees in Gallura cover about half of the land cultivated by the same crops in the South of Sardinia, the total number of hectares cultivated is very similar (1382 ha in Basso Sulcis and 1402 ha in Gallura), thus also the water outflow. Compared to the previous case studies, in Palermo 2 consortium the total production is more than double, thus the total water abstract from the reservoir to satisfy crop water needs is proportioned (about 0.9 Mm^3). While in Sardinia the highest values were estimated under RCP 4.5, in Sicily they are under the worst RCP scenario. The greatest difference in water outflow is accounted for in Bradano-Metaponto consortium, where the highest water abstraction is expected to be 10.86 Mm^3 under RCP 8.5, i.e. about 7 Mm^3 more than under RCP 4.5.

In addition, in San Giuliano reservoir is also computed the greatest mean annual water storage change between future and baseline, specifically a total water amount equal to about 50 Mm^3 less under RCP 8.5 than in the baseline. The difference between the two RCPs is about 18 Mm^3.

The mean change in water stored ranges from about -8 Mm^3 to -15 Mm^3 in Palermo 2 consortium, and from -10 Mm^3 to -13 Mm^3 in Gallura, and in both the strongest water

reduction is estimated under the worst scenario. Similar values are related to the similar inflow and outflow conditions.

Despite the reservoir size, the irrigated agriculture is more vulnerable (-0.3<VI<-0.46) in Bradano-Metaponto consortium, and this is due to the very relevant reduction of annual water stored in the basin, specifically related to the greatest effective precipitation reduction. The risk of vulnerability to climate change is higher under RCP 8.5. The future decreasing of annual water availability reduces the reservoir resilience. The same behaviour is noticed also in the other reservoirs even though the entity of the issue is lower.

Vulnerability indices values (from -0.1 to -0.15) are similar in Palermo 2 and Gallura consortia. Both show the best resilience under RCP 4.5. The lowest risk of irrigated agriculture vulnerability to future changes is estimated in the South of Sardinia, in Monte Pranu basin, under RCP 4.5 (-0.07). In general, the vulnerability of the reservoirs under investigation is almost the same, except for the biggest one.

In conclusion, the irrigated agriculture is defined under vulnerable risk in each case study. Since a future water deficit is expected to characterize each consortium, a decreasing reservoir resilience is estimated. Anyway, despite the mean effective precipitation tended to decrease and crop water demand to increase under climate change conditions, all reservoirs are considered resilient, and this is explained by their capacity and water entering into the basin which is always higher than water distribution volumes.

At this stage, only Italian reservoir mainly used for irrigation are taken into account to assess irrigated agriculture vulnerability, but future work will be dedicated to assess the vulnerability of the other Euro-Mediterranean reservoirs, where agriculture is also expected to undergo relevant future climate changes. An in-depth vulnerability study on Euro-Mediterranean reservoirs and resilience to global warming may be useful to address political decisions target to develop strategies to better manage water resources in irrigation consortia.

REFERENCES

Amayreh, J., Al-Abed, N., 2005. Developing crop coefficients for field-grown tomato (Lycopersicon esculentum Mill.) under drip irrigation with black plastic mulch. Agricultural Water Management 73, 247–254. Elsevier.

Cancelliere, A., Rossi, G., 2011. Drought and water scarcity risk in the Mediterranean. Meeting of the EC Expert group on Water Scarcity and Drought FEM, Venice 13-14, October 2011.

DAI, ACED, 2011. Moldovan Tomato Value Chain Study. Stiopca, O., Cipciriuc, L., Bejan, A. Agricultural Competitiveness And Enterprise Development Project (ACED). USAID/Ukraine Regional Contract Office.

Favati, F., Lovelli, S., Galgano, F., Miccolis, V., Di Tommaso, T., Candido, V., 2009. Processing tomato quality as affected by irrigation scheduling. Scientia Horticulturae 122, 562–571.

Fekete, B.M., Vörösmarty, C.J., Grabs, W., 2000. Global, Composite Runoff Fields Based on Observed River Discharge and Simulated Water Balances. Report No. 22. Global Runoff Data Centre (GRDC), Federal Institute of Hydrology (BfG) Koblenz, Germany.

Fouad, E., 2016. Tomatoes are Morocco´s agricultural export hit. Agri Benchmark. http://www.agribenchmark.org/agri-benchmark/did-you-know/einzelansicht/artikel//tomatoes-are-1.html.

Gabriels, D., 2007. Aridity and drought indices. College of Soil Physics. International Centre of Theoretical Physics.

http://indico.ictp.it/event/a06222/material/4/2.pdf.

Gallo, A., 2015. Assessment of the Climate Change Impact and Adaptation Strategies on Italian Cereal Production using High Resolution Climate Data. Ph.D. thesis. University of Sassari.

Garrote, L., Iglesias, A., Granados, A., Mediero, L., Carrasco, F.M., 2015. Quantitative Assessment of Climate Change Vulnerability of Irrigation Demands in Mediterranean Europe. Water Resources Management 29, Issue 2, 325–338. Springer.

Harrison, P.A., Dunford, R., Savin, C., Rounsevell, M.D.A., Holman, I.P., Kebede, A.S., Stuch, B., 2014. Cross-sectoral impacts of climate change and socio-economic change for multiple, European land- and water-based sectors. Climatic Change, http://dx.doi.org/10.1007/s10584-014-1239-4.

Helyes, L., Lugasi, A., Pék, Z., 2012. Effect of irrigation on processing tomato yield and antioxidant components. Turkish journal of agriculture and forestry 36, 702-709, TÜBİTAK, doi:10.3906/tar-1107-9.

IPCC, 2001. Climate Change 2001: Impacts, Adaptation, and Vulnerability. Contribution of Working Group II to the Third Assessment Report of the Intergovernmental Panel on Climate Change. McCarthy, J.J., Canziani, O.F., Leary, N.A., Dokken, D.J., White, K.S. Cambridge University Press, Cambridge, United Kingdom and New York, NY, USA.

IPCC, 2014. Summary for Policymakers. In: Climate Change 2014: Mitigation of Climate Change. Contribution of Working Group III to the Fifth Assessment Report of the Intergovernmental Panel on Climate Change Edenhofer, O., R. Pichs-Madruga, Y. Sokona, E. Farahani, S. Kadner, K. Seyboth, A. Adler, I. Baum, S. Brunner, P. Eickemeier, B. Kriemann, J. Savolainen, S. Schlömer, C. von Stechow, T. Zwickel and J.C. Minx. Cambridge University Press, Cambridge, United Kingdom and New York, NY, USA.

Jedlička, J., Paulen, O., Ailer, S., 2015. Research of effect of low frequency magnetic field on germination,growth and fruiting of field tomatoes. Acta Horticulturae et Regiotecturae 1. Nitra, Slovaca Universitas Agriculturae Nitriae, 1–4.

Jędrszczyk, E., Skowera, B., Kopcińska, J., Ambroszczyk. A.M., 2012. Te Influence of Weather Conditions During Vegetation Period on Yielding of Twelve

Determinate Tomato Cultivars. Notulae botanicae Horti Agrobotanici 40 (2): 203-209, ISSN 0255-965X, Electronic 1842-4309.

Jensen, C.R., Battilani, A., Plauborg, F., Psarras, G., Chartzoulakis, K., Janowiak, F., Stikic, R., Jovanovic, R., Li, G., Qi, X., Liu,F., Jacobsen, S.E., Andersen, M.N., 2010. Deficit irrigation based on drought tolerance and root signalling in potatoes and tomatoes. Agricultural Water Management 98, 403–413.

Kadioglu, M., Şen, Z., 2001. Monthly precipitation-runoff polygons and mean runoff coefficients. Hydrological Sciences Journal 46:1, 3-11, doi:10.1080/02626660109492796.

Kapur, B., Steduto, P., Todorovic, M., 2007. Prediction of climatic change for the next 100 years in the Apulia region, Southern Italy. Italian Journal of Agronomy 4, 365-371.

Kosmas, C., Kirkby, M., Geeson, N., 1999. The Medalus project Mediterranean desertification and land use, Manual on key indicators of desertification and mapping environmentally sensitive areas to desertification. Energy, environment and sustainable development. European Commission, Community Research.

Lehner, B., Verdin, K., Jarvis, A., 2008. New global hydrography derived from spaceborne elevation data. Eos 89, 93–94, doi:10.1029/2008EO100001.

Lehner, B., Reidy Liermann, C., Revenga, C., Vörösmarty, C., Fekete, B., Crouzet, P., Döll, P., Endejan, M., Frenken, K., Magome, J., Nilsson, C., Robertson, J., Rödel, R., Sindorf, N., Wisser, D., 2011. High resolution mapping of the world's reservoirs and dams for sustainable river flow management. Frontiers in Ecology and the Environment 9 (9), 494-502, http://dx.doi.org/10.1890/100125.

Mancosu, N., 2013. Agricultural water demand assessment using the SIMETAW# model. Ph.D. thesis. University of Sassari.

McDonald, R.I., Green, P., Balk, D., Fekete, B.M., Revenga, C., Todd, M., Montgomery, M., 2011. Urban growth, climate change, and freshwater availability. Pacific Institute for Studies in Development, Environment, and Security, Oakland, CA.

McDonald, R.I., Weber, K., Padowski, J., Florke, M., Schneider, C., Green, P.A., Gleeson, T., Eckmann, S., Lehner, B., Balk, D., Boucher, T., Grill, G., Montgomery, M., 2014. Water on an urban planet: urbanization and the reach of urban water infrastructure. Global Environmental Change 27, 96–105, http://dx.doi.org/10.1016/j.gloenvcha.2014.04.022. Meehl, G.A., Bony, S., 2011. Introduction to CMIP5. CLIVAR Exchanges 16, 2–5.

Mercy Corporation, 2014. Protect and Provide Livelihoods in Lebanon: Tomato Value Chain Assessment.

Mereu, S., Sušnik, J., Trabucco, A., Daccache, A., Vamvakeridou-Lyroudia, L., Renoldi, S., Virdis, A., Savić, D., Assimacopoulos, D., 2016. Operational resilience of reservoirs to climate change, agricultural demand, and tourism: A case study from Sardinia. Science of the Total Environment 543, 1028–1038. Elsevier.

Mohamedova, M., Deleva, E., Stoeva, A., Harizanova, V., 2016. Comparison Of Pheromone Lures Used In Mass Trapping To Control The Tomato Leafminer Tuta Absoluta (Meyrick, 1917) In Industrial Tomato Crops In Plovdiv (Bulgaria). Agricultural University – Plovdiv, Agricultural Sciences VIII, Issue 19.

Monfreda, C., Ramankutty, N., Foley, V., 2008. Farming the planet: 2. Geographic distribution of crop areas, yields,physiological types, and net primary production in the year 2000. Global Biogeochemical Cycles, 22, GB1022, doi:10.1029/2007GB002947.

Moriones, E., Aramburu, J., Riudavets, J., Arnò, J., Lavina, A., 1998. Effect of plant age at time of infection by tomato spotted wilt tospovirus on the yield of field-grown tomato. European Journal of Plant Pathology 104, 295-300.

Nam, W.H., Choi, J.Y., 2014. Development of an irrigation vulnerability assessment model in agricultural reservoirs utilizing probability theory and reliability analysis. Agricultural Water Management 142, 115–126. Elsevier.

Ozbahce, A., Tari, A.F., 2010. Effects of different emitter space and water stress on yield and quality of processing tomato under semi-arid climate conditions. Agricultural Water Management 97, 1405–1410.

Paciello, M.C., 2015. Building Sustainable Agriculture for Food Security in the Euro Mediterranean Area: Challenges and Policy Options. Edizioni Nuova Cultura – Roma, ISBN: 9788868125080.

Patanè, C., Cosentino, S.L., 2010. Effects of soil water deficit on yield and quality of processing tomato under a Mediterranean climate. Agricultural Water Management 97, 131–138. Elsevier.

Patanè, C., Tringali, S., Sortino, O., 2011. Effects of deficit irrigation on biomass, yield, water productivity and fruit quality of processing tomato under semi-arid Mediterranean climate conditions. Scientia Horticulturae 129, 590–596. Elsevier.

Portas, C.A.M., Oliveira, W., Stilwell, M.R., Calado, A.M., Dias, V.M.B., Ruiz-Altisent, M., 1986. The Tomato Processing Industry in Portugal. Hortscience, 21 (1).

RAS, 2002. Campagna di sensibilizzazione per un uso consapevole e amorevole dell'acqua,scheda No. 8. Progetto altriponti, osservatorio mediterraneo: un ponte d'acqua. Regione Autonoma della Sardegna.

Rockel, B., Will, A., Hense, A., 2008. The regional Climate Model COSMO-CLM (CCLM). Meteorologische Zeitschrift 17 (4), 347-348.

Rodriguez-Diaz, J.A., Weatherhead, E.K., Knox, J.W., Camacho, E., 2007. Climate change impacts on irrigation water requirements in the Guadalquivir river basinin Spain. Regional Environment Change 7, 149–159.

Saadi, S., Todorovic, M., Tanasijevic, L., Pereira, L.S., Pizzigalli, C., Lionello, P., 2014. Climate change and Mediterranean agriculture: Impacts on winter wheat and tomato crop evapotranspiration, irrigation requirements and yield. Agricultural Water Management. Elsevier.

Syrian Economic Forum, 2015. Agriculture in Eastern Ghouta, Current Situation Study, www.syrianef.org.

Tanasijevic, L., Todorovic, M., Pereira, L.S., Pizzigalli, C., Lionello, P., 2014. Impacts of climate change on olive crop evapotranspiration and irrigation requirements in the Mediterranean region. Agricultural Water Management 144, 54–68. Elsevier.

Tosti, G., Benincasa, P., Farneselli, M., Pace, R., Tei, F., Guiducci, M., Thorup-Kristensen, K., 2012. Green manuring effect of pure and mixed barley – hairy vetch winter cover crops on maize and processing tomato N nutrition. European Journal of Agronomy 43, 136–146. Elsevier.

Tubiello, F.N., Donatelli, M., Rosenzweig, C., Stockle, C.O., 2000. Effects of climate change and elevated CO_2 on cropping systems: Model predictions at two Italian locations. European Journal of Agronomy 13, 179–189.

UNEP, 1992. World atlas of desertification (United nations environment programme). edited by N. Middleton and D.S.G. Thomas. Edward Arnold, London, ISBN 0 340 55512 2, ix + 69 pp.

UNESCO, 1979. Map of the world distribution of arid region. Explanatory note. United Nations Educational, Scientific and Cultural Organization. Paris, ISBN 92-3-101484-6.

Willmott, C.J., Matsuura, K., 2001. Terrestrial Air Temperature and Precipitation: Monthly and Annual Time Series (1950 - 1999), http://climate.geog.udel.edu/~climate/html_pages/README.ghcn_ts2.html. UDel_AirT_Precip data provided by the NOAA/OAR/ESRL PSD, Boulder, Colorado, USA, from their Web site at http://www.esrl.noaa.gov/psd/.

World Food Summit, 1996. Report of the World Food Summit. Food And Agriculture Organization Of The United Nations Rome, http://www.fao.org/docrep/003/w3548e/w3548e00.htm.

Yano, T., Aydin, M., Haraguchi, T. 2007. Impact of climate change on irrigation demand and crop growth in a Mediterranean environment of Turkey. Sensors 7, 2297-2315.

Žnidarčič, D., Trdan, S., Zlatič, E., 2003. Impact of various growing methods on tomato (Lycopersicon esculentum Mill.) yield and sensory quality. Zb. Bioteh. Fak. Univ. Ljublj. Kmet. 81 - 2.

Websites

ENAS, 2017. Ente Acque della Sardegna - RAS:
http://www.enas.sardegna.it/il-sistema-idrico-multisettoriale/laghi-artificiali/monte-pranu.html
http://www.enas.sardegna.it/il-sistema-idrico-multisettoriale/laghi-artificiali/liscia.html
http://www.enas.sardegna.it/il-sistema-idrico-multisettoriale/laghi-artificiali/alto-temo.html
http://www.enas.sardegna.it/il-sistema-idrico-multisettoriale/laghi-artificiali/cuga.html

CBNurra, 2017. Consorzio di bonifica della Nurra:
http://www.bonificanurra.it/regolamenti/RI2002.htm
http://www.bonificanurra.it/index.php/comprensorio/24-tavole.html

CBGallura, 2017. Consorzio di bonifica della Gallura: http://www.cbgallura.it/index.php?option=com_content&view=article&id=47&Itemid=54.

CBBasso-Sulcis, 2017. Consorzio di bonifica del Basso Sulcis: http://www.consorziobassosulcis.it/servizioirr.asp

EUROSTAT, 2017: http://ec.europa.eu/eurostat/statisticsexplained/index.php/Agricultural_production_-crops.

ISTAT, 2010. Censimento Agricoltura 2010. http://daticensimentoagricoltura.istat.it/Index.aspx?lang=it#.

Basilicata, 2017: http://www.adb.basilicata.it/adb/risorseidriche/idrografico.asp

http://appsso.eurostat.ec.europa.eu/nui/show.do?dataset=orch_total&lang=en

http://www.bradanometaponto.it/SanGiuliano.html

http://www.bradanometaponto.it/PianoClassifica.html

http://www.fao.org/nr/water/aquastat/data/query/index.html?lang=en

http://www.fao.org/3/a-bc824e.pdf

https://www.regione.sardegna.it/documenti/1_470_20161129104147.pdf

http://www.waterboards.ca.gov/water_issues/programs/swamp/docs/cwt/guidance/513.pdf

http://adpaloha.altervista.org/wp-content/uploads/2012/10/ROSAMARINA.pdf

ACKNOWLEDGMENTS

My deep gratitude goes to Chair Professor Donatella Spano for her precious and expert advice, unfailing support, and motivation to give my best. She has become over the years a reference point on which to put faith and esteem. Thank you for giving me the opportunity to work in different contexts, increasing my knowledge and opening up my mind to new experiences and points of view.

I would like to give my special thanks to my supervisor Dr. Serena Marras who patiently and constantly guided and encouraged me in each step of this experience. Thanks for all your expert and valuable advice and suggestions that were crucial to strengthen this work, and to my personal and professional progress. Your professionalism has been an inspiration for me during these years.

My thankfulness to my tutor Dr. Costantino Sirca for imparting his know-how and expertise in this study. Thank you also for the constructive discussions and suggestions useful to improve different aspects of this work.

I really would like to express my special thanks to my co-tutor Dr. Antonio Trabucco for his constant availability and for conveying me his enthusiasm and passion for this thesis, and for the research field of work. Thanks so much to share your knowledge with me, and to valuable support and guide me day by day in the development of this work with your constructive advice and suggestions, contributing to my personal and professional growth.

I am grateful to Dr. Simone Mereu for the useful and constructive discussions which contribute to improve the content of this work. I really would like to thank you for giving me, together with my supervisor, tutor, and co-tutor, the wonderful opportunity to do the stage at UNESCO-IHE which was a crucial experience to improve my professional and personal life.

A sincere thank to Professor Richard Snyder for his unfailing availability and kindness, and for dedicating to this work as much time as possible during his stay at

the University of Sassari, and along these years. Thank you very much for your essential contribute to this thesis.

The third chapter of this work would not have been possible without the support of the UNESCO-IHE Institute for Water Education, and particularly Dr. Janez Susnik, whose professionalism, availability, enthusiasm and kindness were the basis of a very nice and constructive collaboration. Thank you so much for making my stage at the UNESCO-IHE unforgettable.

I also need to thank the SIM4NEXUS project, which has partially funded collaboration activities during my PhD research, the Water Authority of Sardinia (ENAS), and the Regional Ministry of Environment, for their support.

I would like to acknowledge the principal investigators of each FLUXNET site cited in the first part of the thesis to provide me data and useful information.

I thank the University of Sassari that funded the mobility abroad in the framework the Erasmus+ programme, Key Action 1, Learning Mobility of Individuals.

I would like to thank everybody working at the Department of Science for Nature and Environmental Resources, and at the Department of Agricultural Sciences at the University of Sassari. I thanks all professors, researchers, colleagues, and administrative people I met during these years.

A special thank for Dr. Michele Salis, Dr. Valentina Mereu, Dr. Valentina Bacciu, Dr. Gavriil Kyriakakis for their passion for the world of the scientific research that was a source of inspiration for me over the years.

I really would like to thank my colleagues and friends, particularly Andrea Gallo, Veronica Bellucco, Viviana Guido, Noemi Mancosu, Liliana Del Giudice, Carla Scarpa, Olga Muñoz Lozano, José Maria Costa Saura, Lourdes Morillas, Laura Lai, Matilde Schirru, Giovanni Zucca, Lucia Corona, Luana Sale, Lalla Dessena, Caterina Mele, and Matteo Cabras.

A special thank for Mauro Lo Cascio, Andrea Badurina Cantore, Antonio Caddeo, and Enrico Vagnoni to make the last three years so pleasant, and for the amazing time spent together, both in joyful and stressful circumstances…plenty of good memories.

A deep and special thanks goes to my dearest friends, in particular to Simona, Antonella, Claudio, Giancarlo, Giommaria, and Barbara with whom I had the pleasure and the fortune to share these years. I thank them from the depths of my heart for encouraging me and helping me in the most difficult moments and sharing with me the happiest ones.

My special gratitude goes to Carlo who encouraged and motivated me in each step of this thesis, and my life in general. Thanks so much to believe in me, to support me in my decisions, and to share with me the good and the bad days. Words are not enough to thank you for always being there for me with your patience, smile, and love.

Finally, the deepest gratitude to my wonderful family, my mother, my father, and my sister Chiara that always trust in me and push me in doing my best. Thanks so much to support and embolden me every single day of my life, and for your patience and sacrifice over the year. Thanks for helping me growth.

I would also like to thank all people who are not mentioned here, and that contributed to this thesis, and to the achievement of this important goal.

APPENDIX 1

ID	*ZONE_NAME*	*Grape - Bud break literature*
5	Algeria	Same as Morocco
15	Austria	PEP725
26	Bosnia and Herzegovina	PEP725
35	Bulgaria	Same as Romania
66	Egypt	Same as Morocco
74	Czechia	Same as Slovakia
83	France	Jones and Davis 2000; Andreini et al., 2009; Valdez-Gomez et al., 2009; Nendel, 2010
93	Germany	PEP725, Nendel, 2010; Schwab et al., 2000
97	Greece	Anderson et al., 2014
106	Croatia	PEP725
107	Hungary	Same as Slovakia
116	Italy	Cortesi et al., 1997, Novello and Palma 2008, Tomasi et al., 2011; Mancosu, 2013
140	Slovakia	PEP725, Nendel 2010
153	Macedonia	Same as Greece
156	Morocco	Ezzhaouani et al., 2007
189	Portugal	Same as Spain
196	Romania	Same as Greece and Slovakia
201	Saudi	Same as Morocco
208	Slovenia	Same as Croatia
213	Spain	Camps and Ramos 2012; Lopez - Urrea et al., 2012; Picon - Toro et al., 2012
214	Serbia	Same as Bosnia
220	Syrian	Same as Greece
221	Switzerland	Same as Austria
231	Tunisia	Same as Morocco
232	Turkey	Same as Greece

ID	*ZONE_NAME*	*Grape - Harvest literature*
5	Algeria	Same as Morocco
15	Austria	PEP725
26	Bosnia and Herzegovina	PEP725
35	Bulgaria	Same as Romania
66	Egypt	Same as Morocco
74	Czechia	Same as Slovakia
83	France	Jones and Davis, 2000; Valdez-Gomez et al., 2009
87	Georgia	Same as Greece
93	Germany	PEP725; Schwab et al., 2000; Christoph et al., 2003
97	Greece	Anderson et al., 2014
106	Croatia	Same as Italy
107	Hungary	Same as Austria
116	Italy	Tomasi et al., 2011; Mancosu, 2013
140	Slovakia	Same as Austria
153	Macedonia	Same as Greece
156	Morocco	Ezzhaouani et al., 2007
189	Portugal	Same as Spain
196	Romania	Same as Greece and Slovakia
201	Saudi	Same as Morocco
208	Slovenia	Same as Italy
213	Spain	Camps and Ramos 2012; Lopez - Urrea et al., 2012; Picon - Toro et al., 2012
214	Serbia	Same as Bosnia
220	Syrian	Same as Greece
221	Switzerland	PEP725; Meier et al., 2007
231	Tunisia	Same as Morocco
232	Turkey	Same as Greece

APPENDIX 2

ID	*ZONE_NAME*	*Tomato - Sowing and harvest literature*
5	Algeria	Same as Morocco
7	Albania	Same as Greece
26	Bosnia and Herzegovina	Same as Italy
35	Bulgaria	Mohamedova et al., 2016
66	Egypt	Same as Morocco
83	France	Same as Italy
97	Greece	Jensen et al., 2010
106	Croatia	Same as Italy
107	Hungary	Helyes et al., 2012
115	Israel	Same as Lebanon
116	Italy	Favati et al., 2009; Patanè and Cosentino 2010; Patanè et al., 2011; Tosti et al., 2012
123	Jordan	Amayreh and Al-Abed, 2005
136	Lebanon	Mercy Corporation, 2014
140	Slovakia	Jedlička et al., 2015
148	Moldava	DAI/ACED, 2011
153	Macedonia	Same as Greece
156	Morocco	Fouad, 2016
163	Montenegro	Same as Italy
173	Poland	Jędrszczyk et al., 2012
189	Portugal	Portas et al., 1986
196	Romania	Same as Hungary
208	Slovenia	Žnidarčič et al., 2003
213	Spain	Moriones et al., 1998
214	Serbia	Same as Bosnia and Herzegovina
220	Syria	Syrian economic forum, 2015
231	Tunisia	Same as Morocco
232	Turkey	Ozbahce and Tari, 2010